ALADIN-HIRLAM Newsletter

No 8, January 2017

Grand Tour of ALADIN & HIRLAM

ALADIN Programme, c/o P. Termonia, IRM, Avenue Circulaire 3, 1180 Bruxelles, Belgium

HIRLAM-B Programme, c/o J. Onvlee, KNMI, P.O. Box 201, 3730 AE De Bilt, The Netherlands

CONTENTS

:

Introduction

Patricia Pottier

I am happy to provide you with the eighth edition of the combined Newsletter of the HIRLAM and ALADIN consortia.

This edition is mainly dedicated to a "Tour d'ALADIN et d'HIRLAM", with contributions describing the main achievements at our meteorological services in 2016.

Besides these scientific and technical articles, you will find in this Newsletter an "summary report of a "recent workshop on a relevant subject to our community where a few of us have been involved" and an overview of operational configurations.

The "Publications and PhDs"pages will be back in the ninth edition of the Newsletter.

I hope you enjoy reading the eighth ALADIN-HIRLAM Newsletter, thank the authors for their contributions and hand it off first to Philippe Bougeault who will update you with the last important news at the consortia level., the signature of the ALADIN-HIRLAM cooperation agreement.

For additional information, please visit the ALADIN and HIRLAM websites, or just ask the authors of the articles.

ALADIN-HIRLAM cooperation agreement signing by M. Benko and Mme. Thyrring (with the Program Managers, P. Termonia and J. Onvlee, and P. Bougeault from MF)

Editorial

Philippe Bougeault

Last december, the Chairs of ALADIN GA and HIRLAM Council signed the new cooperation agreement between the two Consortia. This is putting a welcome end to a two-year quarrel on data policy, and I am glad to thank all Members for their willingness to compromise. These discussions have raised the awareness of the difficulties that our services are facing, each operating under different legal and economic constraints. In that sense, they have helped us to better understand each other, which will certainly benefit the cooperation.

The joint GA/Council has also reaffirmed the objective to replace the existing two consortia by a single new consortium by 2020, and tasked the two Project Managers to continue their highly appreciated hard work to solve the remaining issues.

First, we must agree on the mission perimeter of this future consortium: will it concern only NWP stricto sensu, or will it also cover Air Quality and/or Regional Climate models? Which will the priority areas be? What level of diversity/duplication is acceptable for new developments? What will be the responsibility of the consortium in terms of Quality Assurance and Monitoring of the operational systems? These questions have been explored in the 2016 Strategy meeting, and will be further discussed in 2017.

We must also agree on the way we will share the property of the various developments, and on the governance and funding mechanisms: a collaboration of 26 organizations has never been easy, and we must create an harmonious synthesis of the two existing systems.

I am very optimistic that we can make good progress on all issues this year. The amount of scientific and technical expertise in our services is tremendous. We are developing a world-leading regional NWP system, to cover a great diversity of geoclimatic conditions, observation systems, and operational constraints. The challenge is to turn this diversity into a strength – the strength of Cooperation!

Events announced for 2017 (and later on)

1 Meetings

- Joint 27th ALADIN Workshop & HIRLAM All Staff Meeting 2017, 3-7 April 2017, Helsinki, Finland
- 14th PAC and 5th HAC/PAC meetings , 22 May 2017, Copenhagen, Denmark
- 39th EWGLAM and 24th SRNWP meetings, 2-5 October 2017, place t.b.d.
- Regular 22nd General Assembly and 3rd joint ALADIN GA and HIRLAM Council, 21-22 November 2017, Cracow, Poland

In 2018 :

- Joint 28th ALADIN Workshop & HIRLAM All Staff Meeting 2018 , 16-20 April 2018, Toulouse, France

2 Working Weeks / Working Days

- HARMONIE WD on DA algorithms, 9-13 January 2017, De Bilt, Netherlands : dedicated page on HIRLAM wiki
- ALADIN-HIRLAM Clouds WW, 16-18 January 2017, Toulouse, France
- 1st SURFEX Users Workshop, Feb 27 – Mar 1, 2017, Toulouse, France
- ALADIN DA basis kit WD, dates t.b.d., Lisbon, Portugal
- Working week on GLAMEPS, HarmonEPS, EPS calibration and HARP for EPS, May 29 - June 2, 2017, place t.b.d.

- More information on-line

3 Regular video meetings

Roger Randriamiampianina took the initiative to organize regular group video meetings on atmospheric Data Assimilation via google hangouts, for DA staff from both ALADIN and HIRLAM.

First year experience with google hangouts showed that it offers good platform for discussion, sharing ideas and experiences. Last year, we had twice meetings per topics and few meetings on specific topics. The dedicated topics for video meetings on data assimilation are the following: radar data processing, conventional observations and COPE, retrieval observations, radiance observations and algorithm issues (3D-VAR, 4D-VAR, LETKF, Initialization, OOPS, etc …).

More information on hirlam wiki.

Video meeting became more and more popular also for other projects in HIRLAM and ALADIN.

4 About the past events

Find on-line information about the past ALADIN-HIRLAM common events such as the joint ALADIN Workshops & HIRLAM All Staff Meetings, the minutes of the HMG/CSSI meetings, the joint HAC/PAC meetings, the joint ALADIN General Assemblies and HIRLAM Councils.

The video of the last Wk/ASM in Lisbon (April 2016) are on-line, on the “Partners part” of the aladin website (please “log in” with the ALADIN/HIRLAM access - ask Patricia in case you don’t know it). The agenda and the presentations of this Wk/ASM are on the public part (without login).

Desert dusts modeling in AROME: Contribution of physical parameterizations at convective scale.

Abdenour AMBAR, Mohamed MOKHTARI

1 Introduction

The interest of modeling the cycle of desert aerosols in Algeria is important because the Sahara covers more than 75% of the country's surface area. This interest is reinforced by the fact that desert dust has a direct impact on the economy, the environment and public health.

Since February 2014, the prediction of atmospheric cycle of desert dust at the ONM (Office National de la Météorologie-ALGERIA) is based on the operational model ALADIN_DUST with 14 km of horizontal resolution (Mokhtari et al., 2012). In order to investigate the contribution of physical scheme implanted in the convective-scale model AROME to the quality of desert dust cycle prediction, an AROME_DUST configuration based on cycle 40 was updated during the scientific stay of M.Mokhtari and A.Ambar at Meteo France in September 2016 (http://www.cnrm-game-meteo.fr/aladin/IMG/pdf/stay_report_mokhtari_ambar_2016.pdf). We carried out meteorological simulations of a particular event (sandstorm in south Algeria, 1st April 2016). AROME_Dust outputs are compared with observations.

2 AROME model and Dusts modules

The AROME convective scale model (Seity et al., 2011) is operational at the National Center for Meteorological Forecasts (Algeria) since April 2014, covering the northern part of the country (Latitude: 28°N-40°N, Longitude: 3°W-9°E). An AROME covering all the country was configured basing on cycle 40 in order to simulate dust aerosol cycle (Tab 1).
Physical parameterizations of the model are inherited from the Meso-NH search model whereas the dynamic part is an adaptation for the fine scale of the ALADIN dynamic. Desert dusts emission processes are managed by the DEAD model which is integrated into copled system AROME-SURFEX (Grini et al., 2006). The transport, deposition and leaching processes are managed by the ORILAM log-normal aerosol scheme (ORganic Inorganic Log-normal Aerosol Model, Tulet et al., 2005).
Initially, desert dust modules was activated in the ALADIN configuration (cycle 36 and 38) (Mokhtari et al., 2012, Mokhtari et al., 2015) and AROME (cycle 33) (Kocha, 2011) in order to provide predictions of dust events during the FENNEC measurement campaign (Chaboureau et al., 2016).
Connecting dust modules in AROME was made in the prediction step (E001) by activating a set of keys in NAMARPHY namelists, in particular LRDUST and LRDEPOS. Then, we added desert dust variables: 9 variables for passive scalars (YEXT) and 7 variables for diagnostics (YEZDIAG). Desert dust fields are extracted in the fullpos step by asking for them in the namelists blocs NAMAFN, NAMFPC and NAMGFL (For more details, see the following link: http://www.umr-cnrm.fr/aladin/IMG/pdf/stay_report_mokhtari_ambar_2016.pdf).

Tab. 1: Characteristics and computational costs of the Model

Model		AROME
Cycle		40
Resolution		3 km
Levels		60
Grid		1024 x 972
Area	Latitude	18°N – 42°N
	Longitude	10°W– 13°E
Initial conditions		ALADIN (8km)
Starting time		00h
Cycle interval		01h
Verification times		09h, 12h, 15h, 18h
Number of processors (NPROC)		16 x 16
Computational costs	Dust on	7260 sec
	Dust off	4740 sec

3 Simulations and discussion

This situation was chosen on the based on METAR (an aviation routine weather report issued at hourly or half-hourly intervals) and SPECI (an aviation special weather report issued when there is significant deterioration or improvement in airport weather conditions) broadcasted from several stations in southern Algeria. Many extreme weather situations related to desert dust were observed, which paralyzed road traffic in the north-south direction and vice versa.
We compared the MSG-SEVIRI satellite images and AOD observations of Tamanrasset station (AERONET) with AROME_Dust outputs. For the concentration, since we do not have measurements of dust concentrations, we applied an empirical equation (1) relating desert dust concentrations and horizontal visibility (Bertrand, 1976). We can then use observations of the visibility available on various aerodrome stations in Algerian Sahara and compare it to AROME_Dust outputs.

$$VV = \left(\frac{1897}{C}\right)^{1/0.91} \quad \text{..... (1)}$$

- VV : visibility in meters.
- C : Concentration in mg*m-3.

Aerosols optical depths (AOD)

The 1st April 2016 event was characterized by a strong depression centered in the Algerian Sahara (Fig. 1-A). The wind speeds during this event exceeded the erosion thresholds in most of the Sahara, raison for which we observed a dust uprising spell. The Aerosol Optical Depth AOD simulated for this event (Fig. 3), exceeded 1 in several locations in southern Algeria. These values were confirmed by the AERONET data of AOD (Fig. 1-B and 1-C) measured at Tamanrasset station (we choose this station because it is the only one to provide AOD measurements). Indeed, the analysis of the AOD's daily variation during April (Fig. 1-B) shows that this spell was marked by relatively high AOD values.

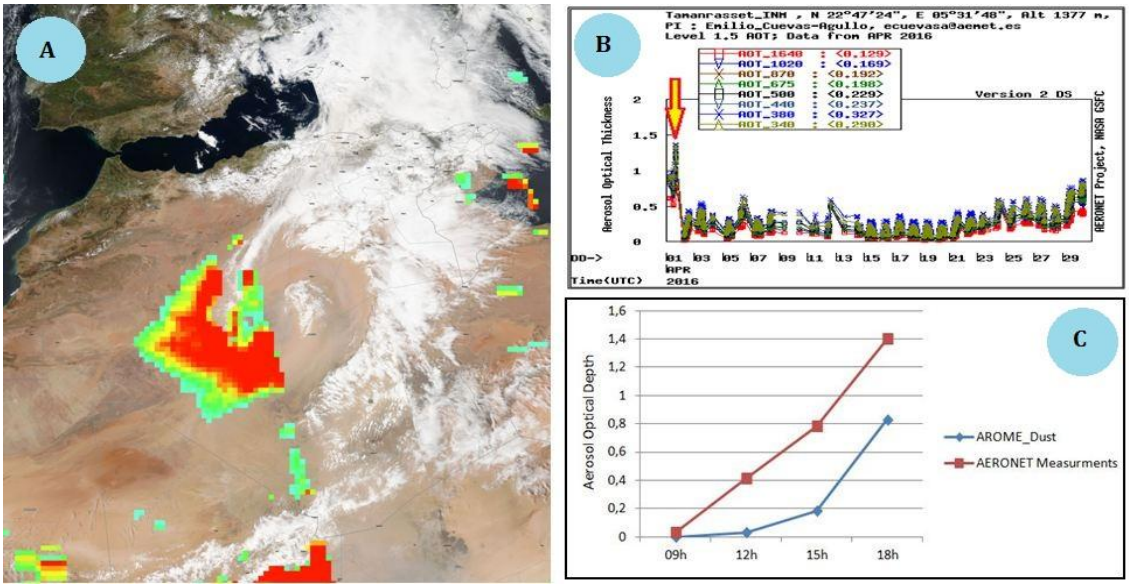

Fig. 1: **-A:** *The Aerosol Optical Depth obtained by the combination of satellite images MODIS/AQUA with the corrected reflectance Suomi NPP / VIIRS, for April 1st 2016 at 12:45utc.*
-B: *AOD daily average recorded during April2016 in Tamanrasset station (Source: http://aeronet.gsfc.nasa.gov/).*
-C: *Aerosols optical depths measured and simulated at the Tamanrasset station on April 1st 2016.*

Figure 3 shows Aerosols optical depths (AOD) predicted by AROME_Dust on April 1st 2016. From the perspective of spatial distribution, AROME_Dust has well simulated the AOD in the Algerian Sahara, compared to the MSG-SEVIRI satellite image (Fig. 2). However, predicted AOD are underestimated versus observations at Tamanrasset station (Fig. 1-C). This is due to the nature of this region and its texture. Indeed, this region is excluded from the source areas, while in reality it contains important dust deposit areas surrounding mountains including the Hoggar and Tassili, which can be subsequently reactivated by the wind.

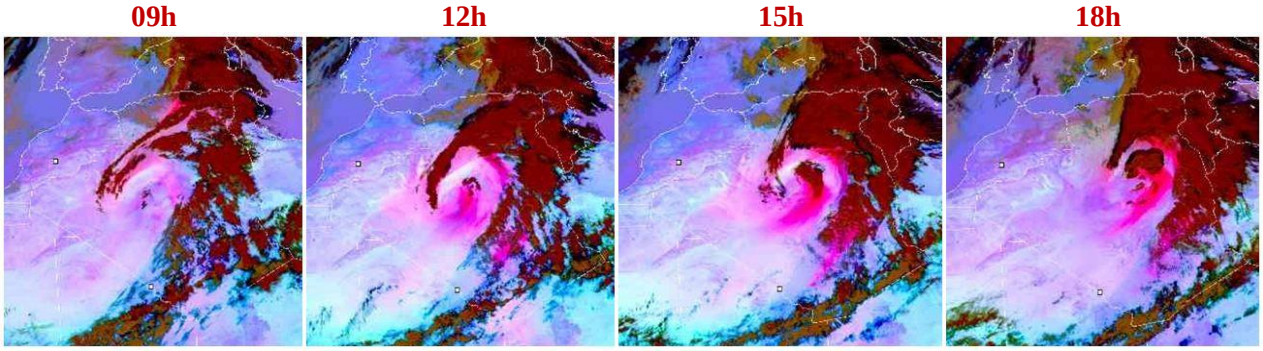

Fig. 2: MSG-SEVIRI satellite image over Algeria for 1st April 2016.

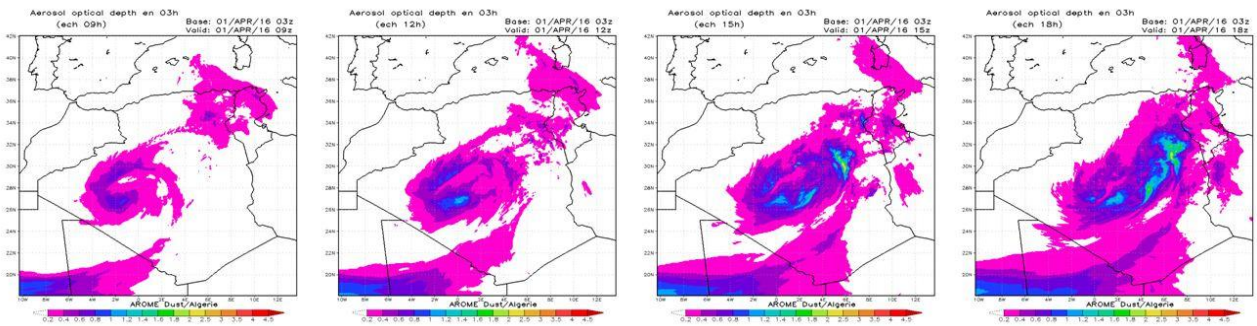

Fig. 3: Aerosols optical depths (AOD) simulated by AROME_Dust on April 1st 2016.

Aerosols concentration and visibility

Figure 4 shows that the dust plume of this event was well predicted by AROME_Dust. The spatial extent of desert dusts observed on the satellite images MSG-SEVIRI (Fig. 2) corresponds to that simulated by the model.
Values of concentration converted to visibility are comparing to the observations of various stations (Fig. 5). These results are very satisfactory. At first sight, we notice that AROME_DUST underestimates the visibility compared to observations in five measurement stations among the six stations picked. However, the difference between the two values (simulated and observed) is not as large and sometimes the two curves are very close (examples in fig. 5: B. B. Mokhtar, H. Messaoud, Adrar). The most important thing is that the model follows the same trend as observations.

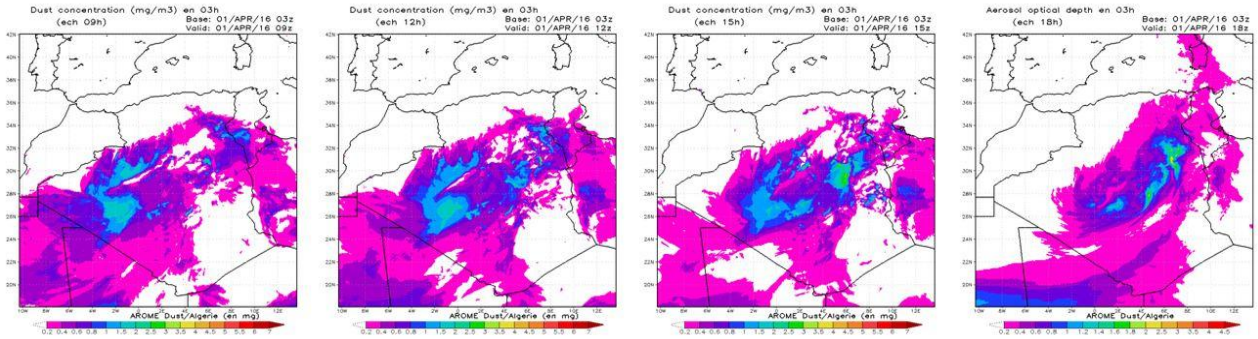

Fig. 4: Concentrations of desert dust simulated by AROME_Dust on April 1st, 2016 (09h,12h,15h,18h).

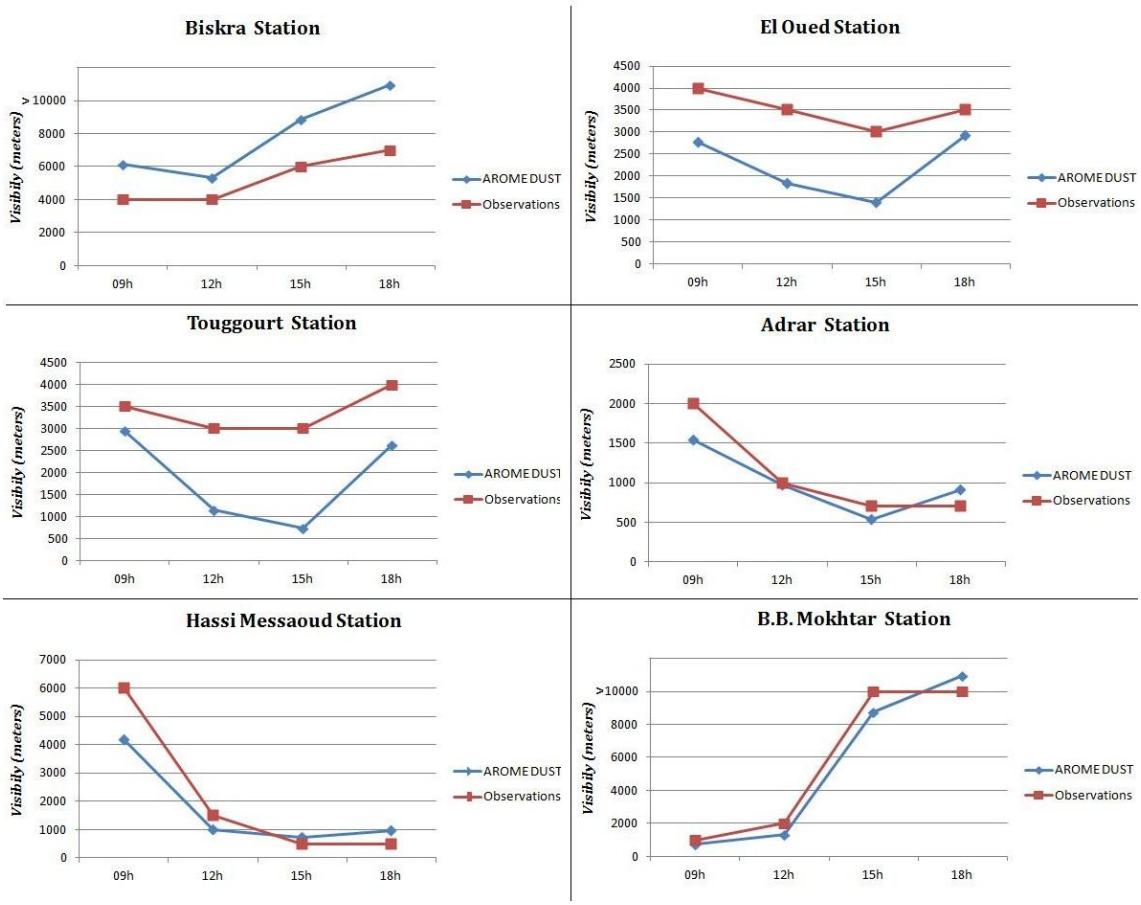

Fig. 5: Visibility measured (METAR observations) and simulated (AROME_DUST) at several stations in southern Algeria on April 1st 2016.

4 Conclusion

This work aims to show the contribution of the physical parameterizations at convective-scale in the modeling of the desert aerosols cycle. The physical scheme used in AROME was mainly developed at the CNRM (Centre National de Recherches Meteorologique - Meteo France) in order to better understand the processes that occur at small-scale.
Overall, high resolution atmospheric simulations carried-out by AROME (resolution of 3km) coupled with dust module over southern Algeria allowed us to improve the prediction of desert dusts cycle. Aerosol optical depth fields obtained follow the same shape of the fields observed with the MSG-SEVIRI satellite images. The conversion of concentration fields to visibility was very efficient, since it gave us a precious tool to validate our results. These visibilities simulated were close to those observed at several stations in southern Algeria which offer to forecasters in meteorological departments an additional tool to use in complex situations related to desert dust uprisings.

Acknowledgments: *The visibility data come from the observation network of ONM (Office National de la Météorologie – Algeria). MODIS/AQUA aerosol optical depth images used in this study were produced with the Giovanni online data system, developed by the NASA Goddard Earth Sciences (GES) Data and Information Services Center (DISC). MSG-SEVIRI satellite images are downloaded from the EUMETSAT website. The authors wish to thank Yves BOUTELOUP and Claude FISCHER at Meteo-France for their help and advices.*

5 References

Chaboureau, J.-P., Flamant, C., Dauhut, T., Kocha, C., Lafore, J-P., Lavaysse, C., Marnas, F., Mokhtari, M., Pelon, J., Reinares Martínez, I., Schepanski, K. and Tulet, P.: *Fennec dust forecast intercomparison over the Sahara in June 2011*, Atmos. Chem. Phys., 16, 6977-6995, doi:10.5194/acp-16-6977-2016, 2016.

Bertrand, J.: *Visibilité et brume sèche en Afrique*. La météorologie, VI, 6, 201-211, 1976.

Grini, A., Tulet, P. and Gomes, L.: *Dusty weather forecasts using the MesoNH mesoscale atmospheric model*, J. Geophys. Res., VOL. 111, D19205, doi: 10.1029/2005JD007007, 2006.

Kocha, C.: *Interactions entre poussières désertiques et convection profonde en Afrique de l'Ouest: observation et modélisation à échelle convective*, Thèse de Doctorat de l'Université de Toulouse 3, 2011.

Mokhtari, M., Gomes, L., Tulet, P. and Rezoug, T. : *Importance of the surface size distribution of erodible material: an improvement on the Dust Entrainment And Deposition (DEAD) Model*, Geosci. Model Dev., 5, 581–598, 2012, doi:10.5194/gmd-5-581-2012, 2012.

Mokhtari, M., Tulet, P., Fischer, C., Bouteloup, Y,. Bouyssel, F. and Brachemi, O.: *Three-dimentional dust and extinction climatology over northern Africa simulated with the ALADIN numerical prediction model from 2006 to 2010*. Atmospheric Chemistry and Physics, doi: 10.5194/acp-15-9063-2015, 2015.

Improvement of microphysical processes in HARMONIE

Pleun Bonekamp and Sander Tijm

1 Introduction

HARMONIE has weaknesses regarding the microphysics. The aim of this study is to improve the representation of Harmonie38h1.2 for winter precipitation. This will be done by tuning the microphysical processes in Harmonie38h1.2 and testing these tunings for several case studies. The results of the freezing rain event of 5 January 2016 for the Netherlands will be discussed. During this freezing rain event Harmonie 38h1.2 (and Harmonie36h1.4 either) predicted solid precipitation (snow and graupel) instead of freezing rain, which influenced the decision for issuing a weather alarm. In these type of situations, it is essential that HARMONIE predictions can be trusted to warn the Dutch population accordingly. In Harmonie38h1.2 several problems are present:

1. too much cloud water if -35 °C < T< 0 °C and almost no cloud ice
2. too much graupel in clouds and therefore too litte snow
3. too much graupel in snow events
4. not enough frozen precipitation that reaches the surface (precipitation melts too fast)
5. liquid precipitation that refreezes to snow instead of to graupel
6. too dense fog
7. too strong wind gusts due to too fast evaporation

In this study, an adjusted version of the microphysical scheme is proposed that diminishes the first 5 weaknesses in Harmonie38h1.2 mentioned above. This new version of HARMONIE is called Harmonie41 in this report. The adjustments include a precipitation conversion, adding a minimum hydrometeor concentration and adding a temperature dependency to several key processes in the microphysical scheme. The temperature dependency is combined with a threshold value of the vertical velocity in the atmosphere, to add a condition that accounts for the presence of ice condensation nuclei in the atmosphere. In this study an overview will be given regarding the weaknesses and proposed adjustments in HARMONIE, and its effects on weather forecasts will be shown. It will become clear that the adjustments enable the model to predict the freezing rain event more accurately and introduces no negative effects on other weather events investigated so far.

2 Microphysical scheme

The microphysical scheme used in HARMONIE is complex, as it involves many coupled processes (Figure 1). Liquid and ice clouds behave differently and a reverse transition between them is possible with different consequences. Firstly, the reversible conversion from ice to liquid water result in a significant latent heat release (or gain) of $\sim$ 10% of the energy necessary for evaporation (or condensation). This release (or gain) of energy contributes to slower melt (or refreezing) of particles by a negative feedback. Secondly, a liquid water droplet has a higher terminal fall speed than an ice particle with the same mass. This implies that solid hydrometeors are airborne for a longer time than liquid ones. Thirdly, light scattering properties are different for cloud water droplets compared to cloud ice particles, which therefore should be treated different in a cloud radiative transfer

scheme. The shape of ice crystals is diverse and complex, which leads to uncertainties in representation of both aerodynamic and morphological properties. Several relationships are proposed to relate the shape of an ice crystal to its mass, volume and terminal fall velocity. HARMONIE makes use of a bulk parameterisation scheme with 3 ice categorizations, which is the minimum of categories to cover most of the precipitating cases [MESO-NH, 2009].

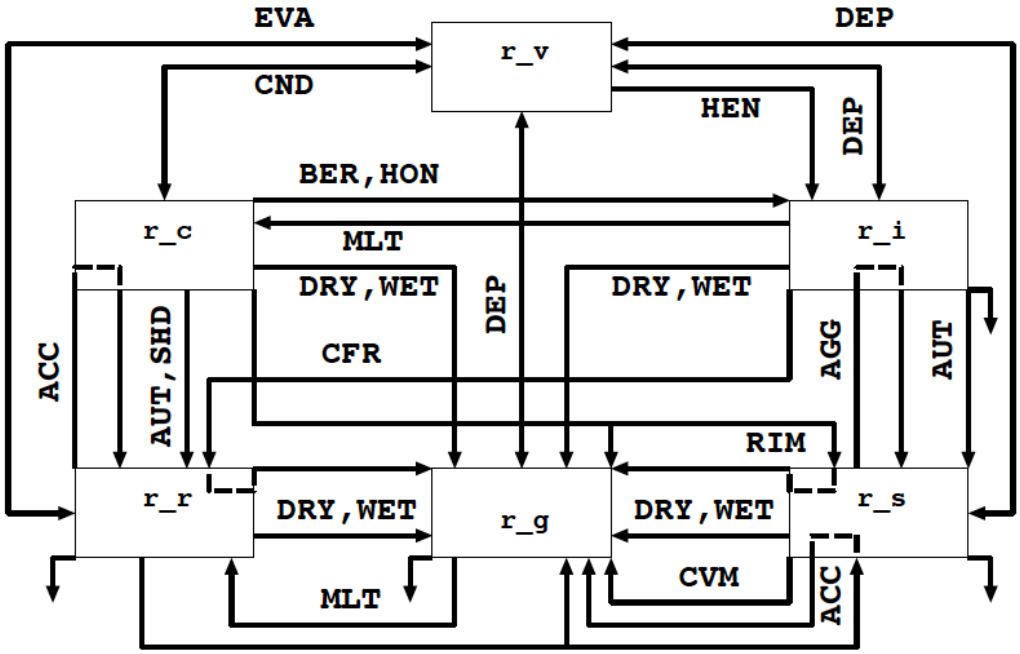

Figure 1: Schematic summary of the microphysical processes in HARMONIE. Taken from [MESO-NH].

3 Method

Several experiments are performed to find the processes that are responsible for the weaknesses mentioned in the introduction. A short overview of the involved processes will be given below, the section numbers refer to the sections in the subroutine rain_ice.f90, KI to Karl-Ivar Ivarsson and PB for Pleun Bonekamp adjustments:

KI1	Section 3.1.1	Reduce the amount of cloud ice
KI2	Section 3.4.6	Reduce the amount of graupel in clouds
PB1	Section 5.2.4	Rain accretion now towards graupel instead of to snow
PB2	Section 6.5	Slowing of melting process
PB3	Section 3.1.1	Heterogeneous cloud ice formation
PB4	Section 5.2.	Accretion process
PB5	Section 5.1.4	Riming
PB6	Section 3.4.3	Snow deposition
PB7	Section 6.4	Dry growth of graupel

These adjustments will be discussed one by one in this section.

3.1 KI1: Reduce amount of cloud ice

KI proposed a change in OCND2 to reduce the deposition and evaporation of snow and graupel with 10% and 25% respectively compared to Harmonie38h1.2. These factors are determined empirically. For the cloud ice water, the deposition and evaporation rate is calculated with the mean ice spherical crystal, which corresponds to a particular ratio of cloud ice and a fixed amount of ice crystals per unit volume. This reduces the deposition and evaporation rate with a factor 10-100, by which more specific cloud water is expected [Ivarsson, 2014].

3.2 KI2: Reduce amount of graupel

This change accounts only for graupel reduction in clouds. If the mixing ratio of graupel (r_g) ~ 0 and the relative humidity of ice, (RH_i), ≥ 115 %, all graupel is converted to snow, since graupel is assumed to be very small. Under high supersaturation conditions, a snow-flake-like crystal growth on those ice pellets is likely. The adjustment account for no conversion to snow if:

$$RH_i \leq 100\% \text{ or}$$
$$r_g \geq 1.0^{-7} \text{ kg} \cdot \text{kg}^{-1}$$

3.3 PB1: Snow accretion towards graupel

In ICE3, rain that is colliding with a frozen particle is converted to snow. In reality this will lead to a frozen particle that more closely resembles graupel/hail (frozen rain) than snow. In ICE3 this is one of the processes that causes the overprediction of snow under freezing rain conditions. This change accounts for the conversion of snow to graupel when a snow particle undergoes accretion. In previous versions, accretion on snow leads to more snow, however this process however is not intuitive. In the code (line number 2485):

$$ZRSS = ZRSS + ZZW,$$

is converted into

$$ZRGS = ZRGS + ZZW.$$

ZZW is the amount of rain, that accretes on snow particles, ZRGS and ZRSS denotes the amount of graupel and snow at a certain timestep, respectively. This change indicates that the amount of rain, which will freeze by accretion will be added to the amount of graupel in stead of to snow.

3.4 PB2: Slowing of the melting process

Currently graupel melts if $T_a > 0$ °C. The rate of melting has a temperature dependence and several constants. The melted water formed at the surface of the graupel is transferred to rain. The melting rate seems to be too fast in the current scheme and is proposed to become twice as slow, as not enough solid precipitation reaches the surface.

3.5 Temperature and vertical velocity dependent processes

Several processes are made temperature dependent in Harmonie41 by:

$$T_a < 273.16 - \text{C\_Bonekamp},$$

where in Harmonie38h1.2 C_Bonekamp = 0 °C, and in HARMONIE41 C_Bonekamp = 20 °C. In combination with the vertical velocity, this threshold value is made more weather regime dependent. Supercooled water

can be present if the temperature is below -20 °C or even at lower temperatures, when no ice condensation nuclei are present to form (solid) precipitation. Therefore the proposed adjustments are made dependent of the vertical velocity in the subroutine rain_ice.f90, which is a measure for the vertical movement in the atmospheric column and therefore the possible presence of ice condensation nuclei. During stable atmospheric conditions the amount of condensation nuclei in the atmosphere will be small, since little vertical movement of air is present and the condensation nuclei that are present initially will precipitate towards the surface and will not be replaced by new ones. During unstable conditions, mixing in the atmosphere is present, by which ice condensation nuclei will be added constantly. Therefore, the adjustments made in HARMONIE41 holds under conditions with little vertical motion. The processes mentioned below are needed to make the growth of snow and graupel slower, since too large amounts of graupel and snow are observed.

3.5.1 PB3: Heterogeneous cloud ice formation

In Harmonie38h1.2 cloud ice can be formed directly if T < 0 °C. However, this is often not observed. Furthermore, in Harmonie36h1.2 cloud ice can only be formed if T < -2 °C. There are many conditions where cloud ice is not formed and where the clouds are 100% liquid even with temperatures well below 0 °C. Therefore we propose to apply the threshods proposed in Section 3.5 on the process of cloud ice formation.

3.5.2 PB4: Accretion

Accretion in Harmonie38h1.2 takes place where:

ZRRT $> 10^{-20}$ kg·kg^{-1}; ZRST $> 10^{-15}$ kg·kg^{-1}; ZRRS > 0.0 kg·kg^{-1} and T_a < 273.16-C_Bonekamp,

where the minimum mixing ratio of rain (ZRRT) and snow (ZRST) at a certain time should be greater than 10^{-20} and 10^{-15} kg·kg^{-1} respectively, the mixing ratio of the rain source (ZRSS) larger than 0.0 kg·kg^{-1} and the temperature below the triple point of water (273.16 K) minus a threshold value (C_Bonekamp). In Harmonie38h1.2 C_Bonekamp=0 °C, for Harmonie41 C_Bonekamp=20 °C in combination with the vertical velocity conditions mentioned in Section 3.5.

3.5.3 PB5: Riming

Riming occurs in Harmonie38h1.2 if $T_a < 0$ °C. However this process is proposed to be made active if T_a < C_Bonekamp. As a result, the growth of snow flakes is reduced and this process can be used to tune the amount of snow. If the diameter of an aggregate reaches a certain threshold, the aggregates will be converted into graupel. This process is therefore influenced as well. Riming of aggregates is proposed to be active when the condition stated in Section 3.5 is met.

3.5.4 PB6: Snow deposition

Deposition on snow occurs in the current scheme when $T_a < 0$ °C, however in reality growth of snow due to deposition of water vapor occur at a lower temperature regime. The deposition of snow is proposed to be active when the conditions stated in Section 3.5 are met.

3.5.5 PB7: Dry growth of graupel

In general the surface temperature of a graupel particle is larger than its environment during accretional growth, since the freezing of liquid water will release the latent heat of fusion. When the surface temperature of graupel

is below 0 °C, all liquid water that sticks to the graupel will freeze. This process is called dry growth (DRY) of graupel. Wet growth (WET) of graupel occurs when the surface temperature of graupel equals 0 °C. Not all collected raindrops can freeze and a thin liquid layer will remain. Harmonie determines the growth regime (WET or DRY) that is active by comparing the DRY and WET growth rates. The lowest growth rate determines the regime and is limiting process, since the amount of liquid water, which can be converted, is important. WET is the maximum rate of the freezing of water on the graupel. So when WET > DRY, enough water can freeze into graupel. Complementary if DRY>WET, not all water can freeze at the graupel. The dry growth rate of graupel involves the number density of graupel and rain particles, the collision efficiency, the fall velocity and some particle dependent parameters. In the present scheme this process is active when T_a < 0 °C. However, T_a < -5 °C is more reliable, since there is latent heat release at the graupel surface, which increase the surface temperature of the graupel. Therefore, the air temperature should be lower than 0 °C for freezing of water on graupel. The condition stated in Section 3.5 is added.

4 Case study

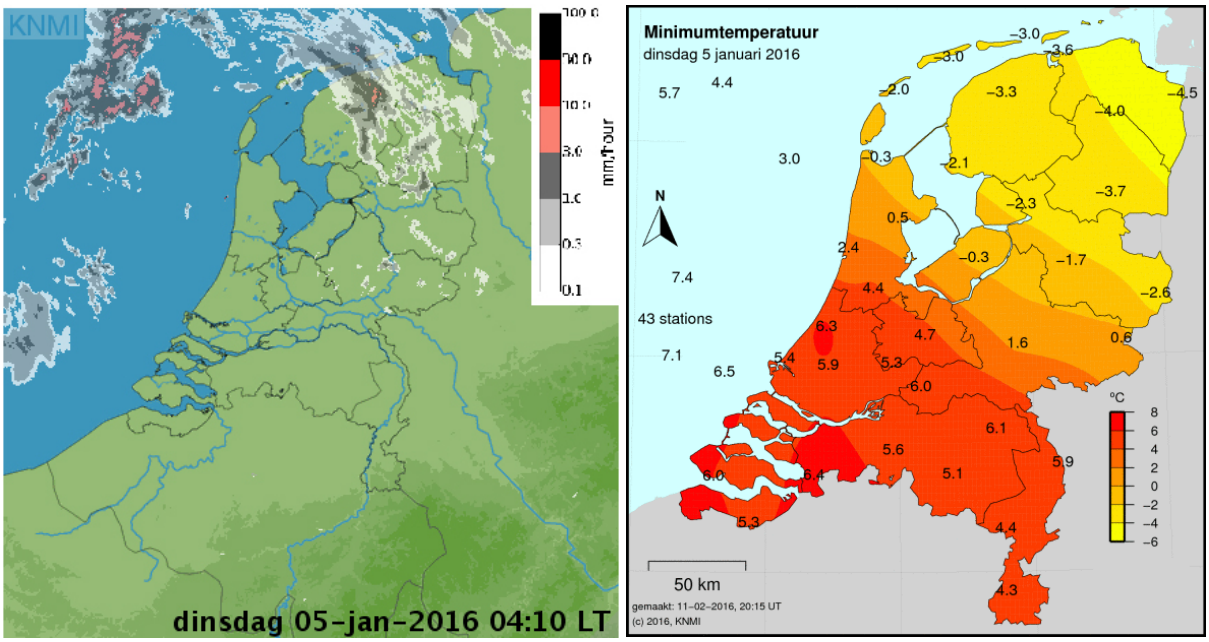

Figure 2: Precipitation radar for January 5^{th}, 2016 4:10 local time (left) and the minimum temperature for January 5^{th}, 2016 (right). Figures are taken from the KNMI archive [2016].

On January 5^{th}, 2016 rain was observed, which in combination with near surface temperatures below 0 °C resulted in freezing rain in the northern part of the Netherlands during the night. During the day almost no precipitation had fallen, but during the day temperatures remained below 0 °C and in the evening more supercooled rain and therefore freezing rain occured. The model results for this case study are discussed in the following section.

5 Results

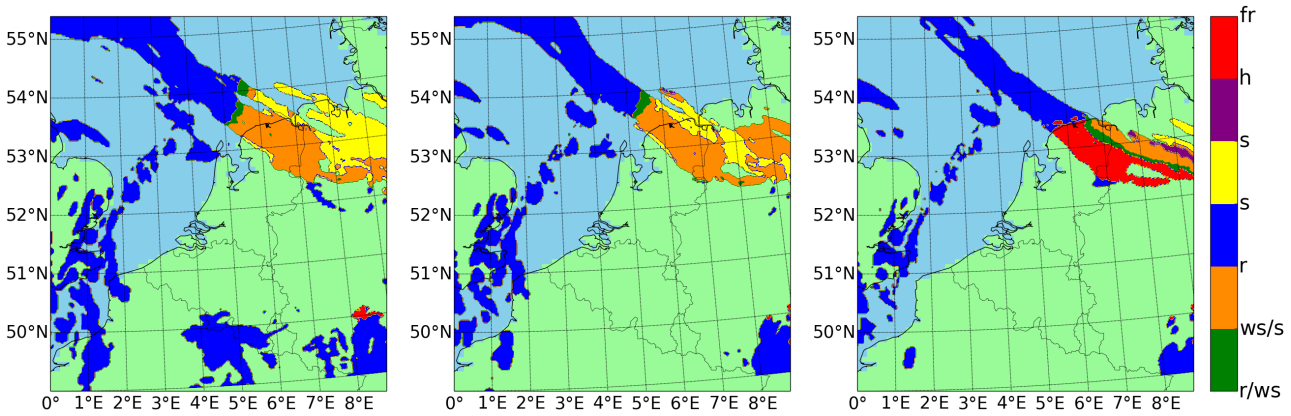

Figure 3: Precipitation type for January 5^{th} 2016 5 UTC for Harmonie36h1.2 (left) Harmonie38h1.2 (middle) and Harmonie41 (right). The meaning of the colors can be found in Table 1.

Table 1: Thresholds used to determine the type of precipitation, with r=rain, g=graupel, s=snow, T_s=surface temperature.

Type precipitation	Mix between r, g and s	Rain	Snow	graupel	Color
Rain/wet snow	r+g >50 %	-	-	-	Green
Wet snow/snow	s+g >50 %	-	-	-	Orange
Rain	-	>90 %	-	-	Blue
Snow	-	-	>90 %	-	Yellow
Snow	s+g+ r>90 %	-	>50 %	-	Yellow
Hail/ ice rain	-	-	-	>90 %	Purple
Freezing rain	r >90 % and T_s <0 °C	-	-	-	Red

As can be observed in Figure 3, Harmonie36h1.2 and Harmonie38h1.2 do not predict freezing rain (yellow and orange colors), while Harmonie41 captures this event (red color). The thresholds to determine which precipitation type is falling is shown in table 1. When the vertical profiles in Eelde (53.07N, 6.35E) of Harmonie38h1.2 and Harmonie41 are compared (see Figure 4) some clear improvements are found:

The amount of snow is increased at the expense of graupel (880 hPa).

The cloud ice in the lower atmosphere is removed (985 hPa).

Specific cloud water is increased and shows a smoother transition (900 hPa).

The melting of graupel, and therefore the increase in rain is more smooth, it takes longer for the graupel to melt completely (910 hPa).

No refreezing to snow or graupel in the lowest part of the atmosphere is present (1000 hPa).

Accretion process is significantly less active, no snow or graupel are accreting in the lowest layer (1000 hPa).

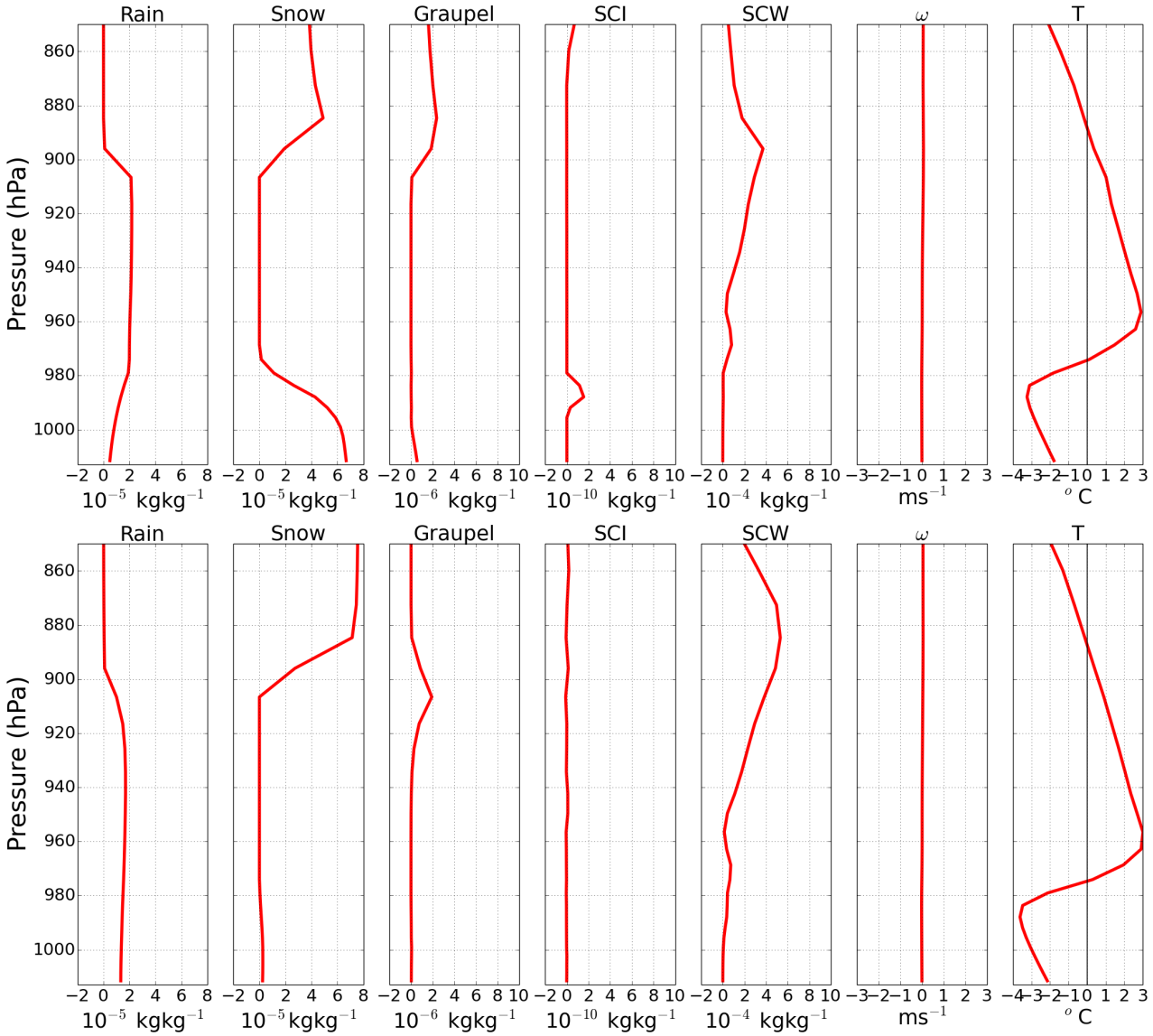

Figure 4: The vertical profiles for Eelde (53.07N, 6.35E) for January 5^{th} 2016, 5 UTC for Harmonie38h1.2 (top) and the proposed Harmonie41 (bottom).

These adjustments are also tested for various other cases in the Netherlands:

27 April 2016 Small showers with graupel, captured by Harmonie41.

24 January 2015 Snow and freezing rain event, captured by Harmonie41.

20 January 2013 Winter convection and freezing rain event, captured by Harmonie41.

10 September 2011 Summer convection. The effects on the adjustments are small.

17 December 2010 Winter convection, snow area more continuous in Harmonie41.

For the winter cases this leads to an improvement of the weather forecast and a more specific precipitation type forecast closer to what was observed, while for the summer case no negative effects are found. Something to mentioned is the more structured patterns of summer convection and a tendency for a decrease of high wind speeds in Harmonie 38h1.2 and therefore in also Harmonie41 compared to Harmonie36h1.2. Further testing should make clear the decrease in high wind speeds does not lead to an underestimation of the wind gusts.

6 Conclusions and recommendations

The adjustments mentioned in Section 3 are proposed to include in a new version of HARMONIE for a more specific prediction of precipitation type and therefore a more reliable weather forecast. Freezing rain events in the Netherlands are captured by Harmonie41, with a threshold of 90% supercooled rain in combination with a surface temperature below freezing point. This means that the current threshold of the presence of 5% supercooled rain can be increased to 90%, which indicates a better representation of what occurs in reality and may lead to a more reliable weather forecast in these situations. The melting rate of graupel is lowered, which could decrease problems of too little solid precipitation at the surface, especially in mountain regions. These adjustments are proposed to be included, or at least to be the basis (or inspiration) for changes in new versions of Harmonie.

A more detailed report of these findings can be found in: *Improvement of microphysical processes in HARMONIE* by PNJ Bonekamp, MSc thesis *Meteorology, Physical Oceanography and Climate* at Utrecht University (IMAU), The Netherlands, 2016.

7 Acknowledgements

I would like to thank Sander Tijm for his supervion during the project and his view on this topic. Also thanks to Karl-Ivar Ivarsson who gave me the opportunity to test his adjustments, which helped a lot.

8 References

[MESO-NH] MeteoFrance, The Meso-NH Atmospheric Simulation system: Scientific Documentation. Part III: Physics, H6: Microphysical scheme for Atmosheric ice, 105-137, 2009

[Ivarsson, 2014] Documentation of the OCND2 option in the ICE3 cloud- and stratiform condensation scheme in AROME, Karl-Ivar Ivarsson,2014.

[KNMI archive, 2016] *http://www.knmi.nl/nederland-nu/klimatologie*, Online; accessed 2016-01-05

2016 ALADIN Highlights in TURKEY

Alper GUSER, Unal TOKA, Yelis CENGIZ, Duygu AKTAS
(Turkish State Met. Service)

1. Introduction

New HPC tender finished in December and SGI ICE XA (4032 core, E5-2690 v4, 2.60GHz) will be installed in February 2017. By the way, TSMS planned main changes in operational suite such as domain enlargement, resolution upgrade, 3dvar DA with ALARO and operational AROME (4 times/day with 2.5km resolution) in 2017. Also ALARO-1 cy40t1 is operational since June 2016 in TSMS. Studies on test DA system and developments on interactive applications related with ALADIN System are still continued during the 2016.

2. Continuing Application Development related with ALADIN System

2.1 The Highway Forecast System

The Highway Forecast System (HFS) is developed for planning highway travels, having a safe journey and transports throughout the Turkish cities. User can generates the weather forecast and conditions such as temperature, humidity, wind speed and directions, precipitation area by defining the travel points (cities), departure date, time and durations.

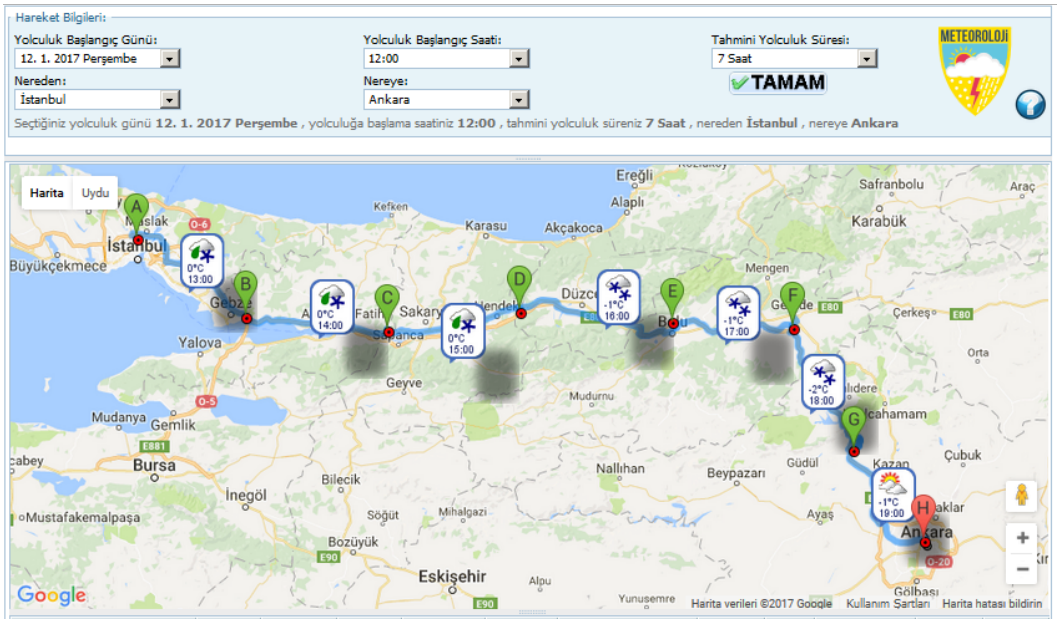

Hareket Aralığı	Gun	Saat	Sıcaklık	Yol(km)	Hava Durumu	Hava Durumu Acıklama	Bulut Kapalılık	Bağıl Nem	Ruzgar Yönü	Ruzgar Hızı	Yağışlı Alan
Kağıthane - Gebze arası	Perşembe	12:00-13:00	0 °C	0-66.km		Karla Karışık Yağmur Sa	% 99	% 98	G.Batı/K.Batı	5 Knot	% 100
Gebze - Kocaeli arası	Perşembe	13:00-14:00	0 °C	66-132.km		Karla Karışık Yağmur Sa	% 65	% 96	K.Batı/G.Batı	3 Knot	% 100
Kocaeli - Hendek arası	Perşembe	14:00-15:00	0 °C	132-196.km		Karla Karışık Yağmur Sa	% 79	% 96	K.Doğu/K.Batı	3 Knot	% 100
Hendek - Bolu arası	Perşembe	15:00-16:00	-1 °C	196-263.km		Kar Yağışı	% 88	% 94	G.Doğu/K.Batı	3 Knot	% 100
Bolu - Gerede arası	Perşembe	16:00-17:00	-1 °C	263-325.km		Kar Yağışı	% 88	% 93	K.Batı/G.Batı	5 Knot	% 100
Gerede - Kızılcahamam arası	Perşembe	17:00-18:00	-2 °C	325-392.km		Kar Yağışı	% 82	% 89	G.Batı/K.Batı	6 Knot	% 96
Kızılcahamam - Altındağ arası	Perşembe	18:00-19:00	-1 °C	392-454.km		Parçalı Bulutlu	% 82	% 87	G.Batı/K.Batı	9 Knot	% 21

Figure 1:The Highway Forecast System (http://khts.mgm.gov.tr/YOL/3.0/khts_v3.php)

Numerical Weather Predictions are the main component of HFS. It is constructed by processing and interpreting of ALARO model outputs. Model outputs are update 4 times in a day.

Besides weather forecast, for instance in the precipitation column how much area of the road will be affected by the precipitation takes place as percentage. The type of the precipitation was determined by giving precedence to the ones which may affect the travels. When it is predicted that there are more than one precipitation type, the type of the precipitation on the road is indicated considering the most harmful precipitation primarily freezing rain or snow.

2.2 Interactive SkewT-LogP Diagram Application

Interactive SkewT–LogP Project, which enables the user to plot the Temp diagram of any given point when clicked on google based map. The diagrams are produced based on WRF and ALARO models. In the project, open source codes and softwares were used and code improvements were done by Turkish Aladiners.

User-friendly SkewT diagrams are produced for the given point instead of generating this diagram for every point in the map and user can make alteration on the diagram. In this context, the computer resources are used more efficiently. Therefore, it was a necessity to switch to interactive applications.

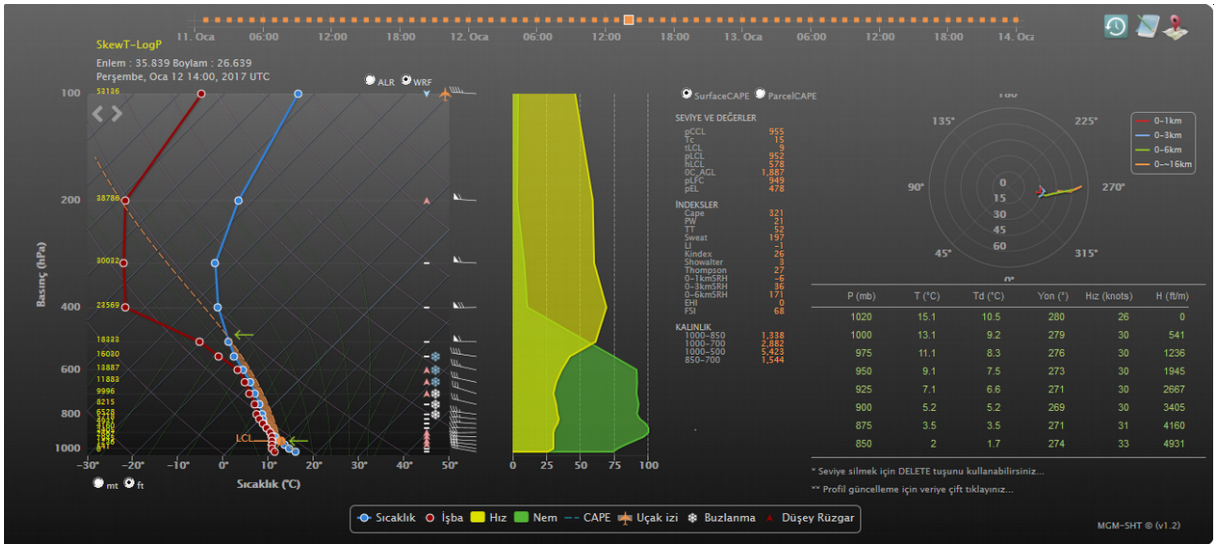

Figure 2:SkewT-LogP Diagram and airport/point selection (http://212.175.180.126/skewt/index.html)

This application generates the following parameters: Temperature, Dew-Point, Velocity, Humidity, CAPE, Contrail, Icing, Vertical Wind, Instability Indices and Thickness. The parameters such as, icing, contrail and vertical wind are calculated to be used for aviation purpose. “Surface CAPE” and “Parcel CAPE” identify the CAPE values calculated by different calculation methods.

For each pressure level, temperature, dew-point temperature, wind speed and direction and the height of the pressure level are shown in a table. The application allows the user to make changes in values and atmospheric profile. After the modifications, all instability indices are recalculated.

In addition, the application has hodograph feature. Wind shear is plotted in 0-1, 0-3, 0-6, 0-16 km height ranges on the hodograph.

Now the source code of this application is shared with Poland Met.Serv.(IMGV).

Sea surface temperature in operational forecast (example of Adriatic Sea)

Martina Tudor, Stjepan Ivatek-Šahdan, Antonio Stanešić

1 Introduction

The operational LAM forecast uses the sea surface temperature (SST) provided in the coupling files. There are two sets of coupling files available operationally from the global models ARPEGE and IFS. Initial values of the SST field do not change during the forecast (72 hours) but do change from one analysis to the next one. SST from the coupling files was compared to in situ measurements available on the Adriatic and parts of western Mediterranean (using measurements from Croatia and Italy). Several alternatives for SST were tested on Croatian domains in 8 and 2 km resolutions (the work was applied on the 4km domain but the results are not presented here):

- OSTIA (Operational Sea Surface Temperature and Sea Ice Analysis [UK Met Office(2005)])
- MUR (The Multiscale Ultrahigh Resolution, [JPL MUR MEaSUREs Project(2015)]) analysis
- ROMS (Regional Ocean Modelling System, [Shchepetkin and McWilliams(2009)]) model output computed daily at Rudjer Bošković institute [Janeković et al.(2014)].

Adriatic Sea is small, but numerous islands along the eastern side and large SST variability make it complicated. This is further enhanced by warm Eastern Adriatic Current (EAC arriving from south through Otranto) and cold Western Adriatic Current (WAC) that forms a narrow stray of cold SST along Italian coastline. To make things more interesting, oceanographers use different naming convention, so the current going towards nortwest is a northwest current and towards southeast is a southeast current (the opposite than meteorological convention for wind). Furthermore, local phenomena, such as cold and dry northeast wind (from notheast, meteorological convention) can cool the sea surface (and the whole water column) by more than 5K in few days.

2 Analysis of available SSTs

The SST from the coupling files was compared to measurements done in situ on a number of stations in Croatia and Italy (see Figure 1 for locations). It was found that there was a strange warm bias on several locations in the data from IFS during winter months. This got fixed during 2013. Then, during winter months, SST is far too warm along the western Adriatic shore and the error can exceed 10K in cold winters, such as in February 2012 (Figure 2).

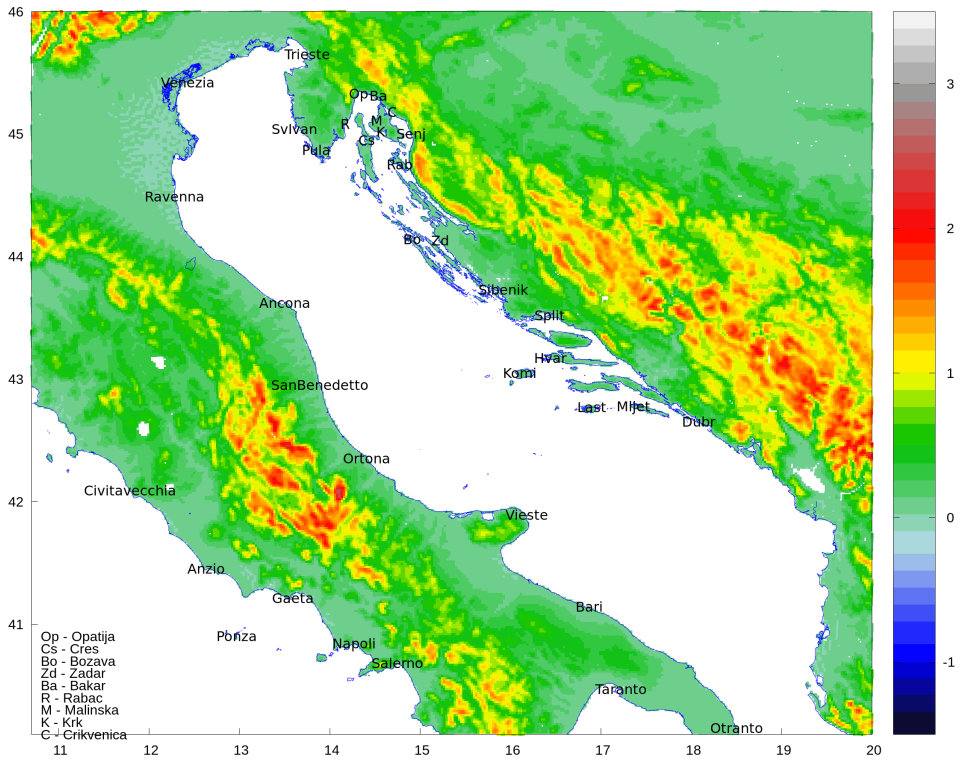

Figure 1: Terrain height (km) in the model domain in 2 km resolution. The locations of stations are marked on the map. There are operational SST measurements for a number of stations in Italy from ISPRA web page www.mareografico.it. Sea below Velebit mountain (north of Zadar, southeast of Senj) is the Velebit channel. Western Adriatic Current (WAC) flows along the west Adriatic shore.

3 Experiments with different SSTs

3.1 SST shift

In the first set of experiments, SST effects on forecast precipitation are analyzed by modifying the SST field in the initial file by shifting the SST field uniformly. For each model forecast, the operational SST field is modified by increasing or decreasing SST values by 2K and 5K. These values have been chosen on the basis of evaluation of model and analyzed SST against in situ data.

Increasing SST enhances precipitation and decreasing SST reduces the precipitation (Figure 3). The effect is not uniform, but it also affects precipitation above land, relatively far from the coastline.

3.2 SST from different sources

The initial SST fields used for the ALADIN operational forecast in 8km and 2km resolutions are taken from the initial file of the global operational forecast that is also used for forecast lateral boundary conditions. The ARPEGE operational SST analysis combines AVHRR satellite data and in situ measurements in the operational oceanographic model Mercator [Bahurel et al.(2004)]. However, in a case of operational failure there were some alternatives used. In situ SST reports by ships and buoys are combined with NCEP SST analysis or a

previous analysis (from 6 hours before) are combined [Météo France(2012)]. If this fails, Reynolds global cimatology at 1 degree resolution or ECMWF SST analysis [Lebeaupin et al.(2006)] can be used.

On the other hand, it is generally assumed that SST in the initila file of IFS is from OSTIA [UK Met Office(2005)] analysis.

OSTIA analysis is used from JPL (NASA) server using:

```
wget http://podaac-opendap.jpl.nasa.gov:80/opendap/allData/ghrsst/data/L4/
GLOB/UKMO/OSTIA/${YYYY}/${DOY}/${YYYYMMDD}-UKMO-L4HRfnd-GLOB-v01-fv02-OSTIA
.nc.bz2.nc4?time[0:1:0],lat[2500:1:2840],lon[3400:1:4200],
analysed_sst[0:1:0][2500:1:2840][3400:1:4200] -O ostia.nc4
```

MUR analysis is used from JPL (NASA) server using:

```
wget http://podaac-opendap.jpl.nasa.gov:80/opendap/allData/ghrsst/data/L4/
GLOB/JPL/MUR/${YYYY}/${DOY}/${YYYYMMDD}-JPL-L4UHfnd-GLOB-v01-fv04-MUR
.nc.bz2.nc4?time[0:1:0],lat[11377:1:12922],lon[15473:1:19110],
analysed_sst[0:1:0][11377:1:12922][15473:1:19110] -O mur.nc4
```

Replace YYYY, DOY and YYYYMMDD by numerical values for year, day of year and date and put it as a single line. Thise are examples how to get data zoomed for the Croatian domain in 8 km resolution. ROMS data for Adriatic are available from forecast run at Institute Ruđer Bošković [Janeković et al.(2014)].

```
ftp http://home.irb.hr:40080/Adria/ROMS_ARCHIVE/roms_his_arch_${YYYYMMDD}.nc
```

These data are in 2 km resolution on a native grid.

It is possible to insert this data using EPYGRAM (replace existing SST data by the data from analysis). However this worked for OSTIA and MUR data, but not for ROMS, because it is in old NetCDF format. This is why a small tool was written.

In the subsequent experiments, the surface temperature in the initial file was replaced by SST from the analysis or ocean model by using the data from the closest sea point available with a radius limiting the influence. For this a simple tool was written. The data are converted from the NetCDF format into an ascii file containing data as "lon lat value". Then this data is put into the initial "ICMSH" file using the simple tool. It can be compiled similarly as edf and a source of a working version is:

```
http://radar.dhz.hr/~tudor/sst/ssto.F90
```

It one of the versions tested. It requires a namelist where one defines MDIST as the maximum distance from where the neares sea poin can be used. The rest are the same as for edf. The usage is

```
ssto namsst ${ICMSHFILE} temp${rYYYYMMDD}.dat
```

where namsst is the namelist file, ICMSHFILE is a initial "history" file and the last argument is the name of the ascii file with SST data.

3.3 Impact on forecast (example)

SST in Kvarner Bay and Velebit Channel (northeast Adriatic) is too warm in the coupling files from both IFS and ARPEGE. However it is too warm in the SST analyses from OSTIA and MUR. Only the ROMS ocean model reproduces the cooling of the sea surface there during the bura epsodes (Figure 4).

The data from OSTIA analysis is available for Kvarner bay, but not the Velebit Channel (southeast of Senj) so there is an issue which data to use there. Simple algorythm of using the SST from the closest sea point puts data from Zadar region (warm SST from south) into the southern portion of the Velebit channel. The same procedure can also distort the data on lakes that are close to the coastline (for example lake Skadar in the southeast, on the border between Montenegro and Albania). MUR analysis is in 1km resolution and contains data over the Velebit channel. However, there is also SST data over many islands that should be resolved in that resolution. Since the SST analyses here are based on satellite data, it is reasonable to question the quality of the data due to pollution from the numerous islands along eastern Adriatic coast. Finally, ROMS model data yield much colder Velebit channel than the MUR analysis.

SST in the coupling files is warmer than OSTIA analysis over most of the domain (Figure 5). The resulting precipitation forecast shifts the precipitation northwest (downstream in this case, Figure 6). One should keep in mind that these experiments were performed using the same initial data for all the model variables, except that SST was modified. This means that the temperature in the lowest portion of the atmosphere adapted to new surface conditions above the sea. The atmospheric contitions above the sea (particularly the temperature and the moisture content) were the consequence of original (too warm) SST.

It was more challenging to put the SST data into the initial file for the 2 km non-hydrostatic run. The reason is rather simple - it resolves narrow bays and passages and a number of big islands. Another challenge was the fact that the land sea mask in the old climatology (and other fields describing topography and percentage of water in a grid cell) quite diverged from reality, with false peninsulas along Italian coastline and the islands totally messed up (some features obvious in Figures 7 and 8).

OSTIA cools the SST in the Kvarner Bay and northern portion of the Velebit Channel. The souther portion of the Velebit Channel is still warm. Using SST from ROMS produces much colder SST in the southern portion of the Velebit Channel and makes it colder than the surrounding sea surfaces (Figure 8 left). Since bura wind is very strong there, this cooling is not unrealistic. But the ocean model in 2 km resolution contains few points along the width of the narrow channel so the ocean circulation does not develop as freely as in nature. There is no data measured in situ in that area during extended time periods to validate the model.

The operational forecast in 2km resolution often produced bogus rainfall over Velebit mountain (Figure 9 left). A blob of weak to moderate rainfall woud be there (in 24 hourly accumulated precipitation) for days and sometimes weeks. First of all, it was a challenge to prove if this blob of rainfall was realistic or not. There are no stations there! The only mountain station (Zavizan) is too far north. Radars from Croatia and Slovenia are too far. The mountain is within the range, but on the edge, and it is a mountain. And the radar are inland, and the precipitation is on the coastal side. Using satellite data for cloudiness [Acker and Leptoukh(2007)] and TRMM [Huffman et al.(2007)] precipitation estimate from satellite data finally proved that in many cases, there were probably no precipitation over southern Velebit while the 2km resolution forecast produced it. Since forecasters mostly did not know how to use this high resolution forecast, this persistent precipitation blob was a perfect excuse not to trust the forecast at all. Using more realistic SST from OSTIA analysis and ROMS ocean model removed this precipitation (see Figure 9 right).

3.4 Impact on surface fluxes

Warmer sea means warmer surface and less stable atmospheric layer above. The turbulent fluxes depend on atmospheric stability. Less stable atmosphere allows for stronger fluxes. With too warm SST, the fluxes of heat (Figure 10) and momentum (Figure 11) were too strong. Using more realistic (and in this case colder) SST improved the model fluxes (that were too strong to begin with).

4 Conclusions

SST fields obtained from global meteorological models can have large errors. The error over Adriatc can exceed 10K when compared to measurements. Global SST anayses, even in very high resolution, do not work well in areas where many islands can obstruct the quality of satellite data. The ROMS ocean model provided better data, especially in cases with strong changes in SST. Using improved SST benefited the forecast since the bogus rainfall was removed. Turbulent fluxes over too warm sea surface are exaggerated.

5 References

Acker, J.G. and Leptoukh, G.: Online Analysis Enhances Use of NASA Earth Science Data, *Eos, Trans. AGU,* Vol. 88, No. 2, 2007.

Bahurel, P, Dombrowsky, E., Lellouche, J.M. and the Mercator Project Team: Mercator ocean monitoring and forecasting system, near-real time assimilation of satellite and in situ data in different operational ocean models, paper presented at 36th Colloquim on Ocean Dynamics, Geohydrodyn. and Environ. Res. Group, Univ of Liége, Liége, Belgium, 2004.

Huffman, G.J., Bolvin, D.T., Nelkin, E.J., Wolff, D.B., Adler, R.F., Gu, G., Hong, Y., Bowman, K.P., and Stocker, E.F.: The TRMM Multisatellite Precipitation Analysis (TMPA): Quasi-Global, Multiyear, Combined-Sensor Precipitation Estimates at Fine Scales. J. Hydrometeorol., 8, 38–55, 2007.

Janeković, I., Mihanović, H., Vilibić, I., and Tudor, M.: Extreme cooling and dense water formation estimates in open and coastal regions of the Adriatic Sea during the winter of 2012, J. Geophys. Res. Oceans, 119, 3200–3218, doi:10.1002/2014JC009865, 2014.

JPL MUR MEaSUREs Project. 2015. GHRSST Level 4 MUR Global Foundation Sea Surface Temperature Analysis (v4.1). Ver. 4.1. PO.DAAC, CA, USA. Dataset accessed [2016-03-01] at http://dx.doi.org/10.5067/GHGMR-4FJ04, 2015.

Lebeaupin, C., Ducrocq, V., and Giordani, H.: Sensitivity of torrential rain events to the sea surface temperature based on high-resolution numerical forecasts, J. Geophys. Res., 111, D12110, doi:10.1029/2005JD006541, 2006.

Météo France: Joint WMO technical progress report on the global data processing and forecasting system and numerical weather prediction research activities for 2012. 22 pp. available at www.wmo.int, 2012.

Shchepetkin, A.F., and McWilliams, J.C.: Correction and commentary on "Ocean forecasting in terrain-following coordinates: Formuation and skill assessment of the regional ocean modelling system" by Haidvogel et al., J. Comput. Phys., 227, 3565-3624, J. Comput. Phys., 228, 8985-9000, 2009.

UK Met Office: GHRSST Level 4 OSTIA Global Foundation Sea Surface Temperature Analysis. Ver. 1.0. PO.DAAC, CA, USA. Dataset accessed [2016-04-28] at http://dx.doi.org/10.5067/GHOST-4FK01, 2005.

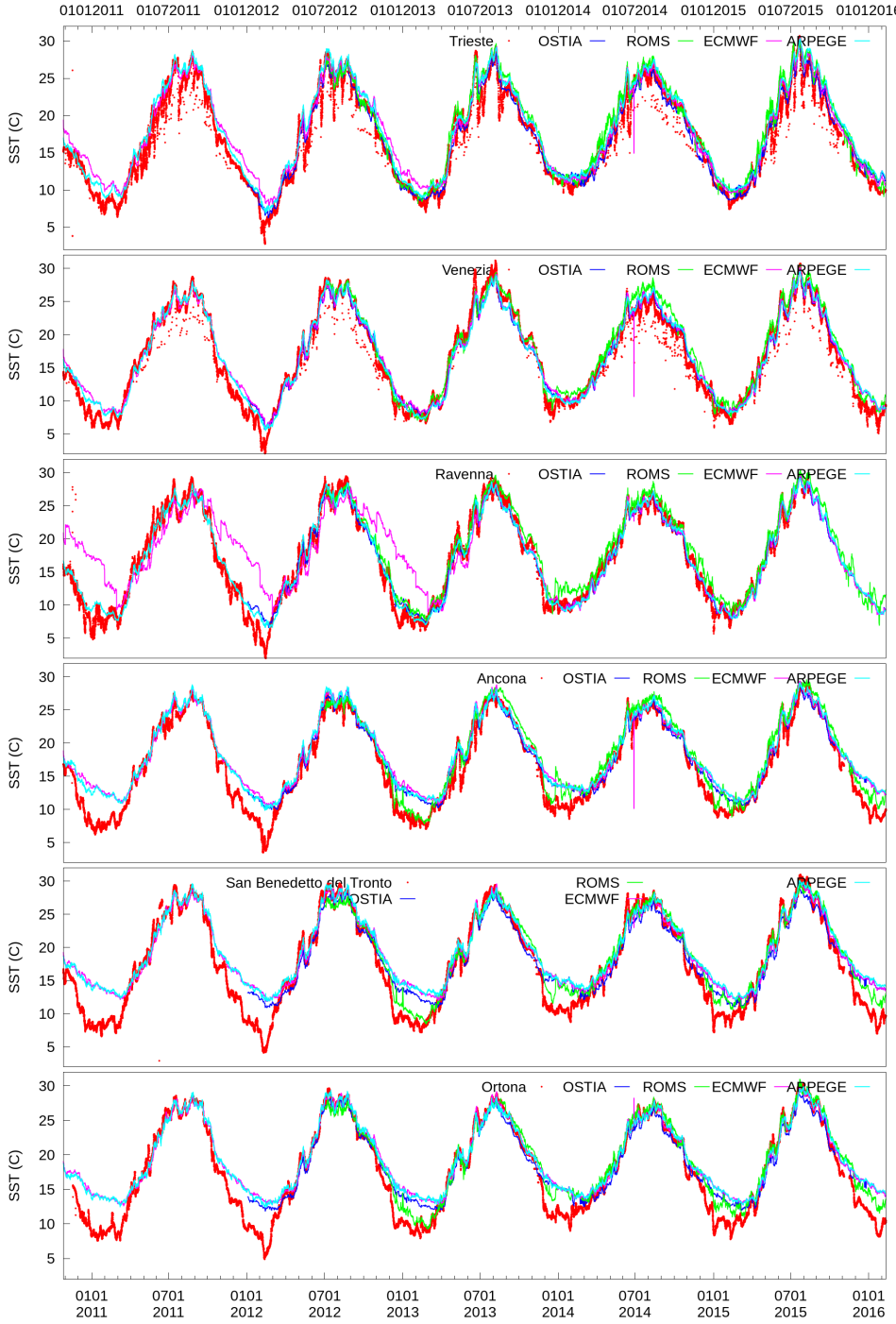

Figure 2: SST from the closest sea point from the initial coupling files of ARPEGE (cyan), IFS (pink), when interpolated to the model grid from the closest sea point of OSTIA (blue) and ROMS (green) and measured in-situ (red) for several stations along the western Adriatic coastline during the period from 27th October 2010 to 6 February 2016.

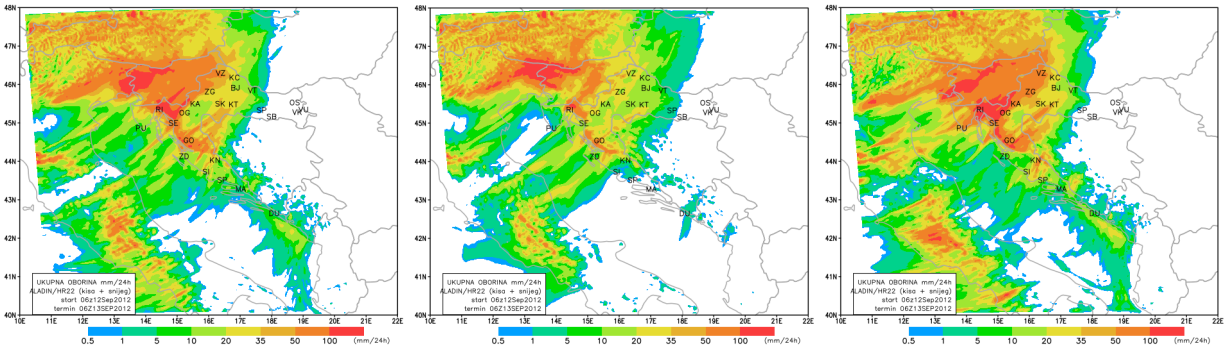

Figure 3: Accumulated 24 hourly precipitation until 06 UTC 13 September 2012 for reference run (left), an experiment when SST is reduced by 5K (centre) and increased by 5K (right) for 2km resolution forecast initialized at 06 UTC 12 September 2012.

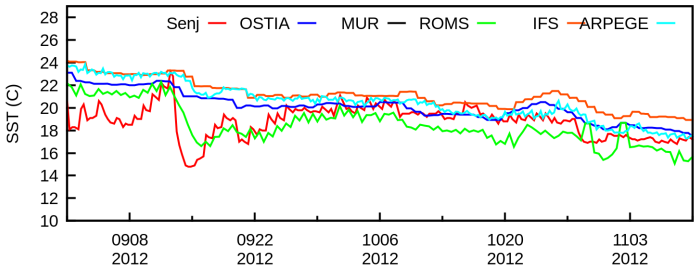

Figure 4: SST from the closest sea point from the initial coupling files of ARPEGE (cyan), IFS (orange), when interpolated to the model grid from the closest sea point of OSTIA (blue), MUR (black), ROMS (green) and measured in-situ (red) for Senj for the period from 5 September to 5 November 2012.

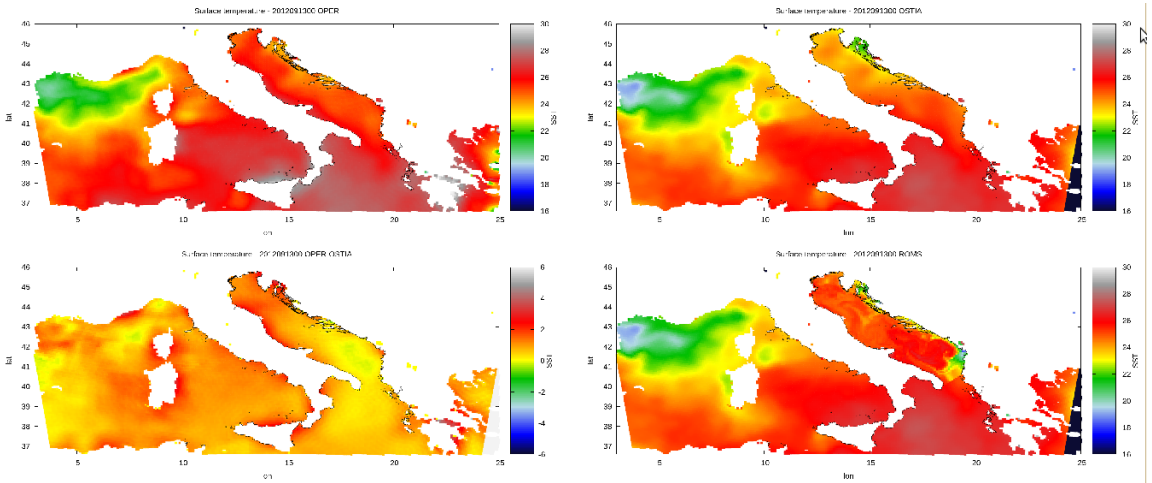

Figure 5: SST in the operational model run in 8km resolution using SST from ECMWF (top left), when OSTIA analysis was inserted (top right), the difference between SST in the operational run and OSTIA (bottom left) and SST when ROMS data were introduced (bottom right).

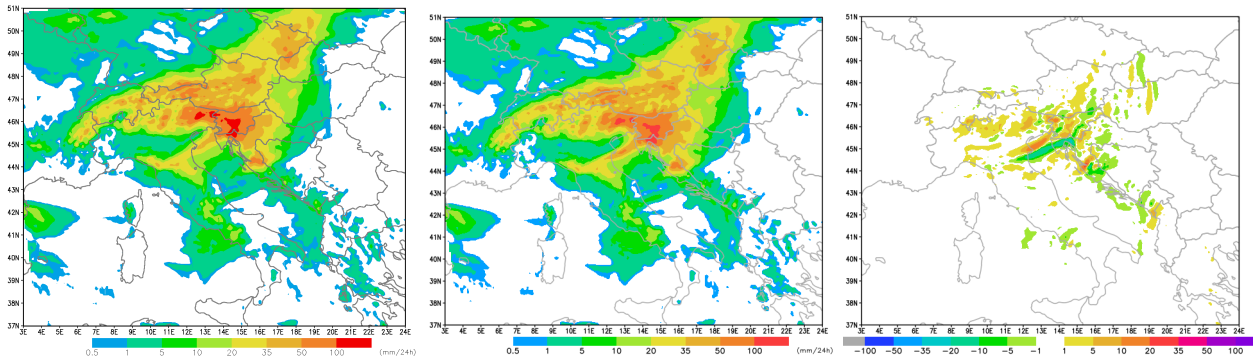

Figure 6: Accumulated 24 hourly rainfall from the reference run in 8km resolution, using SST obtained in the coupling files of the operational IFS (left), from the run using ROMS model SST and OSTIA analysis (centre) and their difference (right).

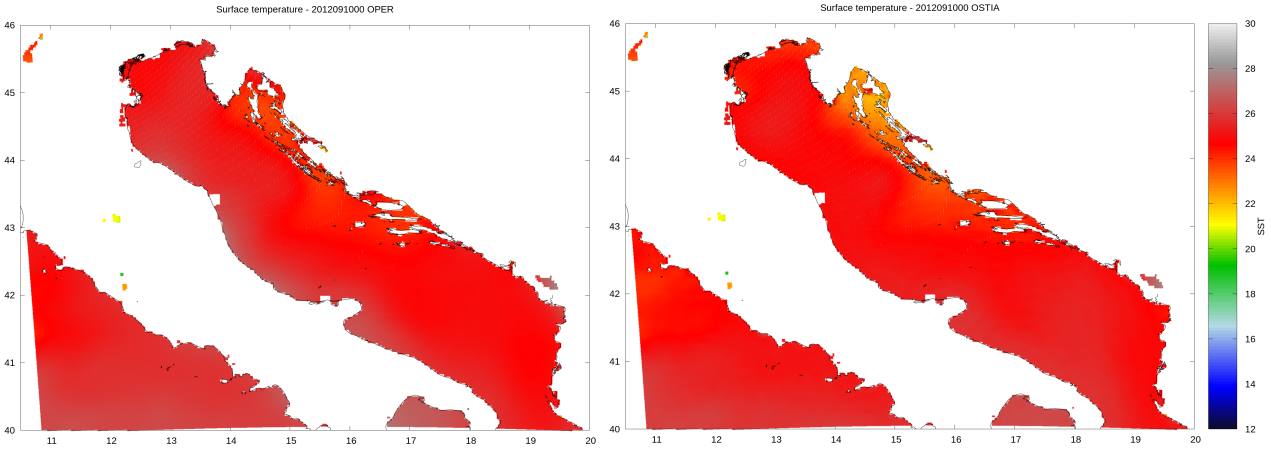

Figure 7: SST from the operational run in 2 km resolution using SST from ECMWF (left) and when OSTIA was inserted (right). The SST over southern portion of the Velebit channel is unchanged.

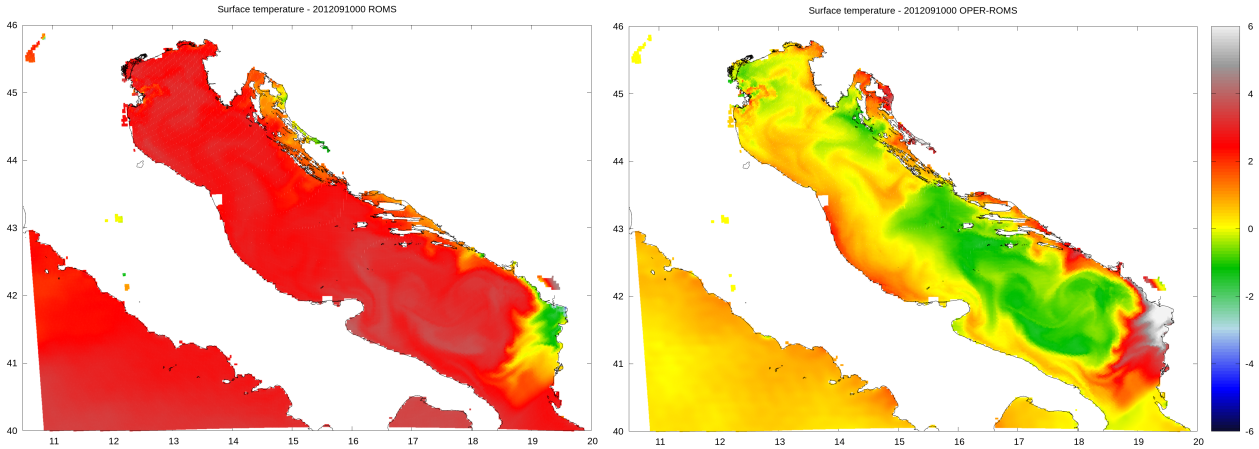

Figure 8: SST from the operational run in 2 km resolution when SST from ROMS was used over Adriatic (left) and the difference to the operational SST (right). The SST in the Velebit channel is considerably colder in ROMS.

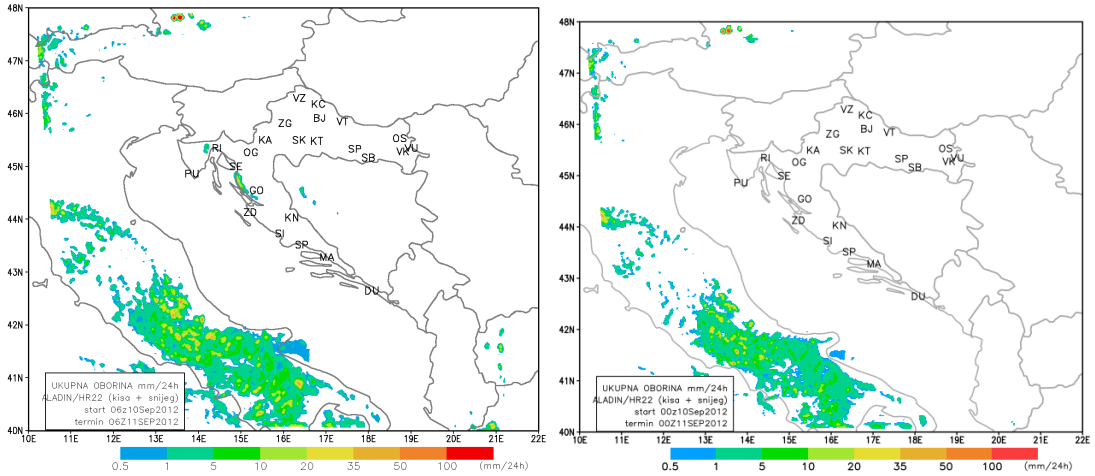

Figure 9: Accumulated 24 hourly rainfall from the reference run in 2km resolution, using SST obtained in the coupling files of the operational IFS (left) and from the run using ROMS model SST and OSTIA analysis (right).

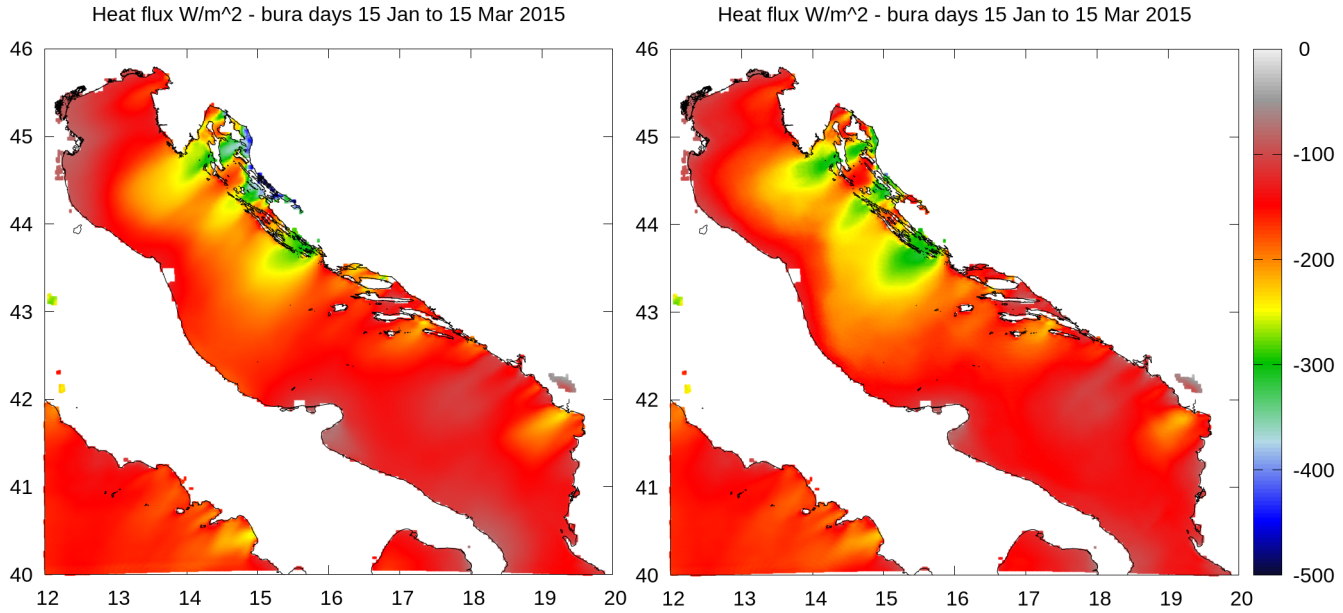

Figure 10: Accumulated heat fluxes from the reference run in 2km resolution, using SST obtained in the coupling files of the operational IFS (left) and from the run using ROMS model SST and OSTIA analysis (right).

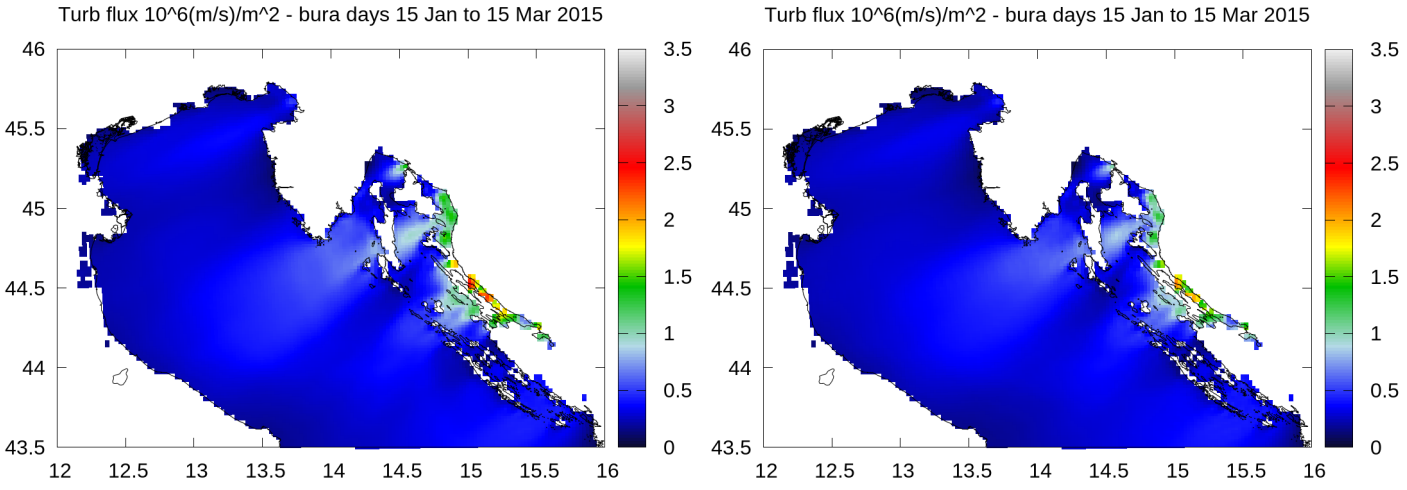

Figure 11: Accumulated turbulent fluxes from the reference run in 2km resolution, using SST obtained in the coupling files of the operational IFS (left) and from the run using ROMS model SST and OSTIA analysis (right).

Application of ENO technique to semi-Lagrangian interpolations

Alexandra Crăciun, Petra Smolíková

1 Introduction

Weighted essentially non-oscillatory scheme was first proposed by Liu, Osher and Chan in [4] and further developped by many authors, see for example [1], [2], [3]. WENO schemes are based on ENO technique with the key idea of finding the "smoothest" stencil among several candidates to interpolate to a high order accuracy and to avoid at the same time spurious oscillations near discontinuities or sharp gradients in the interpolated field. In case of WENO method instead of choosing the "smoothest" stencil possible, the weighted sum of values interpolated on several stencils is used with weights based again on smoothness evaluation. Moreover, the weights can be chosen in such a way that in smooth regions it approaches certain optimal weights to achieve a higher order of accuracy, while in regions near discontinuities, the stencils which contain discontinuities are assigned a nearly zero weight. ENO schemes are not cost effective on vector supercomputers because the stencilchoosing step involves heavy usage of logical statements, which perform poorly on such machines. On the other hand, WENO scheme completely removes the logical statements that appear in the ENO stencil choosing step. As the result, WENO scheme appear to be much faster than ENO scheme on vector machines.

After an extension of the whole interpolation stencil from 4 to 6 grid points following the preparatory work for higher order interpolations being done by George Mozdzynski from ECMWF under the switch NSTENCIL-WIDE = 3, third order ENO technique was implemented in the code in the last year, see [5]. As the next step, the third order WENO interpolation technique was implemented based on previous work and compared with the classical cubic Lagrange interpolation and cubic ENO scheme. The implementation is described shortly in Section 2, several tests are presented in Section 3 and some conclusions are summarized in Section 4.

2 Implementation

To construct a third order WENO interpolation of a field f to the point x, we need to know f in a set $S = \{x_{j-2}, ..., x_{j+3}\}$ of six points, with the subsets $S_k = \{x_{j-3+k}, ..., x_{j+k}\}$, $k \in \{1, 2, 3\}$. Having the

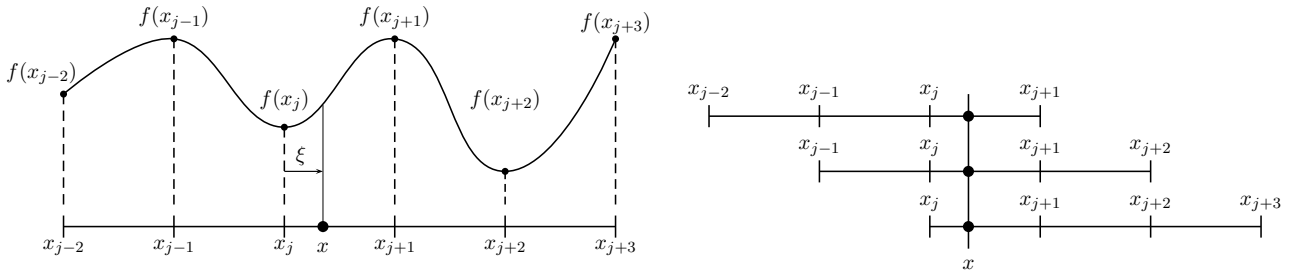

interpolation point x in the central interval $[x_j, x_{j+1}]$ of the big stencil S, the interpolation value is built as a linear combination of the interpolation polynomials on the three stencils S_k, through the following form:

$$P(x) = \sum_{k=1}^{3} \omega_k(x) P_k(x), \tag{1}$$

where the weights are built as follows:

$$\omega_k(x) = \frac{\tilde{\omega}_k(x)}{\tilde{\omega}_1(x) + \tilde{\omega}_2(x) + \tilde{\omega}_3(x)},\ \tilde{\omega_k}(x) = \frac{C_k(x)}{(\beta_k(x) + \varepsilon)^p}. \tag{2}$$

This method should assign to each polynomial P_k a weight ω_k according to the smoothness of the function f on the corresponding sub-stencil S_k. In the above formula, the term β_k is considered to be a *smoothness indicator* and is used to measure the smoothness of the solution on each sub-stencil S_k. There are multiple ways of defining it. If all the stencils are equally smooth according to the definition used for the smoothness indicators β_k, we want to obtain the non-linear weights ω_k in a way that leads to the highest degree approximation for the interpolated function. We can achieve fifth degree for 6 point stencil. The smoother is the function on the stencil S_k, the lower is the value of β_k.

The success of this method depends largely on the definition of the smoothness indicators β_k. One way of measuring the variation of the function is based on L2-norm of high-order variations of the reconstruction polynomials [3]:

$$\beta_k(x) = \sum_{l=1}^{3} \int_{x_j}^{x_{j+1}} (\Delta x)^{2l-1} (P_k^{(l)}(x))^2 dx \tag{3}$$

Similar definitions for β_k were also tested (the difference between them being the derivatives of P_k taken into account):

$$\beta_k(x) = \sum_{l=2}^{3} \int_{x_j}^{x_{j+1}} (\Delta x)^{2l-1} (P_k^{(l)}(x))^2 dx \tag{4}$$

$$\beta_k(x) = \int_{x_j}^{x_{j+1}} (\Delta x)^{3} (P_k^{(2)}(x))^2 dx \tag{5}$$

$$\beta_k(x) = \int_{x_j}^{x_{j+1}} (\Delta x)^{5} (P_k^{(3)}(x))^2 dx \tag{6}$$

Another method ([2],[4]) of estimating the smoothness of the function f on stencil S_k involves undivided differences:

$$\beta_k(x) = \sum_{l=1}^{3} \sum_{i=1}^{4-l} \frac{(f[j+k+i-4, l])^2}{4-l}, \tag{7}$$

where the undivided difference $f[\cdot, \cdot]$ is defined recursively as follows:

$$f[j, 0] = f(x_j),\ f[j, l] = f[j+1, l-1] - f[j, l-1].$$

In the above formula, the "linear weights" C_k are polynomials of degree 2 and P_k are polynomials of degree 3 interpolating the function on each sub-stencil S_k (for our experiments, we used cubic Lagrange polynomials for defining P_k). Following the definition described in [1] and assuming regular grid both in horizontal and vertical (LREGETA=.T.), the "linear weights" have the form:

$$C_1(x) = \frac{1}{20}(2-\xi)(3-\xi),\ C_2(x) = \frac{1}{-10}(2+\xi)(\xi-3),\ C_3(x) = \frac{1}{20}(2+\xi)(1+\xi), \tag{8}$$

where variable $\xi = \dfrac{x - x_j}{\Delta x}$ and Δx is the mesh size.

In equation (2), parameter p in the denominator serves to increase/decrease the dissipation of the scheme (see [3]), and ε is a small positive number used to prevent division by zero. In the experiments, $\varepsilon = 10^{-6}$ and three values of p were tested, namely $p = 0.5$, $p = 2$ and $p = 3$.

The whole 3D interpolation stencil was enlarged from 32 grid points to 120 grid points according to Figure 1. Lateral interpolations remain linear as in the original solution, while the overall number of used ENO/WENO interpolations is 21 giving 63 cubic interpolations and 14 linear interpolations for each grid point.

In order to implement this scheme, new subroutine LAIWENO was designed for computation of weights ω_k. This routine is called from subroutine LAITRI_WENO, LAIDDI_WENO respectively. The choice for the smoothness indicators β_k can be made using variable KDER, which can get integer values from 1 to 5, depending on their definition, respectively, according to equations (3) - (7). Also, the value of p used in the definition of the weights (equation (2)) may be set, through the namelist parameter RALPHA. Variable PDIST is either PDLO (in longitude), PDLAT (in latitude) or PDVER (in vertical dimension) and represents the distance ξ in equation (8).

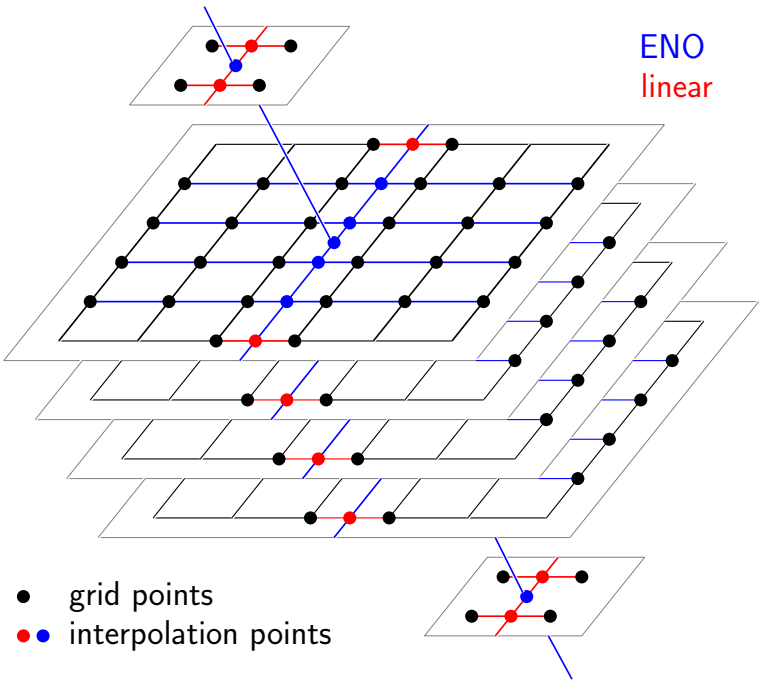

Figure 1: The interpolation stencil for one 3D interpolation.

The WENO scheme may be applied using the general switch LWENO, appearing in the module YOMENO and being declared in the namelist *namdyn*. Other necessary changes were made in subroutines LARCINB and LAITRE_GMV. The modification is available in Prague through the versioning system CVSTUC as the branch Arp_mma130_CY40t1_eno.

3 Testing

For the evaluation of WENO method, several tests were performed. Preliminary 1D tests performed by Ján Mašek and Petra Smolíková include linear advection of a rectangular pulse in a periodic domain and visualisation of the weights ω_k, $k \in \{1, 2, 3\}$ for each definition of the smoothness indicators (equations (3) - (7)), for several values of variable p, as well as the particular case of $\beta_k = 0$, corresponding to the Lagrange interpolation of the fifth order. Figure 2 shows results for several definitions of the smoothness indicator, compared with cubic Lagrange interpolator and ENO scheme. The over/undershoots present in cubic Lagrange solution almost disappear when ENO is used while they are completely eliminated with WENO scheme using definition (4) or (7). In Figure 3 one can see that WENO definitions lead to the expected behaviour: the stencil not containing the discontinuity has bigger value of the weight. It was noticed that even if all definitions give very similar weights after one time step, longer interpolation leads to different weight patterns.

Having this encouraging results we proceeded to 2D experiments - classical test (Andre Robert): warm bubble with sharp boundary rising up in the field of constant potential temperature (300K) without forced horizontal advection. The reference solution uses cubic Lagrange interpolator.

As expected, the results shown in Figures 4, 5 and 6 prove that when WENO scheme is applied, the solution becomes smoother than the one which uses cubic Lagrange interpolator. Smoothness indicators computed as in equation (3), (4) and (7) lead to quite similar solution and better accuracy than for the cases of β_k defined in equations (5) (not shown) and (6), when some of the vortices in the reference solution disappear.

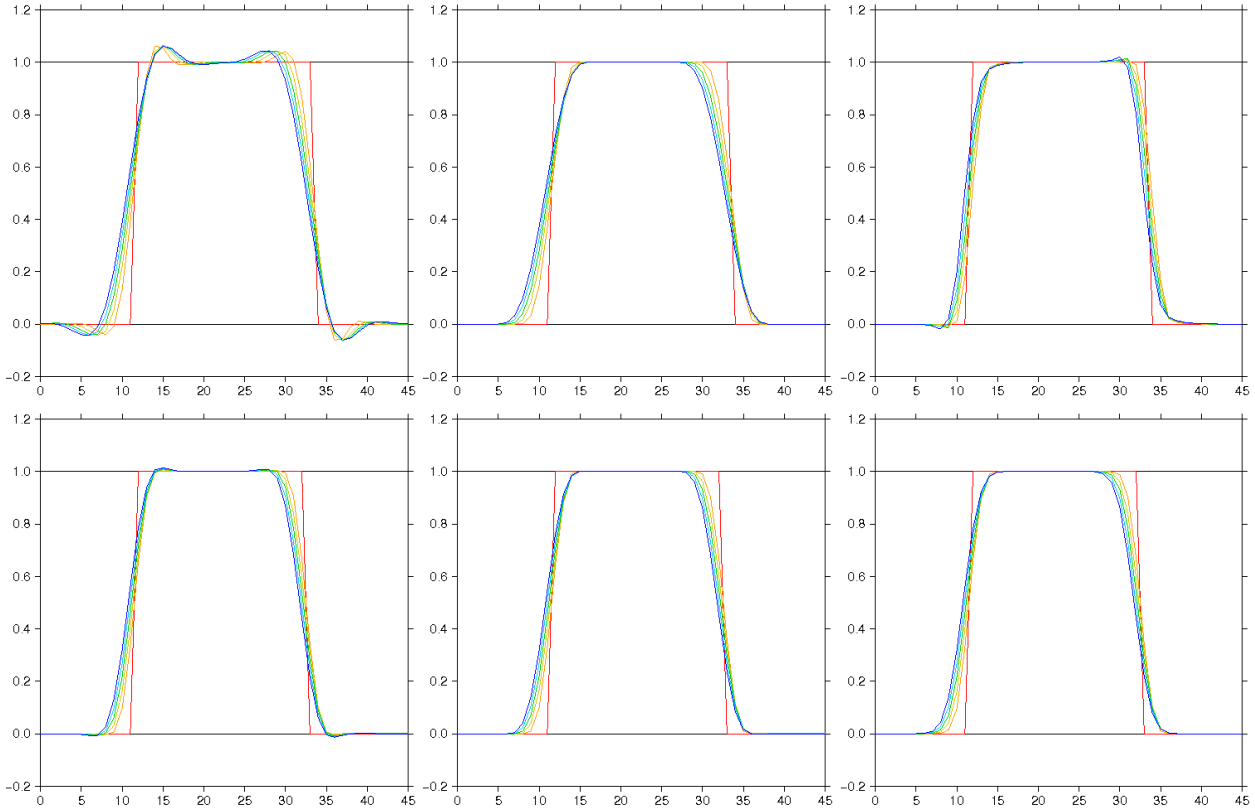

Figure 2: Linear advection of a rectangular pulse in a periodic domain with CFL=0.8, red - original function, orange - after 1 revolution, yellow - after 2 revolutions, green - after 3 revolutions, blue - after 4 revolutions, violet - after 5 revolutions. From left to right: first row - cubic Lagrange interpolator, cubic Lagrange with quasi-monotonic version, ENO scheme, second row - WENO scheme, p=0.5, different definitions for smoothness indicator β_k: equations (3), (4) and (7).

For the same definitions of smoothness indicators, setting value of p either 2 or 3 gives similar results; we show results only for $p = 2$. Moreover, both values of this parameter prove to be too smoothing in comparison with the solution provided by $p = 0.5$ (Figure 6), which seems to be the most similar to the reference solution. Besides, $p = 0.5$ and β_k computed according to definition (3) or (7) remain the best candidates also when the scheme is applied only in horizontal dimension (not shown).

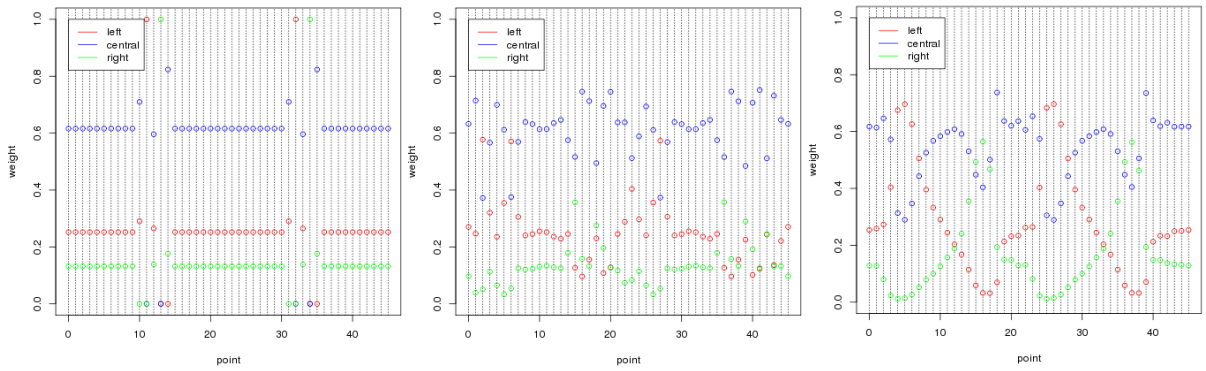

Figure 3: Linear advection of a rectangular pulse: WENO weights ω_1 (red), ω_2 (blue), ω_3 (green) for $p = 0.5$. Definition (3) for β_k after 1 time step on the left and after 280 time steps (5 revolutions) in the middle; β_k according to (7) and 280 steps performed on the right.

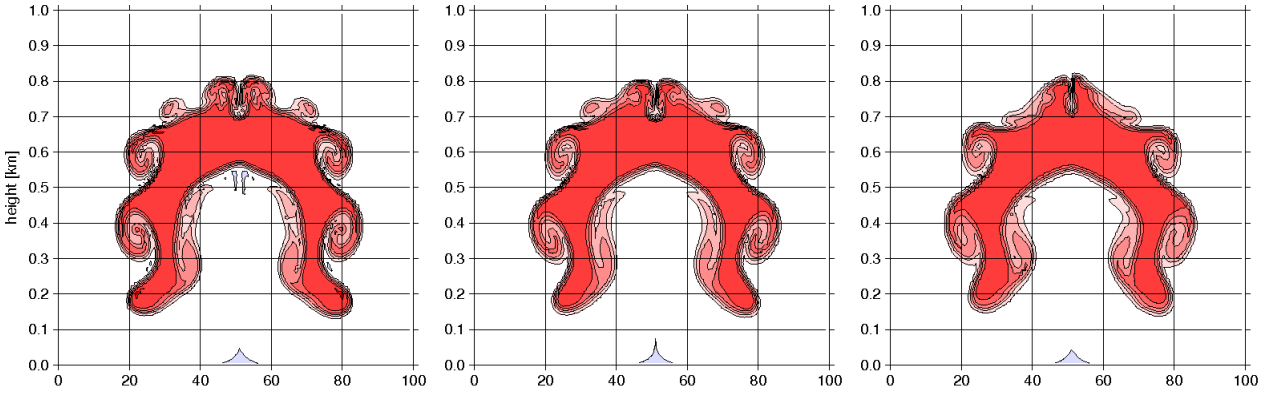

Figure 4: Sharp warm bubble: cubic Lagrange interpolator (left), quasi - monotonic version of cubic Lagrange (center) and ENO (right).

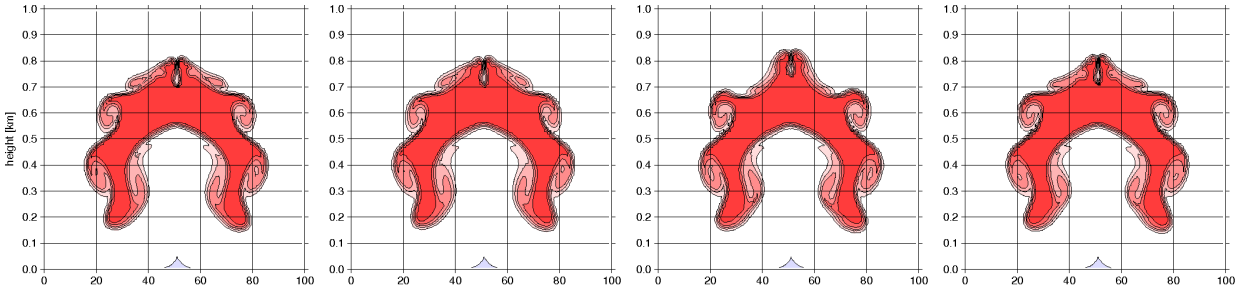

Figure 5: Sharp warm bubble: WENO scheme, p=2, different definitions for smoothness indicator β_k: equations (3),(4), (6) and (7), from left to right.

Another step in the evaluation was to visualize the way this scheme chooses the interpolation stencil. The plots below (Figure 7) show the stencils corresponding to the highest value of weights ω_k ($k = 1, 2, 3$), in horizontal dimension (latitude) in the second layer of the whole 3D-interpolation grid used (see [5] for details). Parameter IWLOC (in subroutine LAIWENO) is equal to 1 when the highest weight was obtained on the central stencil (white color), 2 for the right stencil (red color) and 3 for the left stencil (blue color).

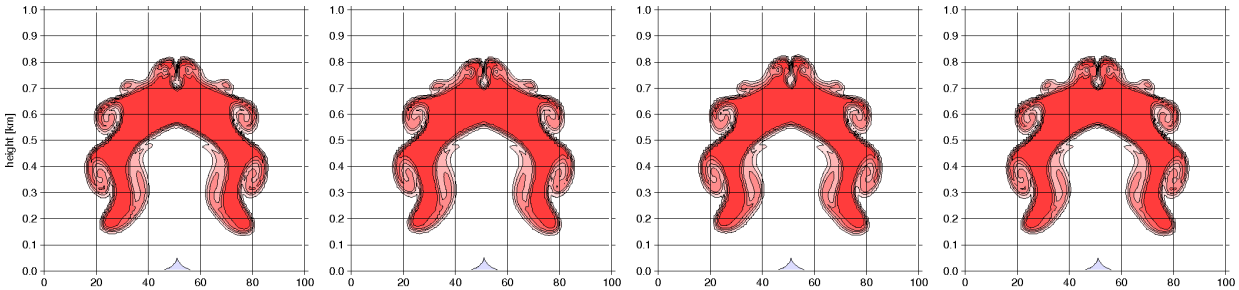

Figure 6: The same as Figure 5 but with p=0.5.

It can be seen that the WENO scheme behaves as expected near discontinuities, for example, the right stencil is chosen mostly on the left side of the bubble's vortices, the left one on the right side and the central stencil elsewhere. One can see that for WENO with $p = 2$ lateral stencils are used more often then for WENO with $p = 0.5$.

Furthermore, in order to assess where under/overshootings appear for distinct interpolators, parameter IPARQM was introduced in subroutine LAIWENO (and LAITRI, for the case of cubic Lagrange interpolator). This parameter is set to 1, when the interpolator overshoots, 2 when it undershoots and 0 when the interpolator stays within the bounds given by values of the function to be interpolated, and was obtained using a similar approach

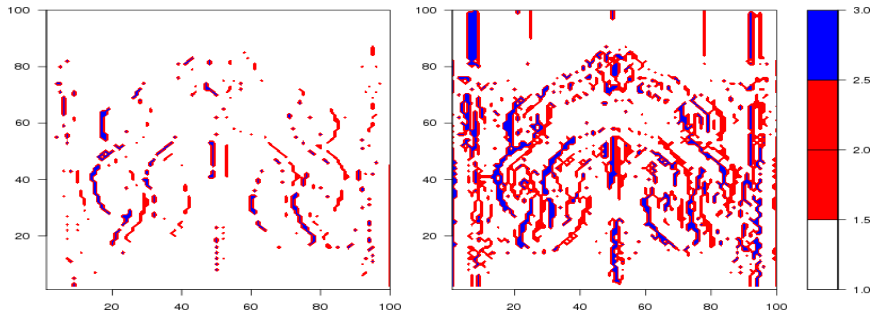

Figure 7: Stencil choice, WENO scheme after 80 steps, smoothness indicator β_k as in equation (3): p=0.5 (left) and p=2 (right).

as for the case of quasi-monotonous treatment of interpolations, found in subroutine LAITRI. With WENO scheme applied in both horizontal and vertical directions, IPARQM was plotted either for the vertical direction only (see Figure 8 - first row) or the horizontal direction only, for the second layer of the six used in the whole 3D-interpolation grid (see Figure 8 - second row).

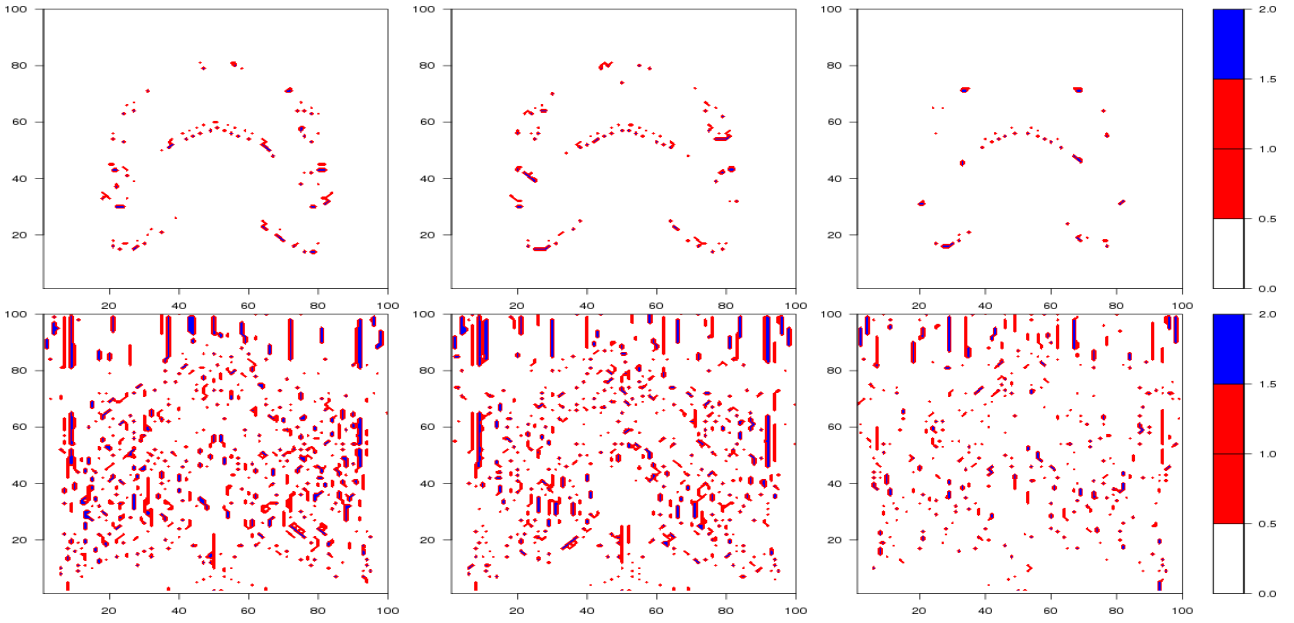

Figure 8: Over- and undershooting detection (in vertical - first row, in horizontal - second row), sharp warm bubble after 80 steps: cubic Lagrange interpolator (left), WENO scheme with β_k as in equation (3), p=0.5 (center) and p=2 (right).

It can be seen that both schemes lead to overshooths in specific areas of the bubble. Moreover, p=0.5 leads to comparable results to cubic Lagrange interpolation, for overshoots computed either in vertical or in horizontal direction.

In addition, the values of these under/overshootings were analysed. These were computed under variable ZOVER, in subroutine LAIWENO (and LAITRI, for the case of cubic Lagrange interpolator). Figure 9 shows the values of ZOVER computed in horizontal direction, for the second layer of the six used in the whole 3D-interpolation grid (with WENO scheme applied in both horizontal and vertical directions). It can be observed that the two values of p lead to different results after 80 steps. When p is set to 2, overshoots have smaller values (analogous result could be also observed in Figure 5). At the same time, the case with $p = 0.5$ presents slightly less overshoots when compared with cubic Lagrange interpolation.

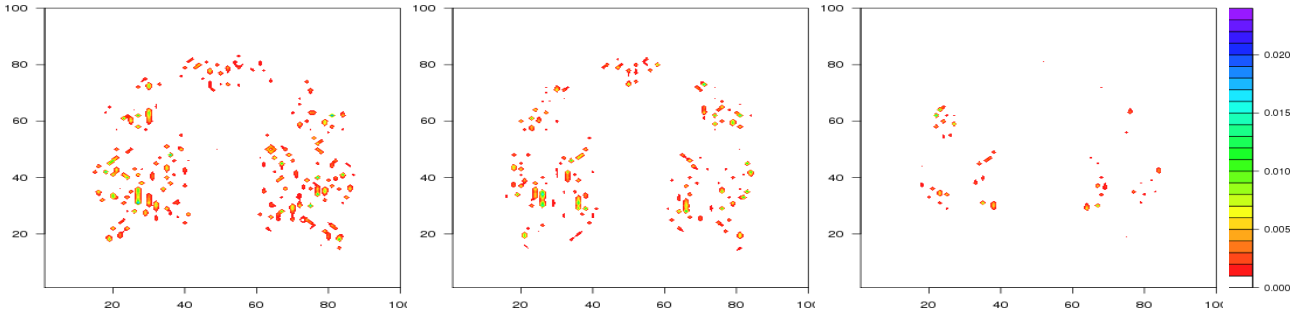

Figure 9: Sharp warm bubble after 80 steps: cubic Lagrange (left), WENO scheme with β_k as in equation (3), p=0.5 (center) and p=2 (right).

4 Conclusion

The WENO (Weighted essentially non-oscillatory) scheme was implemented to semi-Lagrangian interpolations of the model ALADIN with several possible definitions. Overall, the results show that the WENO scheme, for all definitions of smoothness indicators and values of parameter p that were tested, produces slightly smoother solution than cubic Lagrange interpolator. To conclude, the best choice for the smoothness indicators was the one in equation (3), with all derivatives (up to third order) of the reconstruction polynomials taken into consideration. The case with $p = 0.5$ showed increased accuracy than $p = 2$ and $p = 3$. Besides, the implementation gives fifth order Lagrange interpolation in case β_k are set to zero.

We may say that interpolations are subject of a trade off between accuracy and noise production near discontinuities. More smoothing schemes give less over/undershoots while more accurate results suffer from noise created near sharp gradients or discontinuities in the interpolated field.

It seems to us that slight improvement in the production of over/undershoots observed for the best behaving choice of the β_k and p parameters (β_k according to definition (3) and $p = 0.5$) does not compensate the increase in the computational cost of the new WENO scheme compared to the classical cubic Lagrange solution.

5 Acknowledgements

We are very grateful to Ján Mašek for the basic idea and first tests leading to the work presented here.

References

[1] Carlini E., Ferretti R. and Russo G., *A Weighted Essentially Nonoscillatory, Large Time-Step Scheme for Hamilton–Jacobi Equations*, SIAM J. Sci. Comput., 27(3), 1071-1091, 2005.

[2] Jiang G.-S., Shu C.-W., *Efficient Implementation of Weighted ENO Schemes*, Journal of Computational Physics, Volume 126, Issue 1, Pages 202-228, June 1996.

[3] Jung C.-Y., Nguyen T. B., *A New Adaptive Weighted Essentially Non-Oscillatory WENO-θ Scheme for Hyperbolic Conservation Laws*, arXiv:1504.00731, 2015.

[4] Liu X.-D., Osher S., Chan T., *Weighted Essentially Non-oscillatory schemes*, Journal of Computational Physics, Volume 115, Issue 1, Pages 200-212, November 1994.

[5] Crăciun A., *Application of ENO techniques to SL interpolations*. RC-LACE stay report, http://www.rclace.eu/?page=13, 2015.

Assimilation of ATOVS and GNSS ZTD data in the HARMONIE-AROME model configuration run at AEMET

Joan Campins, Jana Sánchez-Arriola, María Díez, Javier Calvo and Beatriz Navascués

1 Introduction

The present article describes the implementation and evaluation of the assimilation of ATOVS and Ground Based Global Navigation Satellite System (GNSS) zenith total delay (ZTD) data in the HARMONIE-AROME model configuration, which is part of the shared ALADIN-HIRLAM system. This system is run operationally on the AEMET bullx computer over the two domains shown on Figure 1 and these integrations serve as Regular Cycle of Reference (RCR) to monitor the quality of the HARMONIE reference system.

The impact of using ATOVS and GNSS ZTD observations has been assessed separately through two different parallel suites on the domain centered on the Iberian Peninsula. The current operational run, that only assimilates conventional observations, is used as control experiment. Over Canary Islands, only the impact of ATOVS data has been evaluated. All the experiments have been carried out over the same period, from July to November 2016.

The impact studies performed are especially relevant for the atmospheric moisture initial state. In the current operational suite, the only direct humidity measurements assimilated are vertical profiles from radiosondes (TEMP). ATOVS humidity soundings and GNSS ZTD data provide additional sources of information and it is expected that they can contribute to better simulation of the mesoscale atmospheric distribution of moisture.

This paper shortly describes the main features from the collection of this data at AEMET, to the observations selection and its usage within the data assimilation system. Both types of observations show biases with respect to model background. As observation bias can systematically damage the data assimilation process, and finally the quality of the forecasting system, the bias correction is an essential step before the assimilation. To correct the observation biases for both types of observations, the adaptive variational technique VarBC (Dee 2005, Auligné et al. 2007) has been used. An objective verification of all the experiments has allowed to assess the impact on forecasts, with emphasis on the shorter lead times to better understand the influence of the assimilation of these data types.

The control and experimental suites are presented in Section 2. The observation handling and the variational bias correction procedure, for both ATOVS and GNSS ZTD, are described in Sections 3 and 4, respectively. In Section 5, the forecast impact is assessed. Finally, some concluding remarks and future work are presented in Section 6.

2 Control and Experimental Suites

Control suite

The control experiment used for this study is the cycle 40h1.1 of the HARMONIE-AROME configuration that is the operational AEMET NWP suite run on the local computer. The model is run at 2.5 horizontal resolution and 65 vertical model levels extending up to 10 hPa, over two domains: one centered on the Iberian Peninsula that includes the Balearic Islands (called AIB), and other centered on the Canary Islands (called AIC). Figure 1 shows the geographical areas covered by both suites. Boundary conditions from ECMWF are applied at 1-hr intervals.

The main differences compared to the AROME-France cycle 40t1 set-up are described in Bengtsson et al. (2017), and references there in. These include radiation settings and updates in cloud and condensation schemes known as OCND2 concerning specially the separation between cloud water and cloud ice treatment. Also it includes a major update of the turbulence scheme known as HARATU which produces a significant reduction of the 10m wind speed bias, a reduction of the cloud cover and an increase in clouds base height compared to the CBR scheme. The turbulence scheme works in combination with dual mass flux scheme EDMFm for the shallow convection.

The upper-air assimilation is run with a 3-hr cycle using 70 minutes cut-off time for the observations. For the upper levels a 3DVar scheme is applied including for the base configuration the following observations: TEMP, AIREP, AMDAR, SYNOP, BUOY and SHIP. For the surface analysis, CANARI OI is used followed by SURFEX Offline DA (SODA) using the optimal interpolation option with conventional observations, to update SURFEX variables. The large scale from the host model is included in the analysis through a scale selection method (LSMIX).

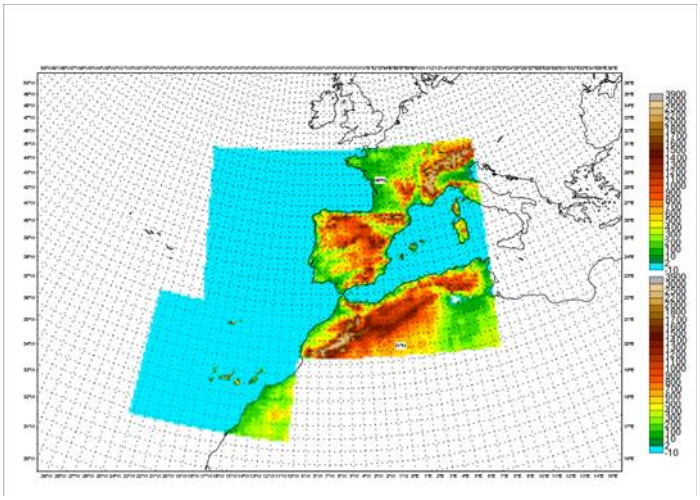

***Figure 1**: Domain of Iberian Peninsula and Canary Islands Suites.*

ATOVS experiment description

The HARMONIE configuration is able to assimilate, among many other observation types, microwave radiances from the so-called Advanced TIROS Operational Vertical Sounders (ATOVS) on board of several polar-orbiting satellites. ATOVS comprises AMSU-A, AMSU-B (Advanced Microwave Sounding Unit A and B) and MHS (Microwave Humidity Sounder; which has replaced the old AMSU-B) instruments. In AEMET, ATOVS radiances are available via EUMETCast (local) for NOAA-18, NOAA-19, METOP-A and METOP-B. All these satellites are equipped with AMSU-A and MHS instruments.

In order to explore the impact of the ATOVS assimilation in the current operational suite, two parallel experiments, one for the Iberian Peninsula and the other for the Canary Islands domains, have been prepared. These experiments, named AIB_ATOVS and AIC_ATOVS respectively, are identical to their control counterparts, but they also assimilate ATOVS radiances from different satellites. In Section 3, a detailed description of the data selection, and particularly to the variational bias correction, is presented.

GNSS ZTD experiment description

This experiment is based in previous efforts on the HARMONIE-AROME configuration to assimilate ground based GNSS ZTD observations (Sánchez Arriola et al., 2016). A suite parallel to AIB run has been prepared for the operational assimilation of GNSS ZTD observations in addition to the conventional data. This run has been called AIB_GNSS**.** GNSS ZTD observations are fetched from the EUMETNET E-GVAP European program server via ftp in ASCII format.

3 ATOVS observation handling

The AMSU-A instrument measures the radiance that reaches the top of the atmosphere in 15 channels, that are sensitive mainly to atmospheric temperature in different vertical layers. As the uppermost model level is 10 hPa, the assimilation of those channels with weighting functions having a significant contribution from vertical layer above that value is not recommended. For this reason, the HARMONIE reference system exclude AMSU-A channels 11-15, and it is questioned if AMSU-A channel 10 should be used. AMSU-A channels 1-5 are not used as their weighting functions are close to the surface, so they are affected by surface emissivity and model biases at surface.

MHS instrument measures the radiance at the top of the atmosphere in 5 channels, 3 of them (channels 3 to 5) are atmospheric sounding channels, sensitive to atmospheric humidity in different vertical layers. Weighting functions for channels 3-5 are peaking at middle and high levels (above the model top), being channel 5 the lowest peaking and 3 the highest peaking of the atmospheric sounding channels.

As default, we utilize channels 6-10 from the AMSU-A and channels 3-5 from the MHS instruments. However, due to the poor quality of some channels (this information is confirmed by different satellite monitoring websites as http://www.star.nesdis.noaa.gov/icvs) we exclude channels 7-8 AMSU-A from NOAA-19 and METOP-A, and MHS NOAA-19

channel 3. The selection of satellites-instruments-channels is done within *mf_blacklist.b* routine.

Satellite data are subjected to a horizontal thinning for two main reasons: to reduce the data volume and to avoid the effects of observation error spatial correlation. In HARMONIE two thinning distances are introduced: RMIND_RADC1 and RFIND_RAD1C. The first one is the minimum horizontal distance allowed between two observations, and the second one is the resulting average horizontal thinning distance between two observations after thinning. Due to the different characteristics of the AMSU-A and MHS instruments, RMIND_RAD1C are different, lower for MHS (40 km) than for AMSU-A (60 km). On the contrary, RFIND_RAD1C is the same (80 km) for both instruments.

ATOVS Variational Bias Correction

Background departures for ATOVS observations present biases that can be due to systematic errors in the satellite instrument itself, deficiencies in the radiative transfer model, or bias in the first guess. In HARMONIE, bias correction for ATOVS radiances is carried out using the Variational Bias Correction scheme (VarBC), which is a particular adaptive scheme that is embedded inside the assimilation system and then the bias correction coefficients are continuously updated as part of the assimilation. The evaluation and tuning of VarBC for HARMONIE-AROME is extensively explained in Lindskog et al. (2012), and next we only will underline the outstanding issues.

Bias is estimated by means of a linear combination of predictors (p_i). In the reference system, a set of 5 predictors (i= 0, 1, 8, 9 and 10) are used for AMSU-A channels 6-10 and for MHS channels 3-5, where $p_0 = 1$ to allow a constant component for the bias, p_1 depends on the atmospheric state at the observed location and p_8-p_{10} depend on viewing angle relative to nadir. The convergence of the predictors to a certain timescale is set by means of the NBG_AMSUA and NBG_MHS parameters. In the HARMONIE AROME 2.5 reference system NBG value is set to 2000 for AMSU-A and MHS.

Before the assimilation of the satellite data, the spin-up of the VarBC coefficients for each assimilation cycle HH is needed. This is achieved by running the data assimilation with ATOVS data in passive mode. As it was mentioned before, with a NBG = 2000, a month is enough to get steady VarBC coefficients for the Iberian domain (this result is similar to that obtained in Lindskog et al., 2012 for a different region).

The calibration of the VarBC coefficients for the Canary Islands domain during the spin-up period has taken about 10 days longer than for the Iberian Peninsula and Balearic Islands domain, as can been seen in the Figures 2 and 3. This could be related with the southernmost latitude and the smaller area of the AIC domain and with the lower observations density in this area.

During this spin-up period, the passively assimilated observations were monitored, that is, the time series of number of observations, bias correction and the background and analysis departures were examined. This monitoring allows to prevent the utilization of satellite data with a small sample of data (for instance those from paths at the edge of the domain), which may create unstable bias correction coefficients. In this case, the blacklisting of those data can be performed by means of the LISTE_LOC_HH files in the observations pre-processing step.

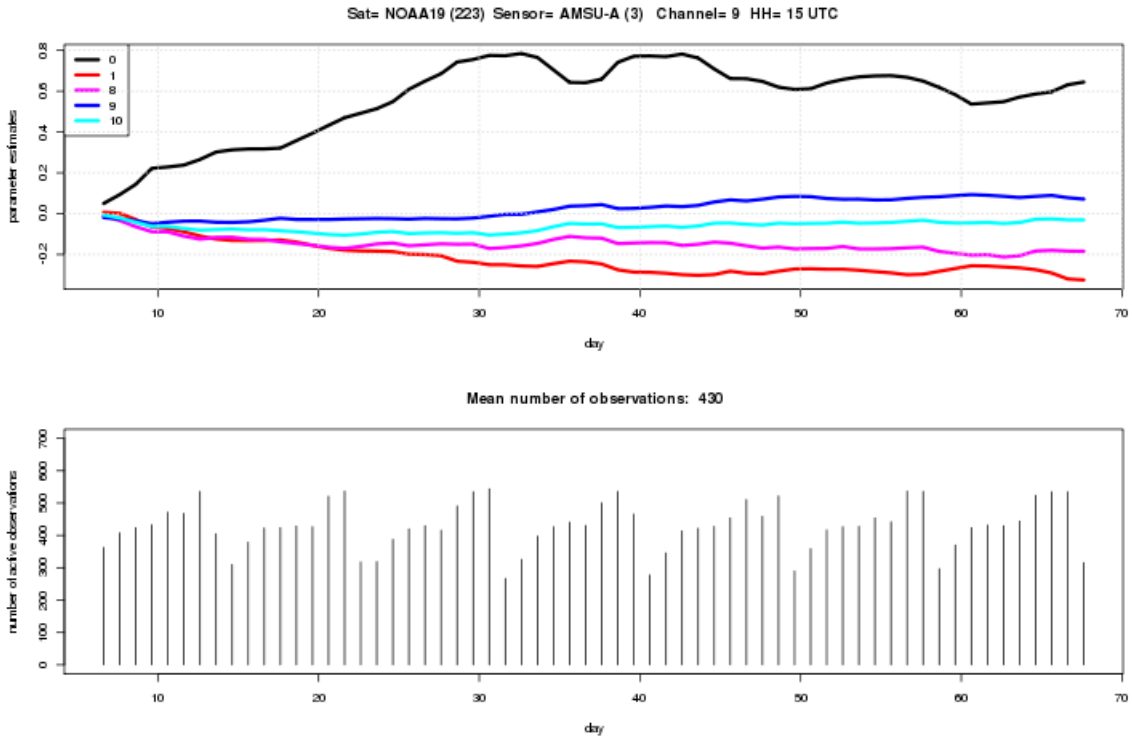

***Figure 2**: Evolution of the VarBC coefficients for the AIB_ATOVS suite (Iberian Peninsula and Balearic Islands) during the spin-up period*

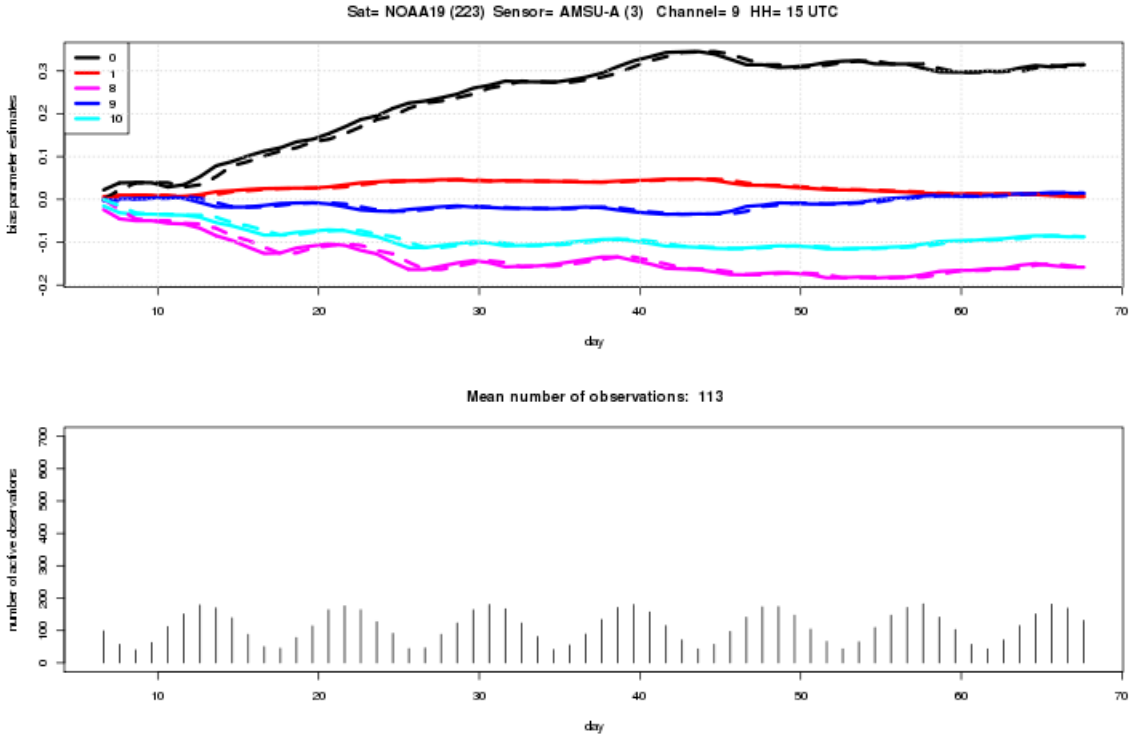

***Figure 3**: Evolution of the VarBC coefficients for the AIC_ATOVS suite (Canary Islands) during the spin-up period showing that it needs a longer period to stabilize the VarBC coefficients.*

Also, the monitoring can reveal large departures that can worsen the analysis, a channel with poor quality or not properly. In this case it is better to keep this channel as passive.

After this spin-up period, those satellites-instruments-channels, that the bias correction seems to properly reduce the first-guess systematic departures, can be assimilated as active. For AIB_ATOVS and AIC_ATOVS, the active assimilation channels are all the aforementioned, except AMSU-A channel 10, that we have decided to keep as passive. Figure 4 displays the first-guess (corrected and non-corrected) and analysis departures (top panel) and number of assimilated observations (bottom panel) for channel 6 on NOAA-18 AMSU-A, from 1st to 30th September 2016 at 18 UTC for AIB_ATOVS experiment (observations over land are displayed in green and over sea in blue). It shows that bias correction is able to significantly reduce departures (non-corrected departures in dashed lines with triangles and corrected in solid lines with circles), close to analysis departures (solid line with squares). Data availability oscillates daily. Overall the number of observations over land is lower than over sea, among other reasons because observations over high orography are rejected.

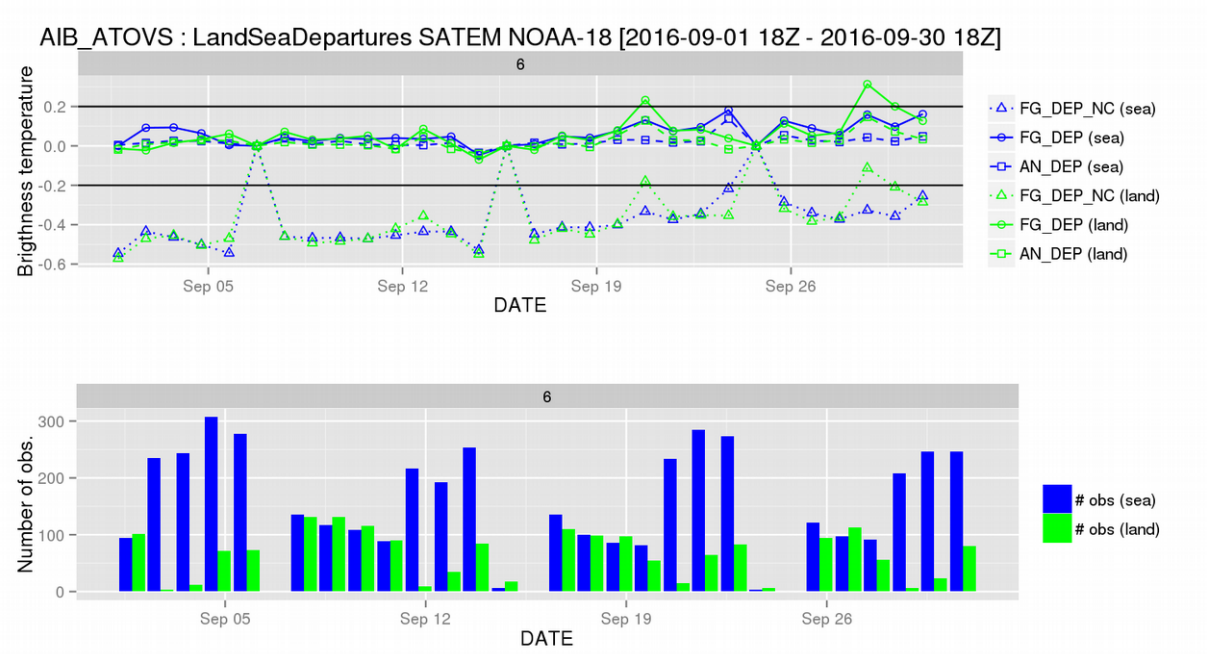

Figure 4: *AIB_ATOVS departures statistics (top) and number of observations (bottom) for NOAA-18 AMSU-A Channel 6 from 1st to 30th September 2016 at 18 UTC for data over sea (in blue) and over land (in green).*

4 GNSS ZTD observation handling

The GNSS ZTD observation processing includes data selection, quality control, and also a Variational Bias Correction to handle the systematic discrepancies between model equivalents and observed values. The available files within the cut-off time of 70 min, have been fetched by ftp, filtered, and prepared to be assimilated by the model at every assimilation cycle.

There are many ground based GNSS sites which raw data are processed by more than one GNSS ZTD analysis center. So, the first step consists on creating a “White List” containing the best quality of station-analysis center pairs. The White List is based on the statistics of the

ZTD departures, the observation-background counterpart in observation space. The criteria taken to select the best pair station-analysis center into the White List was the smallest standard deviation, provided that the skewness did not exceed a predefined threshold. Time series of background departures for this White List construction were obtained through a one month long run before the starting date of the experiment, where the GNSS ZTD data entered in passive mode to the data-assimilation system.This White List used contains 783 sites all around Iberian Peninsula and the sites chosen are from ASI_, ROBH, SGN_, IGE2 and METO GNSS ZTD analysis centers; its distribution can be seen at Figure 5.

In the pre-processing step, the available data from a selection of the best quality station-analysis center pairs, chosen through the White List, is further reduced by applying a temporal thinning in order to retain from each station the ZTD observation closest to the analysis time (ZTD time frequency is about 15 min). No spatial thinning has been applied to these data.

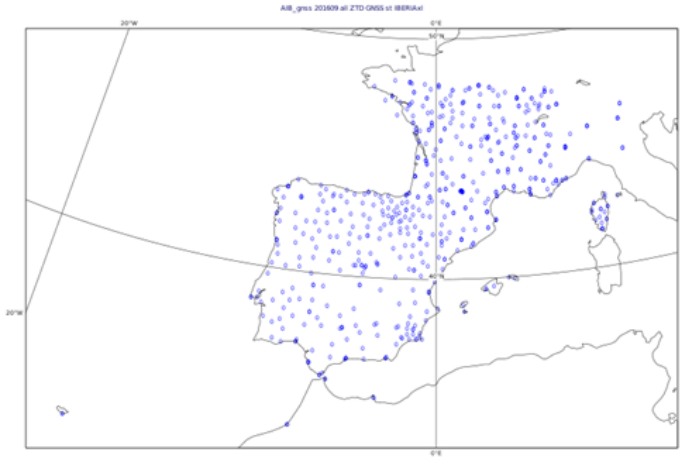

***Figure 5**: Distribution of the stations contained in the White List used for this study.*

GNSS ZTD observations Variational Bias Correction

The sources of bias of background departures for ZTD observations come from GNSS data processing algorithms (that may even differ from one Analysis Centre to another), systematic errors in both the ZTD observations operator and the model field, the relatively low model top (10 hPa) used by the HARMONIE AROME 2.5 model configuration that leads to an underestimation of the ZTD model equivalent value, and also the interpolation and extrapolation from the model orography to the real one. The bias derived from all of these sources is estimated by applying a VarBC method to these observations. It is based on a single constant predictor. So, the systematic differences between the observations and the model equivalent are parameterized as site dependent offset parameter, one value per site that is updated every 3 hours. These biases have been first tuned in a 5-6 weeks spin-up period previous to the assimilation of GNSS ZTD observations, during which these data entered to the analysis in passive mode only and so, did not influenced the model state. Variational bias-correction coefficients are in general very sensitive to the bias present in closely located sites during the spin-up period, and that is the reason why the spin-up period used here has been long enough, a bit more than a month, to be able to remove the bias of all stations, taking into account that the adaptivity corresponds to a stiffness coefficient in the variational bias correction scheme (nbg_sfcobs_ndays110) equal to 15.

The functionality of this bias correction is represented by the time evolution (here a month is shown) of the GNSS ZTD observation (obs raw), the bias corrected observation (ob), the first guess (fg) and the analysis (an), shown in Figure 6, where it is possible to see how the variational data assimilation scheme has managed to correct the observation from the systematic bias along the previous period of spin-up, for this particular site of MALLIGE2 that is shown as an example.

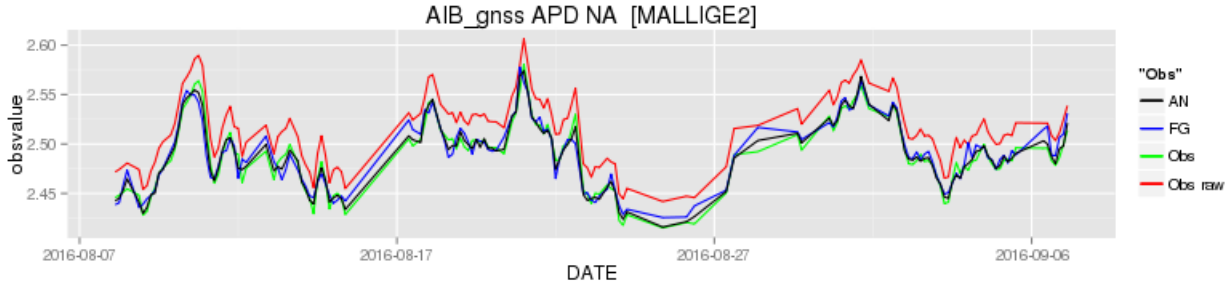

***Figure 6**: One moth time series of bias correction for MALLIGE2 site. Red line is raw observation with no bias correction, green line is bias corrected observation, blue line is first guess and black line is the analysis.*

5 Impact on forecast

The impact of the assimilation of ATOVS and GNSS ZTD data has been assessed through the forecast objective verification of all the experiments against SYNOP and TEMP observations during the test period (July-November 2016). Only the shortest lead times are shown here to draw more clear conclusions about the influence of the extra observations assimilation on the forecast skill.

Overall, the impact found is rather small in most of the variables. It has to be taken into account that, among other reasons, the large scale mixing with the host model prevents a larger influence of these observations in the assimilation cycle. Nevertheless, some rather consistent features seem to indicate a benefit of the assimilation of both types of data.

Figure 7 displays the vertical distribution of bias and rmse of temperature and relative humidity for the different experiments in the Iberian Peninsula and Balearic Islands domain. Both types of observations moisten the model (GNSS ZTD the most), and a positive impact is observed at the vertical profiles of humidity rmse due to the assimilation of either ATOVS (from 700 hPa upwards), or GNSS ZTD (up to 700 hPa) data. This last data type also produces a slight reduction of the cold bias in the lowest atmospheric layers.

The smaller cold bias due to the assimilation of GNSS ZTD data is also visible in T2m scores, accompanied by a reduction of the positive/negative biases of mslp and rh2m, respectively (see Figure 8). Precipitation skill scores (see KSS in Figure 8) are consistent with those obtained in humidity and show the benefit of the assimilation of both data types.

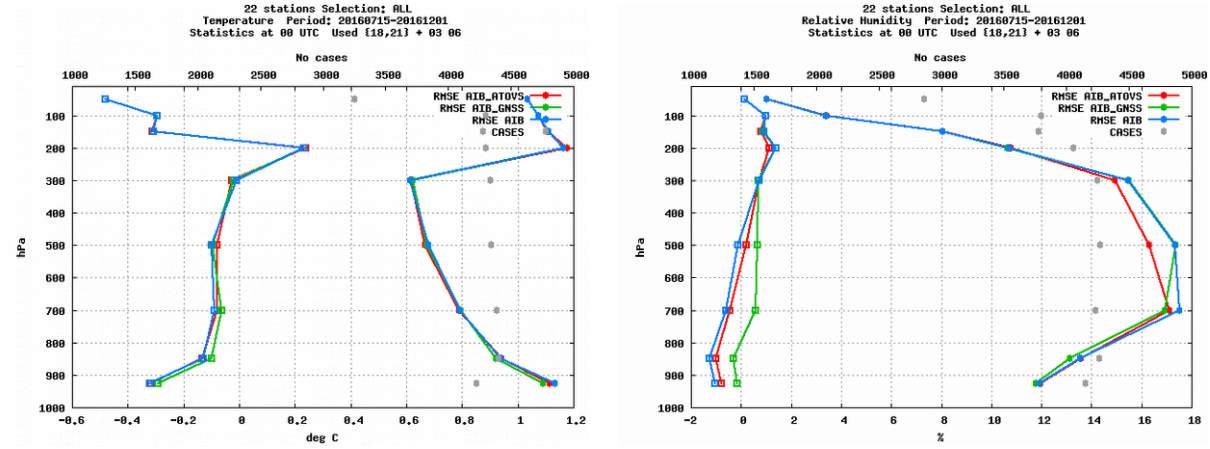

***Figure 7**: RMSE and BIAS against soundings at 00 UTC for the AIB domain comparing ATOVS (red), GNSS (green) and control (blue). RMSE and BIAS for temperature (left) and relative humidity (right)*

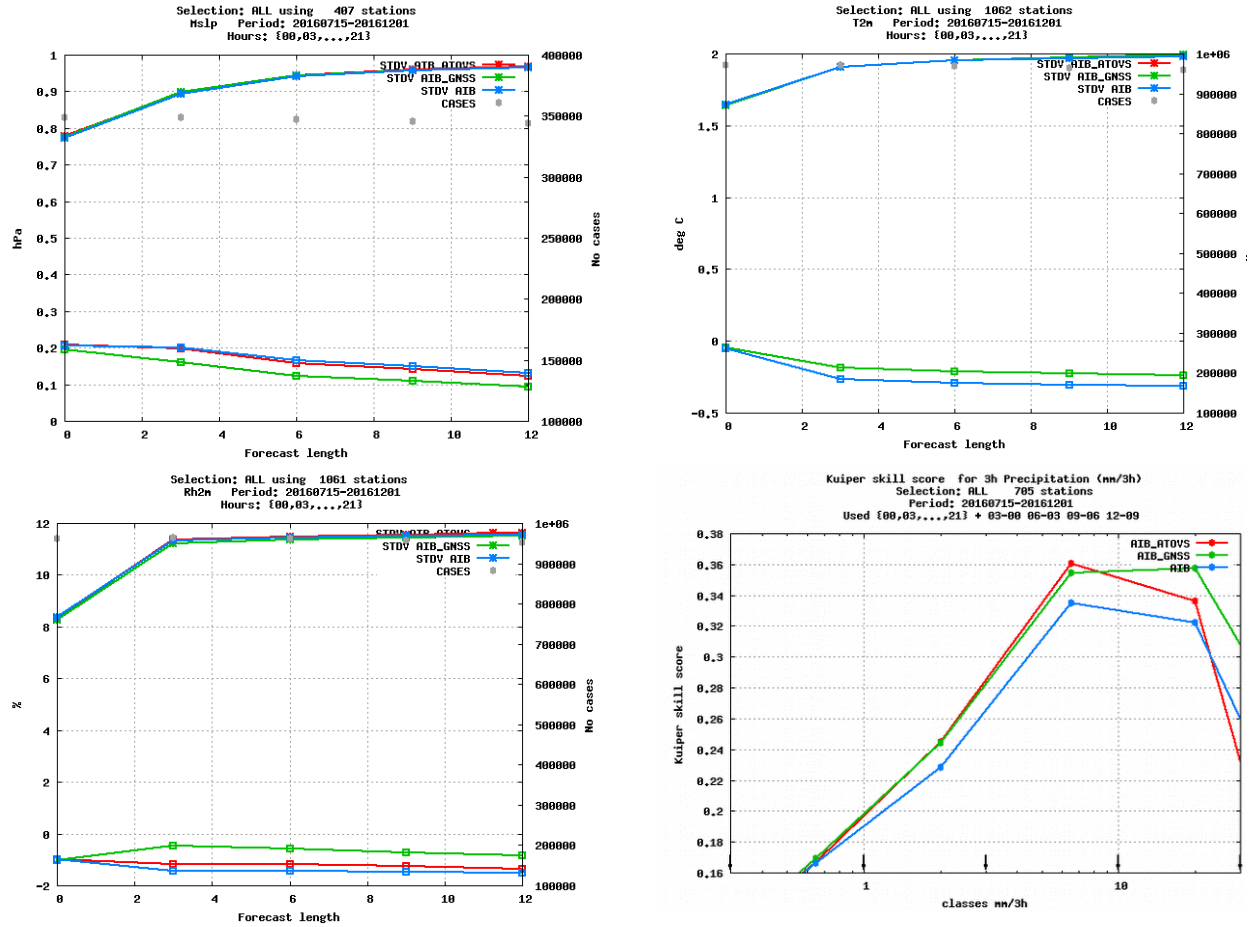

***Figure 8**: STDV and BIAS against synop function of the forecast length for the AIB domain comparing ATOVS (red), GNSS (green) and control (blue). MSLP (top left), 2m temperature (top right) and 2m relative humidity (bottom left). The KSS for different precipitation categories is shown on bottom right plot.*

The influence of ATOVS assimilation in the Canary Islands region is qualitatively very similar to that found in the Iberian Peninsula domain. Only the humidity vertical profile seems to be affected, being AIC_ATOVS slightly moister than AIC, and having a smaller rmse, as it is displayed in Figure 9. This Figure also shows that AIC model also presents in this area a cold bias in the lowest atmospheric levels, that ATOVS assimilation is not able to correct (similarly to the northernmost geographic domain). The impact found in other surface parameters (mslp, T2m, rh2m) is also neutral. Precipitation events have been rare in this area during the test period, and the number of observations and the complex orography of these islands makes difficult to draw conclusions of the objective verification performed for this variable.

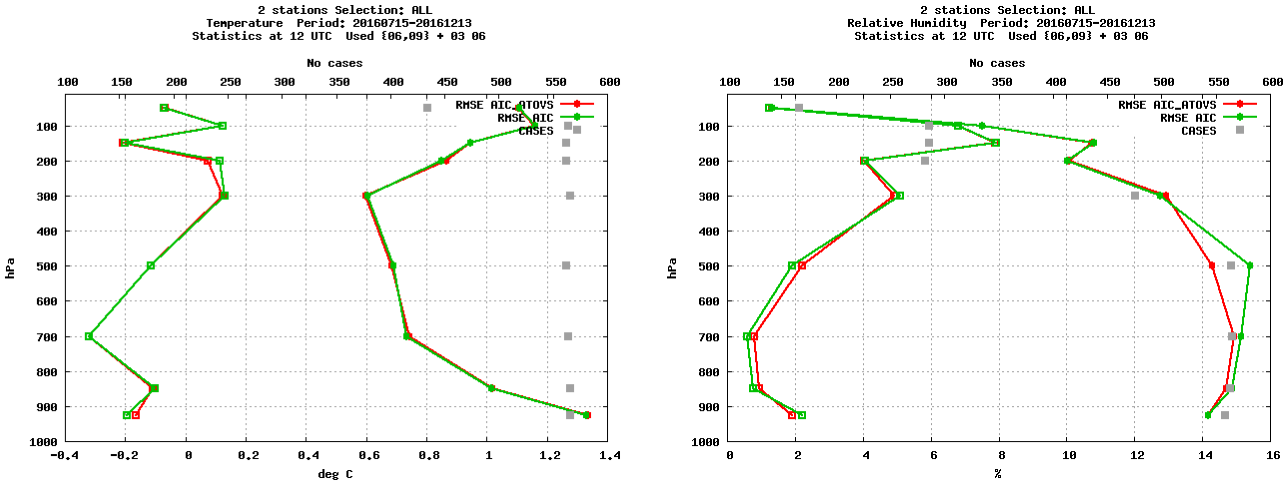

***Figure 9**: RMSE and BIAS against soundings at 12 UTC for the Canary Islands domain (AIC) domain comparing ATOVS (red) and control (green). RMSE and BIAS for temperature (left) and relative humidity (right). Note that only 2 soundings are available for this domain.*

6 Conclusions and future work

A series of parallel experiments have been carried out at AEMET to prepare the assimilation of ATOVS and ground based GNSS data in the operational NWP suite. This system comprises two independent HARMONIE runs covering the Iberian Peninsula and Balearic Islands, and Canary Islands. Apart from the effort needed for a local reception of the different data types, considerable work has been devoted to the setup of the different assimilation experiments. It included, among others, the creation of a White List for GNSS ZTD data, further pre-processing of these data, and three HARMONIE-AROME suites running spin-up periods during which data was introduced in passive mode. These spin-up periods have allowed to calibrate the corresponding VarBC coefficients, to monitor the different observations, and to select the satellites-instruments-channels to be assimilated at each assimilation cycle. Once this training step has been completed, the three experiments assimilating ATOVS in the two domains, and GNSS data in the Iberian Peninsula region, have been run and monitored in parallel to the operational ones over the period July to November 2016.

The impact on forecast produced by the assimilation of these extra observations has been assessed by means of an objective verification against surface and vertical profile

observations. The results obtained indicate an overall neutral impact in most of variables. However, and in both geographical regions, the assimilation of ATOVS clearly improves the atmospheric humidity in middle-upper levels. The assimilation of GNSS data produces a positive impact on the humidity, up to 700hPa, and it is also able to decrease the bias observed in temperature at or close to the surface, and in rh2m and mslp. Both data types improve the forecasted precipitation in the Iberian Peninsula and Balearic Islands domain.

The results obtained show a statistically significant sensitivity of the humidity linked variables in the HARMONIE-AROME model, to the initial state of the atmospheric moisture.

Work is on-going for the joint assimilation of both data types over the Iberian Peninsula and Balearic Islands domain. In the Canary Islands region, the next step is to start the assimilation of ground based GNSS observations.

7 Acknowledgements

Gema Morales is responsible for the installation and maintenance in AEMET of the obsmon tool which results have been widely used in this work. Daniel Martín support for the local installation of HARMONIE-AROME model is very much appreciated.

8 References

Auligné T., McNally A.P., Dee D.P., 2007: Adaptive bias correction for satellite data in a numerical weather prediction system. *Q. J. R. Meteorol. Soc.,* **133**: 631-642.

Bengtsson, L., Andrae, U., Aspelien, T., Batrak, Y., Calvo, J., de Rooy, W., Gleeson, E., Sass, B. H.,Homleid, M., Hortal, M., Ivarsson, K.-I., Lenderink, G., Niemelä, S., Nielsen, K. P., Onvlee, J., Rontu,L., Samuelsson, P., Santos Muñoz, D., Subias, A., Tijm, S., Toll, V., Yang, X., Køltzow, M. Ø., 2017:The HARMONIE-AROME model configuration in the ALADIN-HIRLAM NWP system, Monthly Weather Weather Review, accepted for publication, January 2017

Dee D. 2005: Bias and Data assimilation. *Q. J. R. Meteorol. Soc*. **131**: 3323-3343.

Lindskog M., Dahlbom M., Thorsteinsson S., Dahlgren P., Randriamampianina R., Bojarova J., 2012: ATOVS processing and usage in the HARMONIE reference system. *HIRLAM Newsletter*, **59**: 33-43

Sánchez Arriola J., Lindskog M., Thorsteinsson S., Bojarova J., 2016: "Variational bias correction of GNSS ZTD in the HARMONIE modeling system". *Journal of Applied Meteorology and Climatology* 55(5), 1259-1276; DOI: 10.1175/JAMC-D-15-0137.1.

AROME-France convection-permitting EPS

François Bouttier, Laure Raynaud, Claude Fischer, Patricia Pottier

1 AROME-France-EPS

A convective-scale ensemble prediction system has been developed at Météo-France. It has the same model configuration as the deterministic AROME-France suite, except for the horizontal resolution (2.5km in the ensemble, 1.3km in AROME-France, and 90 vertical levels for both).
It uses 12 perturbed forecasts of the AROME-France model coupled with the ARPEGE global ensemble prediction system (PEARP[1]).
Each member is perturbed in order to represent the main sources of uncertainty, including the error on initial conditions, surface conditions, clustered boundary conditions from the PEARP global ensemble, and the model. Initial conditions are perturbed using a simple scheme based on re-scaled PEARP initial perturbations. Surface conditions are perturbed using auto-correlated random modifications applied to various aspects of the SURFEX surface model. Lateral boundary conditions are selected among the PEARP 35-member ensemble forecasts using a clustering technique. Atmospheric model errors are represented by SPPT perturbations correlated in time and space modifying the wind, temperature, and humidity tendencies of the AROME physical parameterizations.

2 Research & development & Verification

Recent research results

- Extensive validation using HyMeX SOP1 data shows that it not important to have consistent initial and lateral boundary perturbations => use of ensemble data assimilation (EDA) for initial perturbations or cheaper alternative (to add small-scale random noise to the initial conditions) with improvment over the simple downscaling from a larger-scale ensemble.
- Surface perturbations improve the ensemble performance; explicit surface perturbations are necessary.
- Spatial correlations of ensemble forecasts are highly sensitive to the correlations of surface perturbations, at low levels. The correlation sensitivity to SPPT correlation structures, or to correlations in the initial perturbations, seems to be negligible after a few hours.
- The introduction of a tolerance in space and time when computing the precipitation probabilities, can be proven to improve the forecast scores, by filtering small-scale noise and increasing the apparent ensemble size.

Preparation of the operational utilisation of PEARO

The AROME-France-EPS system has been used and evaluated by forecasters during two forecast exercises in October 2014 and June 2015. The preparation to the future operational utilisation of PEARO has continued during fall 2015, during which a pre-operational run of AROME-France-EPS has been run in near real time once per day, in order to organize weekly training sessions on recent past events. These exercises offered the possibility to examine the behaviour of AROME-France-EPS on a wide range of situations, among which several cases of strong winds, fog and heavy precipitation. They also contributed to more accurately define work methods, as well as relevant parameters and diagnoses, and appropriate visualisation tools necessary to fully make use of ensemble forecasts..

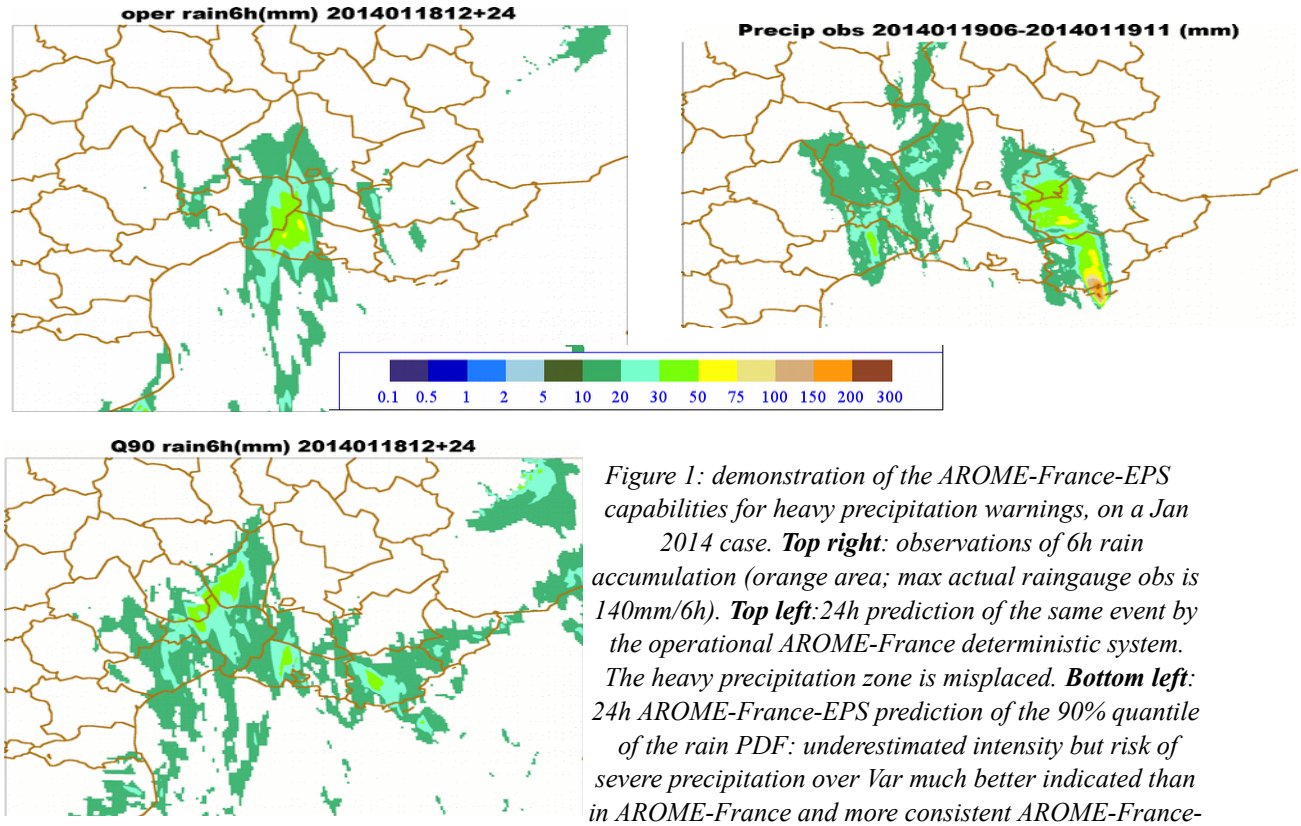

*Figure 1: demonstration of the AROME-France-EPS capabilities for heavy precipitation warnings, on a Jan 2014 case. **Top right**: observations of 6h rain accumulation (orange area; max actual raingauge obs is 140mm/6h). **Top left**:24h prediction of the same event by the operational AROME-France deterministic system. The heavy precipitation zone is misplaced. **Bottom left**: 24h AROME-France-EPS prediction of the 90% quantile of the rain PDF: underestimated intensity but risk of severe precipitation over Var much better indicated than in AROME-France and more consistent AROME-France-EPS forecasts in time*

Objective verification

The objective verification of AROME-France-EPS, performed over nearly one year of simulation, indicates a significant improvement over PEARP, especially regarding precipitation (see figure 2) and 10-meter wind speed.

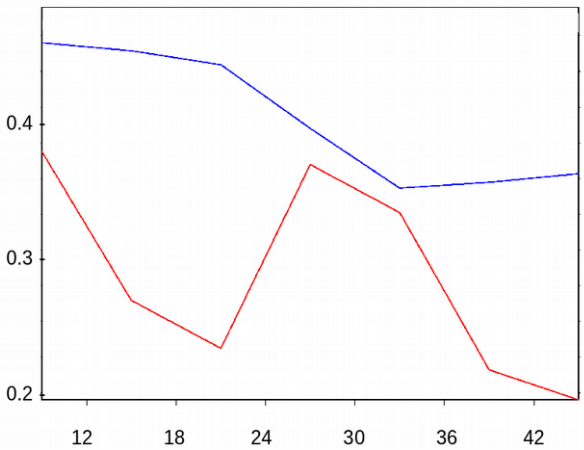

Figure 2: Brier Skill Score, added value of PEARO (blue line) vs PEARP (global system), red line threshold event is RR >1mm/6h, computed over 302 instances of the EPS systems (Dec. 2015 - Oct. 2016). The higher the Brier Skill Score, the better the probabilistic system performed for that event.

3 Conclusion

The AROME-France-EPS system benefits from the advances of the AROME model configuration such as the increased capability to forecast more accurately high impact convective weather (storms, heavy precipitation etc.). Objective verification, performed over nearly one year of evaluation, indicates a significant improvement over an existing global probabilistic prediction system based on ARPEGE, especially regarding precipitation and 10-meter wind speed. AROME-France-EPS is operationally produced on the Météo-France supercomputer since Oct 2016. It runs twice a day, at 09 and 21 UTC, to provide forecasts up to a 45h range.

4 References

[1] Descamps L., C. Labadie, A. Joly, E. Bazile, P. Arbogast, P. Cébron: PEARP, the Météo-France short-range ensemble prediction system. *Quart. Jour. Roy. Meteor. Soc.*, 141,1671–1685. DOI: 10.1002/qj.2469

[2] Bouttier F., L. Raynaud, O. Nuissier and B. Ménétrier: Sensitivity of the AROME ensemble to initial and surface perturbations during HyMeX. *Quart. Jour. Roy. Meteor. Soc.*, 142, Issue Supplement S1, 390–403. DOI: 10.1002/qj.2622

ALADIN related activities @SHMU (2016)

Mária Derková, Jozef Vivoda, Oldřich Španiel, Martin Belluš, Martin Dian, Viktor Tarjani

1 Introduction

The summary of ALADIN related activities at Slovak Hydrometeorological Institute in 2016 is given. The setup of ALADIN operational system is described and some research and development activities are highlighted.

2 The ALADIN/SHMU NWP system

The ALADIN/SHMU system setup

The ALADIN/SHMU system has been ported to new HPC and thoroughly upgraded in 2016 both in resolution, code version and physical parametrizations. This new version of the ALADIN/SHMU system has been declared quasi-operational on 28/07/2016. It covers so-called LACE domain with 4.5 km horizontal resolution and 63 vertical levels. It is running 4 times per day up to 3 days. Current model version is based on CY40T1_(pre)bf06 with ALARO-1vA physics and ISBA surface scheme, coupled to Arpege global model. The spectral blending by digital filter is applied for the upper-air pseudo-assimilation using Arpege analysis. For surface the CANARI data assimilation scheme using additional local observations is active. More ALADIN/SHMU details are given in Table 1. A comparison of old and new HPC is illustrated in Table 2.

Table 1: ALADIN/SHMU – (quasi-)operational setup, HPC parameters

Model version	CY40T1_(pre)bf06
Resolution	4.5 km
Levels	63
Area	2812 x 2594 km (625 x 576 points), [2.31; 33.77 SW, 39.07; 55.88 NE]
Initial conditions	CANARI surface analysis & upper-air spectral blending by DFI, 6 h cycling
Boundaries	ARPEGE, 3 h coupling frequency
Starting times	00, 06, 12, 18 UTC
Forecast length	+78 h/+72 h/+72 h/+60 h
Surface scheme	ISBA
Physics	ALARO-1vA
Dynamics	2TL SL hydrostatic; SLHD

Table 2: The SHMU supercomputers

old HPC	new HPC
IBM p755	IBM Flex System p460
4x Power7 8core CPUs (3.6 GHz), 256 GB RAM	4x Power7+ 8core CPUs (3.6 GHz), 256 GB RAM
10 nodes	12 nodes (in total ~1.26x stronger than old HPC)
AIX 6 SE OS; xlf 13.1.01	Red Hat Enterprise Linux; gfortran 4.9.3 (xlf 15.1.0)

The activities in 2016 related to the operational system

Technical and operational activities were mostly concentrated on porting and validation of NWP system and system-related tools to new HPC.

- The necessary environment and the technical and supporting tools to run operational and user applications are gradually being ported to new hpc, with emphasis to use grib_api whenever possible (lambert and latlon projections).
- Mirror of the e-suite based on CY38T1_bf03 with ALARO-0 baseline was ported and validated on new HPC as a basis for new operational environment, declared on 29/04/2016.
- CY40T1.bf05_export version was ported to new HPC including future bf06 and newest development of T2m/RH2m interpolation in ALARO-1 ACTKECLS (by M. Dian and J. Masek + bf of L. Gerard).
- In this configuration whole assimilation and production chain works under the operational environment (so called run_app system), declared pre-operational on 28/07/2016. New system shows overall improvement with respect to the old one in almost all parameters, as illustrated on Figure 1 for 2m temperature (top left) and vertical profile of temperature (top right) for September 2016. There is a problem with the wind speed in the mountains that is sometimes too low (Fig. 1 bottom left), which might require to retune the turbulence scheme. Another problem is the scores of MSLP at the analysis time (Fig. 1 bottom right), that we think is related to the missing initialization. Therefore the incremental digital filter algorithm will be investigated.

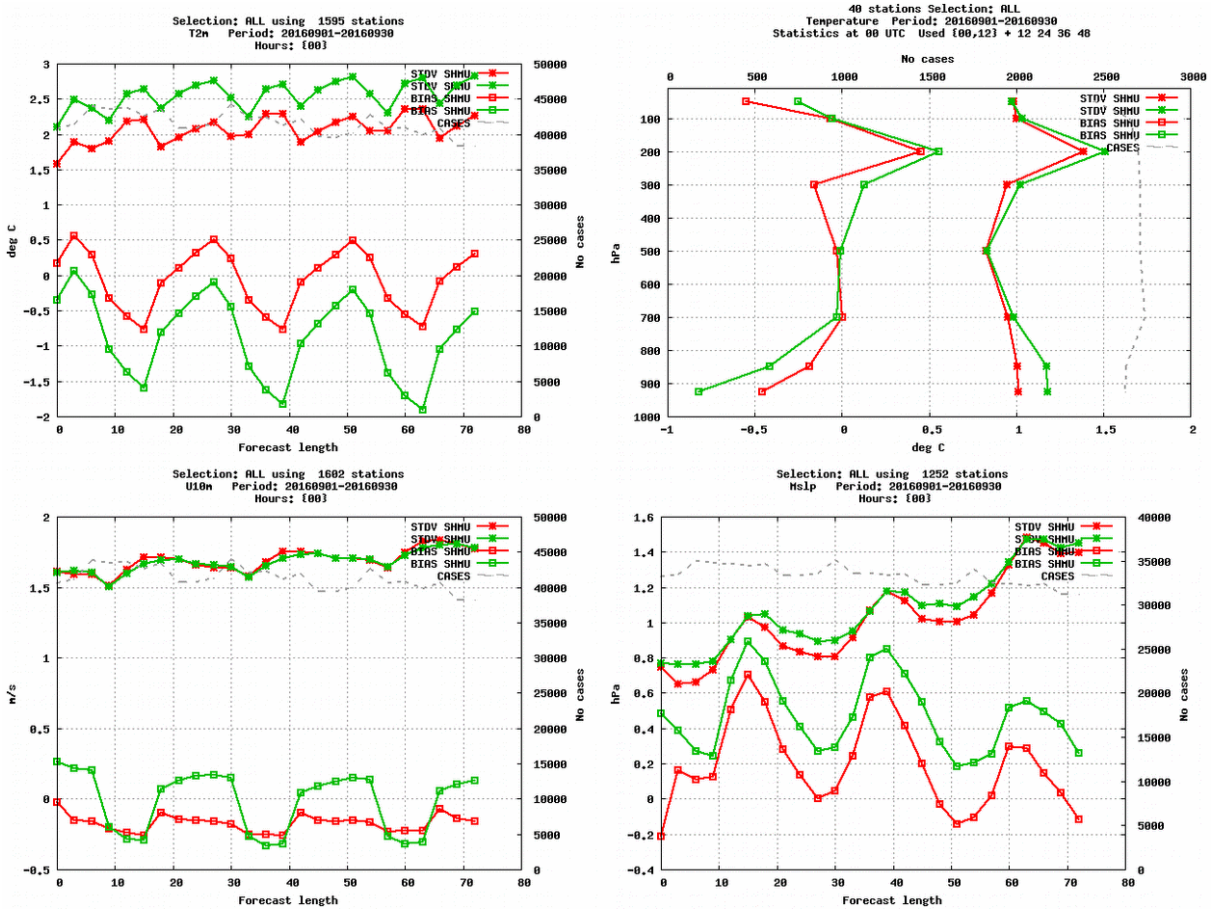

Figure 1: The verification scores of 2 m temperature (top left), vertical profile of temperature (top right), 10 m wind speed (bottom left) and MSLP (bottom right) for September 2016 for the new operational setup (red) and the old one (green).

3 Research and Development activities

Improving the screen level parameters computations in ALARO-1 (M. Dian, RC LACE stay)

The temperature at 2 m computed from the lowest model level TL and temperature on the model surface TS showed oscillating behavior in stable conditions with ALARO-1/TOUCANS, as illustrated on the Figure 2, green line. New interpolation formula was proposed, following Geleyn 1988 methodology to simplified Gratchev et. al. 2007 solution. The oscillations disappeared, as displayed on the Figure 2 with orange line. For more details see the LACE report.

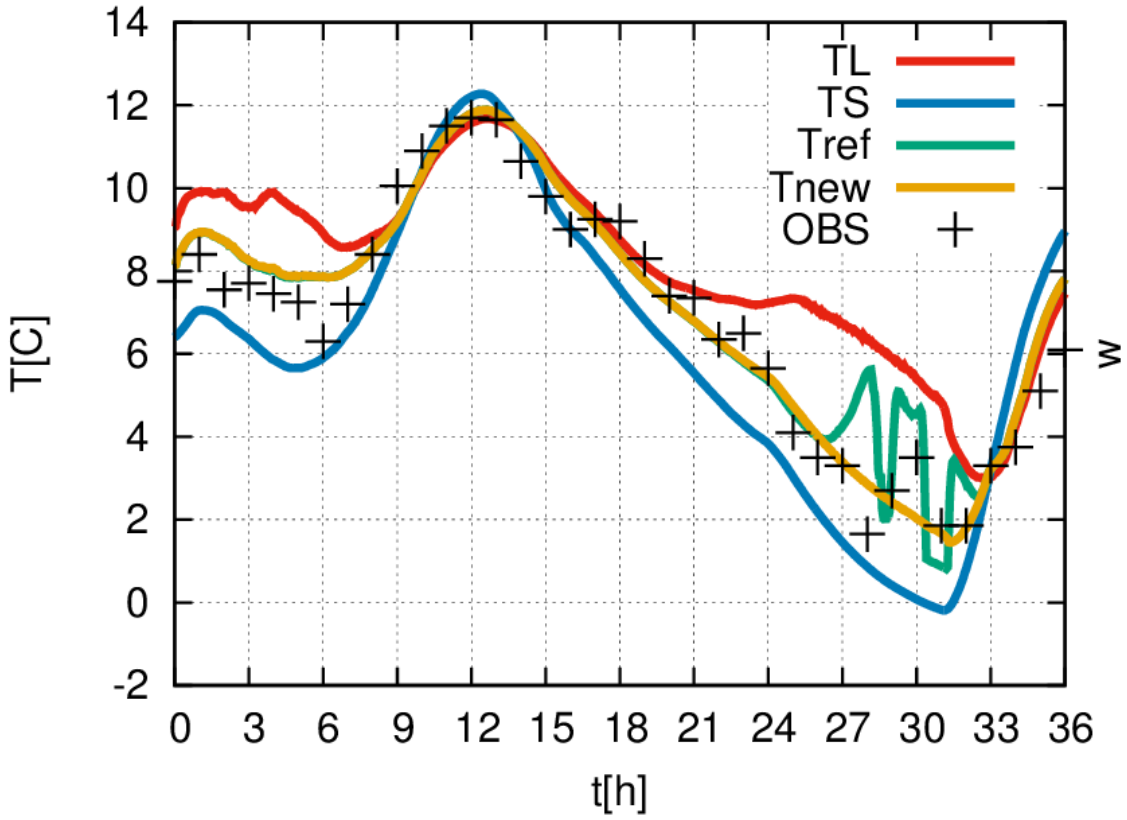

Figure 2: The evolution of 2 m temperature forecast for Prague, 23/12/2015. Surface temperature in blue, the lowest model level temperature in red, the reference temperature forecast in green and newly implemented formulation for T2m computation in orange. The observation are in black crosses.

Vertical finite element discretization in NH kernel of ALADIN system (J. Vivoda, RC LACE stay)

A work has been accomplished on:
(a) definition of knots and explicit values of eta on half and full levels (from B-spline basis of order C-1 and C, when levels are located either in spline maxima or in so called Greville points);
(b) reimplementation of variation diminishing method for approximate operators;
(c) redefinition of full level A and B.

ALADIN-LAEF (M. Bellus, RC LACE stay)

The ALADIN-LAEF system has been upgraded to cycle 40t1 with ALARO-1 physics while the model resolution was increased to 5 km and 60 levels. At the same time the domain must have been reduced as displayed on Figure 3 due to the planned operational implementation. The new method Ensemble BlendVar was technically implemented. It should replace the functional but obsolete Breeding-Blending method for generating the initial perturbations at the model levels. BlendVar is the combination of the upper-air spectral blending technique (the same as in case of Breeding-Blending method) and 3DVar assimilation procedure involving the perturbed observations. The statistical scores for the old domain and new domain (dynamical adaptation) are shown on Figure 4 for temperature at 2 m (BIAS, RMSE, CRPS and outliers).

The paper titled "Perturbing surface initial conditions in a regional ensemble prediction system" (Bellus, Wang, Meier) has been published in Monthly Weather Review.

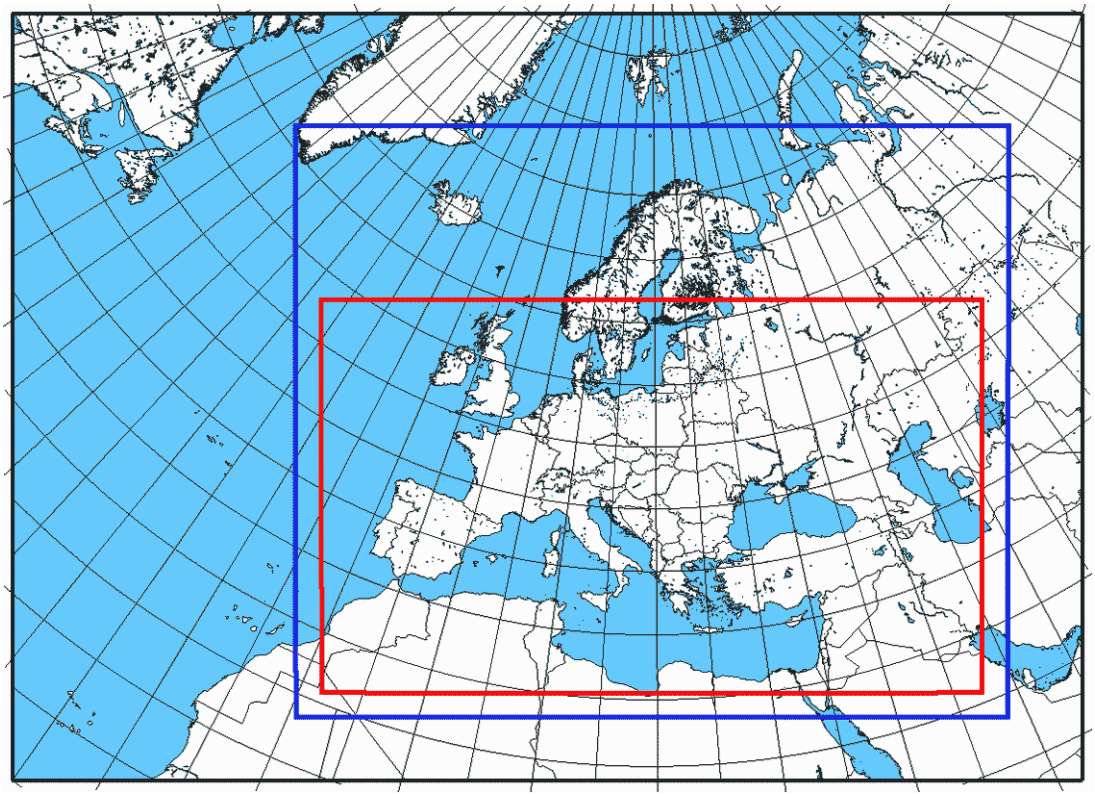

Figure 3: New ALADIN-LAEF domain in red compared to the old domain in blue.

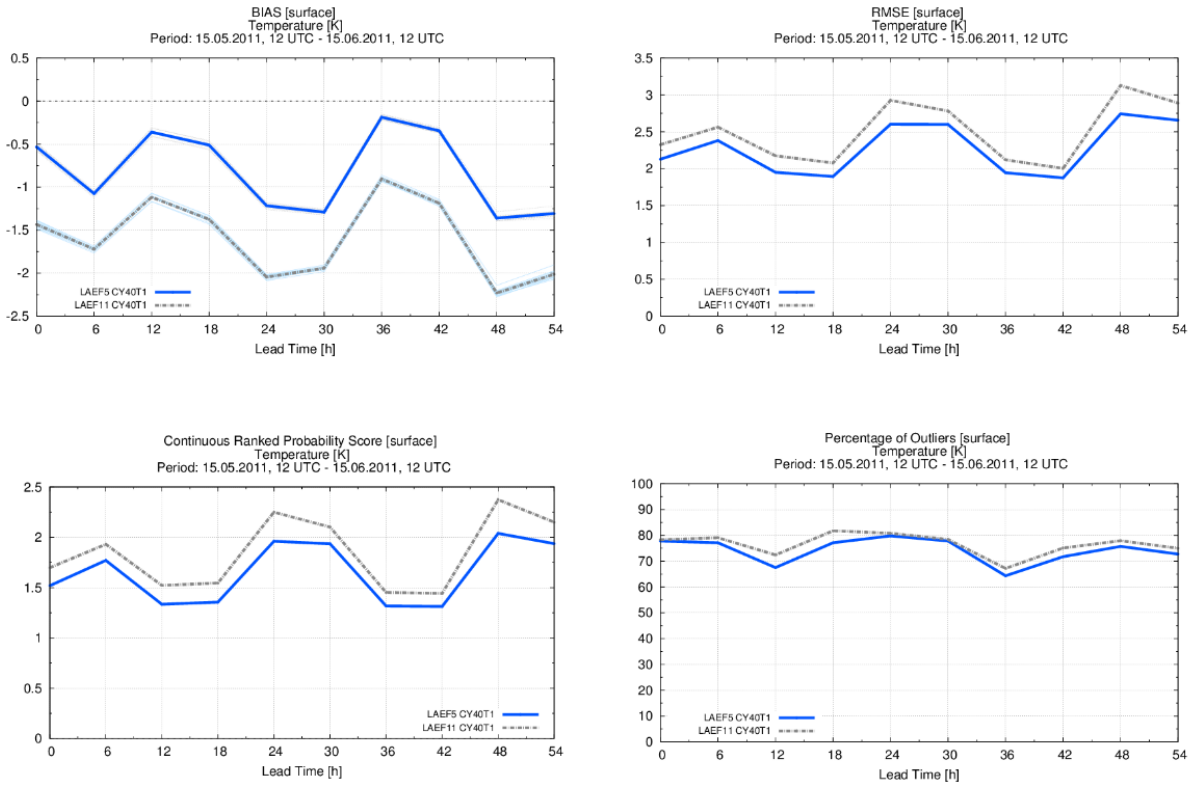

Figure 4: BIAS, RMSE, CRPS and outliers for T2m for new ALADIN-LAEF domain (blue) and the old one (dashed grey).

AROME experimental setup (J. Vivoda, M. Nestiak, M. Dian)

The AROME configuration was ported for CY40T1_bf05. The experimental domain with 2.5 km/63 levels (the same as for ALADIN) has been prepared (Figure 5, left). 1 week experiment (15.-21.2.2016) has been run in downscaling mode (sanity check) for 00, 06, 12 and 18 UTC networks. The outputs were verified against Slovak automatic stations and compared to INCA (in red), operational, ALARO-0 (in blue) and ALARO-1 (in violet) versions for T2m (Figure 4 right). The AROME scores are in orange. 3DVAR assimilation is being technically tested.

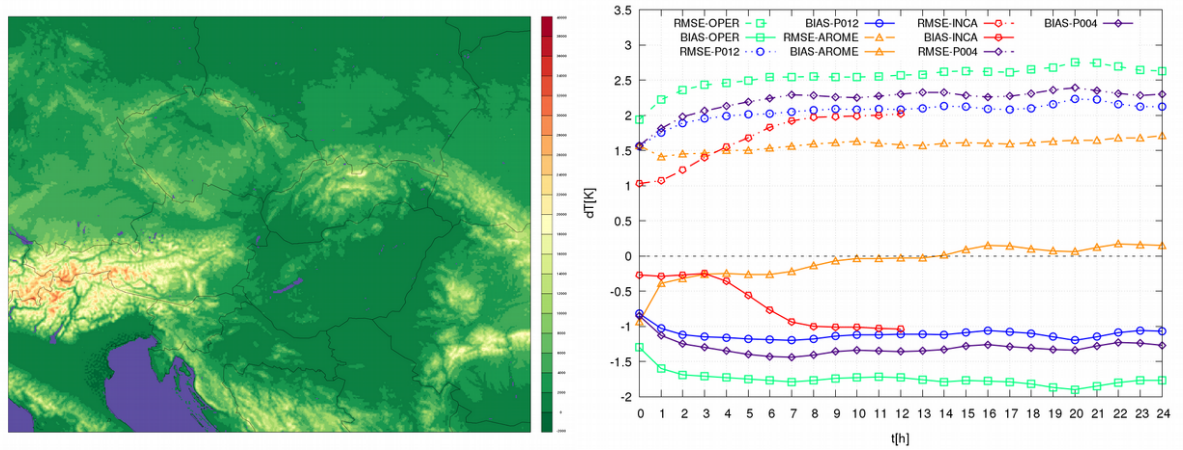

Figure 5: Left: The experimental AROME domain with orography . Right: The scores for 2m temperature for several forecasts explained in the text above.

SURFEX experiment (V. Tarjani, J. Vivoda, R. Habrovsky, I. Prcuch)
Test suite based on the offline SURFEX forced by analyses of INCA-SK nowcasting system aiming to improve the snow cover description was prepared. 2 m temperature and relative humidity, 10 m wind and precipitation (rain, snow based on radar measurements and conventional observations) analyses are used to drive the SURFEX offline. Radiative forcing (short and long wave) is taken from the most actual ALADIN-SK forecast. Forcing time step is 1 hour and SURFEX is initialized with the short-range ALADIN forecast. The snow profile evolution during last winter period have been re-analysed using the three alternative schemes: CROCUS, ES (explicit snow) and D95 (all three are part of the SURFEX export) and compared with measured data where possible. Single-column and also full-domain (INCA-SK) experiments were carried out. SURFEX tuning and verification is now in progress. The preliminary results indicate that all 3 schemes give comparable results (Figure 6).
Experiment aims to prepare a detailed analysis/forecasts of snow profiles in mountain regions of Slovakia (interest for the avalanche prevention center).

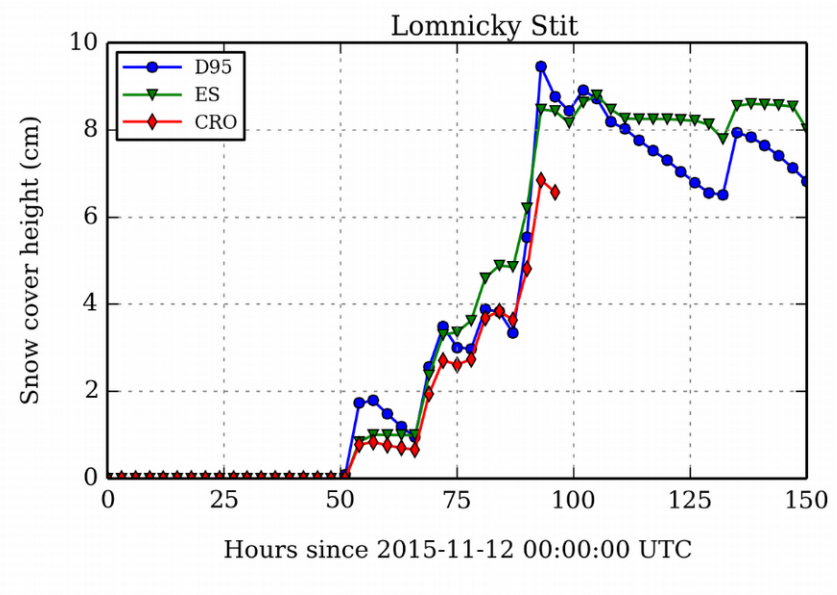

Figure 6: The snow cover height for Lomnicky stit station for 3 different snow schemes: D95 in blue, CROCUS in red and explicit snow scheme (ES) in green.

4 References

Bellus, M., Wang, Y., Meier, F., 2016: Perturbing Surface Initial Conditions in a Regional Ensemble Prediction System. MWR, vol. 144, 3377–3390. DOI: 10.1175/MWR-D-16-0038.1

Belluš, M., 2016: New high resolution ALADIN-LAEF on CY40T1 with ALARO-1 physics. Report on stay at ZAMG, 25/04~13/05 + 06/06~10/06, 2016, Vienna, Austria (available on www.rclace.eu)

Dian, M., 2016: Improving the computation of screen level fields (temperature, moisture). Report on stay at CHMI, Prague, April 2016 (available on www.rclace.eu)

HARMONIE activities at the Icelandic Meteorological Office in 2016

Bolli Pálmason, Guðrún Nína Petersen, Nikolai Nawri, Sigurður Þorsteinsson, Halldór Björnsson

1 Introduction

HARMONIE has been run operationally at the Icelandic Meteorological Office (IMO) since autumn 2011, version 38.1h2 since September 2015. There were little changes made to the operational NWP set up at IMO in 2016. However, in December it was necessary to change the initial SST field due to error in the ECMWF output. During 2016 IMO and the Danish Meteorological Office (DMI) worked on a joint HARMONIE domain for Iceland and southern Greenland (IGA) that became operational in December, see Yang et al. (2017). The reanalysis project, ICRA-2016 (Pálmason et al., 2016; Nawri et al., 2017), finished in early 2016 and the results were investigated during the year.

2 Replacing ECMWF SST and sea ice with fields from MyOcean

On November 8 we noticed an error in the ECMWF high resolution forecasts that are used as initial and boundary conditions for the IMO HARMONIE runs. These problems relate to a long-standing issue with using satellites to identify sea ice cover. In this case sea ice was incorrectly identified at the north and west coast of Iceland and resulted in significantly too low temperatures in coastal areas. Figure 1, left panel, shows the 6 hour HARMONIE forecast of sensible heat flux from the surface. In bay areas in northwestern and western Iceland, close to the coast, sea ice was incorrectly identified. The resulting sensible heat flux is towards the surface (up to 77 W/m2) while over nearby ocean undisturbed by the error the flux is of similar or larger magnitude from the surface. ECMWF implemented a new cycle (cycle 43rl) at the end of November but there were no improvements in this matter. Early in December ECMWF installed a temporary fix to the SST that decreased the error, but did not remove it. Internally these low temperatures were becoming a significant problem, not only for the medium range but also for our HARMONIE runs. A decision was made to replace the ECMWF sea ice fraction (CI) and SST with data from the ocean model MyOcean until a permanent solution was found at ECMWF, see Figure 1, right panel. The solution replaces the CI and SST in the ECMWF model data for the HARMONIE analysis step and since these parameters are kept constant for the whole forecast range it eliminates the problem. The solution was implemented on December 3.

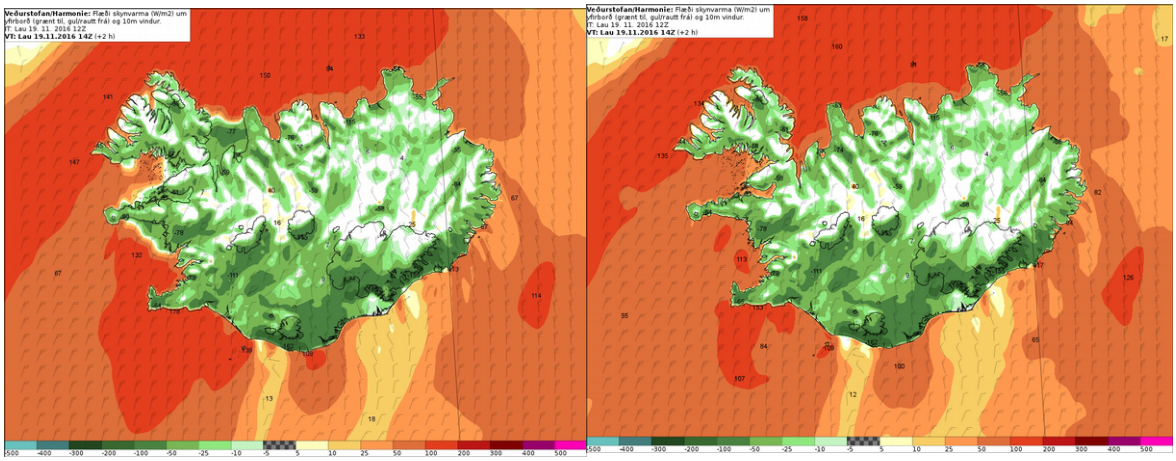

Figure 1: Sensible heat flux (W/m2), positive values are from the surface. Forecast 2016-11-19 12 UTC + 6h. With initial values of sea ice and SST from ECMWF (right panel) and MyOcean (left panel).

3 ICRA-2016: Parameterisation of sensible heat fluxes at the surface

We investigated the role of the turbulent sensible heat flux parameterisation on low-level air temperature biases. The basis for this analysis was data obtained during the ICRA-2016 reanalysis project conducted by IMO between the autumn of 2015 and the spring of 2016 (Pálmason et al., 2016). The model version used was HARMONIE 38h1.2, run in numerical weather prediction mode, with Arome physics, SURFEX 7.2 surface scheme, atmospheric analysis in blending mode, CANARI_OI_MAIN for inline surface analysis, applied before the atmospheric analysis. Initial and boundary conditions were provided by ERA-Interim reanalyses from ECMWF.
The data used here is for 2010, as during the cold months of that year the western half of Iceland was predominantly snow free, and the eastern half predominantly snow covered.
Sensible heat fluxes from the ground to the atmosphere can be parameterised as,

$$H = - \rho \, Cp \, (T_{2m} - T_{s)} / R_{ah} \, , \qquad (1)$$

with air density ρ, specific heat capacity of air Cp, surface air temperature T_s, 2-m air temperature T_{2m}, and aerodynamic resistance to heat transfer R_{ah} (e.g. Viney, 1991). Sensible heat fluxes then depend on the low-level vertical air temperature gradient, and the intensity of turbulence near the ground.

Sensible heat fluxes and vertical temperature gradients

As shown in Figure 2, with positive temperature lapse rates, there is indeed a near-linear relationship between the downward sensible heat flux, H, and the vertical temperature gradient ($T_{2m} - T_s$). However, within inversion layers, contrary to the relationship suggested by (1), turbulence effects on sensible heat transfer increase in significance, whereby a larger temperature gradient is counteracted by increased stability. These effects fall into two main categories:

- Increased overlying temperature (stronger inversion) leading to increased stability, reduced turbulence, and mostly unaffected downward sensible heat flux. As seen below, this is usually associated with weak wind conditions.
- Despite an unchanged vertical temperature gradient, turbulence and downward sensible heat flux are increased. As seen below, this is usually associated with increased turbulence due to strong wind conditions.

Sensible heat fluxes and low-level wind speed

As shown in Figure 3, during the cold season and with a prevalence of near-surface inversion layers, sensible heat transfer is driven primarily by low-level wind speed, rather than the vertical temperature gradient. This effectively decouples near-surface and overlying temperatures, resulting in extreme low-level temperature profiles and negative biases. This effect is particularly strong under weak wind conditions, when any warming on the overlying model levels is essentially ignored by the surface scheme.

Conclusions

Based on lapse rate, a switch happens in the model between two approximate linear relationships:

- With a positive lapse rate, changes in sensible heat flux are driven mostly by changes in the magnitude of the near-surface lapse rate.
- With a negative lapse rate (inversions), changes in sensible heat flux are driven mostly by changes in low-level wind speed.

Snow cover contributes to the creation of inversion layers, and therefore to a decoupling between temperatures on the lowest model levels and those closer to the surface, as determined by SURFEX.
However, snow-free grid points, especially in January 2010, show relationships between lapse rate, wind speed, and sensible heat flux that are very similar to those of snow-covered grid points (see again Figures 2 and 3).

Therefore, the main factors contributing to the large negative 2-m temperature biases in HARMONIE simulations in winter appear to be low-level temperature inversions, while snow characteristics, such as maximum albedo and emissivity, only have an indirect effect.
Significant improvement in the simulation of 2-m temperature could be achieved if the same sensible heat flux parameterisation that is used for positive lapse rates were also applied within inversion layers, rather than a more sophisticated turbulence scheme that emphasises the role of the low-level wind.

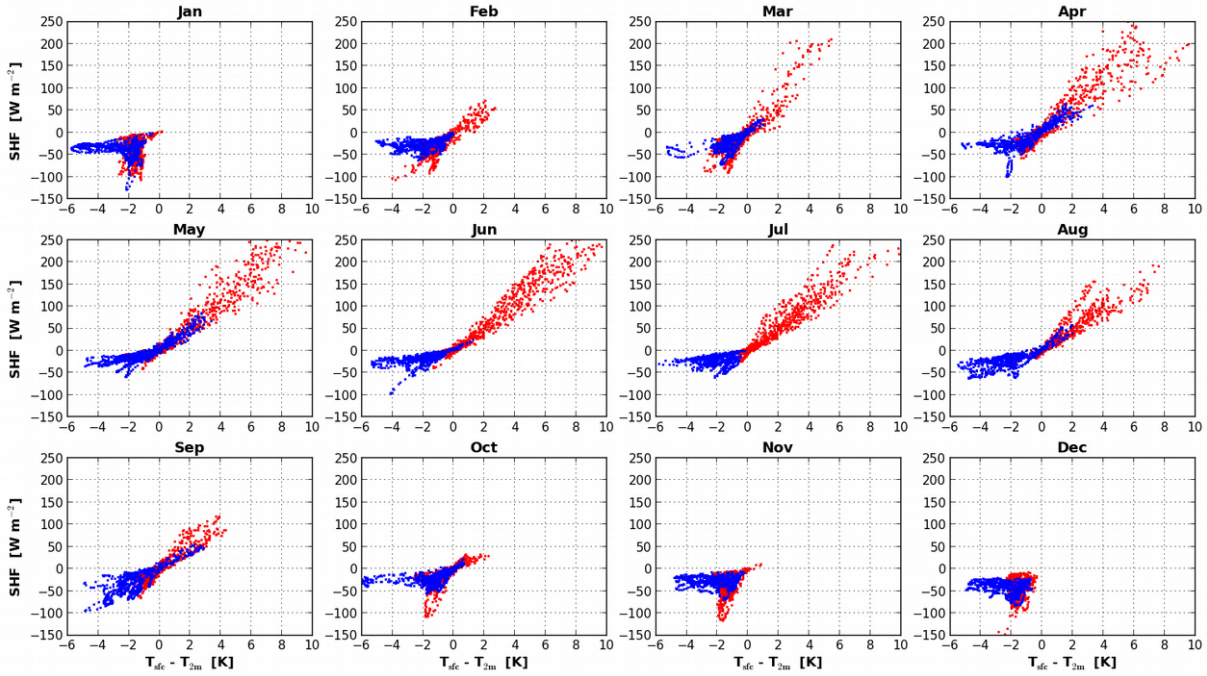

Figure 2: Hourly mean values of the surface-to-2-m temperature lapse rate and sensible heat flux. Red dots represent spatial averages over all snow-free land-based grid points, whereas blue dots represent spatial averages over all snow-covered grid points.

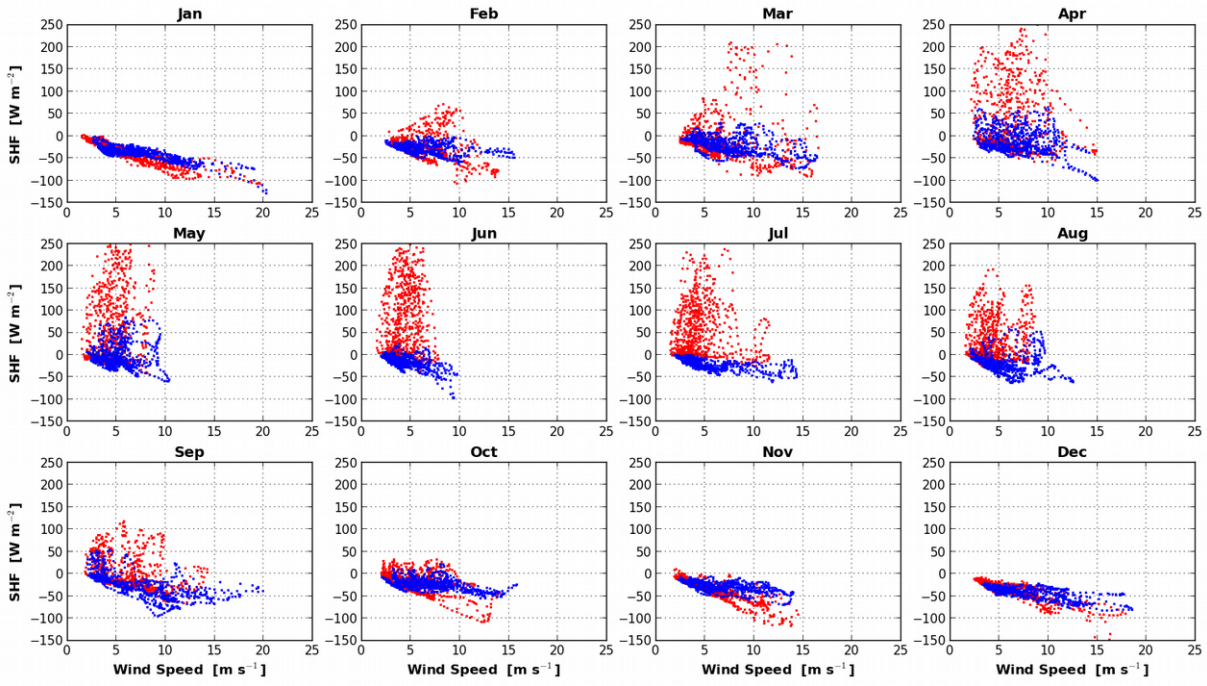

Figure 3: As Figure 2, but for the relationship between 10-m wind speed and sensible heat flux.

4 References

Nawri, N., B. Pálmason, S. Thorsteinsson, G. N. Petersen, H. Björnsson, 2017: The ICRA-2016 atmospheric reanalysis project for Iceland, Report, Icelandic Meteorological Office, Reykjavik, Iceland. In preparation.

Pálmason, B., S. Thorsteinsson, N. Nawri, G. N. Petersen, H. Björnsson, 2016: HARMONIE activities at IMO in 2015, ALADIN-HIRLAM Newsletter no.6, February 2016, 72–75.

Viney, N. R., 1991: An empirical expression for aerodynamic resistance in the unstable boundary layer, Boundary-Layer Meteorology, 56 (4), 381–393.

Yang, X., B. Pálmason, B. S. Andersen B. H. Sass,, B. Amstrup, M. Dahlbom, C. Petersen, K. P. Nielsen, R. Mottram, N. W. Nielsen, A. Mahura, S. Thorsteinsson, N. Nawri, G. N. Petersen, 2017: IGA, Joint Operational HARMONIE by DMI and IMO, ALADIN-HIRLAM Newsletter no.8, February 2017.

Modelling activities at the Hungarian Meteorological Service

Antal Fischer, Viktória Homonnai, Máté Mile, Panna Sepsi, Balázs Szintai, Mihály Szűcs
Hungarian Meteorological Service

1 Introduction

This short paper describes the current research and development activities at the Hungarian Meteorological Service (OMSZ) related to the ALADIN/AROME modelling system. At the end of 2016, three limited are systems from the ALADIN/AROME model family are run operationally at OMSZ, which are described in Table 1.

Table 1: Operational model configurations at OMSZ.

	AROME	**ALADIN**	**ALADIN-EPS** (11 members)
Resolution	2.5 km	8 km	8km
Levels	60	49	49
Number of points	500x320	360x320	360x320
Modle version	CY38T1	CY38T1 (ALARO-1)	CY38T1 (ALARO-1)
Boundaries	ECMWF deterministic (1h coupling)	ECMWF deterministic (3h coupling)	ECMWF ENS (6h coupling)
Runs per day	00, 06, 12, 18 (+48h), 03, 09, 15, 21 (+36h),	00 (+60h), 06 (+48h), 12 (+60h), 18 (+36h)	18 (+60h)
Data Assimilation	3 hourly (SYNOP, TEMP, AMDAR, MODE-S)	6 hourly (SYNOP, TEMP, AMDAR, SEVIRI, AMV, ATOVS)	-

This paper describes the developments related to these operational systems.

2 Research and development activities

Eight AROME forecast runs per day

Since 9th March 2016 AROME at the Hungarian Meteorological Service is run eight times per day, using analyses from the three hourly Rapid Update Cycle (RUC) of AROME. For the time being the runs starting at 03, 09, 15 and 21 UTC are run for +36h only, but this is planned to be extended in future. The main motivation for the introduction of the new forecast runs was that in situations with severe weather events the more frequently updated AROME products could help forecasters in issuing warnings. Figure 1 show scores of the new AROME runs over Hungary during summer 2016. It can be concluded that the new runs could give a benefit as compared to older runs only in the first 3-4 hours of the forecasts (especially for temperature), after this range the systematic errors of the model dominate. However, it is expected that after the operational introduction of the assimilation of remote sensing instruments (Radar, satellites, GNSS) this time range could be extended.

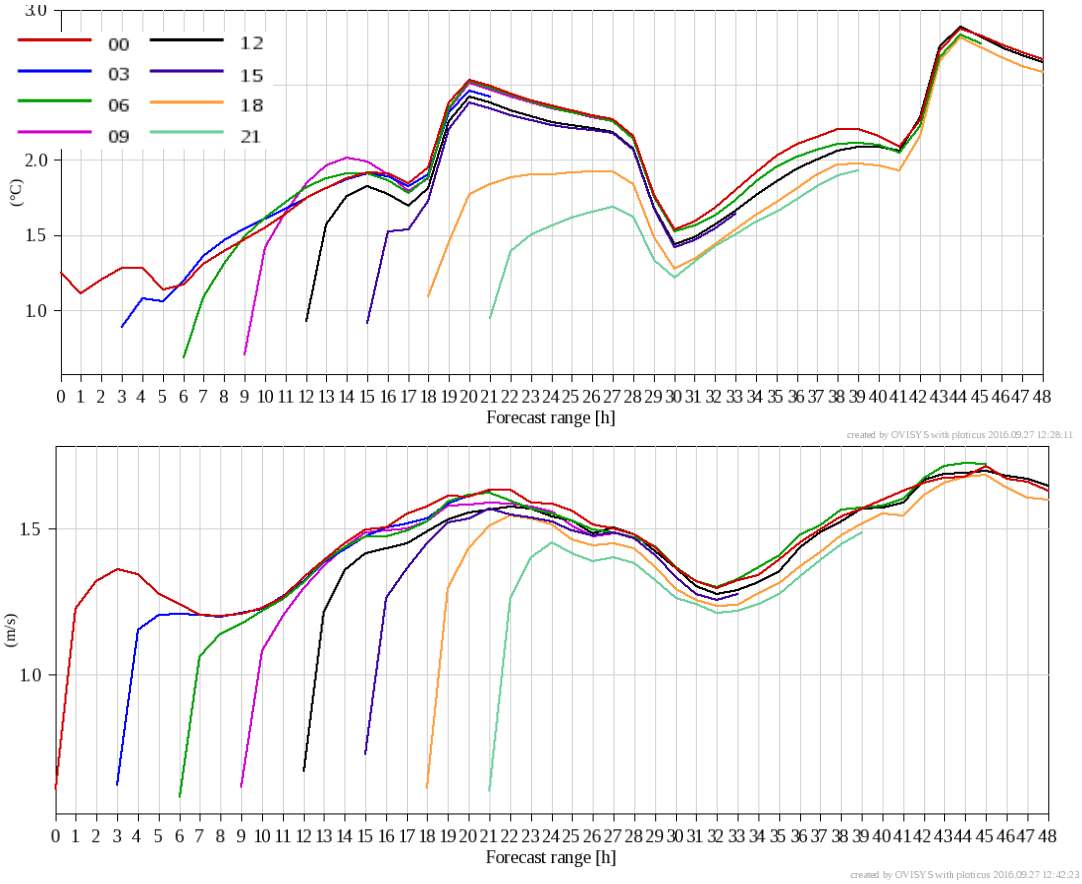

Figure 1. RMSE of 2 metre temperature (upper panel) and 10 metre wind speed (lower panel) for the eight AROME runs for the period 2016-06-01 – 2016-08-31.

Assimilation of AMDAR-humidity

Direct temperature and wind measurements from aircraft are important data in our operational AROME data assimilation system because we use only conventional observations. Recently, humidity data are also available in more and more AMDAR reports not only in the USA but also in Europe. These data are especially useful when the aircraft is in descending or ascending phase so it observes vertical characteristics of the troposphere more frequently than radiosondes. The sensor measures mixing ratio of water vapor which can be converted to specific humidity for the assimilation.

As a first step radiosonde and aircraft humidity data were compared when both observation types were available. Visual check of vertical profiles indicates a good agreement between the two measurements so in the next step only single specific humidity profile from AMDAR report was assimilated. On the vertical profile of the first guess and the analysis it can be seen well that after the assimilation, humidity profile is closer to the observations, but without these measurements this is not the case (Fig. 2).

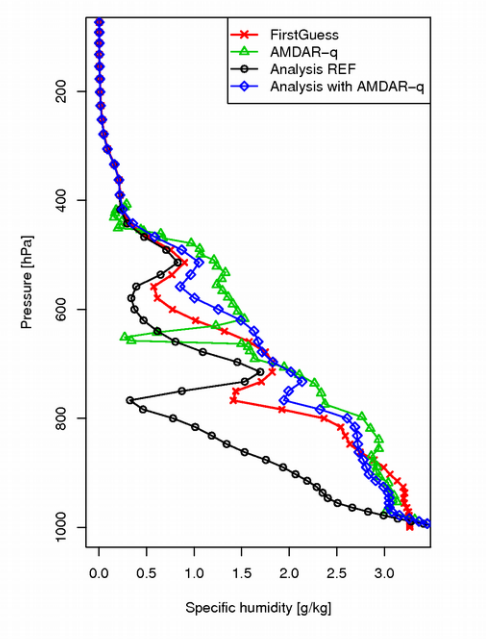

Figure 2. Vertical profiles of specific humidity of AMDAR (green), first guess (red), analysis without AMDAR-q (black) and analysis with AMDAR-q (blue) on 25th March 2016 at 18UTC over Budapest.

The impacts of AMDAR humidity were studied on a longer time period. A summer period was chosen from 1st to 22th June 2016. 24 hours forecasts from 00, 09 and 12 UTC were prepared with 3-hour data assimilation cycle. Biggest impact can be seen in the 09 UTC run (no radiosondes), especially in cloud cover (Fig. 3).

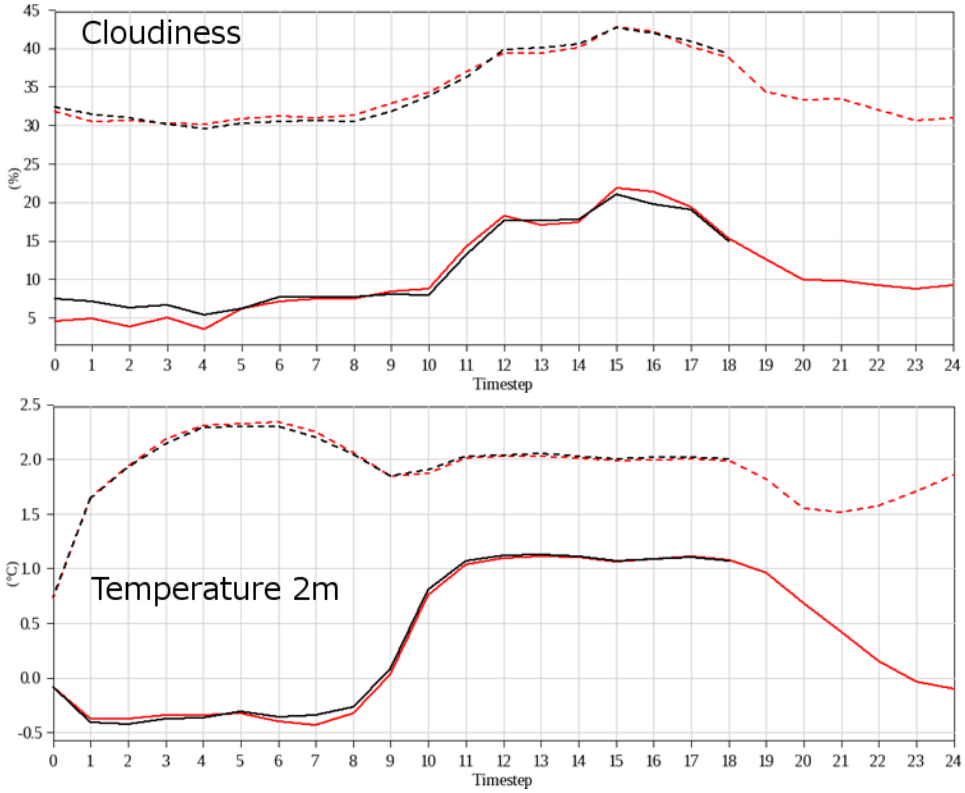

Figure 3. BIAS (solid) and RMSE (dashed) verification scores as a function of lead time for the three-weeks summer period (09 UTC runs). SYNOP stations below 400 m were used for the calculations. Black lines indicate the operational run and red lines are the experiment with additional AMDAR humidity data.

Changes in Lateral Boundary Conditions of ALEPS at the Hungarian Meteorological Service

OMSZ's limited-area ensemble activity started almost a decade ago. Météo-France's global ensemble system (Prévision d'Ensemble ARPEGE, or PEARP) had been used to produce boundary conditions until November 2016.

OMSZ had been interested in ECMWF's ENS boundary conditions (ENS-BCs) because of the possibility of using the same coupling method for ensemble than high resolution model. Since Hungary is a Co-operating State, ENS-BCs were not available until the extension of ECMWF's Optional BC Project in July 2015, which made ENS-BCs available in a similar way to HRES-BCs.

Experiments proved that ENS-coupled version of OMSZ's limited-area ensemble system (ALEPS-ENS) produced forecasts that were significantly different from those produced by the previous version (ALEPS-PEARP). Single members were more accurate for most variables, so the root-mean-square error (RMSE) of the ensemble mean was lower. At the same time, the system was less dispersive (Fig 4). These results motivated us to change LBCs in our operational system.

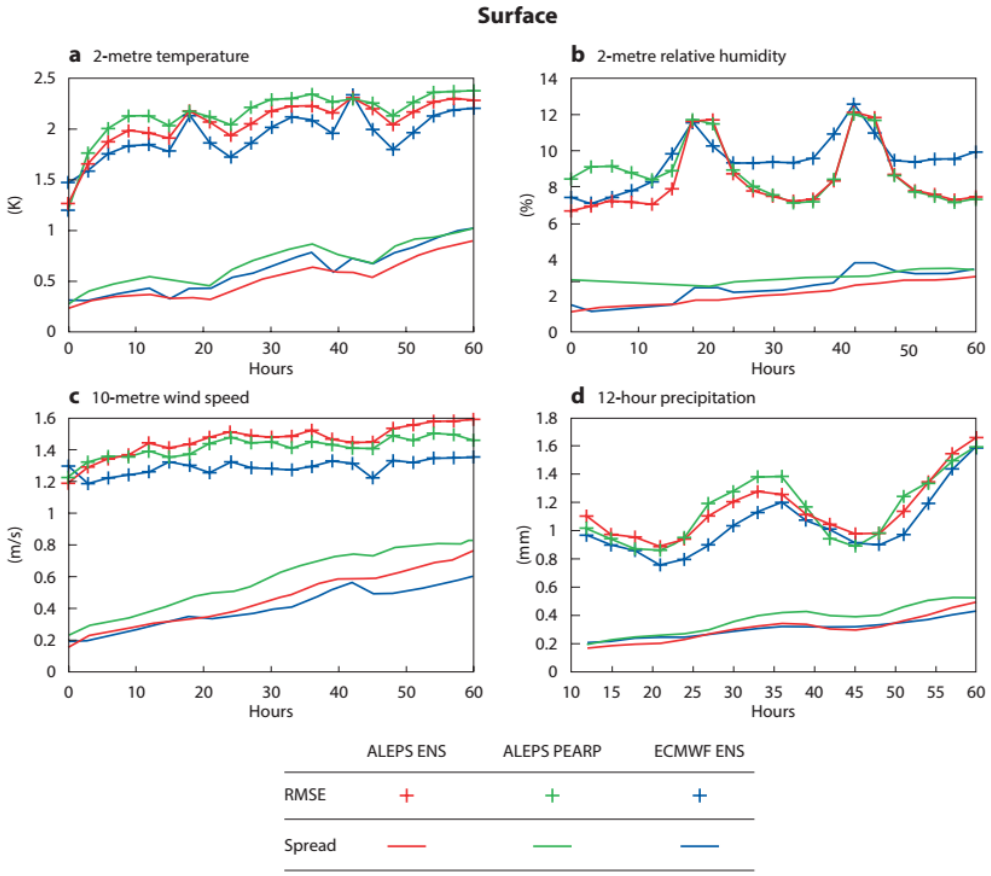

Figure 4. RMSE of the ensemble mean and spread around the ensemble mean of forecasts up to 60 hours ahead run at 18 UTC every day between 11 December 2015 and 31 January 2016 for (a) 2-meter temperature, (b) 2-meter relative humidity, (c) 10-meter wind speed, and (d) 12-hour precipitation

In OMSZ's modified operational system (ALEPS-ENS), we integrate 11 ensemble members using boundary conditions derived by simple dynamical downscaling of the 11 members of ECMWF ENS. The first is coupled to the ENS control and the others to the first 10 of the 50 perturbed members. Model runs start at 18 UTC every day and cover the next 60 hours.

Atmospheric perturbations are derived from interpolated global ICs and LBCs while surface fields are identical for all ensemble members at the beginning of the model runs. Coupling is realized every three hours based on the outputs of the 18 UTC ECMWF's ENS run. In addition, we get ENS-BCs for 12-hour periods from the other three ENS production times (00, 06 and 12 UTC). These can support our future plans for maintaining an ensemble of data assimilation cycles.

The surface processes in ECMWF's Integrated Forecasting System (IFS) are quite different from those in the ARPEGE and ALADIN models, which makes not feasible to initialize surface fields directly from the IFS at the beginning of an ALADIN run. Since there is no surface data assimilation at OMSZ, the issue can simply be resolved by obtaining surface fields from the deterministic ALADIN surface analysis files. However, if such a procedure were to be used for all members, it would lead to the elimination of the surface field perturbations in ENS. Since we would like to preserve such perturbations, we decided to add them to the surface fields obtained from the ALADIN analysis.

For the integrations we use the ALADIN model in hydrostatic mode with 8 km horizontal resolution and 49 model levels. Our domain covers most of continental Europe. Parametrized processes are described by the ALARO physics package.

ALADIN in Poland - 2016

Marek Jerczynski, Bogdan Bochenek, Marcin Kolonko, Malgorzata Szczech-Gajewska, Jadwiga Woyciechowska

1 Introduction

Various efforts were carried out at IMGW in 2016. Among them were: switching to AROME 2km, further testing and usage of CROCUS snowpack for hydrologic and meteorological purposes, installation of HARP verification package for operational use and work on data assimilation, with computation of B matrix.

2 Operational activities

During 2016 two operational NWP suites were used at IMGW. First was sub-regional one based on ALARO-1 model, with 4.0 km resolution. Its domain covers almost whole area of Europe (see Figure 1). Second was high resolution suite, which domain covers Central Europe. It has 2 km grid-size and is based on AROME model (see Figure 2). Both suites use CY40T1bf5 code version of ALADIN system. Table 1 summarizes main features of the suites.

Table 1: Current operational configurations

Suite	Sub-regional	HiRes
Domain	E040	P020
Model	CY40T1 / ALARO-1	CY40T1 / AROME
Resolution	4.0 km	2.0 km
Area	3156 km x 3156 km	1600 km x 1600 km
Grid	800 x 800	810 x 810
Levels	60	60
Coupling zone	16	10
Runs	4 / day	4 / day
Starting times	00, 06, 12, 18 UTC	00, 06, 12, 18 UTC
Forecast range	66h, 66h, 66h, 60h	30h
Coupling model	ARPEGE	ALARO - E040
Coupling frequency	3h	1h

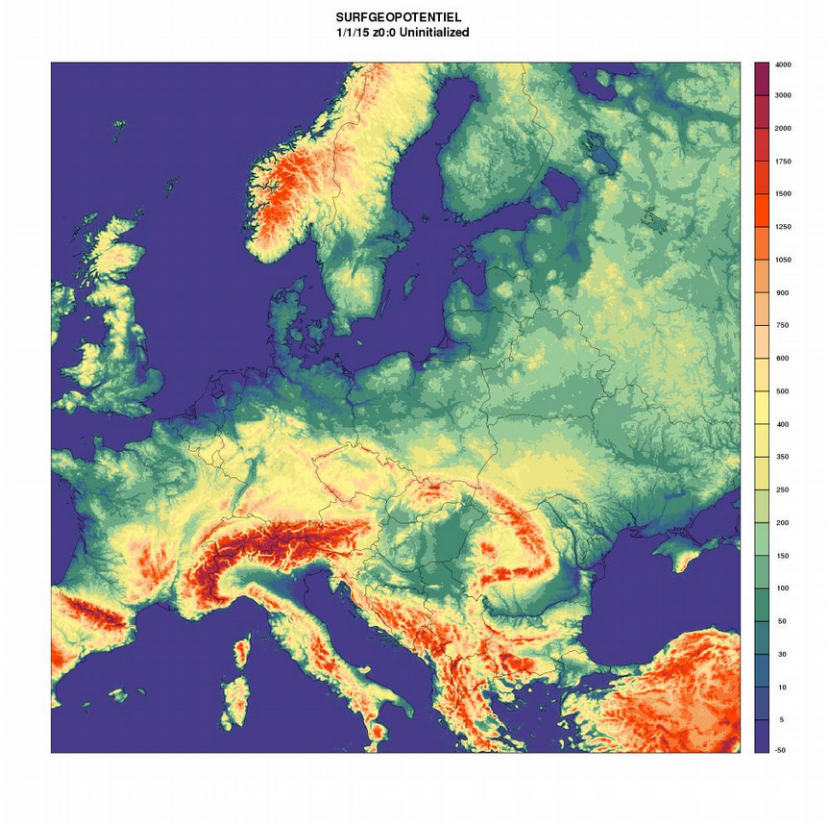

Figure 1: Domain E040

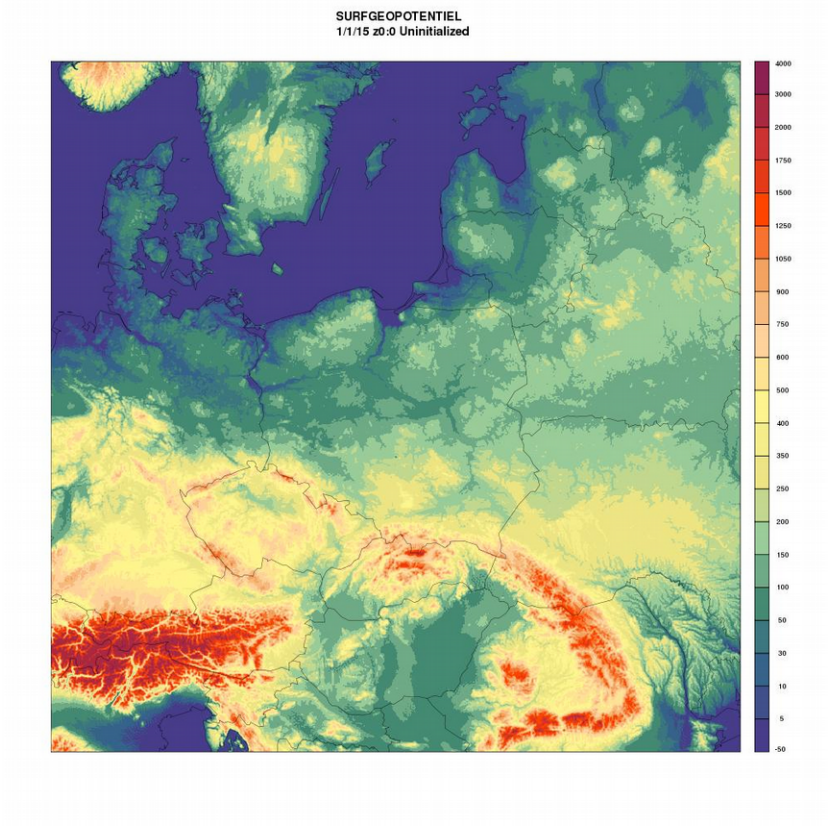

Figure 2: Domain P020

Further work was done with implementation and testing of snow model CROCUS. Validation of model results was done for various winter seasons, stations from Tatra Mountains are shown, (see Figure 3) and new applications were prepared, accumulation of SWE in Sola river basin is presented (see Figure 4). Impact of CROSUS results on hydrological models is currently studied for some river basins in Poland.

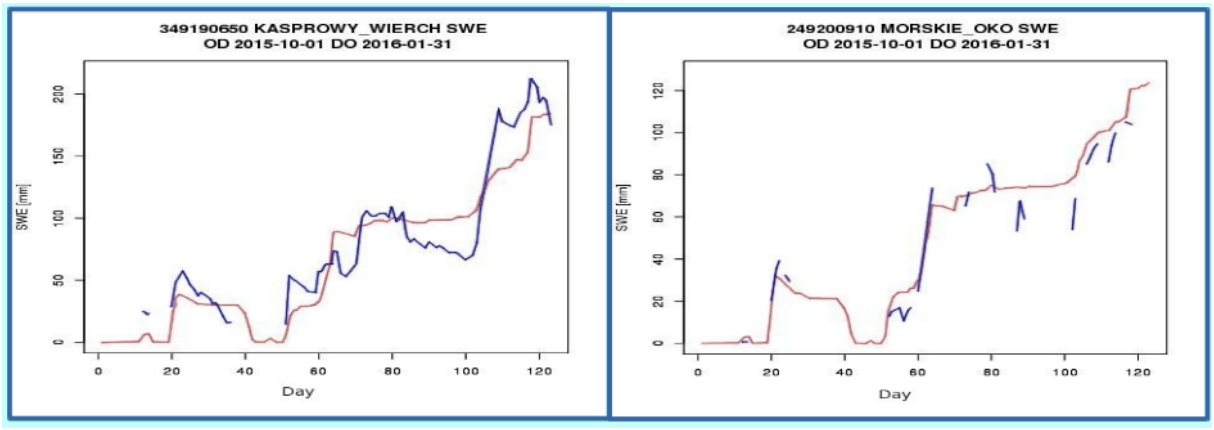

Figure 3: CROCUS validation

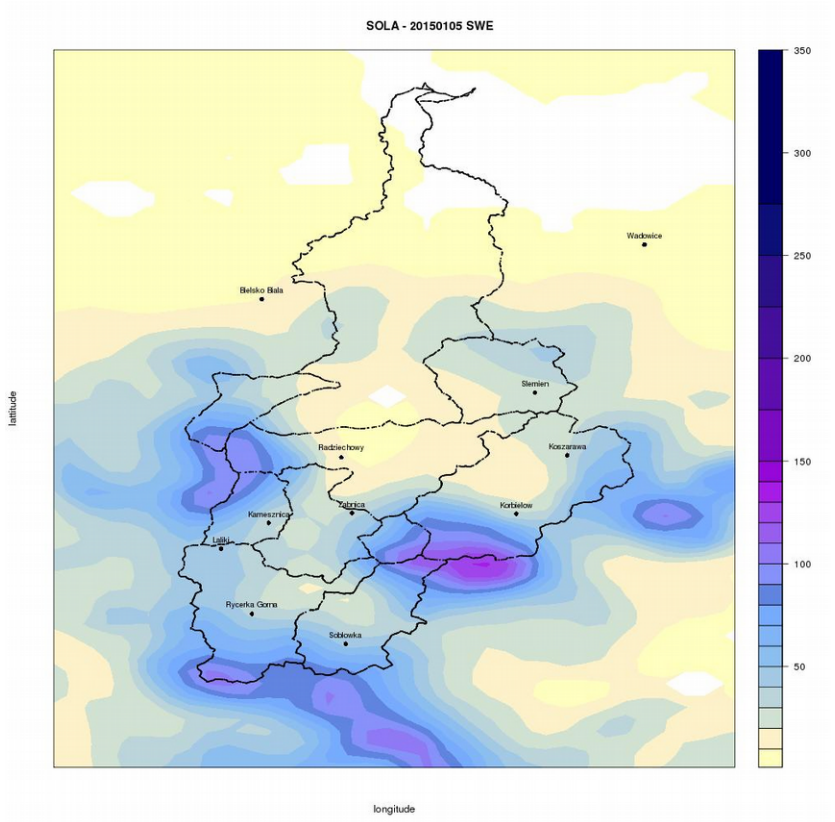

Figure 4: CROCUS applications

HARP – Hirlam-Aladin R-Package is a common framework for verification. It already runs operationally for Aladin-Poland. As it works on-line user can choose parameters such as: 2m temperature, msl pressure, 10m wind speed and uv-direction, 12h precipitation accumulation, total cloud cover and 2m relative humidity. User can also determine a period for verification and kind of scores (Spread & Skill, Mean bias, Median bias or Mad) to plot. This point-to-point verification can be

done as well for single station as for all stations together, and it is used for deterministic forecast. There are three meteorological models we may verify: ALARO, AROME and GFS. Observational data used for this verification are data from synoptic stations (see Figure 5).

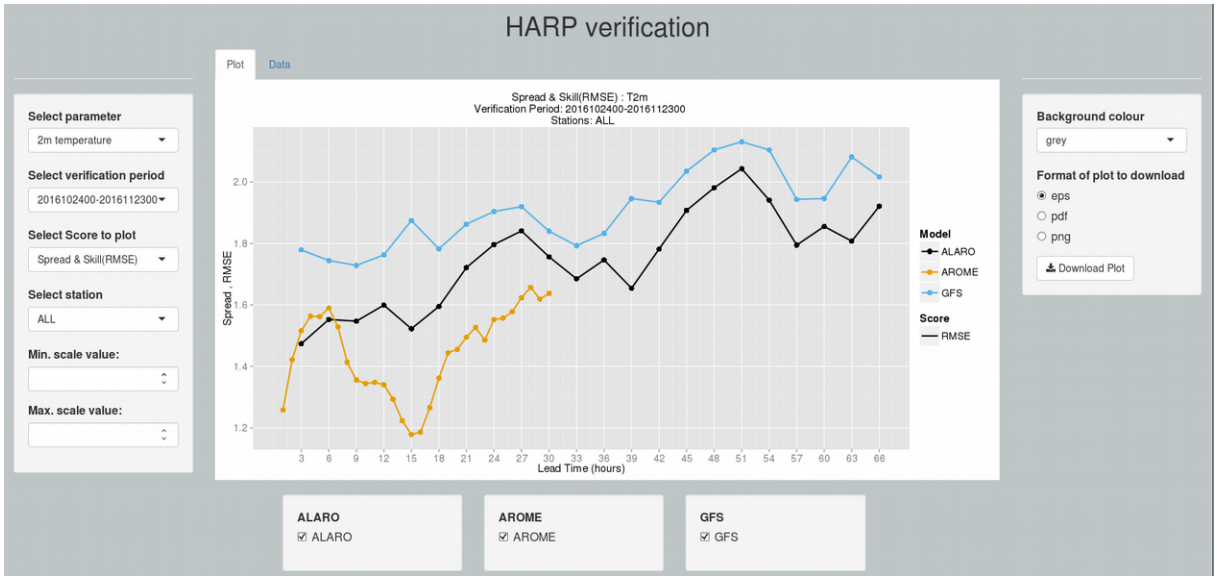

Figure 5: HARP in Poland

Preparations for Data Assimilation in AROME had started. B matrix was built on the base of our domain AROME ensamble forecast, with LBC from AEARP. This domain was with 799x799 grid points, 2km horizontal resolution and 60 vertical levels. Ensemble forecast was run for 6 members, two times per day with lenght for 30 days (see Figure 6).

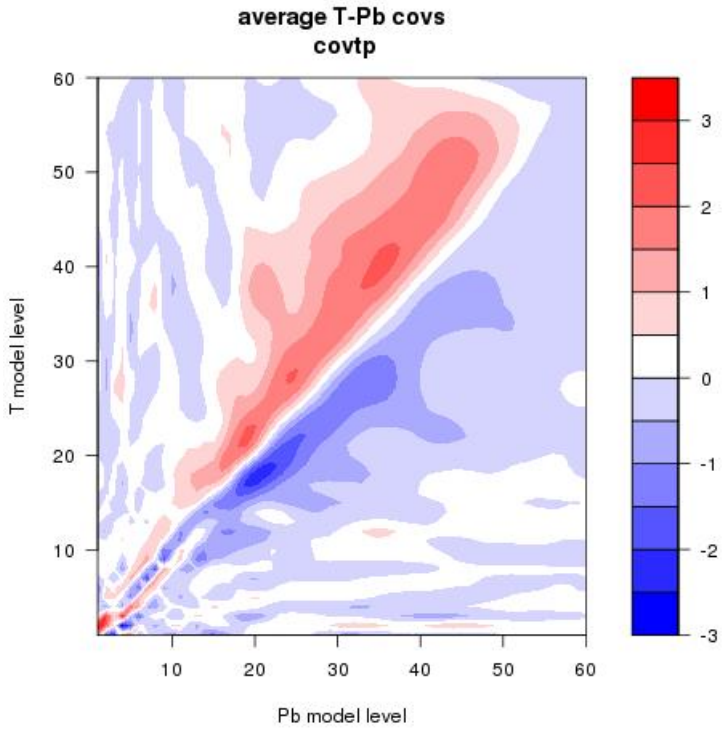

Figure 6 B matrix for AROME in Poland.

RMI-EPS: a prototype convection-permitting EPS for Belgium

Geert Smet

1 Introduction

In recent years, there have been several high-profile thunderstorms in Belgium, in particular the Pukkelpop thunderstorm of 2011, resulting in five casualties, and the Pentecost storms of 2014, leading to hundreds of million euros of damage. These cases highlighted again the importance of having a good forecast and warning system for severe weather. Probabilistic guidance from ensemble forecasts should be an important forecast tool for these events, since predicting their exact timing, location and intensity is generally very difficult, if not impossible.

With improved prediction of severe weather in mind, most European countries have started with the development of convection-permitting EPS in the last few years. At the Royal Meteorological Institute of Belgium (RMI), an experimental high-resolution (2.5km) ensemble with 11 ALARO members and 11 AROME members is currently being tested. This is meant to be a prototype for a future operational convection-permitting EPS over Belgium. In this article, we describe the current set-up of the system and discuss some forecast results for several thunderstorm episodes in August 2015. The performance of the ALARO and AROME members, and the usefulness of combining them in an ensemble is investigated. Additionally, a comparison is made with the global EPS of ECMWF and the pan-European mesoscale GLAMEPS. We conclude with our future plans toward an operational convection-permitting RMI-EPS.

2 Ensemble system configuration

The RMI-EPS system currently consists of 22 ensemble members, 11 with AROME physics and 11 with ALARO physics, all using cy38h1.1 with SURFEX, and running at 2.5km horizontal resolution with 65 vertical levels. Initial condition (IC) perturbations and lateral boundary conditions (LBC) are taken from the ensemble system of ECMWF (hereafter referred to as ECEPS). Each member has an independent surface assimilation cycle (CANARI). There are two control members, one AROME control (mbr000) and one ALARO control (mbr001), that both take their lateral boundary conditions from the ECEPS control member. They both have a 3DVAR (upper-air) data-assimilation cycle. Only conventional observations (SYNOP, AIRCRAFT, BUOY, TEMP en PILOT) are used, no satellite or radar data.

Initial conditions for the perturbed RMI-EPS members are created by adding initial perturbations of ECEPS members to the analysis (after 3DVAR) of the control members. This is done in pairs, in order to prevent that all perturbations of one type are added to only one type of physics. Namely the first perturbed member is an ALARO member (mbr002), taking IC perturbations and LBC from the first perturbed member of ECEPS, the next two members are then AROME members (mbr003 and mbr004) taking IC perturbations and LBC from the second and third perturbed member of ECEPS, and then again two ALARO members (mbr005 and mbr006), taking IC perturbations and LBC from the fourth and fifth perturbed member of ECEPS, and so on. This gives 10+1 AROME members and 10+1 ALARO members.

Currently, the forecast range is 36 hours, twice a day at 00 and 12 UTC, with a 6 hour data-assimilation cycle at 06 and 18 UTC. Computations are done at ECMWF's computing facilities (ecgate/cca) and only some standard

products (probability maps, forecasts interpolated to locations,...) will be automatically transfered to RMI. A combination of the HarmonEPS system (cy38h1.1) with RMI preprocessing and postprocessing scripts is used. In order not to have to recompute the B-matrix for the data-assimilation, and to possibly allow comparisons with convection-permitting EPS from Météo-France and DWD, first tests were done with the default HarmonEPS_1 domain, shown in figure 1. In the future, a custom domain centered over Belgium will be defined and tested.

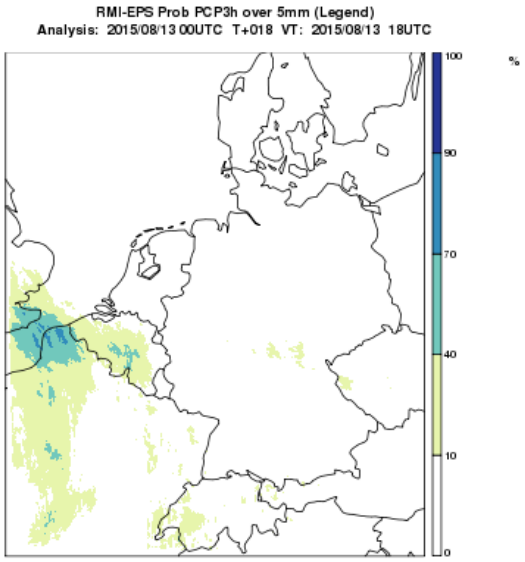

Figure 1: Probability plot RMI-EPS for 3h accumulated precipitation ($> 5mm$). Forecast of 13 August 2015 (00 UTC run) over full domain.

3 Thunderstorm case studies

We studied a series of thunderstorm events over Belgium occurring in August 2015, with generally positive results for the RMI-EPS system. As an illustration, we take the thunderstorms of 13 August 2015 shown in figure 2. This case was interesting as our operational deterministic LAM model gave very little precipitation over Belgium (figure 2), while our forecasters nevertheless gave a 'code orange' warning for the west of the country. In reality, the largest amount of precipitation was actually observed in the east of the country, and this was in fact nicely predicted by the RMI-EPS, as shown by the regional probabilities in figure 3.

4 Verification

A preliminary statistical verification over 15 forecasts around several thunderstorm episodes in August 2015 also gave encouraging results. Figure 5 and 6 show the RMSE and ensemble spread for 6h accumulated precipitation and 2-meter temperature, with scores being averages over 10 standard WMO weather stations evenly spread over the whole of Belgium (as shown in figure 4).

For precipitation, the RMSE of RMI-EPS is comparable with those of GLAMEPS and ECEPS, while the ensemble spread is clearly larger and closer to the RMSE. For 2-meter temperature, the RMSE is somewhat smaller than GLAMEPS and ECEPS in the first 24h, and somewhat larger thereafter. The ensemble spread on the other hand is clearly worse than GLAMEPS, but still much better than ECEPS.

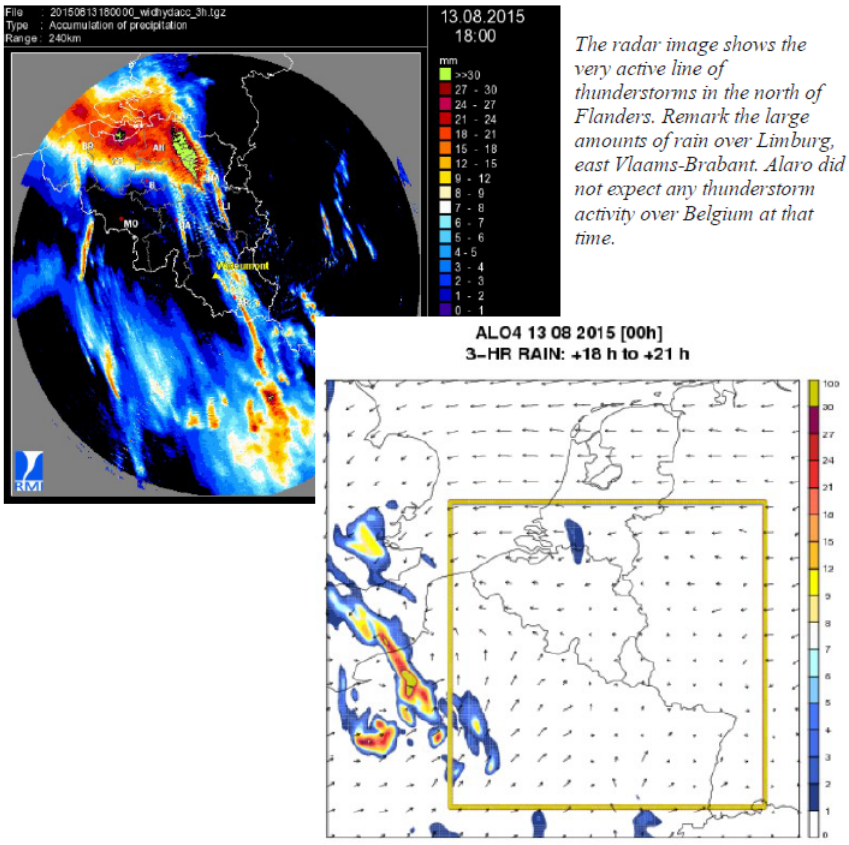

The radar image shows the very active line of thunderstorms in the north of Flanders. Remark the large amounts of rain over Limburg, east Vlaams-Brabant. Alaro did not expect any thunderstorm activity over Belgium at that time.

Figure 2: Thunderstorm over Belgium on 13 August 2015: radar (left) and operational deterministic model ALARO4 (right). (Courtesy: S. Caluwaerts)

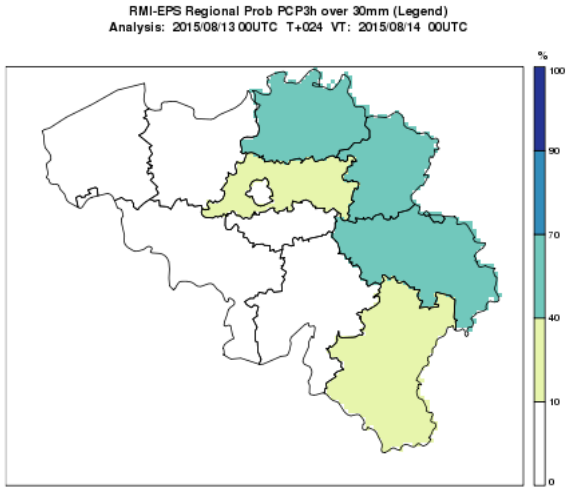

Figure 3: Regional probability plot RMI-EPS for 3h accumulated precipitation ($> 30mm$). Forecast of 13 August 2015 (00 UTC) for lead time +24h.

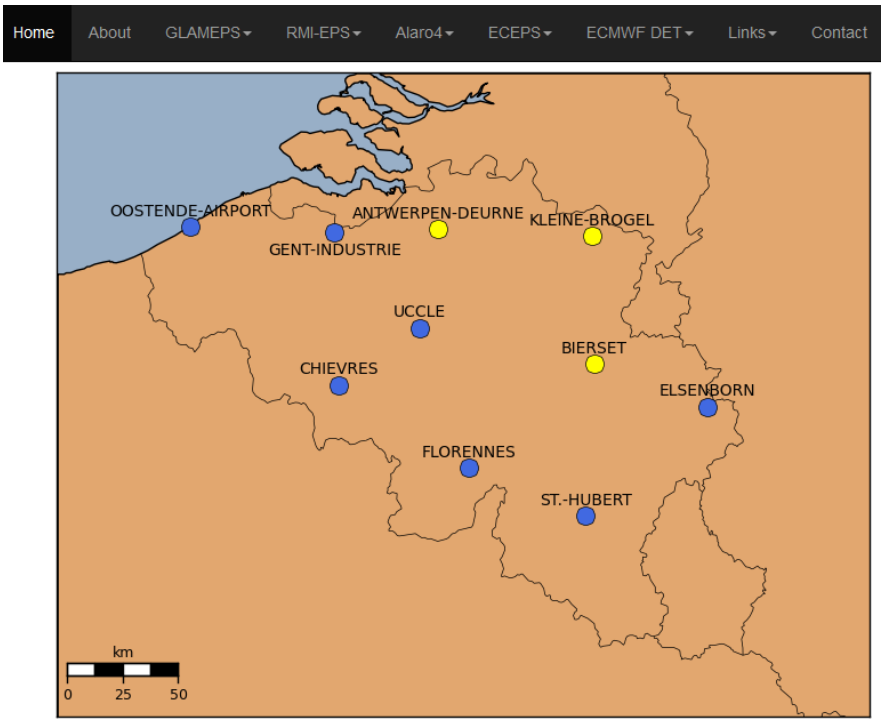

Figure 4: Location of the 10 standard synop stations used in the verification.

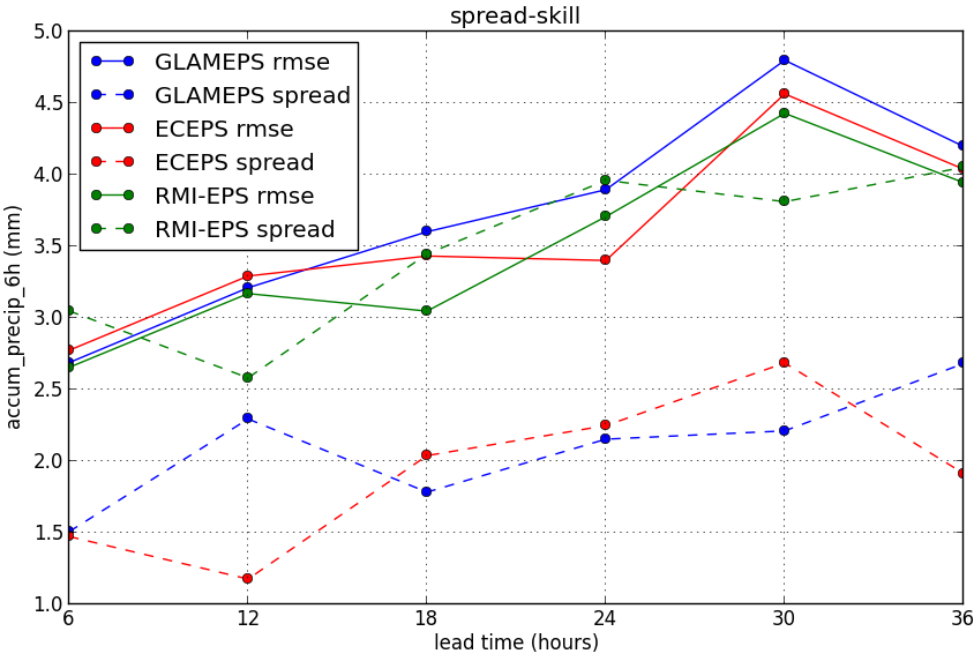

Figure 5: RMSE and spread for 6h accumulated precipitation: thunderstorm cases of August 2015. Comparison of RMI-EPS with GLAMEPS and ECEPS.

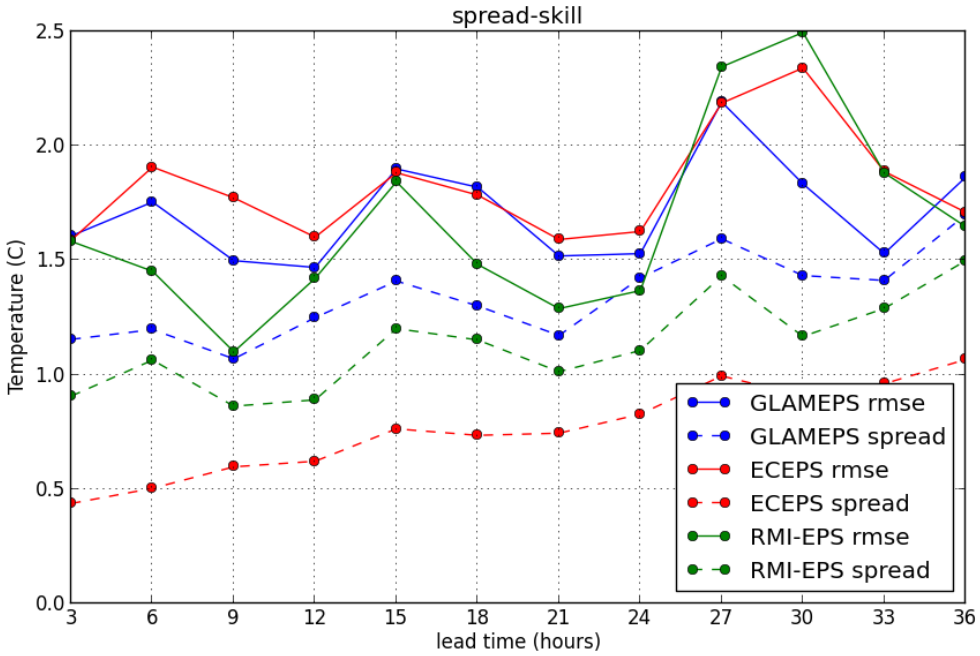

Figure 6: RMSE and spread for 2-meter temperature: thunderstorm cases of August 2015. Comparison of RMI-EPS with GLAMEPS and ECEPS.

Comparing the contribution of the AROME and ALARO members to the RMI-EPS ensemble, we see that the AROME members tend to overestimate the amount of precipitation, while the ALARO members tend to underestimate the amount of precipitation, but curiously the bias of the two models conspire to cancel out almost perfectly, see figure 7. The ALARO members are clearly underspread (partly due to missing a thunderstorm event completely), but have a better RMSE than the AROME members (although they might suffer unduly from the double penalty problem), see figure 8. Nevertheless, combining them improves both the spread and RMSE, as the scores of RMI-EPS in figure 8 show. It also leads to a better CRPS, as can be seen in figure 9.

5 Conclusion and future plans

Even though there are still many improvements possible to the current RMI-EPS set-up, its performance is already surprisingly good, or to use ALADIN parlance 'better than expected'. The RMI-EPS system was able to predict some severe thunderstorms that were completely missed by our operational deterministic model, and preliminary verification scores suggest it compares well with already existing state of the art ensemble prediction systems like ECEPS and GLAMEPS. The AROME and ALARO physics seem to be good complements to each other. They can give rise to quite different results in extreme cases, and combining members from both models improves bias, RMSE, spread to RMSE ratio and CRPS.

At the moment, all the perturbed members have the same physics (and dynamics) settings as their corresponding control member. In the future, multiphysics options (e.g. different tunings, parameterizations,...) for the perturbed members will be tested. An upgrade to ALARO-1 physics is also planned, but for this some issues with SURFEX will first have to be resolved. To improve the spread for 2-meter temperature, additional surface perturbations (on top of the current independent surface assimilation cycle) will be investigated.

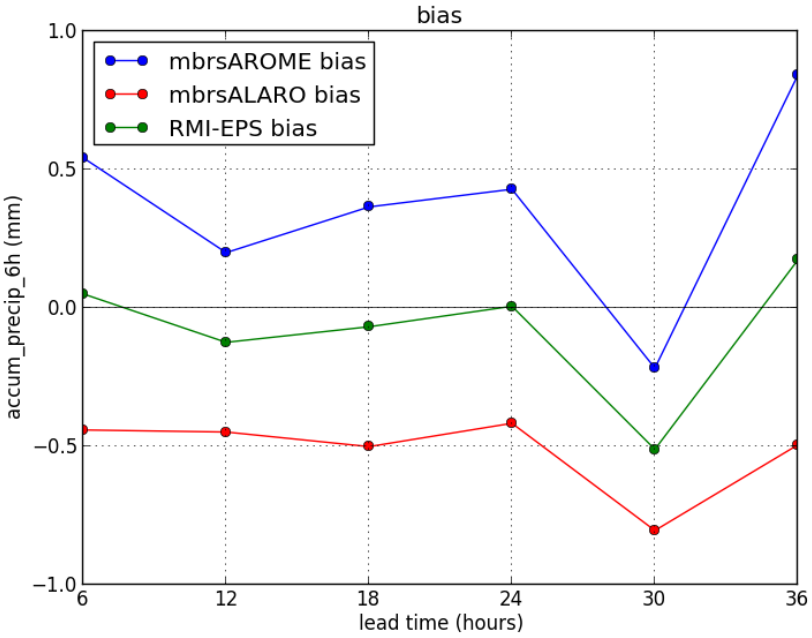

Figure 7: Bias for 6h accumulated precipitation: thunderstorm cases of August 2015. Comparison of the ALARO and AROME members within RMI-EPS.

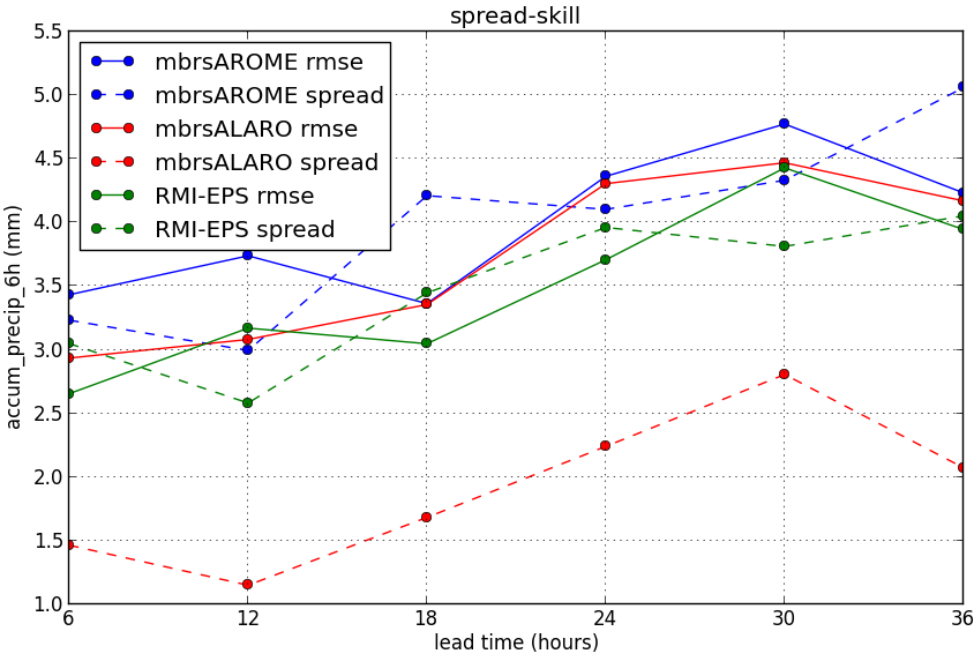

Figure 8: RMSE and spread for 6h accumulated precipitation: thunderstorm cases of August 2015. Comparison of the ALARO and AROME members within RMI-EPS.

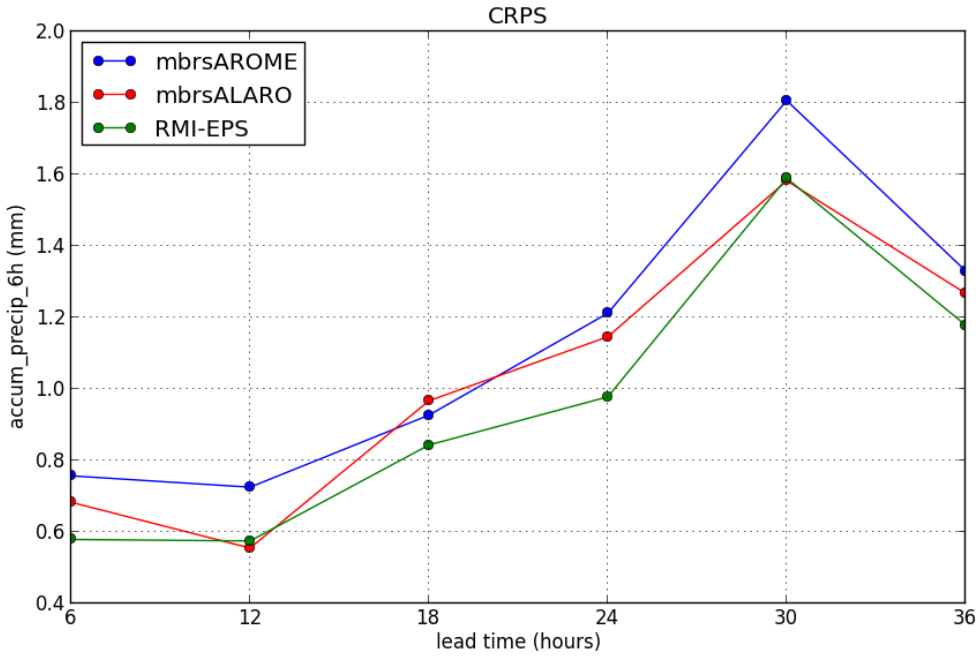

Figure 9: CRPS for 6h accumulated precipitation: thunderstorm cases of August 2015. Comparison of the ALARO and AROME members within RMI-EPS.

In the course of 2017, daily semi-operational runs are going to be implemented, and a new domain centred around Belgium will probably be used. Lagged boundaries or a longer forecast range might also be considered, if they turn out beneficial in an operational context.

6 Acknowledgements

The author wants to thank Joris Van den Bergh at the Royal Meteorological Institute of Belgium (RMI) for help with the RMI-EPS verification, and Steven Caluwaerts at Ghent University (UGent) for help with the thunderstorm case studies.

ALADIN Highlights for IPMA, I.P. (Portugal)

Maria Monteiro, João Rio, Vanda Costa, Manuel João Lopes, Nuno Moreira

1 Introduction

Since the last year no changes have taken place on the local operational NWP system and developments have undergone mostly towards the creation of a local data assimilation system for the AROME-Portuguese Mainland (AROME-PT2) model version. In this publication, we summarise the main achievements on these two different aspects.

Foreseen activities are expected to occur on the already implemented surface data assimilation and on the implementation of a local 3D-Var system. Meanwhile, new procedures are taking place to upgrade the NWP computing systems. And, as a consequence of the recently organization of the 2016 ALADIN workshop and HIRLAM All Staff Meeting in Lisbon, new research groups have shown interest to participate on the local NWP activities.

The document is organized as follows: in section 2, details are given on the local NWP system current status and foreseen changes; and, in section 3, the efforts and progress done in order to provide AROME-PT2 with a data assimilation cycling are described.

2 Local NWP operational system status

Main developments on the operational system during 2016 occurred as a follow up of recently available resources, in particular, the entrance in to operations of a new HPC system (the IBM p7+, with 9 nodes) and the new ARPEGE dissemination features.

In April 2015, the new cycle CY38T1_bf03 became operational in all the Portuguese system configurations and geographical domains (see Monteiro et al. (2015) for further details). Simultaneously several changes have taken place, namely: the increase of the ARPEGE (from Météo-France) coupling fields horizontal resolution from 18 km to 10 km; the enlargement of the AROME-PTG domain eastward; the upgrade of the climatologies to CY38; and, the implementation of a new AROME initialization by direct coupling with the ARPEGE model analysis, instead of using ALADIN as an intermediate coupling model. This last change, in particular, has had a strong negative impact on the short-range wind forecasts due to the increase of the model spin-up (actual AROME-PT2 horizontal resolution is 2,5 km).

The new ARPEGE dissemination features have given rise to set a new model suite where the local version of AROME (CY38T1_bf03) is running 4 times a day with 60 levels for all geographical domains. This suite is now in pre-operational mode.

To validate the impact of increasing the number of levels from 46 to 60 on the local version of AROME, a statistical study has been performed over the 48-hour forecasts of the 12 UTC runs during a 3-month Summer-fall period (20150807-20151004). Screen level as well as accumulated precipitation fields were examined using 110 Portuguese synoptic stations. The 60-level model version has been run over an enlarged domain over the Iberian Peninsula, the domain AROME-IBE. The 46-level version was integrated over the smaller operational domain, the AROME-PT2. Figure 1 illustrates some of the results. In this figure other configurations not so

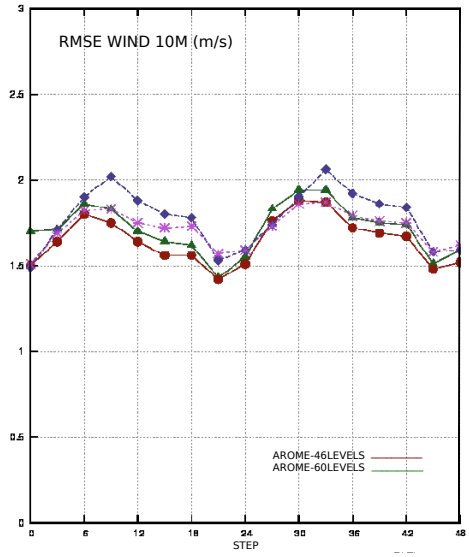

Figure 1: RMSE of the 10-meter wind forecasts, starting at 12 UTC over a Summer-fall period (20150807-20151004), using different Iberian geographical domains and vertical discretizations: AROME-IBE (60 levels, in green) and AROME-PT2 (46 levels, in red).

important for the conclusions to take are so illustrated. As a conclusion we could find a general positive impact (not shown) on the 60-level model version, although the slight degradation on the wind fields shown in Figure 1.

3 Towards a Data Assimilation system in AROME-PT2

At present, the local versions of the AROME model do not contain its own data assimilation system. On each local operational model configuration (one per different geographical domain) the 2,5 km resolution surface initial conditions of AROME-PT2 are supplied by an horizontal interpolation of the surface ARPEGE coupling fields at 10 km.

The lack of small scale structures in its initial conditions is mostly responsible for the large model spin-up which has impact on the 10-meter wind forecast quality in particular, at its first ranges as mentioned before. In order to introduce localised information coming from the observations on the H+00 model fields a 6-hour cycling surface data assimilation system was recently created by the OI-MAIN scheme. The so-called OI-MAIN scheme applies the Optimum Interpolation method described in Giard and Bazile (2000) to produce soil moisture and temperature increments that are used to update the surface and deep soil initialization fields of the in-line surface model SURface EXternalisée (SURFEX, LeMoigne et al., 2012). The analysis fields produced this way are then used to initialize a 24-hour integration of the AROME-PT2 model (with 46 vertical levels) at the 00 UTC network.

The surface data assimilation system here mentioned is locally running on a daily basis so that its quality may be assessed. It uses surface observations (of SYNOP type) over the Iberian Peninsula domain and in order to have a good coverage of the Iberian surface conditions at each network, a neighborhood real-time share of Binary Universal Form for data Representation (BUFR) information through the Global telecommunications System (GTS) has started this Summer between IPMA and AEMET (from around 330 stations). In this way, a back-phased version of BATOR code (Monteiro, 2016) compliant with WMO BUFR template is now locally in use.

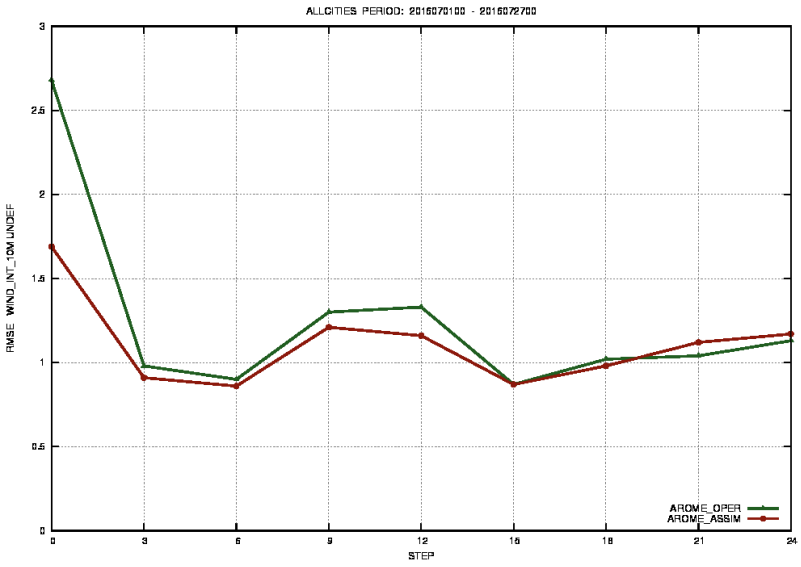

Figure 2: RMSE of the 10-meter wind forecasts (in m/s), starting at 00 UTC over a Summer period (20160701-20160727), using different surface initializations on the AROME-PT2 model version: by interpolation of ARPEGE fields (AROME_OPER, in green) and by the OI-MAIN method (AROME_ASSIM, in red).

To assess the impact the new initialization system has on the AROME-PT2 forecasts, a first statistical study over a short Summer period of 2016 has been performed using the locally available verification tools (with data coming from 110 Portuguese synoptic stations). Figure 2 illustrates some of the results. As a general conclusion, this preliminary study has shown that the analysis fields had a weak adjustment to the screen level observations (not shown) meaning that further work is needed on the system. However, a positive impact on the short-range forecasts of 2-metre temperature and 2-metre humidity was achieved, for the model runs starting at 00 UTC and up to the sun rising moment when the atmospheric movements at lowest levels tend to be dominated by processes more vertically turbulent.

Furthermore, a positive impact could be immediately seen on the 10-metre wind forecasts up to H+18, decreasing in a clear way the large model spin-up. As future work, progress is expected under the form of diagnostic studies in order to understand the surface data assimilation scheme and to set a 3-D analysis structure to AROME-PT2.

4 References

Giard, D., & Bazile, E. (2000): Implementation of a new assimilation scheme for soil and surface variables in a global NWP model. Monthly Weather Review, 128, 997-1015.

LeMoinge, P., et al. (2012) SURFEX SCIENTIFIC DOCUMENTATION, SURFEX v7.2 - Issue no 2 - 2012, CNRM/GAME, from Météo-France/CNRS, Toulouse, France.

Monteiro (2016): Validation of a back-phased version of the source code BATOR. ALADIN Project Stay report - version 2.0. From http://www.rclace.eu/?page=11.

Monteiro et al. (2015): ALADIN Highlights for IPMA, I.P. (Portugal). ALADIN-HIRLAM Newsletter no.6, January 2016. From http://www.umr-cnrm.fr/aladin/IMG/pdf/nl6.pdf.

Met Éireann NWP Highlights 2016

Eoin Whelan, Rónán Darcy, Emily Gleeson, John Hanley

1 Introduction

Met Éireann's Numerical Weather Prediction (NWP) research and development during 2016 was focussed mainly on the porting of the operational NWP suite to ECMWF (Section 3) and MÉRA, the Met Éireann regional reanalysis project (Section 4). For completeness the current Met Éireann operational NWP suite is described in Section 2

2 Current operational suite

This section provides a summary of Met Éireann's operational NWP suite. There were no significant changes to the operational suite during 2016.

The HARMONIE-AROME configuration of the shared ALADIN-HIRLAM system (harmonie-37h1.1), hereafter HARMONIE-AROME, is used operationally by Met Éireann as its short-range forecast model as well as a research tool by Met Éireann scientists. The HIRLAM model also continues to be run as part of the Met Éireann operational NWP suite and remains popular with forecasters. Table 1 provides a summary of the configurations of both models.

Table 1: HARMONIE-AROME and HIRLAM operational configurations

Model	HARMONIE-AROME (37h1.1)	HIRLAM (7.2)
Domain	540 x 500 grid points (Δx =2.5 km)	654 x 424 grid points ($\Delta x = 0.1^{\circ}$)
Vertical levels	65 levels up to 10 hPa, first level at 12 m	60 levels up to 10 hPa, first level at 31 m
Forecast cycle	6 hours	6 hours
Data assimilation	Surface analysis with blending	4DVAR
Observations	Conventional only (cut-off 20 min)	Conventional only (cut-off 2 h)
Forecast	54-hour forecast every 6 hours	54-hour forecast every 6 hours

HIRLAM is run over an Atlantic domain and provides short-range guidance for forecasters, Figure 1b. The HARMONIE-AROME domain covers Ireland, the United Kingdom and a small area of France. The shorter cut-off and earlier delivery time (2 hours) provides Met Éireann forecasters with early guidance focussed on high-impact weather events. With the availability of ECMWF computing resources for operational NWP in 2017 it is hoped that the HARMONIE-AROME implementation can be significantly improved.

3 Port of operational suite to ecFlow/ECMWF

In this section we provide a summary of the port of Met Éireann's operational NWP suite to ECMWF.

Met Éireann has been running its operational NWP suite at the Irish Centre for High-End Computing (ICHEC) since 2007. From early 2017, the suite will run at ECMWF under the "Framework for Member State time-

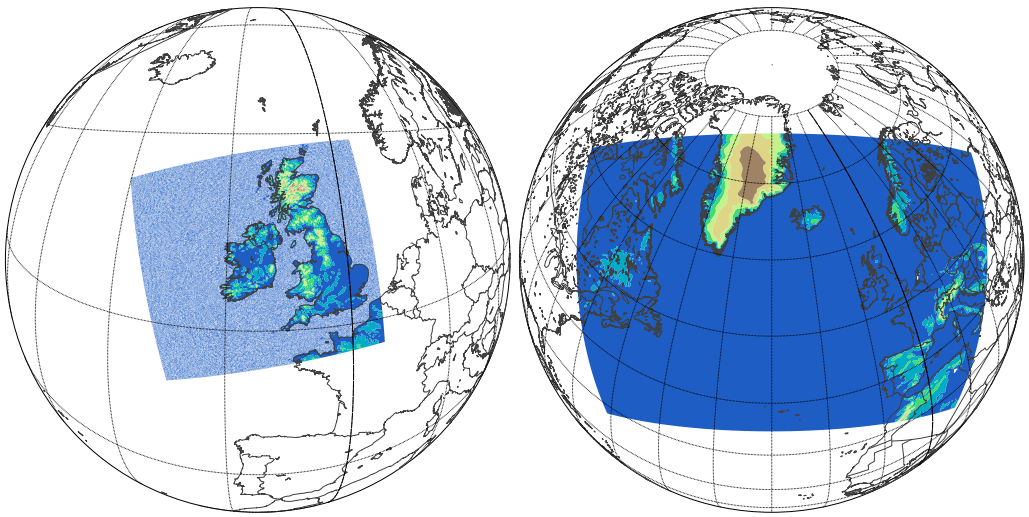

(a) (b)

Figure 1: (a) Operational HARMONIE-AROME domain (2.5 km grid spacing) and (b) operational HIRLAM domain (0.1° grid-spacing).

critical applications" using service option 2, Member State ecFlow (or SMS) suites monitored by ECMWF. This will enable ECMWF operators to provide first-level monitoring of Met Éireann's NWP products.

In order to use this service, the suite must comply with the requirements set out in the Framework for Time-critical Applications document [ECMWF, 2015]. Among these criteria is the stipulation that all products should work under the ecFlow work flow package. HARMONIE-AROME and HIRLAM currently run using the mini-SMS job scheduler at ICHEC, so the migration process involved updating the scripting systems to work with ecFlow. In addition to the NWP models, other suites were built under ecFlow to run and monitor operational tasks such as boundary processing and observation retrieval, as well as various non-operational administrative tasks. As ecFlow allows complex inter-suite triggering, this enabled a logical and robust work flow to be constructed. Models wait for necessary boundary files before initialising and then wait for the latest observation files before the forecast begins, and delayed runs can be dealt with elegantly.

Time critical users at ECMWF have access to two identical Cray XC40 clusters, cca and ccb, as well as two storage clusters, sc1 and sc2. The target node or cluster may be selected by assigning a variable at the suite level in ecFlow, allowing rapid and straightforward switching of hosts in the event of a slowdown or failure. There will be an overlap period during which time the models will run both at ICHEC and ECMWF to allow for forecast verification, and to allow the suites at ECMWF to be tested for robustness and reliability.

4 MÉRA update

In this section we provide an update on MÉRA, the 35-year very high resolution (2.5 km horizontal grid) regional climate reanalysis for Ireland, carried out using the shared ALADIN-HIRLAM system.

The reanalysis covers the same area as the Irish operational domain, Figure 1a. Seven separate simulations were set up to run for five years at a time, with a one year spin-up period for each simulation. A spin-up period of 1 year was deemed necessary to allow deep soil parameters to reach an equilibrium. Each simulation was run on ECMWF's Cray XC30 system, cca. The output data are, temporarily, stored in ECMWF's data handling system, ECFS. The project has produced approximately 750 TB of forecast and observation feedback data, 200 TB of which will be archived. MÉRA will continue to be updated in real-time.

Preliminary analysis shows that it takes almost 12 months to spin-up the deep soil in terms of moisture, justifying the choice of running year-long spin-up periods. No systematic biases were found in MSLP, surface humidity and screen-level temperatures but there is a positive bias in 10 m wind speed after 2005 which coincides with the automation of many synoptic stations. Soil temperatures are well represented by the model. 24-hour accumulations of precipitation generally exhibit a small positive bias of ~1 mm per day and negative biases over mountains due to a mismatch between the model orography and the geography of the region.

The forecast model performance was validated by comparing observed surface parameters and MÉRA output. Here we compare MÉRA 3-hour forecasts with synoptic observations available over Ireland rather than the entire MÉRA domain. Figure 2 shows 2 m temperature and 10 m wind speed verification results for the years 1981-2014. In figures 2a and 2c all available synoptic observations for each time-step are included whereas in 2b and 2d only the set of synoptic stations available at the start of the time period (1981) are included throughout the entire time-series. Note that there are some gaps as the data archiving process is still under way; we only use the archived data where the large HARMONIE-AROME files have been split down and stored by parameter to readily usable smaller files. The results in Figure 2 indicate consistent model performance over the time period in terms of 2 m temperature as well as MSLP and 2 m relative humidity (not shown). However, the bias in 10 m wind speed increased significantly after 2005 when synoptic stations began to be automated and new stations were also opened (Figure 2c). This increase in bias is not seen in the corresponding figure (Figure 2d) which does not include the new or automated stations.

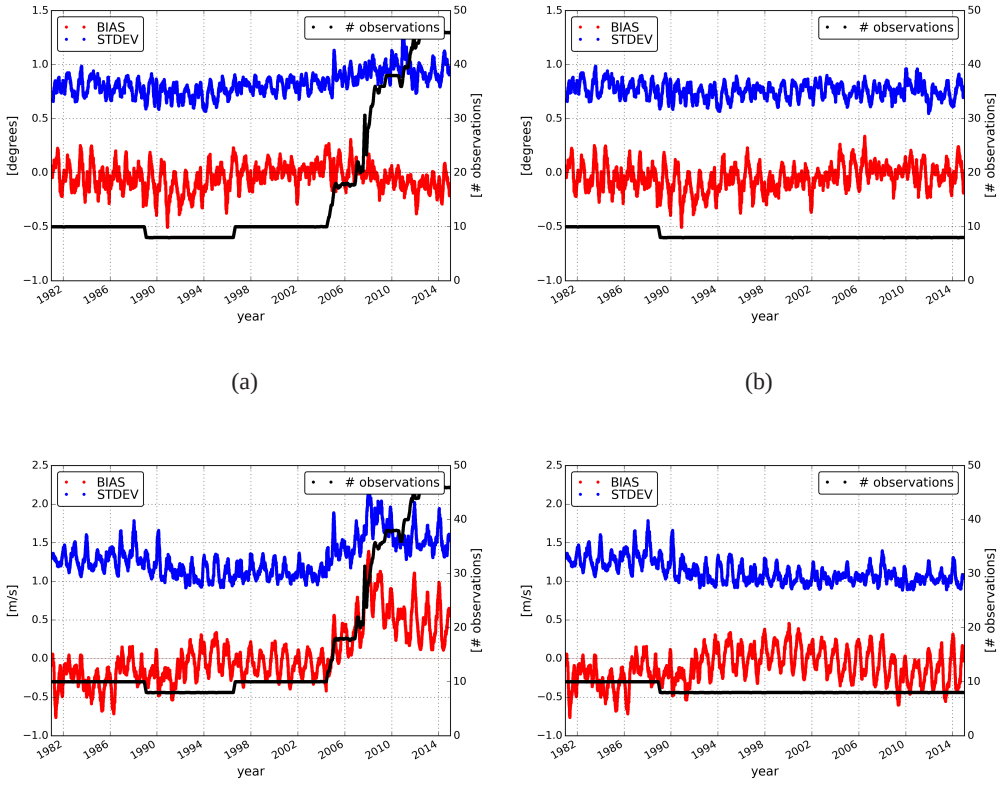

Figure 2: Time-series of verification scores for MÉRA 3-hour forecasts of (2a, 2b) 2 m temperature and (2c, 2d) 10 m wind speed compared with SYNOP observations. The average error, or bias, is shown in red and the standard deviation of the errors is shown in blue. A 2-month running average is applied to the data. In 2a and 2c all available Irish synoptic observations are included; in 2b and 2d only observations from the same stations available in 1981 are included.

A more thorough validation of the entire dataset is under way, with the aim of quantifying all biases in the dataset. This will enable improvements to be made to Met Éireann's operational NWP suite and will also help in the design of a proposed high resolution ensemble forecasting system.

Further details can be found in Whelan and Gleeson [2016a] and Whelan and Gleeson [2016b]. A manuscript has also been submitted to the European Meteorological Society ASR journal and is currently under review.

5 Outlook for 2017

The MÉRA production simulations were almost completed in 2016 with significant progess made with the work of data processing and analysis. Met Éireann's operational suite has been ported to ECMWF with an overlap period for evaluation and testing during early 2017 prior to making the ECMWF suite operational.

During 2017 Met Éireann plans to complete the initial evaluation of the MÉRA dataset and make the dataset available to external researchers midway through the year. We also plan to evaluate and implement the 40h1 version of the shared ALADIN-HIRLAM system (harmonie-40h1). A larger domain, upper-air data assimilation (3DVAR) and higher frequency (3-hour) cycling should lead to improved forecast skill. Initial tests of an ensemble system will also be carried out during the second half of 2017.

References

ECMWF. *Framework for time-critical applications*. European Centre for Medium-Range Weather Forecasts, 2015. URL `https://software.ecmwf.int/wiki/display/UDOC/Time+Critical+applications`.

E. Whelan and E. Gleeson. A mesoscale regional reanalysis for ireland. *ALADIN-HIRLAM Newsletter*, 7: 93–99, 2016a. URL `http://www.umr-cnrm.fr/aladin/IMG/pdf/nl7.pdf`.

E. Whelan and E. Gleeson. Met Éireann High Resolution Reanalysis for Ireland. In *Proceedings of the National Hydrology Seminar 2016*, Office of Public Works, 2016b. URL `http://edepositireland.ie/handle/2262/77869`.

IGA, the Joint Operational HARMONIE by DMI and IMO

Xiaohua Yang[1], Bolli Palmason[2], Bjarne Stig Andersen[1], Bent Hansen Sass[1], Bjarne Amstrup[1], Mats Dahlbom[1], Claus Petersen[1], Kristian Pagh Nielsen[1], Ruth Mottram[1], Niels Woetmann Nielsen[1], Alexander Mahura[1], Sigurdur Thorsteinsson[2], Nikolai Nawri[2], Guðrún Nína Petersen[2]

1. Danish Meteorological Institute
2. Icelandic Met Office

1. Introduction

In 2015, Danish Meteorological Institute (DMI) and the Icelandic Met Office (IMO) entered a bilateral agreement concerning collaboration around installation of the DMI-HPC (Cray XC30) at IMO headquarter in Iceland. The agreement also involved a joint development and operation of weather forecast setup for Iceland and south Greenland. Under this framework, DMI operates the HPC facility remotely, with IMO ensuring continuous operation of site infrastructure. The DMI-HPC with two Cray XC30 clusters was installed in November 2015 and became operational in March 2016. In 2 December 2016, the joint operational Numerical Weather Prediction (NWP) setup, HARMONIE-IGA (Iceland Greenland domain A) was declared operational at DMI.

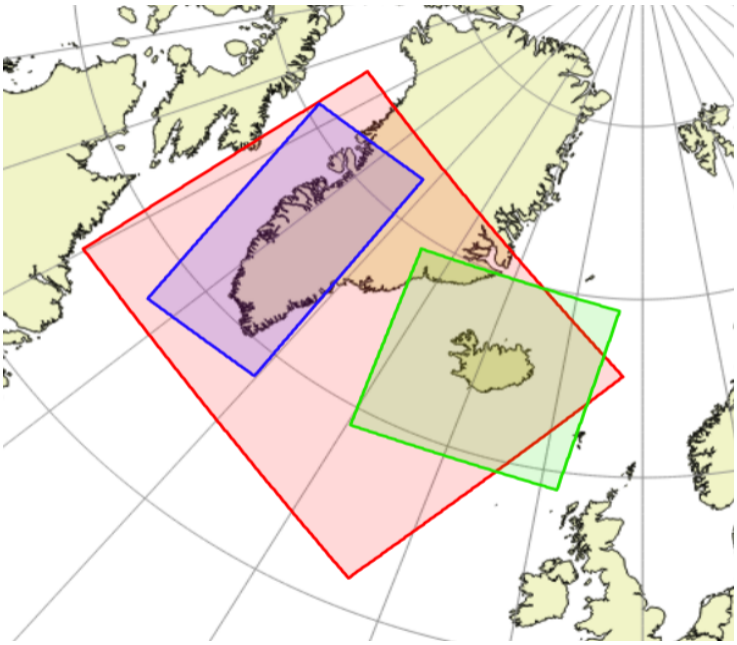

Figure 1. The new operational HARMONIE domain IGA (in red, 2.5 km grid) in comparison to the previous operational one at DMI, GLB (in blue, 2 km grid) and at IMO, ICELAND (in green, 2.5 km grid). IGA runs every 6 hours at 00, 06, 12 and 18 UTC.

This note presents briefly the IGA model system configurations, its adaptations from the reference HARMONIE 40h1.1 and some examples of forecast performances. The detailed description, including results from validation study and operational monitoring, will be featured in a separate, extended report.

2. Model configurations and adaptation

Domain and configuration

During the past years both DMI and IMO have implemented the high-resolution HARMONIE model for operational NWP forecasts. At DMI, a HARMONIE-GLB configuration with 400x800 horizontal mesh and a grid distance of 2 km had been in operational use since 2014 covering southwest Greenland. The HARMONIE-ICELAND domain at IMO runs on a 500x480 mesh, with 2.5 km grid size, covering Iceland and the nearby waters. Thanks to the enhanced computation capacity with DMI-HPC, it became feasible to run a significantly larger operational HARMONIE model domain IGA that covers both of the previous operational domains at the two services (Figure 1). With IGA, HARMONIE model is run on a horizontal mesh of 1000x800 points at 2.5 km grid resolution and 65 levels. The new domain provides an unprecedented high resolution forecast capability for Southeast Greenland and the area between Greenland and Iceland, a region characterised by complex surfaces of high plateaus with ice caps, steep coastal orography, and hence, frequent occurrence of storms. The extended domain coverage has also been observed to improve greatly simulation of the convective events in west of Iceland associated with cold air outbreak. Figure 2 illustrates, e.g., a comparison of precipitation simulation for a convection episode in Dec 2013 by running same HARMONIE model over the IMO domain “ICELAND” (Fig 2a, with domain coverage shown in Fig 1 in green), and over the larger IGA domain (Fig 2b, with domain coverage shown in Fig 1 in red). Interestingly, the simulated precipitation patterns fit remarkably well between the two set-up for the east half of the plots, but rather different for the west half, in which the precipitation pattern in Fig 2a appears to suffer clear distortion due to limitation in domain size for “ICELAND” .

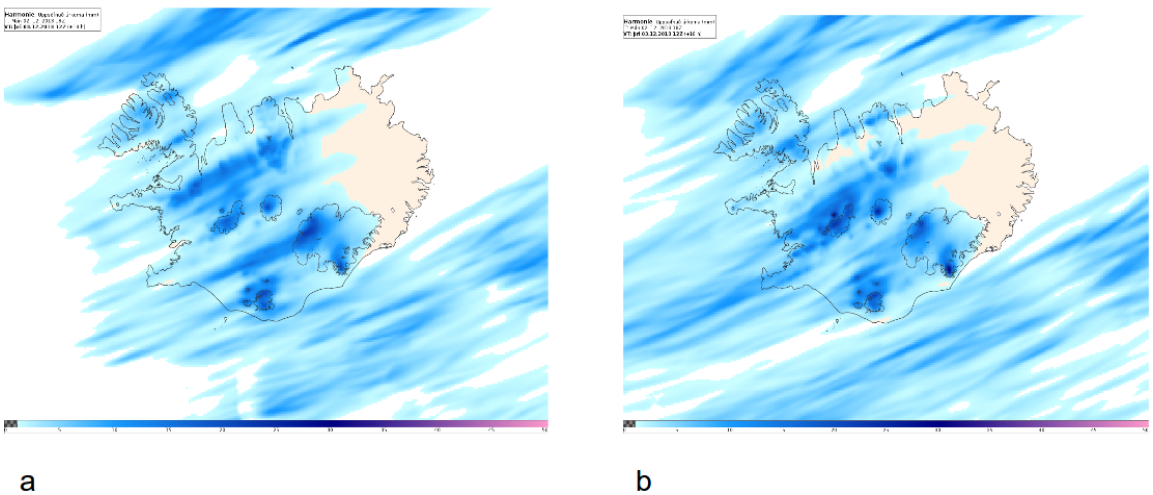

Figure 2: Sensitivity of model domain size on forecast of a convective precipitation event in west Iceland on Dec 3 2013. In this test, HARMONIE model is configured to run on a) the model domain “ICELAND” (as shown in Fig 1 in green) and b) the model domain “IGA” (Fig 1 in red). Start time is 20131202 at 18 UTC, the precipitation shown here is 18h accumulated total.

IGA runs every 6 hours at the synoptic times of 00, 06, 12 and 18 UTC with a 60 hour forecast length, assimilating in-situ surface temperature and humidity observations. The cutoff time for observation data is a half hour after the base times, with a full forecast delivered about 1 hour thereafter. Presently, there is no upper air assimilation. Instead, a "blending" option, as developed in the HIRLAM consortia, is used, in which large scale model states of wind, temperature, pressure and specific humidity, which are valid for the cycle start time, as provided by short range forecast of ECMWF, are blended with the first guess of the HARMONIE model itself, through spectral nudging. A number of additional post-processed forecast quantities have been developed for convenience of end users, on top of the standard HARMONIE postprocessing parameters, using output of the HARMONIE forecast (Yang et al., 2017).

Model adaptation

IGA is based on the reference HARMONIE-40h1.1 as released by the HIRLAM-C programme in late 2016. As detailed in Bengtsson et al (2017), HARMONIE 40h1.1 features an extensive list of updates on various aspects of the forecast system, including several important upgrades in the physical parameterisation of turbulence, radiation and condensation schemes, and an upgrade of SURFEX surface scheme to version 7.3. In order to assure satisfactory forecast performances for operational use in IGA, extensive technical and meteorological tests have been conducted. Among these, major efforts have been devoted to upgrading and testing the physiography database (PGD), selecting and testing of grid type in spectral transform onto grid point space, validation of the turbulence parameterisation scheme HARATU, testing of the subgrid scale orography (SSO) parameterisation, and the mixed phase cloud parameterisation option OCND2 in connection with the shallow convection scheme EDMFM.

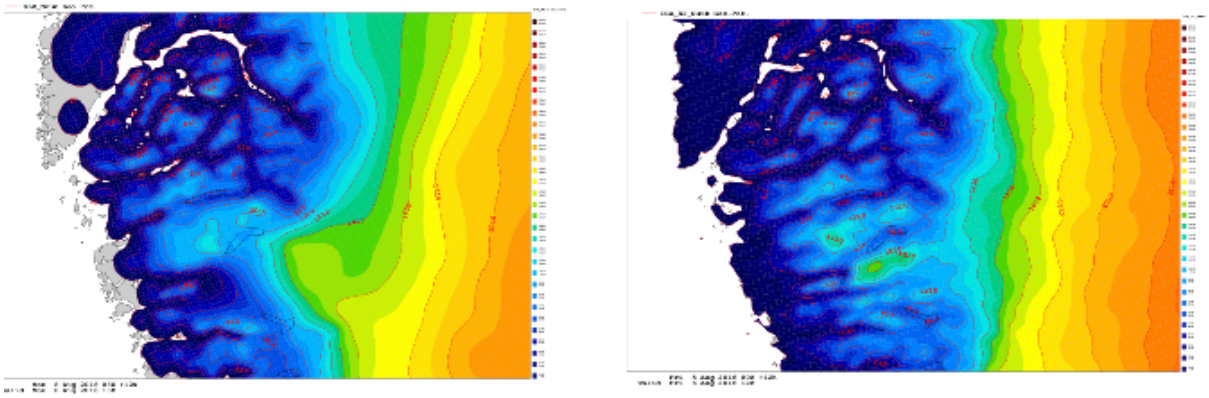

Figure 3: Model resolved orography for area around Nuuk, Greenland, with a) GLB, horizontal resolution 2 km, using GTOPO30 data at 1 km resolution, b) IGA, horizontal resolution 2.5 km grid but using GIMP elevation database at 90 m resolution.

In HARMONIE 40h1.1, the PGD from ECOCLIMAP-II is used to generate invariant or seasonally varying climate constants. Numerous deficiencies have been found in the database for areas of Iceland and Greenland. In fact, the ECOCLIMAP-II has not been updated from ECOCLIMAP-I for this region. Corrections and updates have hence been necessary. For IGA, some of the earlier corrections and improvements in the PGD as implemented by IMO for its ICELAND domain have been ported, including glacier extent, soil characteristics, vegetation fractions, albedo and roughness. These updates have been shown to give significant improvements to the surface fluxes and temperatures (Palmason et al. 2016). Furthermore, surface types for the coast of Eastern Greenland have been updated. Similar update have been done to the FAO/HWSD sand/clay database for Iceland. For the

topographic database, the Greenland Ice Mapping Project (GIMP) topography with a resolution of 90 m has been implemented on top of the data by the USGS Global Multi-resolution Terrain (GMTED) data set at a resolution of 250m. The GIMP dataset has also been used to map the extent of the glacier ice that underlies the seasonally varying snowpack in the ablation zones of the ice sheet.

The use of combined GIMP and GMTED data in IGA enabled construction of a high-quality topography database. Figure 3 illustrates, as an example, the model orography height in HARMONIE-GLB (a) and HARMONIE-IGA (b), for the area around Nuuk, Greenland. While GLB is at a grid resolution of 2 km, the elevation database is from that of GTOPO30 with 1 km resolution. For IGA, the data resolution for aggregation is at 90 m. Comparing Figures 3a and Fig 3b, many differences in details can be identified, such as the land mask (mis-)fit on the west coast and the shape to the orographic gradient toward the eastern border.

The above improvement of PGD for IGA has been validated in a month-long comparative study. It showed clear benefits with the reduction of standard deviation and bias errors for wind speed and a reduction of the average bias in surface temperature (not shown here). Presently, the work on improving the mapping features in PGD for Greenland and Iceland are continuing. Future upgrades are planned for gradual implementation in the operational HARMONIE for this region.

For the NWP community, observation data from conventional in-situ measurement platform are typically shared via the Global Telecommunication System (GTS). For historical reasons the GTS data hub does not contain the complete observation data stream available to individual national weather services. This has been the situation for a majority of surface observation data collected in Iceland by IMO, which are still outside of the GTS exchange due to technical and logistical reasons. Thanks to the bilateral collaboration between DMI and IMO, IGA can benefit directly from the merging of the observation data stream available for operational use, which results in a significant increase of observation data used in IGA surface assimilation. Figure 4 illustrates an example of the increase in observational data due to the merge of the DMI-IMO data streams (Fig 4a) as contrast to the situation in which data from Iceland is only available via GTS for DMI (Fig 4b).

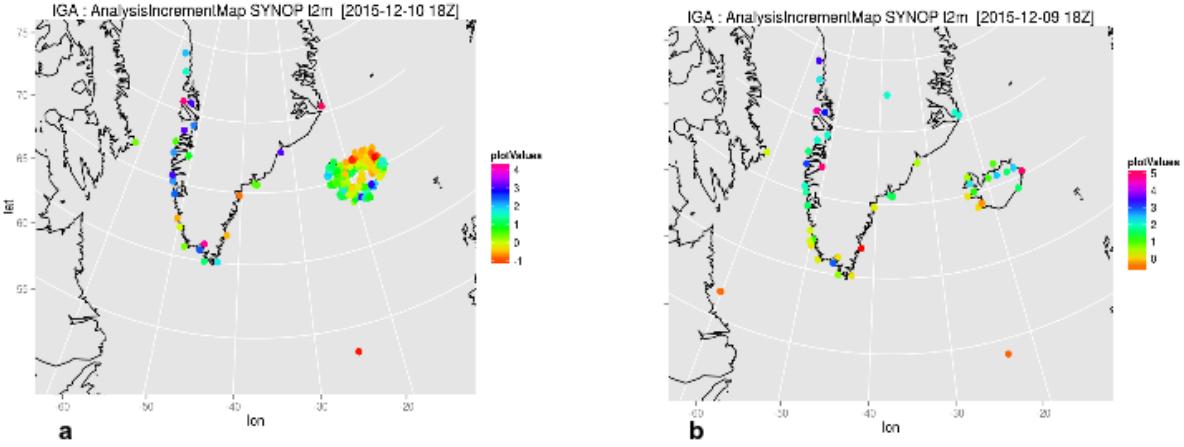

Figure 4: Analysis increment of T2m for IGA on Dec 9 2015 at 18 UTC, with a) combined DMI+IMO observation data stream; b) DMI data stream-only. Note the significantly different

Selection of configuration options

The HARMONIE system contains many alternative configuration options for model setup in dynamics, physics and data assimilation. In the reference 40h1.1, a set of default options have been specified, such as the use of linear grid in spectral transform to grid point space, use of explicit horizontal diffusion, and a time stepping of 60 s for the default domain. 40h1.1 uses the AROME physical parameterisation framework, with some of the deviations developed by the HIRLAM community, such as the turbulence option HARATU, the shallow convection scheme EDMFM with a modified parameterisation for the cloud mixed phase (OCND2) , some modification in parameterisation for cloud optical properties in the IFS-based radiation scheme, and no use of the subgrid scale orographic parameterisation. In the process of operationalise IGA, numerous validation and comparison tests have been performed, in which hindcast runs have been performed by both DMI and IMO teams for selected weather-rich episodes, with a goal to validate the model setup and to determine optimal configuration options in terms of meteorological performance as well as technical effectivity and stability.

The domain of IGA is characterised by complex terrain with frequent occurrence of challenging weather, often associated with small scale surface features. This has been found to pose a great challenge to high resolution NWP model. Strikingly, at the initial validation phase of 40h1.1 for the Greenland and Iceland regions, tests with use of linear grid in spectral transform encountered numerous instability problems. The issue with computational stability caused severe difficulty to carry through several of the scheduled validation tests. On the other hand, using either quadratic or cubic grids have shown remarkable stability, while maintaining satisfactory meteorological quality. From the comparison of using different grid representations, the main sensitivity has been observed for surface wind, in which a slight increase in positive wind bias for cubic grid have been seen for Icelandic stations, less so for quadratic grid (not shown here). Similar sensitivity has been reported in a study over Scandinavia in which surface wind over mountain stations have shown increased wind bias, (Bengtsson et al. 2017, Yang et al. 2017). As concluded in Yang et al. (2017), it is assessed that the slight increase in wind bias, associated with use of higher truncation grids than linear one, is relatively minor and can be compensated for through other means of tuning, such as use of SSO for HARMONIE-NEA at DMI. For IGA, we have selected to use quadratic grid for operational use. Rigorous tests for IGA have also been performed, in which time stepping of 60 s, 75 s and 90 s have been compared in month long runs, achieving meteorologically equivalent results. Based on the tests, a time stepping size of 75 s has been chosen.

In Harmonie 40h1,1, a non-default dynamic option COMAD (COntinuous Mapping about Departure points scheme) is available, which is a correction applied to the standard interpolation weights in the SL scheme that takes into account the deformation of the air parcels along each direction of interpolation. The scheme helps to reduce excessive build-up of cloud hydrometeors in isolated grid-points (Bengtsson et al 2017). After testing, COMAD has now been activated in IGA.

Finally, IGA also deviates from the reference 40h1.1 as the cloud microphysics option OCND2 is not chosen. Based on experience of the HARMONIE-ICELAND-38h1.2 at IMO, a multi-month test of sensitivity regarding OCND2 has been performed for IGA. While OCND2 has been found effective for several Nordic domains in addressing some of the observed weakness in the AROME parameterisation of the mixed phase processes in cloud microphysics (Bengtsson et al, 2017), the test on the IGA domain have shown less favorable results in precipitation, which is of major concern for IMO in view of their use in downstream applications.

3. Operationalisation and forecast performance

A test setup of IGA was configured in late 2015 at the ECMWF HPC with the system based on beta versions of HARMONIE 40h1.1. The setup went through extensive tests, including comparative experiments to examine forecast sensitivity on various configuration options in dynamics and in the physical parameterisations. After implementation onto the DMI Cray XC30 in mid-2016, a real time cycling was established, with monitoring and continuous tuning in the following period until the final operationalisation.

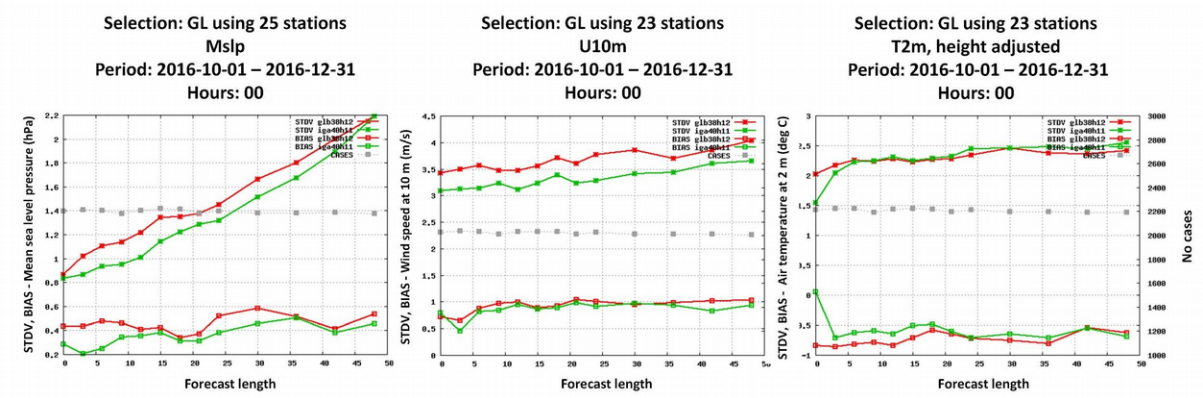

Figure 5: Observation verification of standard deviation (upper curves) and bias error (lower curves) for HARMONIE-IGA (in green, based on 40h1.1) in comparison of the earlier operational model HARMONIE-GLB (in red, based on 38h1.2) during October and December 2016, for the observations of (a) mean seal level pressure, (b) 10-metre wind and (c) 2-metre temperature. These statistics are done for the area in Southwest Greenland, where the model domains overlap.

From intercomparisons of modelled results against surface measurements over a rather extended parallel period, IGA has been found to have a generally satisfactory quality for key forecast parameters, in comparison to the earlier operational models. Figure 5 illustrates the score intercomparison between IGA and the previously operational HARMONIE model for the GLB domain for the last quarter of 2016. Here the verification for MSLP, 10-metre wind and 2-metre temperature all point to a clear reduction in the model errors.

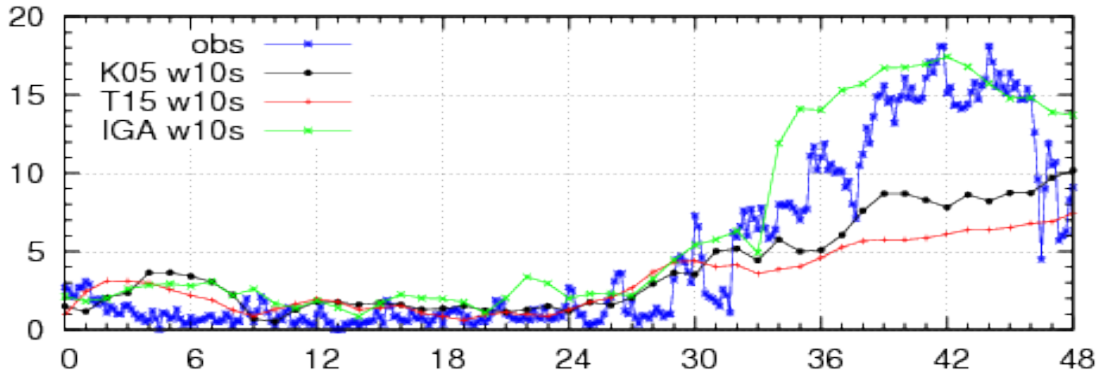

Figure 6: Wind speed time series in hours by model prediction dated 2017010100 with HARMONIE-IGA (green), HIRLAM-K05 (black) and HIRLAM-T15 (red), in comparison with observations (blue) for station Tasiilaq in east Greenland.

South Greenland and Iceland experience frequent storms associated with cyclonic activities. In numerous locations along coastal Greenland, katabatic winds from the cold Greenland icecap can sometimes escalate to hurricane scale in short time. The is often referred to as“piteraq” in local language. From operational experiences, strong local storms in the region are often associated with steep orography along the coastal landscape. Accurate prediction of piteraq has been a major challenge for numerical weather prediction. Thanks to a fine grid resolution over an extensive domain, as well as nonhydrostatic dynamics, HARMONIE-IGA has been found to be especially skillful in predicting hazardous Greenland windy weather. Figure 6 shows a forecast meteogram for a recent Piteraq event at the DMI observation station Tasiilaq in the beginning of 2017 for the HARMONIE IGA, HIRLAM K05 and HIRLAM T15 in comparison to observations. All of the forecasts are initiated from 2017-01-01 00 UTC. As shown in the curves, following a very calm New Year’s Day (January 1st), the Piteraq starts to develop around noon on January 2nd and quickly reaches strong gale wind speeds during the evening. IGA correctly forecast the strength of the event, whereas the lower resolution HIRLAM models K05 and T15 predicted too low wind speeds.

Figure 7 are scatterplots of surface wind speed comparing predictions with HARMONIE-IGA, HIRLAM-K05 and ECMWF-IFS HiRes models against observations for the period from 2016-12-15 to 2017-01-13. Significant variations are seen for the model fits to the high wind speed observations. For these, IGA is clearly superior, demonstrating further an enhanced predictive skill with high resolution HARMONIE in contrast to coarser resolution HIRLAM and ECMWF-IFS forecasts. Meanwhile, as illustrated in Figure 7, the IGA forecasts tend to suffer a larger spread compared to the other models. While the representativity of the observational data itself can be an issue for an area with a complex landscape, there is no doubt that there is still a plenty of room for further improvements of the HARMONIE model.

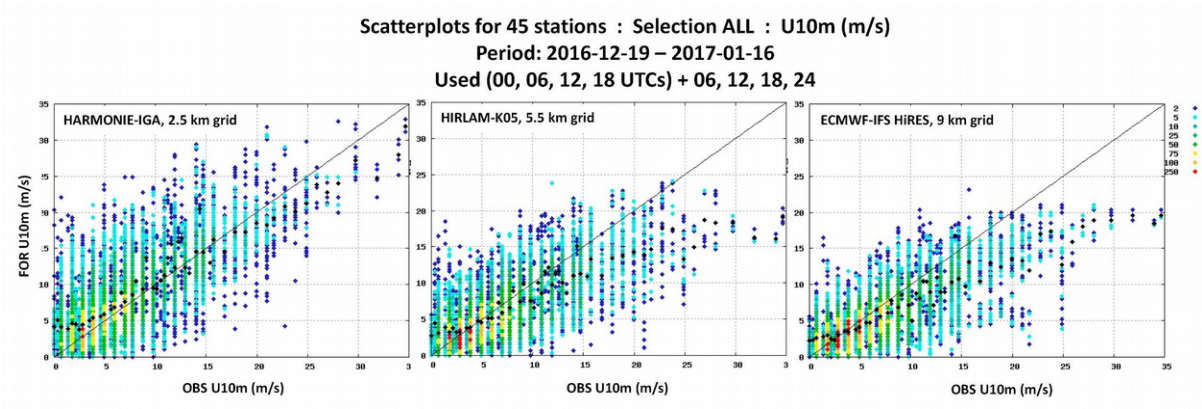

Figure 7: Scatterplots comparing observed (horizontal axis) and modelled (vertical axes) wind speed over the South Greenland and Iceland area with a) HARMONIE-IGA. 2.5 km grid, b) HIRLAM K05, 5.5 km grid and c) ECMWF-IFS HiRES, 9 km grid for the latest one month period between December and January 2017. Dark heavy dotted values are observed wind speed bin averaged values.

4. Outlook

Operational use of the high resolution HARMONIE model in routine numerical weather prediction for the South Greenland and Iceland area has shown remarkable strength in accurate prediction of severe weather associated with complex surface conditions in these geographical regions. As demonstrated in the above summary, forecasts made on an extended domain brings clear advantages for predicting

weather situations in which the representation of the full life cycle of the phenomena is crucially important. It is recognised that, due to limitation in computation capacity, even with the current model domain IGA, it still suffers incomplete coverage of the entire service area of DMI and IMO for Greenland and Iceland. It is hence obvious, that priority should be given to future expansion of the operational HARMONIE forecast domain for the region, so that the entire Greenland is covered. The operationalisation of HARMONIE for such an extended domain is expected in connection with the upcoming installation of next phase of the DMI-HPC during early 2018.

For both climate studies about Greenland Icecap and economic activities in both Greenland and Iceland involving water management and green energy, an adequate characterisation of the surface process of glacier ice is of vital importance. While the recent operational HARMONIE for Greenland and Iceland has forecast the surface temperature evolution over the ice sheet well, a significant deficiency has been identified in relation to the surface snow melt. Recent studies testing a modification of the HARMONIE cy38h1.2 parameterisation for glacier ice within the SURFEX scheme suggest that current model errors, at times when the glacier becomes exposed, can be fixed (Mottram et al. 2017). Looking further ahead, more accurate ice melt and run-off computations should be included in HARMONIE. Such are important both for ice surface mass balance estimations and for commercial applications such as hydropower forecasting. The work to improve the glacier ice physics will be incorporated in coming versions of the SURFEX scheme in collaboration with Météo France.

Presently, preparation to activate 3D-VAR upper air data assimilation for the operational IGA is in progress. Traditionally, data assimilation for the Greenland-Iceland area has been a very challenging task due to severe shortage of observations for the region, e.g. in-situ observations for Greenland have been very sparse. Further, most of the Greenland stations are located along the coastline, with poor representation of the meteorological conditions over the vast Greenland ice sheet. With improving system infrastructure in HARMONIE, data assimilation, and accumulated experience of assimilating large amount of remote sensing (satellite, radar etc.) data for other operational HARMONIE domains, it is considered adequate to start implementing 3DVAR also for the Greenland-Iceland area. This work will focus on the use of remote sensing data such as polar orbiting satellite measurement of radiance, atmospheric motion vectors, radio occultation, GNSS zenith delay etc.

References

Bengtsson, L., Andrae, U., Aspelien, T., Batrak, Y., Calvo, J., de Rooy, W., Gleeson, E., Sass, B. H., Homleid, M., Hortal, M., Ivarsson, K.-I., Lenderink, G., Niemelä, S., Nielsen, K. P., Onvlee, J., Rontu, L., Samuelsson, P., Santos Muñoz, D., Subias, A., Tijm, S., Toll, V., Yang, X., Køltzow, M. Ø.: The HARMONIE-AROME model configuration in the ALADIN-HIRLAM NWP system, Bull. Amer. Meteorol. Soc., accepted for publication, 2017

Mottram R., Gleeson E., Nielsen K. P. and Yang, X., Modelling Glaciers in the HARMONIE-AROME NWP model, 2017, Proceedings for EMS 2016.

Palmason, B., Thorsteinsson, S., Nawri, N., Petersen, G. N., and Björnsson, H.: HARMONIE Activities at IMO in 2015, ALADIN-HIRLAM Newsletter, 6, 72-75, 2016.

Yang, X., B.S.Andersen, M. Dahlbom, B. H. Sass, S. Zhuang, B. Amstrup, C. Petersen, K. P. Nielsen, N. W. Nielsen, A. Mahura: NEA, Operational implementation of HARMONIE 40h1.1 at DMI, ALADIN-HIRLAM Newsletter, 2017.

ALADIN related activities in Slovenia in 2016

Neva Pristov, Benedikt Strajnar, Jure Cedilnik, Jure Jerman, Peter Smerkol, Matjaž Ličar, Matjaž Ličer, Anja Fettich

1 Introduction

This contribution is a summary of ALADIN related activities in Slovenia in 2016. Some developments are highlighted: validation of ALARO-1, the development and evaluation of 2-way coupling between ocean and atmosphere has been further developed (see also previous AHNs); more experiments testing the usage of Zenith Total Delay (ZTD) observations were carried out; Crocus snow model was implemented and first tests were done.

2 Operational

The operational ALADIN system remained the same as in 2014. ALARO-1vA physics package was evaluated over over summer and winter seasons. Winter bias of 2 m temperature is reduced, summer maximum 2 m temperature forecasts are still underestimated, impact is clearly seen in temperature biases, while it is hardly visible in standard deviation of forecast error. Neutral impact on upper-air fields is noticed.
Recomputation of background error covariances was done and consistant model (re)analysis were obtained with 3 hourly assimilation cycle for the period 2011-2015. Our plan is to use ALARO-1vB in the operational suite and to re-compute production forecasts for the period of few years.

It can be also mentioned, that Peter Smerkol checked part of the ALARO-1 TOUCANS code (calculation of the Third order moments corrections to heat and moisture fluxes in acdifv3.F90). He cleaned the code, corrected known bugs listed in TOUCANS documentation by Ivan Bašták Ďurán and the one he found. All of the bug corrections except one produce the negligible differences in norms and in the contributions within DDH.

3 Research and Development Activities

Two-way atmosphere-ocean model coupling

A two-way coupled ocean and atmosphere modeling system comprises 4.4 km ALADIN/ALARO and Princeton Ocean Model (POM) for Adriatic sea and uses Mediterranean Forecasting System (MFS) as ocean component outside the POM model domain. The heat and momentum fluxes between sea surface and atmosphere as estimated by ALADIN model are transferred into POM every model time stamp, and sea surface temperature (SST) is returned from POM to ALADIN. The study was continued by studying the impact of two-way coupling during the data assimilation cycle. As a start the coupled system was tested on several precipitation cases rather than long-term simulations which would presumably lack observational information given no data assimilation for the ocean component.

Various implementation of coupling during a short warm-up periods beforehand the event and the production forecast were evaluated, as well as several approaches to using SST information in ALADIN in the one-way coupled mode (POM, MFS, global atmospheric model). First results suggest that it is important that two-way coupling is applied not only during the long term (e.g. 72 h) forecast but also already in the data assimilation cycle prior to event (Figure 1).

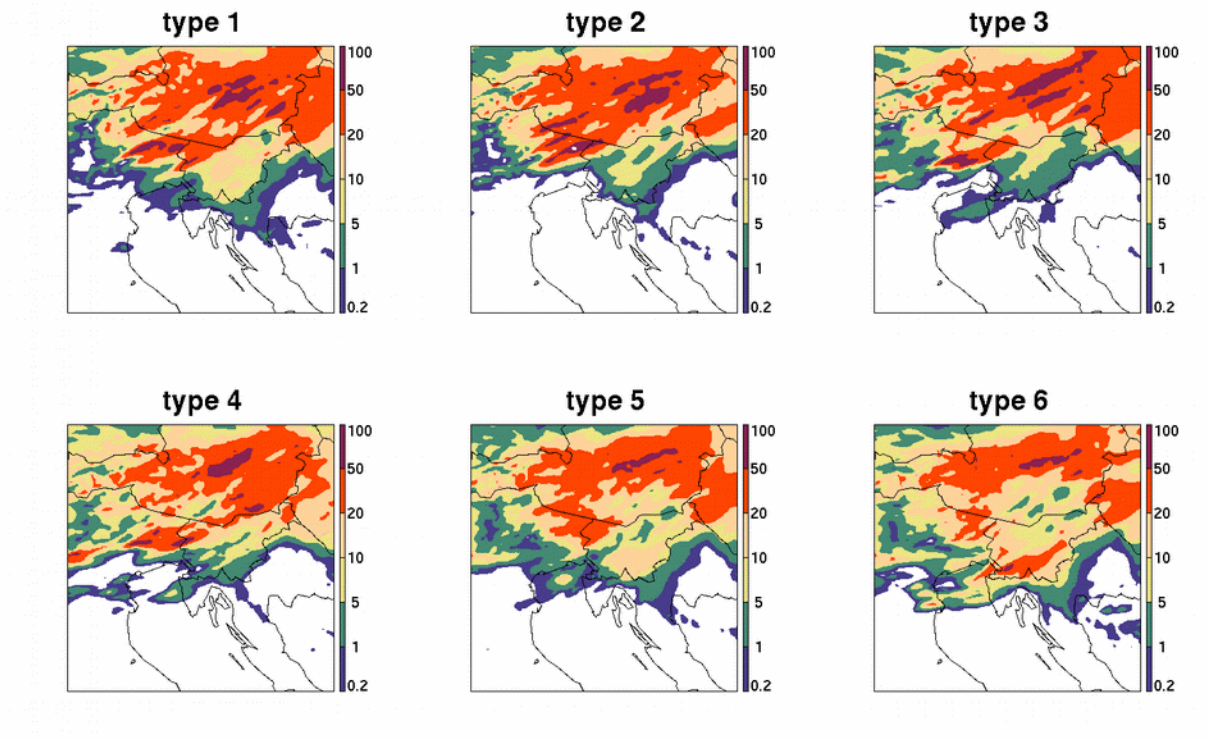

Figure 1:24-hour precipitation accumulation [mm] in different coupling/SST settings. Types 1-3: one-way coupled system using OSTIA (ECMWF), MFS, POM+MFS as SST, respectively. Type 4: same as type 3, but fully coupled during production run. Type 5: 2-way coupled assimilation run, uncoupled production and type 6: 2-way coupled assimilation and production. One month time series of RMS scores for temperature (K) at 500 hPa.

Towards operational use of Slovenian GPS Zenith Total Delay observations

Experiments using a network of approximately 25 Slovenian (plus a small surrounding) GPS stations were continued in 2016, mainly during a 4-week stay of Tunisian colleague Zied Sassy in Ljubljana. We first evaluated observation biases with respect to the model and corrected heights of observations to use geometric rather than ellipsoid heights. Based on previous result using static bias correction where beneficial impact of using approximately 50% of all stations was shown, we now tested the ability of VarBC scheme to adaptively correct the data from the other 50% of stations. It was shown that the correction to bias by VarBC scheme was small and not correcting the remaining large biases in some observations. This confirms that a rather crude pre-selection based on offline static bias estimation will be kept for now and such a setup will be added to operational assimilation in 2017.

Implementation of Crocus snow model

With the great help of Bogdan Bochenek from Polish team (flat-rate stay) the Crocus snow pack model was successfully ported and tested. This was a good basis for the work that followed in scope of which Crocus was implemented to a quasi-operational level. At this stage there are two Crocus ecFlow suites: one in which Crocus is coupled to the operational ALADIN/ALARO production runs at 4.4 km horizontal resolution using consecutive 24 hour forecasts and a second one where the forcing for Crocus is obtained from the INCA nowcasting system runs at 1 km horizontal resolution, the latter is for analysis purposes only.

The validation and verification work is in progress; the plan is also to use station data for forcing of Crocus as a 1D model and test some avalanche oriented tools.

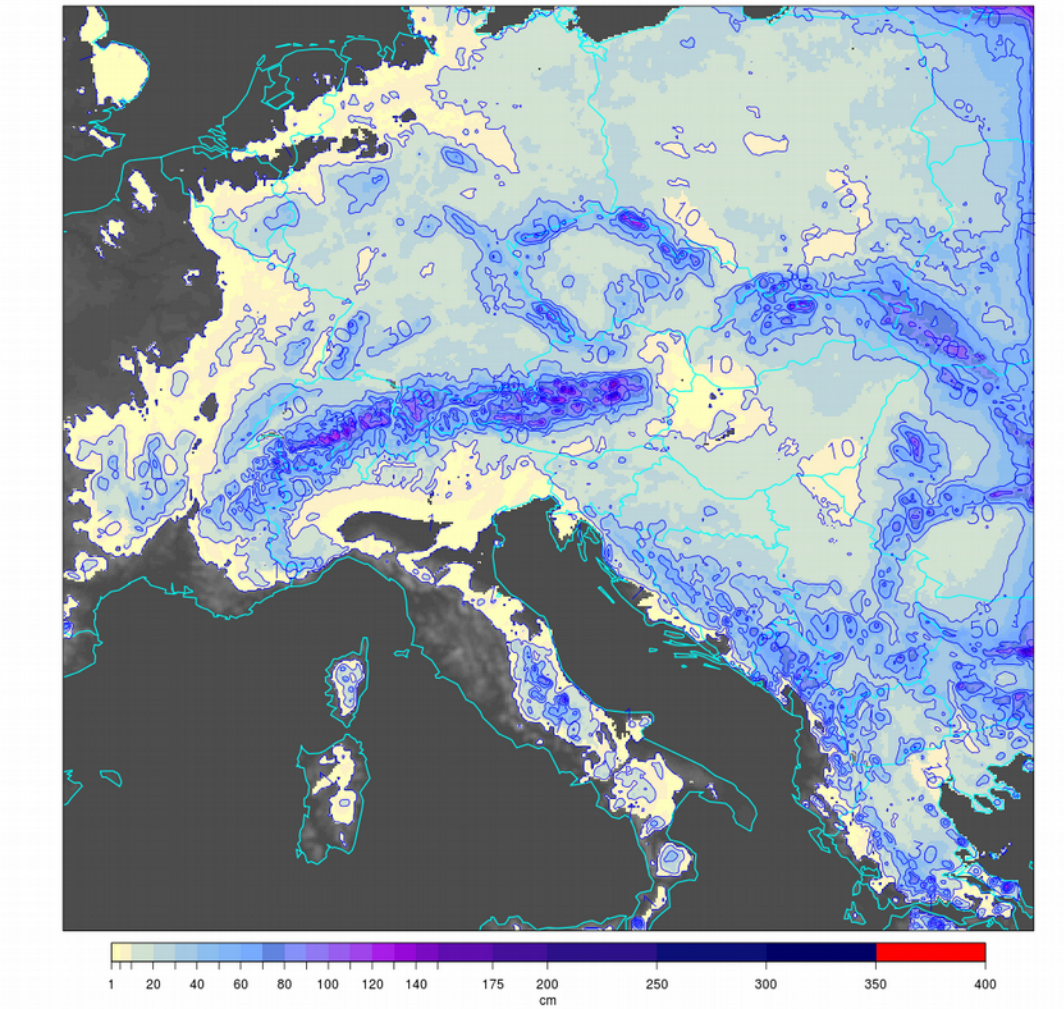

Figure 2: Snow height [cm] from Crocus snow model forced with ALADIN/ALARO. Valid for 16 January 2017.

4 References

Ličer, M. et al., 2016: Modeling the ocean and atmosphere during an extreme bora event in northern Adriatic using one-way and two-way atmosphere–ocean coupling, Ocean Sci., 12, 71-86, doi:10.5194/os-12-71-2016, 2016.

Sassi, Z., 2016: Assimilation of GPS moisture information, stay report in Ljubljana

Smerkol, P., 2016: Debugging and testing Toucans module for Alaro-1, RC LACE stay report in Prague

Strajnar B., 2016: Overview of ALADIN data assimilation activities at ARSO, report for LACE DA

The MetCoOp ensemble MEPS

The MetCoOp team
Corresponding author: Ulf Andræ SMHI

Figure 1: The very first MEPS forecast from 8th of November 2016 06Z showing the ensemble mean MSLP and 12h precipitation.

1 Introduction

MetCoOp is the cooperation around NWP production between Sweden and Norway and Finland. It was established in 2011 and has been running the HARMONIE-AROME configuration in the ALADIN-HIRLAM NWP system operationally since March 2014. The shared tasks involves pre processing of observations and boundaries, the core production and the daily monitoring of the meteorological and technical performance. Post processing and product generation is handled by each institute separately. On the 8th of November 2016 MEPS, the MetCoOp EPS, based on harmonie-40h1.1 was put in production. MEPS replaces the previous deterministic HARMONIE configuration. In the following we describe the MEPS components, the operational implementation, performance, some problems and the plans for the future.

2 The MEPS configuration

2.1 The forecast model and assimilation system

MEPS is based on harmonie-40h1.1 (http://hirlam.org/trac/wiki/Harmonie_40h1) with the forecast model setup as described in (Bengtsson et.al. 2017). The MetCoOp domain, shown as a particularly tasty version in figure 1, covers 750x960 points with 2.5 km horizontal grid spacing and 65 levels in the vertical. Local changes in the forecast model compared to the reference harmonie-40h1.1 includes the COMAD scheme (Malardel et.al. 2015) for the Semi-Lagrangian interpolations, the simplified ice

scheme (SICE) for sea ice and a modified temperature response from melting snow. The model is constrained by hourly ECMWF HIRES boundaries.

The assimilation setup is based on 3DVAR with large scale mixing within a 3h cycle using structure functions derived by downscaling of ECMWF EDA members for a summer and winter period. In addition to the conventional observations AMSU, MHS, IASI, ASCAT, RADAR reflectivity and GNSS data are also assimilated in the system. Compared to the default harmonie-40h1.1 the observation errors have been changed back to the same values as in 38h1.2 and an extra check of duplicated stations has been implemented. The surface assimilation is based on CANARI and SODA using the OI scheme. The impact from T2M/RH2M increments in soil temperature and soil moisture has been adjusted to have a faster response. In addition to SST from ECMWF, MetCoOp also utilizes SST and sea ice concentration from the oceanographic model HIROMB over the Baltic Sea and the lakes Vänern and Vättern in Sweden.

2.2 The ensemble configuration

The ensemble system consists of 1 control and 9 perturbed members with the same domain and forecast model as mentioned above. The control member is the only one running 3DVAR but all members run their own surface assimilation with 6h cycling as compared to 3h for the control. The control member runs up to 66 hours and the perturbed members up to 48 hours. The initial and boundary perturbations are generated from the ECMWF HIRES output using the SLAF method implemented in HARMONIE (Garcia-Moya et.al. 2015) where perturbations are constructed from scaled differences between two forecasts with initial times 6 hours apart, but valid at the same time, see figure 2. The scaling coefficient, SLAFK, is tuned in such a manner that all members have approximately the same standard deviation. We can, however, note that there is a different bias in the perturbations of the different members. This is an inherent property of the method and coming from the fact that the ECMWF model has a surface pressure bias depending on the forecast length.

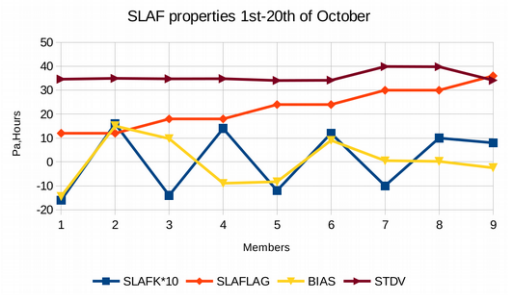

Figure 2: SLAF properties for the different members. The red line shows the lag in hours for the ECMWF forecast used. The blue line shows 10 times the scaling factor. The yellow and brown lines shows surface pressure bias/stdv at initial time respectively.

The ensemble members are distributed over the two HPC resources available for MetCoOp so that six members runs on the Swedish computer Frost and the remaining four on the Norwegian computer Vilje. The triggering and coordination of the run is controlled with ECFLOW from a common server. One of the members on Vilje are used as the backup for the control member having in mind that most of the down stream production is still relying on the deterministic run as the main source of information. This means that this member uses the first guess from the control member on Frost, runs upper air and surface assimilation, and is then perturbed like all the other members.
Running an ensemble system increases the technical challenges manifoldly. Several changes has been done in MEPS with respect to harmonie-40h1.1 to handle the increased amount of data. Worth mentioning is the direct conversion of the distributed IO-server files to GRIB (i.e. no FAcat), OpenMP optimization of the postprocessing in the GRIB conversion step, and the backporting of the asynchronous reading of boundaries developed by Meteo France and available in cy41. An example of the potential performance gain by this is shown in figure 3. In general care has been taken to move postprocessing of variables requiring full model levels for e.g. all ensemble mebers inside the suite so

that less data has to be written to disk and distributed to the users. The technical changes that are not particularly tailored for MetCoOp will be a available in harmonie-40h1.2.

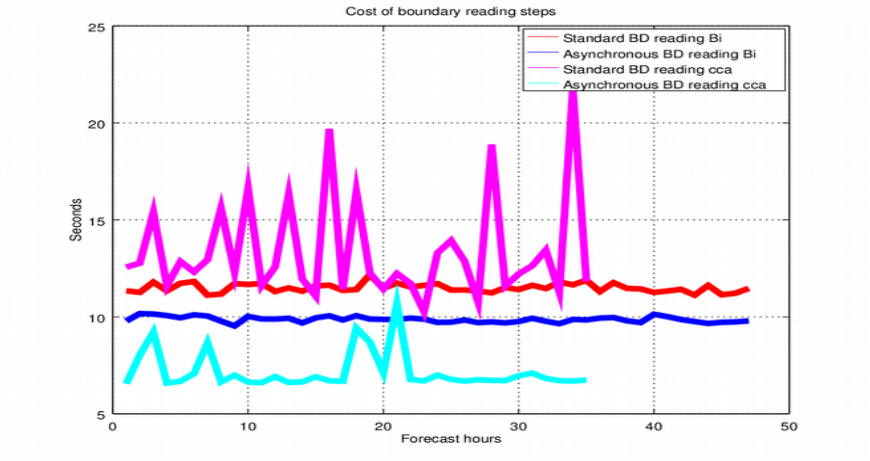

Figure 3q: Impact of asynchronous reading of boundaries from two different platforms. The gap between the red/magenta and the blue/cyan lines is the gain in seconds per input time step for the two different platforms.

3 Deterministic and probabilistic performance

3.1 Performance with respect to 38h1.2

Together with the introduction of MEPS, cycle 40h1.1 replaced the old 38h1.2 version that had been operational since December 2014. Improvements such as reduced positive wind bias and less excessive fog and precipitation can be noted. The scorecards in figure 4 shows a maintained improvement over ECMWF over areas of importance.

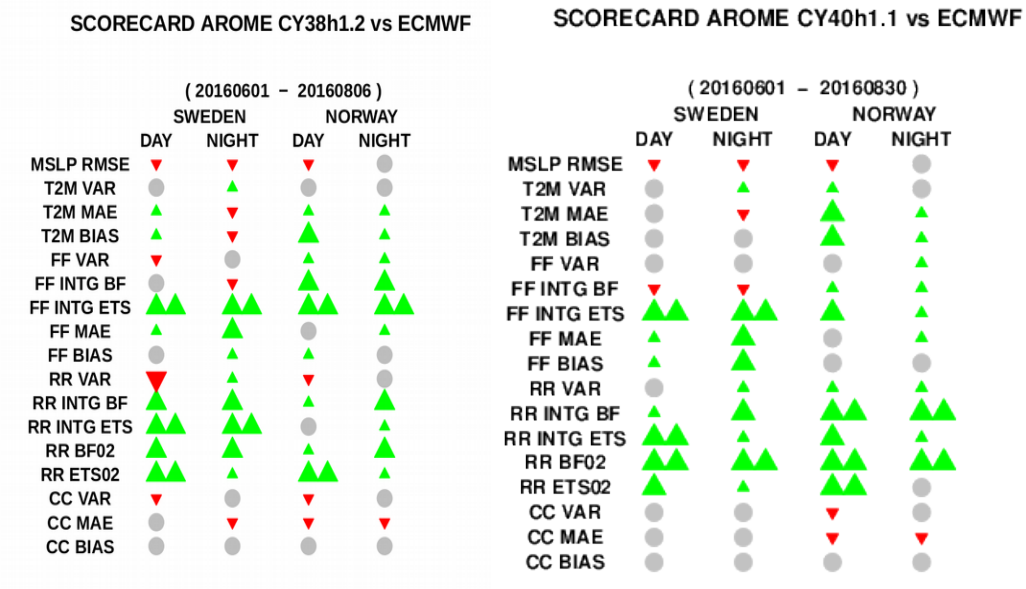

Figure 4: Scorecard for the MetCoOp setup of harmonie-38h1.2 and harmonie-40h1.1 vs ECMWF respectively (RMSE – Root Mean Square Error, VAR – variability of the dataset compared to observed variability, MAE – Mean Absolute Error, INTG BF/ETS – bias frequency/ Equitable Threat Score integrated over a wide range of thresholds, BF02/ETS02 – bias frequency/ETS for 0.2mm/12hr precipitation).

3.1 Ensemble performance

MEPS has been running in near operational mode since mid June 2016 and this allows us to make a comparison with other ensemble systems available for the forecasters such as ECMWF ENS and GLAMEPS. From the spread skill relationship shown in figure 5 it is clear that MEPS and GLAMEPS are comparable whereas ECMWF is under dispersive. For CRPS, figure 6, MEPS has the smallest error although the difference to GLAMEPS is not very large. Note that both ECMWF and GLAMEPS have five times more mebmers than MEPS. MEPS has become useful tool for the duty forecasters and both institues are building up a catalogue of products.

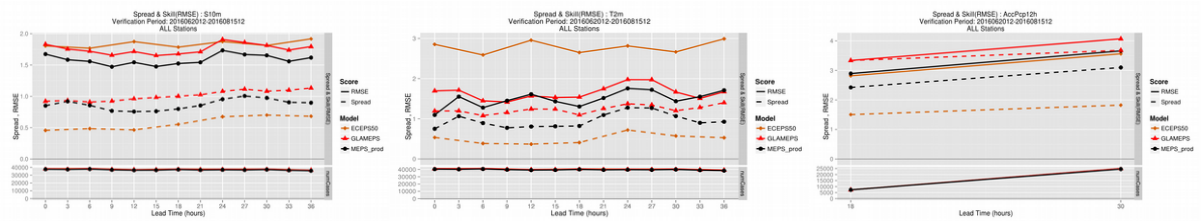

Figure 5: Spread skill for ECMWF ENS (brown), GLAMEPS (red) and MEPS(black). Solid lines denotes skill and dashed spread. The figures shows from left to right: U10m, T2m and 12h precipitation.

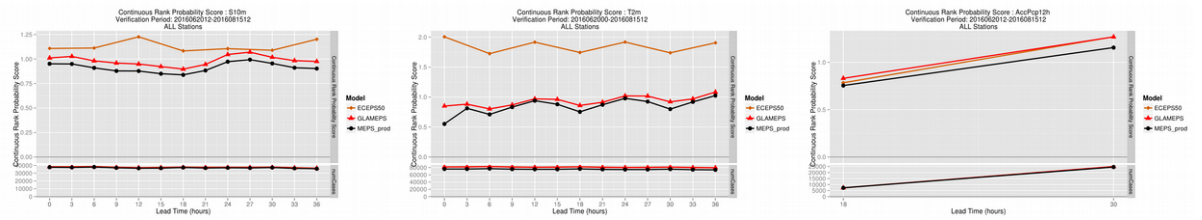

Figure 6: CRPS for ECMWF ENS (brown), GLAMEPS (red) and MEPS(black). The figures shows from left to right: U10m, T2m and 12h precipitation.

4 Future development

4.1 The forecast model

The lack of ability of the model to propely predict freezing rain has be a complaint from the duty forecasters in Sweden and Norway. This has been addressed recently and will be implemented in operations in January 2017. The overall impact is small but the forecasts improves in the specific cases, given that the general atmospheric conditions are correctly forecasted. An example from a case in 2012 is shown in figure 7 where the updated version to the right has a better match with the observations.

The separation of the nature tile in SURFEX into two patches, high and low vegetation, is currently being tested and gives a clear improvement on screen level relative humidity. Figure 8 shows that the positive bias we experience in spring time 2m relative humidity over Scandinavia is reduced when 2 patches are introduced. Although there is still a remaining bias for other reasons. Unfortunately the introduction of 2 patches (in combination with removed atmospheric surface-boundary-layer (SBL) model) now gives a slight negative bias in diagnostic 10m wind speed. We are presently investigating how this wind bias may be reduced.

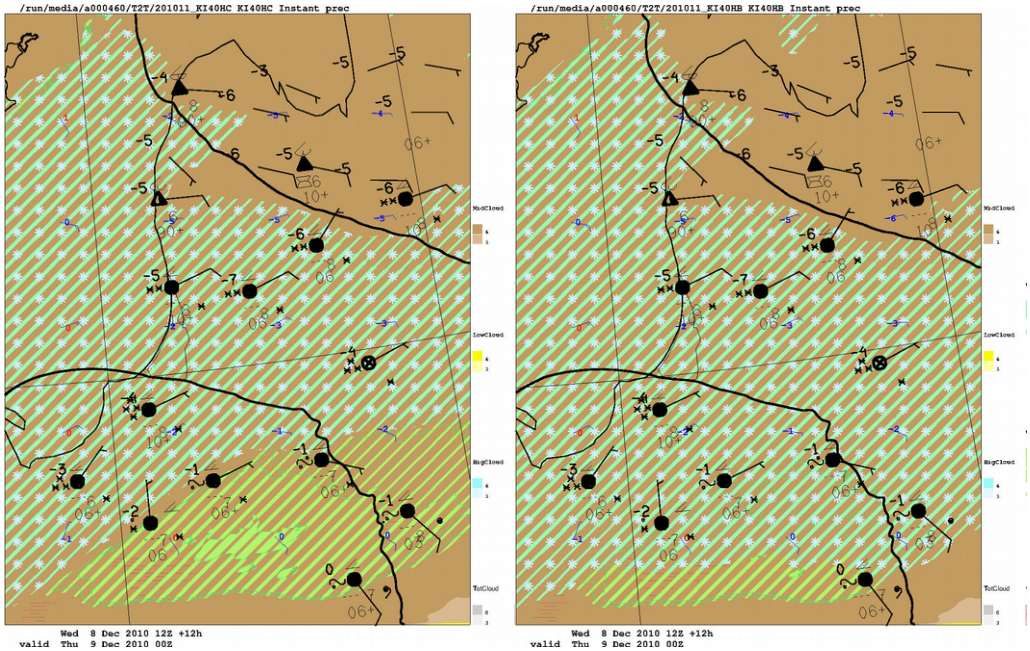

Figure 7: 12 hour forecast issued 2010-12-08-12 over the area south-east of the Baltic sea. Middle level clouds in brown, instant solid precipitation as light blue stars and instant rain as green lines. Observations in black. To the left is the forecast without updates for supercooled rain, to the right -with the updates.

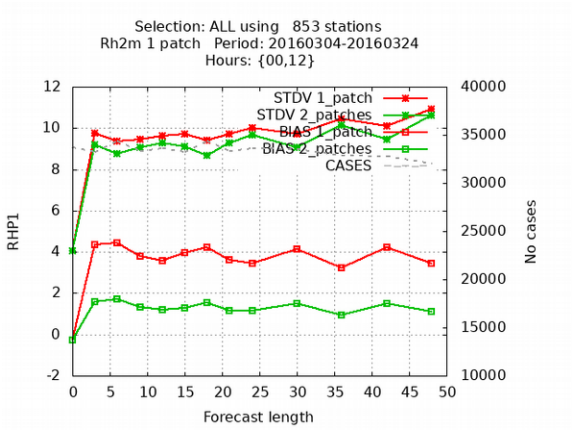

Figure 8: Verification of RH2M for a setup with one (red) or two(green) patches.

4.2 Assimilation

The current structure functions used has been derived using an older version of both the forecast model and the forcing ECMWF EDA system. New structure functions is currently being created using MEPS and the latest ECMWF EDA version. The new structure functions will be generated not only with the traditional downscaling but also by running MEPS in EDA mode as a comparison.
In the current operational setup only radar data over Sweden and Norway is assimilated and this will be extended in the pre-operational suite to include Danish and Finnish radars as well. In addition the number of GNSS stations assimilated will doubled.

4.3 The Ensemble system

Using SLAF as the perturbation method has been shown to give better scores than just using arbitrary members from ECMWF ENS. In addition it has allowed us to extend the former deterministic system

to an ensemble system without changing the boundary data transferred from ECMWF. There are however some limitations in the number of members that can be constructed with this method, something that is desirable as MetCoOp is increasing the capacity by e.g. the inclusion of FMI. There is also a question if the method reflects the real uncertainties in the right way. Consequently we are working with comparisons using the hourly ECMWF ENS data nowadays available four times a day. The work involves clustering of members to maximize the spread as well as rescaling of the perturbations.
The surface perturbation method developed by Meteo France (Bouttier et.al. 2012) has been shown to increase the spread and reduce the RMSE of e.g. T2M, see figure 9. The surface perturbations are now tested in MetCoOp although with a reduced set of parameters, adjusted length scales and perturbation sizes. In the operational setup we have seen problems that are related to the 6h cycling used for the ensemble members, as compared to 3h for the control, and we see a need to redesign this when introducing the surface perturbations.

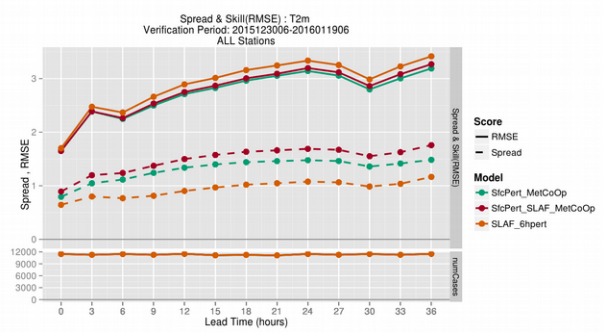

Figure 9: T2M spread and skill for surface perturbations only (green), surface perturbations + SLAF (red) and SLAF perturbations only (brown). Solid lines denotes skill and dashed spread.

4.4 Extending MetCoOp

Since 1st of January 2017 FMI is a part of MetCoOp and the growth implies an increased HPC capacity but of course also an increased domain size to fulfil the needs of FMI. The full switch to a common new domain distributed over three HPC resources is expected to take place during the second half of 2017.

5 References

Bengtsson, L., Andrae, U., Aspelien, T., Batrak, Y., Calvo, J., de Rooy, W., Gleeson, E., Sass, B. H., Homleid, M., Hortal, M., Ivarsson, K.-I., Lenderink, G., Niemelä, S., Nielsen, K. P., Onvlee, J., Rontu, L., Samuelsson, P., Santos Muñoz, D., Subias, A., Tijm, S., Toll, V., Yang, X., Køltzow, M. Ø., 2017: The HARMONIE-AROME model configuration in the ALADIN-HIRLAM NWP system, Monthly Weather Weather Review, accepted for publication, January 2017

Bouttier F, Vie B, Nuissier O, Raynaud L. 2012. Impact of stochastic physics in a convection-permitting ensemble. Mon. Weather Rev. 140: 3706 – 3721

Malardel, S. and Ricard, D. (2015), An alternative cell-averaged departure point reconstruction for pointwise semi-Lagrangian transport schemes. Q.J.R. Meteorol. Soc, 141: 2114–2126. doi:10.1002/qj.2509

Garcia-Moya, J-A et.al, 2015: http://www.umr-cnrm.fr/aladin/IMG/pdf/slaf.pdf

NEA, the Operational Implementation of HARMONIE 40h1.1 at DMI

Xiaohua Yang, Bjarne Stig Andersen, Mats Dahlbom, Bent Hansen Sass, Shiyu Zhuang, Bjarne Amstrup, Claus Petersen, Kristian Pagh Nielsen, Niels Woetmann Nielsen, Alexander Mahura, from Danish Meteorological Institute

1. Introduction

During 2016 DMI added HARMONIE-NEA to its operational NWP suite. NEA (North Europe domain A) features an upgraded source code basis with improved model physics and dynamics, an improved physiographic database, and a significantly increased use of remote sensing data. Further, NEA is configured on a significantly extended model domain, bring improved forecast capability for Denmark and nearby waters, as well as for the Faroe Islands. NEA was launched simultaneously with the model IGA for South Greenland and Iceland (Yang et al. 2017).

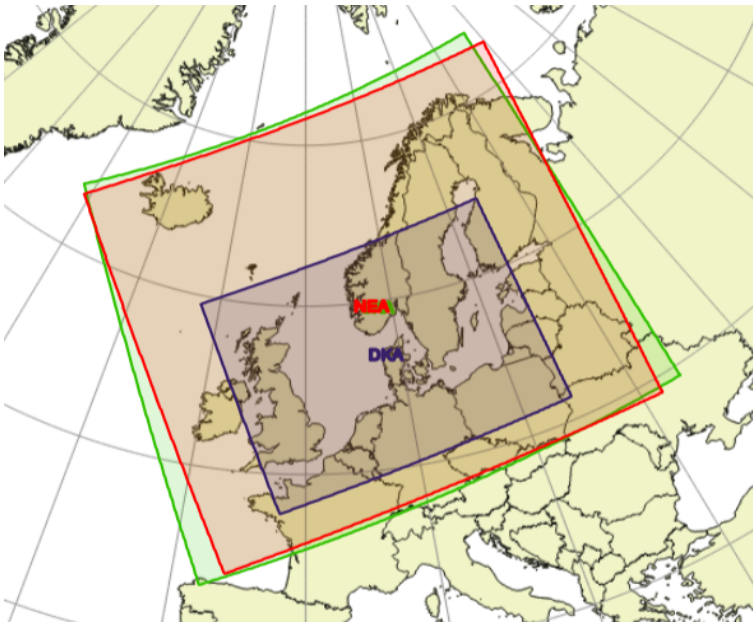

Figure 1: The new HARMONIE operational domain NEA (in red, with a grid resolution of 2.5 km) in comparison to the previous operational HARMONIE domain DKA (in blue, with a grid resolution of 2.5 km) and the operational HIRLAM domain SKA (in green, with a grid resolution of 3.3 km).

NEA is based on the reference Harmonie-40h1.1 as released by the HIRLAM-C programme (Bengtsson et al 2017). An extensive amount of numerical experiments have been conducted using the NEA setup, contributing to the coordinated pre-release validation and tuning in connection with tagging of the reference 40h1.1 in HIRLAM-C. In addition, several local deviations in the configuration options have been implemented following extensive evaluation with an aim to improve the performance. In NEA the data assimilation has been expanded with several new remote sensing data streams such as ATMS, AMV and Radio Occultation (RO) data. Furthermore, an extended set of forecast parameters have been developed for the HARMONIE suites at DMI, with the goal to enable the operational HARMONIE to fully replace the corresponding operational HIRLAM suites and cover the production needs at DMI.

This note briefly presents the NEA model configuration, its main deviations from the reference HARMONIE and some of the associated evaluation examining these deviations. A more detailed description, including results from validation study and operational monitoring, will be featured in a separate, extended report.

2. Model configurations and adaptation

Domain and configuration

NEA is configured on a horizontal grid with 1280x1080 columns with a Lambertian projection, 2.5 km in grid resolution and 65 levels with a terrain-following hybrid vertical coordinate. The lowest model level is about 12 m above the ground and highest level is at approximately 10 hPa. The NEA domain, as shown in Figure 1, covers approximately the same area as that of the previously operational HIRLAM-SKA domain, which had a 3.3 km grid resolution. Compared to the previously operational HARMONIE-DKA, NEA covers an area 1.7 times larger. No doubt, the upgrade of the operational HARMONIE at DMI onto a domain as large as NEA is only feasible with the new HPC installation at DMI with two Cray XC30 clusters. With the operationalisation of NEA, the high resolution HARMONIE forecast is extended to give good coverages of the Faroe Islands in the Northern Atlantic Ocean. The full coverage of NEA includes all nearby waters around Denmark (including the whole Baltic Sea and the North Sea). This makes it feasible to use the HARMONIE model to drive several downstream model applications at DMI, such as the operational storm surge models and the atmospheric dispersion models for emergency preparedness.

NEA is configured with a 3 hourly data assimilation cycling, each running 60 h forecasts. It is run at base times of 0, 3, 6, 9, 12, 15, 18 and 21 UTC. The model runs has 1h 15 m observation cutoff relative to the base time. The full set of forecast results for each cycle is delivered to end users about 3 h after the nominal analysis time (the base time).

Model adaptation and evaluation experiments

In connection with the implementation and validation of HARMONIE-40h1.1, an extensive amount of multi-season evaluation and tuning experiments have been done using NEA configuration. These include comparative sensitivity/impact studies of domain sizes, the upgraded orographic database (in which GMTED2010 in 250 m resolution replaces the previous reference database with GTOPO-30 at a resolution of 1 km), the turbulence parameterisation HARATU, the use of cubic/quadratic grid in the spectral truncation for the grid representation, the test of modified radiation parameterisation settings involving cloud inhomogeneity factor and a correction of the parameterisation of the cloud optical properties. These evaluations have contributed to defining the reference release of HARMONIE 40h1.1 and they are detailed in the system wiki of HIRLAM-C (https://hirlam.org/trac/wiki/Harmonie_40h1/ValidationTests) and a summary report (HIRLAM-C Management, 2016). In this report, we only describe briefly the evaluations associated with the testing in NEA for several configuration options that differ from reference HARMONIE 40h1.1. This include the use of a cubic grid, selection of time step length, the subgrid-scale orographic drag parameterisation (SSO), the derivation of a structure function with EDA, and assimilation of several additional remote sensing data streams in the 3DVAR data assimilation.

Recently, following successful experiences at ECMWF, spectral representation on grid point space using cubic or quadratic grids (instead of a linear grid) has been evaluated in the HIRLAM consortia (Bengtsson et al, 2017). In these studies, higher spectral truncation has been found to be dynamically more stable, and computationally more effective. While higher truncation has been shown to be able to maintain similar quality for most forecast parameters, a tendency with increased wind speed bias has

been observed, typically in areas with steep orography. Figure 2 illustrates the test results with NEA in terms of forecast error of surface wind and temperature for a month-long winter episode. It is shown, e.g. from Fig 2a, that wind speeds over Scandinavia (which include many observation stations over a complex terrain) indeed suffer a larger positive bias with higher truncation cubic grid than runs with less a truncated quadratic grid. The tendency is not as clear though for the Danish area with flat terrain (Fig 2b). On the other hand, as also is shown in Fig 2a, activating orographic surface drag via SSO in the run with cubic grid can quite effectively reduce the wind speed bias. The impact of SSO seems to be to compensate for the increased wind, so that the wind speed bias become a lot less than the run with quadratic grid. Interestingly, use of SSO seems also have impact on wind speed for the area with flat terrain. Meanwhile, the sensitivity of temperature forecasts to these variations seem to be insignificant, as shown in Fig 2c and 2d. Parallel tests have also been made for a summer and an autumn test episode with similar outcomes.

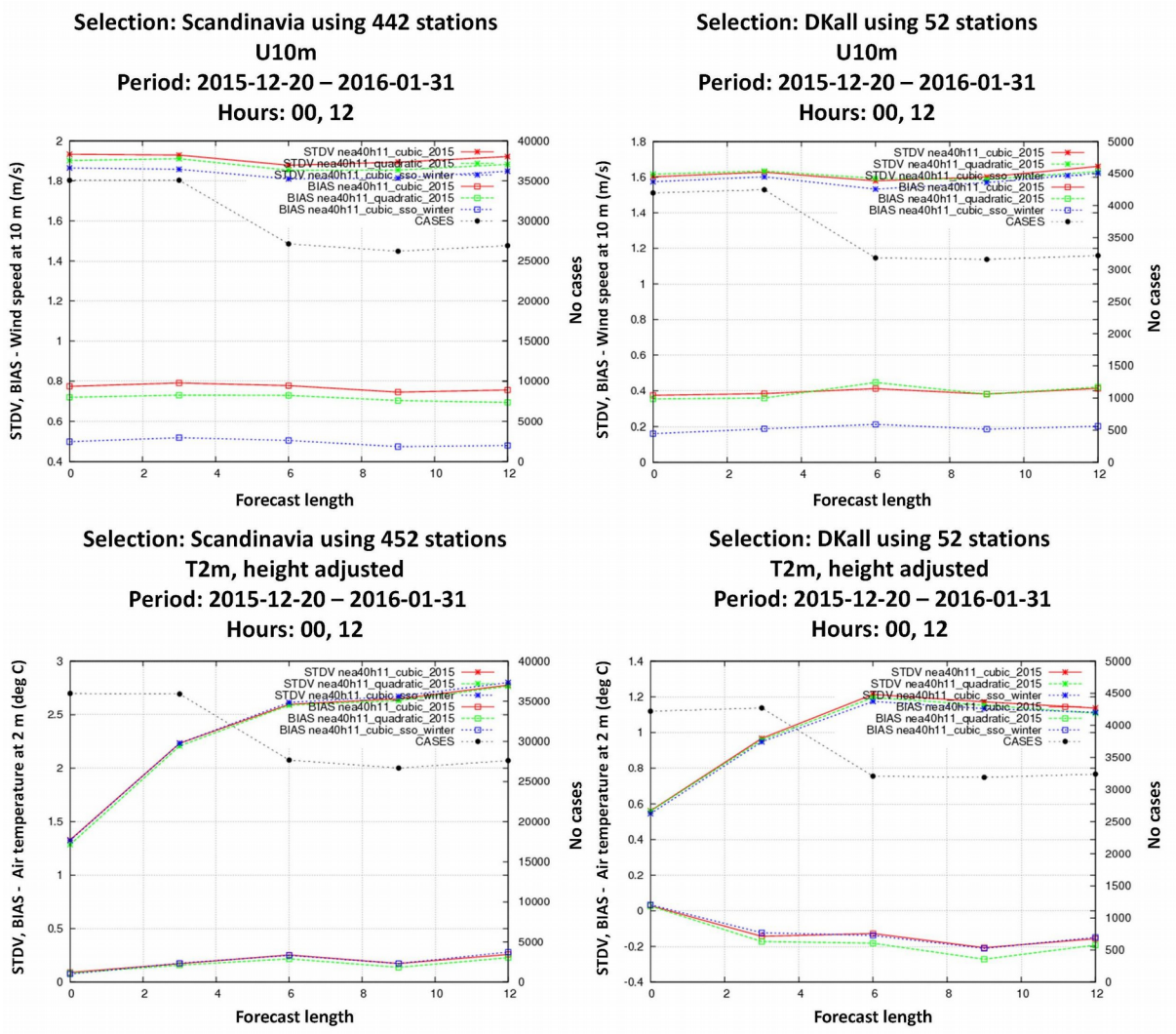

Figure 2 : Averaged model errors as a function of forecast lead-time as compared to surface observations from the period between December 20 2015 and January 31 2016 for a) 10-metre wind over Scandinavia b) 10-metre wind over Denmark, c) 2-metre temperature over Scandinavia and d) 2 -metre temperature over Denmark. The red curves show the results for forecasts using a cubic grid, the green curves for forecasts with a quadratic grid, and the blue curves for forecasts with a cubic grid and the SSO parametrisation.

Experiments with time step length have been made for selected summer and winter episodes, in connection with the test of a cubic grid for NEA. Time step lengths of 60, 75 and 90 s, respectively, have been tested. Figure 3 shows a verification comparison between the experiments for the surface parameters mean sea level pressure (MSLP), 10-metre wind, and 2-metre temperature and humidity for the winter episode, revealing overall rather marginal differences between the forecasts. Similar results have been observed for a summer episode, demonstrating satisfactory robustness of the dynamics settings as selected in the model configuration.

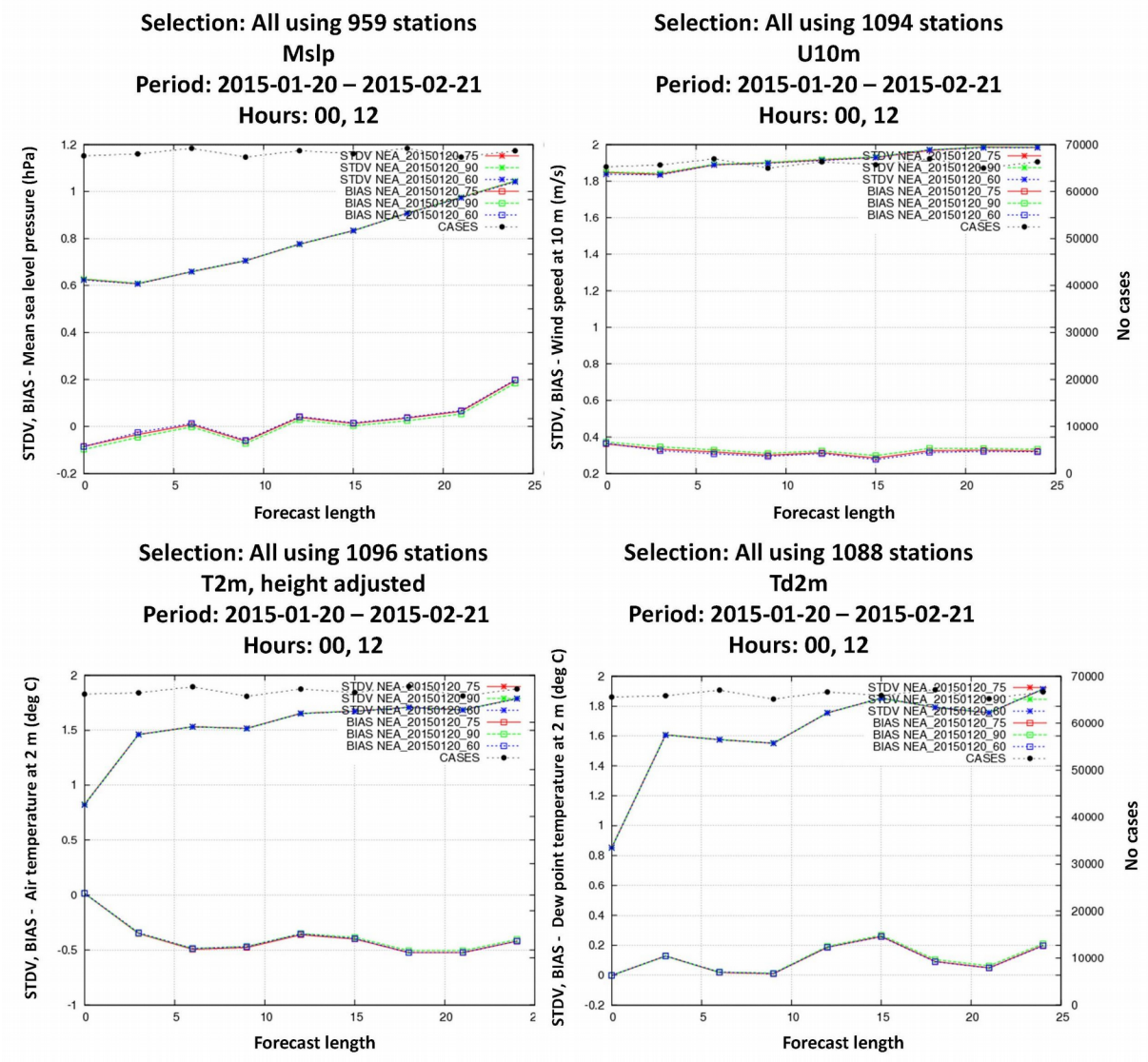

Figure 3: Averaged standard deviation and bias errors as a function of forecast lead time (in hours) with NEA when running with a cubic grid and time step lengths of 60s (blue), 75s (red) and 90s (green) with a) Mean Sea Level Pressure, b) 10-metre wind speed, c) 2-metre temperature and d) 2-metre dewpoint temperature, for the one month winter episode between January 20 and February 21 2016.

Based on the results of extensive validation and tuning experiments, the final configuration of NEA has been chosen as: A cubic grid with 75 s time step length and an activated SSO scheme (with a drag coefficient XFRACO set to 300). Monitoring of the wind forecast skill after the operationalisation of NEA shows the wind forecast of NEA to be rather satisfactory. See further details below.

Data assimilation

HARMONIE 3-Dimensional Variational Data Assimilation (3DVAR) has been used for upper air data assimilation in NEA, with special focus on increasing the use of remote sensing data. For surface assimilation, NEA uses the reference HARMONIE 40h1.1 settings with assimilation of screen level temperature and humidity, as well as snow-depth. SST and sea ice fraction from ECMWF analysis are used to initialise the sea surface conditions.

A two-step boot-stripe approach has been followed to derive background error statistics on the ECMWF HPC. Structure functions for NEA on both cubic and quadratic grids have been derived, following the procedure described below. First, a downscaling run with a 4-member HARMONIE EPS is done with HARMONIE 40h1-trunk. A 10-day uncycled run is launched every 12 h, using the ECMWF EPS (ENDA stream) as initial and lateral boundaries. The differences in 6 h forecasts constitute the sample to generate background error covariance statistics. In second step, the above preliminarily derived structure functions from the first step were adopted to re-generate new structure functions by running Ensemble Data Assimilation (EDA). The EDA consists of an ensemble of perturbed data assimilation cycles and can be used to estimate the background errors in which more mesoscale features are represented than the downscaling method do. The EDA run starts at 2013081500 and end at 2013082418 with 6 h interval and 8 perturbed members. For NEA, a scaling factor of 0.3 for the background term has been chosen, In view of the limited size in the extension zone with 11 points, a data exclusion zone of 150 km has been specified to avoid potential problems with assimilation of observation data close to the lateral boundary.

NEA 3DVAR assimilates considerably more observation data than those in the reference HARMONIE 40h1.1. For conventional observation, it assimilates in addition MODE-S-EHS temperature and wind data as obtained via ftp from KNMI. For remote sensing data, NEA assimilates atmospheric radiance over sea from AMSU-A, MHS and ATMS instruments onboard NOAA 18/19, Metop A/B and NPP. Among these, the Suomi NPP (National Polar-orbiting Partnership) satellite (JPSS-0) carries the Advanced Technology Microwave System (ATMS) instrument that measures brightness temperatures in the atmosphere using 22 channels. These combines the strengths of the AMSU-A and MHS instruments. A subset of channels have been used in assimilation, selected with considerations on model's vertical configuration and quality of the instrument channels. For radiance data, variational bias correction (VARBC) is applied. Atmospheric Motion Vectors (AMV) observations from the geostationary Meteosat-10 are used actively. These observations contains wind information extracted by tracking motions of clouds and other atmospheric constituents and are obtained through the consecutive images (15 min apart). Channels used are the WVCL1, WVCL2, VIS2, IR3 and VIS3. AMV observations are primarily used over sea but are also included over land when the model surface pressure is more than 50 hPa higher than that of the observation. Radio Occultation observations (GNSS-RO) are assimilated using the bending angle from both the Metop-A, Metop-B and the six COSMIC satellites. All of these satellite data are acquired from the Eumetcast system except for ATMS data. The latter is obtained from local receiving stations in Denmark and Greenland. In addition, assimilation of radar reflectivity data has been included in the NEA-suite during pre-operational stage, which has demonstrated an overall positive impact in comparative studies. As illustrated in Fig 4, radar data from 12 countries are assimilated, using data retrieved mainly through the EUMETNET/OPERA data stream, in hdf5 format and quality controlled (QC) using the BALTRAD quality control package. QC is performed in order to clean the data from unwanted and non-precipitating echoes, for example external emitters, ground and sea clutter. The resolution of the

radar volume data is usually much higher than that of the NWP model and hence needs to be thinned, not doing so would be detrimental to both the memory usage of the model and the assimilation process in general. For this purpose, we utilize a preprocessing tool developed within the HIRLAM consortium that harmonizes the OPERA-HDF5 files and reduces the data amount using the supperobbing technique. Radial winds are currently under investigations, however. As OPERA is not requiring the member states to upload radial winds data and hence is not redistributing such observations, i.e. there is precious little such data available compared to radar reflectivities. Presently, in view of stability with data delivery and needs to do more evaluation and tuning, assimilation of radar data is arranged in a parallel suite, with plan to operationalise it at next upgrade.

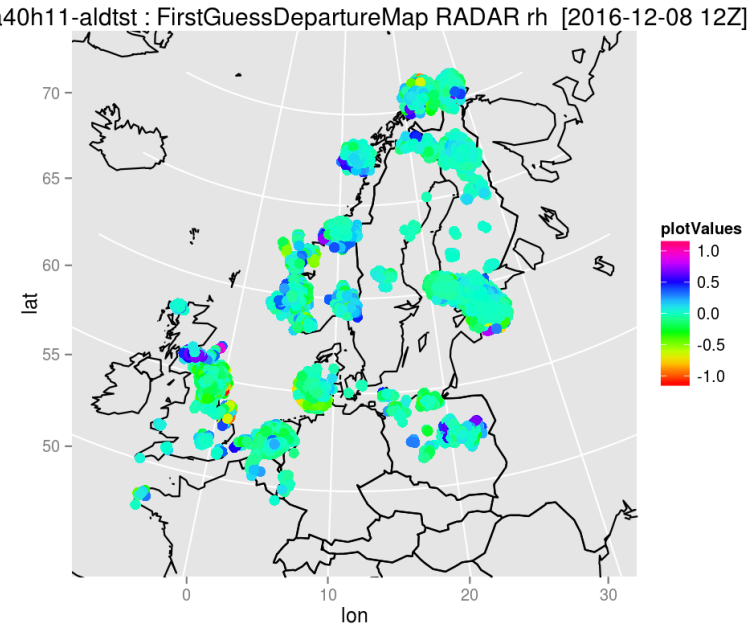

Figure 4: Radar reflectivity data from up to 12 countries have been successfully assimilated in the real time 3DVAR in NEA. The example shown here is the analysis increment of radar reflectivity for assimilation cycle 20161208 12 UTC

Postprocessing

In connection with the HARMONIE upgrade to NEA, an extended range of postprocessing parameters have been generated for end-users. Apart from those available from the reference HARMONIE, additional output stream has been produced by adapting the stand-alone NWP post-processing utility initially developed at DMI for the HIRLAM system for the purpose of addressing service needs in the local production system. Among these, some of the parameters are listed below.

Clear Air Turbulence (CAT). The CAT index is developed for aviation forecasts (Nielsen et al, 2012). It has many similarities to the well known ELROD index but is further elaborated. The index is calculated on all model levels and consists of two indices - a cyclonic and an anti-cyclonic index.

Icing index. This index calculates the risk of icing of aircrafts with an integer (0,1,2,3,4) showing the risk level. It is calculated on all model levels and on some flight levels. Additionally levels for the lowest and highest freezing points are calculated.

Thunder index. This index (Nielsen et al, 2003) calculates the likelihood for lightning with a number between 0 and 1. It takes into account a number of key factors which are typical for high risk of lightning such as stability, CAPE, presence of ice and depth of cloud below and above the ice phase. Additionally the tropopause height, equivalent potential temperature are calculated as input to the thunder index routine.

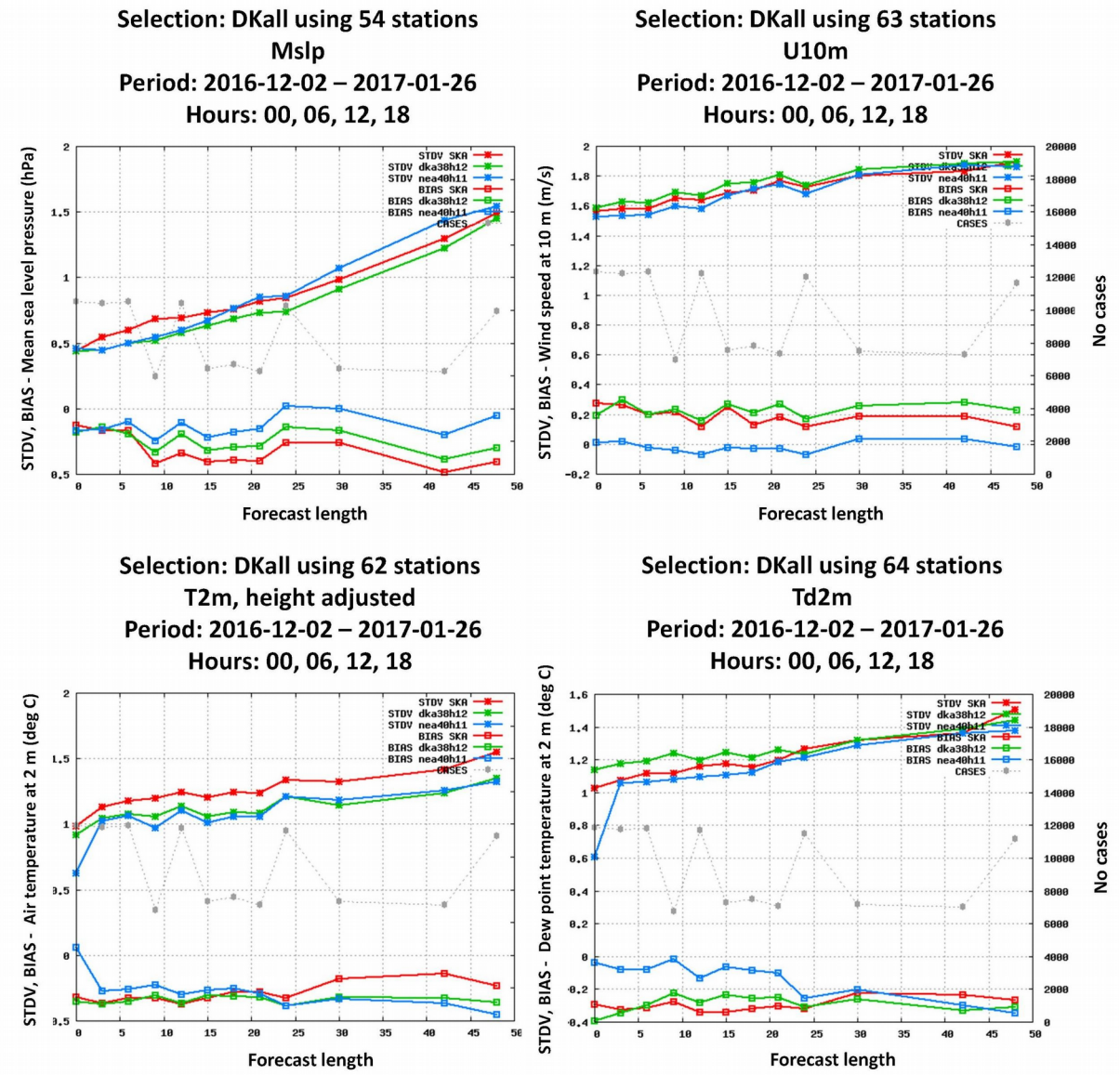

Figure 5 : Averaged standard deviation and bias errors as a function of the forecast lead-time, validated against surface observations of Danish stations since operational launch of NEA, during Dec 2 2016 and Jan 26 2016, for , a) Mean Sea Level Pressure, b) 10-metre wind speed, c) 2-metre temperature and d) 2-metre dewpoint temperature. The red curves are for previous operational HIRLAM-SKA, green for HARMONIE-DKA and blue for HARMONIE-NEA.

Flash-flood (cloud burst) index. This newly developed index attempts to identify locations with high risk of cloudburst. It takes into account stability, precipitable water, wind, CAPE and CIN. A report about the index is currently in preparation.

Cloud visible transparency index. This index supplement the forecast of cloud cover with a number between 0 and 1 which describes the transparency of the clouds at visible wavelengths. E.g. thin cirrus clouds have a high transparency whereas thick frontal clouds have a low transparency.

3. Operationalisation and forecast performance

Following extensive validation and tuning experiments, NEA was implemented for real-time cycling since summer 2016, followed by a pre-operational launch in mid-September and an official launch in beginning of December 2016.

Monitoring of the forecast performance both during experimentation stage and real-time cycling has shown satisfactory performance with HARMONIE-NEA in comparison to the previous operational suites with both HIRLAM and HARMONIE. Figure 5 shows the verification statistics for NEA since its official launch on Dec 2 2016, as compared to those of the previous operational suites HIRLAM-SKA and HARMONIE-DKA for Danish stations. As shown in these comparisons, NEA shows an overall clear improvement of standard deviation errors to varying degree, and a reduction in the bias error for most parameters. NEA is also seen to have improved precipitation forecast scores and reduce the overall positive bias of the cloud cover forecasts.

References

Bengtsson, L., Andrae, U., Aspelien, T., Batrak, Y., Calvo, J., de Rooy, W., Gleeson, E., Sass, B. H., Homleid, M., Hortal, M., Ivarsson, K.-I., Lenderink, G., Niemelä, S., Nielsen, K. P., Onvlee, J., Rontu, L., Samuelsson, P., Santos Muñoz, D., Subias, A., Tijm, S., Toll, V., Yang, X., Køltzow, M. Ø., 2017: The HARMONIE-AROME model configuration in the ALADIN-HIRLAM NWP system, Monthly Weather Weather Review, accepted for publication, January 2017

Nielsen, Niels Woetmann, and Petersen, Claus, 2012: An upper-tropospheric clear and cloudy air turbulence index in DMI-HIRLAM,2012, DMI report No. 12-01, https://www.dmi.dk/fileadmin/Rapporter/SR/sr12-01.pdf

Nielsen, Niels Woetmann, and Petersen, Claus: A generalized thunderstorm index developed for DMI-HIRLAM, 2003, DMI report No. 03-16,https://www.dmi.dk/fileadmin/Rapporter/SR/sr03-16.pdf

Yang, X, B Palmason, B S Andersen, B H Sass, B Amstrup, M Dahlbom, C Petersen, K P Nielsen, R Mottram, N W Nielsen, A Mahura, S Thorsteinsson, N Nawri and G N Petersen, 2017: IGA, Joint Operational HARMONIE by DMI and IMO, Joint ALADIN-HIRLAM Newsletter 8, 2017.

HIRLAM-C Management Group, 2016 : Quality Assessment of HARMONIE-CY40h1.1, HIRLAM system wiki, https://hirlam.org/trac/attachment/wiki/CommunicationWithUsers/Quality-assessment-of-HARMONIE-CY40h1.1-161031.pdf

Construction of a continuous mesoscale EPS with time lagging and assimilation on overlapping windows

Xiaohua Yang, Henrik Feddersen, Bent Hansen Sass, Kai Sattler
Danish Meteorological Institute

1. Introduction

High impact weather such as strongly convective precipitation is often characterized by a rapid development with short spatial and time scales, hence of limited predictability. Forecasting mesoscale extreme weather with a timely warning is a major challenge facing NWP research and operational community. First, resolving such phenomena often requires high resolution NWP with timely assimilation and frequent update. Second, uncertainty information needs to accompany with prediction of extreme weather in order to address limitation in predictability. This calls for an Ensemble Prediction System (EPS) at high resolution and, preferably, also with frequent update and early delivery. For an operational mesoscale ensemble forecast system, the above mentioned need to maintain high spatial and temporal resolution with adequate spread, and a quick and frequent delivery, is associated with significant computation cost, hence, technical affordability is a major concern in system construction.

Recently, the design for a COntinuous Mesoscale Ensemble Prediction System (COMEPS) has been proposed(Yang et al, 2016), with a goal to construct a high resolution, operationally affordable high resolution EPS for routine weather forecast. One of the main ideas in COMEPS is the assembling of a time lagged ensemble using continuously generated forecast members which are produced around clock. Increase of temporal spread, rapid update in data assimilation, frequent delivery and a more balanced, evenly distributed HPC load are among many underlying considerations behind the design. Based on these, a mesoscale EPS system has been developed at Danish Meteorological Institute (DMI) . After extensive real time testing with satisfactory verification results, COMEPS is now ready to be operational at DMI.

At present, COMEPS is a two model ensemble using both HARMONIE and HIRLAM forecast systems, with production on a common grid defined by the DKA-mesh with 800x600x65 and 2.5 km grid spacing. It runs data assimilation each hour and generates a 24-member EPS probabilistic forecast of up to 42-hour on hourly basis. Apart from obtaining spread through time lagging and multi-model approaches, COMEPS also utilises several perturbation techniques to enhance representation of uncertainties, such as use of Scaled LAgged Forecasting (SLAF) for lateral boundary perturbation, use of alternative option mix in physical parameterisation. Another novel configuration feature in COMEPS is the data assimilation cycling, which consists of three parallel sets of data assimilation cycles over overlapping time windows, providing additional opportunity to construct perturbation in initial condition. The design to configure uncycled analysis with short time interval may potentially also be useful in operational nowcasting and 4DVAR.

In this notes, we present main configuration features of COMEPS. A more detailed documentation about COMEPS is in preparation.

2. Configuration with a continuously refreshing EPS

For COMEPS, the concept "continuous" refers both to generation of ensemble members around clock, and to production of probabilistic forecast each hour.

In contrast to a traditional EPS system with control members obtained from intermittent data assimilation with cycling interval of 6-hour, such as GLAMEPS (Iversen et al 2011), DMI-EPS (Feddersen 2009) or 12-hour (ECMWF ENS), COMEPS defines control members to be hourly analyses obtained through assimilating latest available observations. This is then followed by ensemble forecasts with perturbations around initial and lateral boundary states and also around physical parameterisation. To ensure a smooth data flow, every COMEPS data assimilation and the follow-up forecast integration shall be finished well within one hour. This same procedure is repeated in the next hour, and next again.

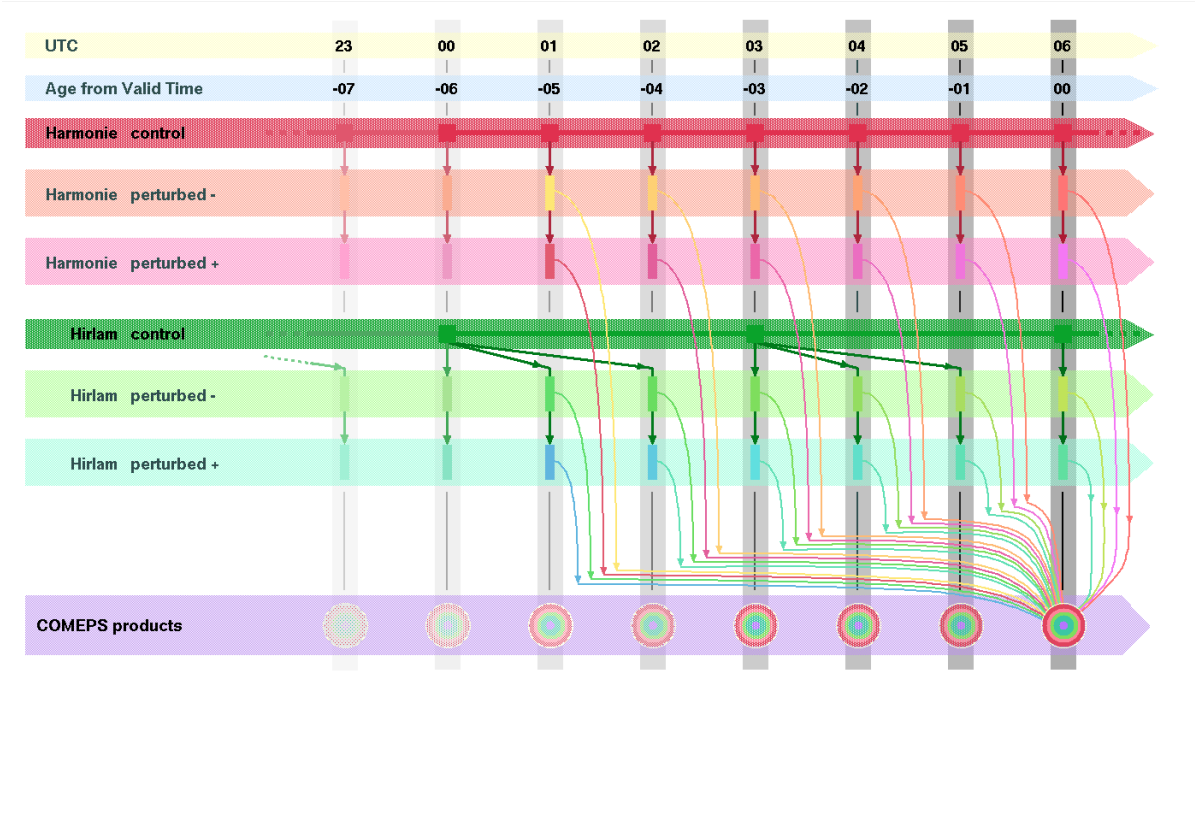

Figure 1: Schematic illustration of the data flow for COMEPS which generates ensemble forecast every hour around clock. For any given base hour, COMEPS ensemble consists of perturbed ensemble members that are generated with base time over the last 6 hours, with 2 perturbed members each hour from HARMONIE and 2 from HIRLAM , thus 4 newly generated perturbed members each hour, summing up to a total of 24 members with time lagging..

Figure 1 illustrates the implementation of the above design in the current DMI-COMEPS. For any given base hour, e.g. 06 UTC, COMEPS ensemble consists of perturbed members that is generated with base time over the last 6 hours (01,02,03,04,05 and 06 UTC), with 2 perturbed members each hour from HARMONIE and 2 from HIRLAM , thus 4 newly generated perturbed members each hour, which sums up to a total of 24 time-lagged members. Applying same approach to any given base hour, a probabilistic forecast can be generated.

One can think of numerous advantages with use of the above approach in ensemble generation. By applying time lagging, a sizable EPS (with 24 members) at rather high resolution is obtained. Use of hourly control analysis allows use of frequent refresh cycling in which latest observation is assimilated, providing better potential for the forecast system to react to the latest weather evolution. Averaging of forecasts with limited length of time shift may potentially be beneficial to reduce the jumpiness often seen from forecasts initiated with intermittent assimilation. Finally, one important advantage here is that the production task has been evenly distributed along time, avoiding the commonly seen problems with uneven use of HPC resources at operational NWP centers. With a final ensemble size of COMEPS at 24, it is unusually large compared to average sizes of LAM ensembles. Moreover, it is continuously produced around clock, even though it in reality only update 4 of the 24 members each hour. With COMEPS, generation of mesoscale EPS becomes easily achievable and feasible.

3. Assimilation cycling with overlapping windows

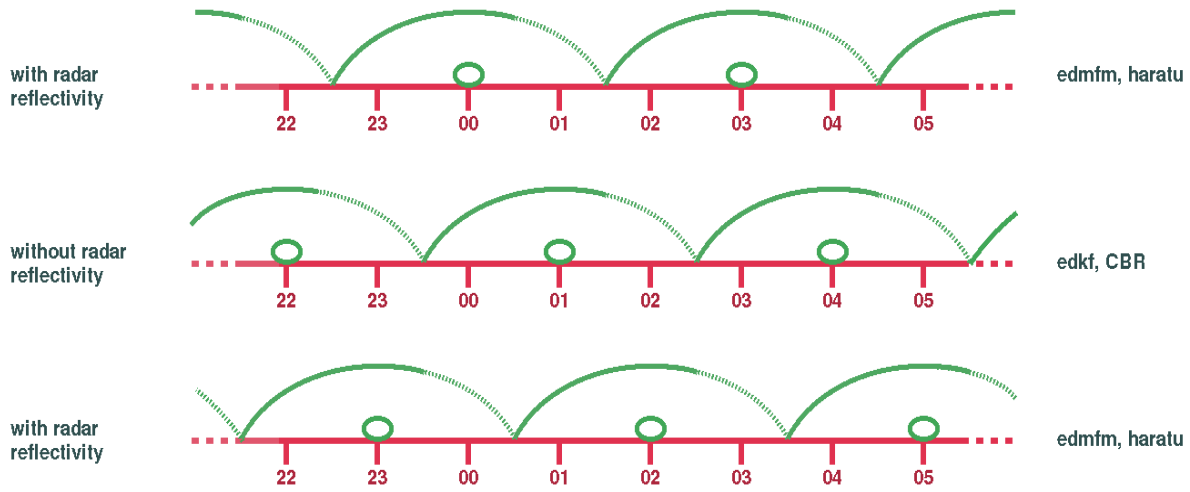

Figure 2: Schematic illustration of the cycling design in COMEPS for generation of hourly control analysis, which is achieved by running three independent data assimilation cycling with shifted base hours (small green circles). For each base hour, a control analysis is made to assimilate observation data over a 3-hour window around the base time, as illustrated by the green lines. This is followed by two ensemble forecast integrations with certain perturbations, including those initial perturbation around the control analyses. Similar procedure is configured for both HIRLAM and HARMONIE sub-ensembles. Note that for any given base-time, say 00 UTC, the suites at neighbouring base hours (23 UTC and 01 UTC), are independent.

COMEPS data flow requires launch of hourly perturbation forecasts around the control analysis that is obtained by assimilating latest observation, facilitating timely update of initial states to capture fast evolving atmospheric states. Technically, this can be easily achieved by setting up hourly assimilation cycling for control members. In the COMEPS implementation, however, we propose an alternative cycling approach to achieve the hourly refresh of control analysis. Figure 2 illustrates the

COMEPS cycling approach with three parallel data assimilation cycling. For both COMEPS-HIRLAM and COMEPS-HARMONIE model components, three parallel suites are configured, each with a 3-hourly cycling. The first suites run on base time at 00, 03, 06..., the second suites run on an one-hour shifted base time at 01, 04, 07..., the third on yet another hour shift at 02, 05, 08.... These three suites are mutually independent, and each suite is defined on observation time window that partly overlap with the other two suites with base time 1 or 2 hours apart. Taking advantage of three mutually independent suites, it is convenient to implement some deviations in the configuration of control members to enhance spread. As illustrated in Figure 2, on/off switch about activation of radar assimilation and selection of physical parameterisation scheme have been configured for the control members in COMEPS-HARMONIE, allowing coexistence of three sets of control members which are statistically of comparable forecast qualities.

Assimilation over overlapping windows have earlier been proposed in other context with the argument to benefit from longer window (eg., Fisher et al, 2011). In the current application, configuration of several parallel data assimilation suites on overlapping windows is also believed to have several advantages. Longer assimilation window is beneficial for assimilation to achieve a more balanced model states which shall also suffer less spin-up problem. Wider assimilation window is also beneficial to utilize more observation, some of which may otherwise be left unused due to longer delivery. Example for the latter is radiosonde as well as some satellite observation with slow delivery. From technical point of view, splitting runs into several parallel, independent cycling help to make operational suites more robust and easier to maintain and troubleshoot. As the suites between consecutive time points are independent from each other, it is easier to handle run-time irregularities occurred on individual suites.

4. Towards operational COMEPS

In the first operational implementation of COMEPS, a system with two-model ensemble has been proposed, combining equal numbered sub-ensembles with one based on HARMONIE forecast system and another on HIRLAM system. A COMEPS forecast consists of 12 ensemble members based on the adapted reference HARMONIE 40h1.1 at DMI (Yang et al, 2017), 12 members based on the adapted HIRLAM 7.3 (Feddersen et al 2009).. HARMONIE is run on the DKA grid of 800x600x65 with 2.5 km grid spacing, HIRLAM is run on the H03 grid of 830x640x65 with a grid resolution 0f 0.03 degree (ca 3.3 km), As described above, for each model component, 2 perturbed forecasts are produced each hour around control analysis assimilating latest available observation. Each hour, COMEPS probabilistic forecast is assembled using ensemble members produced in the last 6 consecutive hours on the common grid defined by DKA, forming a 24 member ensemble.

For perturbation, both of the sub-ensembles apply combination of the approaches as developed in the HIRLAM research community in form of perturbations of initial and boundary conditions and in physical parametrisation.

The advantage of two-model ensemble with COMEPS can be demonstrated by comparing the probabilistic verification scores between the full COMEPS system and that of the HIRLAM and HARMONIE sub-ensembles, individually. Figure 3 shows the Continuous Rank Probabilistic Score (CRPS) along forecast lead-time for COMEPS forecast of screen level temperature, wind and 12-h accumulated precipitation, for the month of December 2016, with verification about all Danish stations. Comparing scores for sub-ensembles, it is clear that the skill scores with the complete COMEPS system are best, indicating that putting individual model sub-ensembles together brings clearly added values.

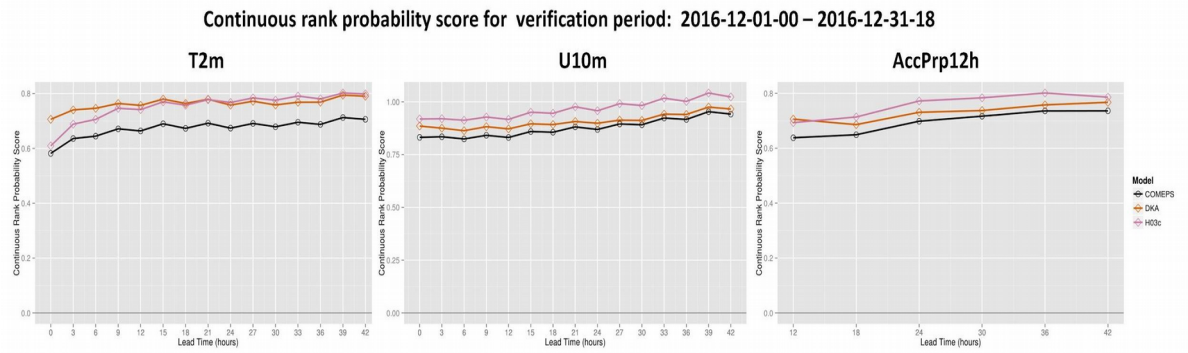

Figure 3:Probabilistic forecast skill of 24-member COMEPS (in black) as measured by Continuous Rank Probabilistic Score (CRPS) along forecast lead-time for Danish stations in December 2016. Also plotted are the corresponding scores of COMEPS-HIRLAM sub-ensemble (in pink) and COMEPS-HARMONIE sub-ensemble (in orange), illustrating added values by combining the two models. The scores here are computed by COMEPS forecasts with basetime at 00, 06, 12 and 18 UTC.

For lateral boundary perturbation, following the experience of using SLAF with the 25-member DMI-EPS system using HIRLAM model at 5.5 km (Feddersen, 2009), it is used in COMEPS for both HIRLAM and HARMONIE components. With SLAF, following the approach described by Ebisuzaki and Kalney (1992) , the forecast error of ECMWF (i.e. the difference between an old forecast and the most recent analysis) is multiplied by a scaling factor and added to or subtracted from the most recent analysis to provide a perturbed initial condition. The scaling factor controls the magnitude of the perturbation so that it becomes approximately independent of the forecast error, i.e. larger forecast errors of older forecasts are damped more than smaller forecast errors of recent forecasts.

UTC	Control member			Perturbed member		
	Shallow convection	turbulence	sso	Shall convection	turbulence	sso
00,06,12,18	edmfm	haratu	z01d	edkf	cbr	z01d
01,07,13,19	edkf	cbr	z01d	edmfm	haratu	z01d
02,08,14,20	edmfm	haratu	none	edkf	cbr	none
03,09,15,21	edmfm	haratu	z01d	edmfm	cbr	none
04,10,16,22	edkf	cbr	none	edkf	cbr	z01d
05,11,17,23	edmfm	haratu	none	edmfm	haratu	z01d

Table 1. Example of varying physical parametrisation options configured for different COMEPS-HARMONIE control and perturbed members. In addition, differential assignment of physical options include also those for LCRIT, GRSN, OCND2, COMAD.

A part of the spread in COMEPS comes from representation of model uncertainty, which is achieved by alternating configurations options for physical parameterisation used in control members and in perturbed members. Configuration of three consecutive suites on overlapping 3-h assimilation windows per model makes it easy to device control members that deviate slightly from each other in configuration options. Table 1 lists e.g. the mapping of options assigned for shallow convection, turbulence and subgrid scale orographic parameterisation in the control and perturbed forecast members of the COMEPS-HARMONIE sub-ensemble with different basetime. It is shown that control members of COMEPS-HARMONIE runs with three somewhat different combinations of physical options, whereas perturbed forecast members run with 6 different set of option combination in physics. For COMEPS-HIRLAM members, representation of model error is realised mainly through alternating use of KFRK and STRACO condensation scheme in the hourly control members, as well as the use of stochastic perturbation of physics tendencies (SPPT) in some of the perturbed members

From operational experiences and the earlier verification statistics of operational HARMONIE and HIRLAM models, it is expected that, while some of the physical parameterisation schemes have distinctively different characteristics in forecast, on average these option combination are expected to be of comparable skill level in the resulted forecasts, hence suitable for the kind of ensemble configurations as exemplified in Table 1.

As discussed in previous section, 3DVAR data assimilation with observation window of 3-hour is performed in both HARMONIE and HIRLAM control models defined on overlapping windows. In COMEPS HARMONIE, all data streams as assimilated in the operational NEA model (Yang et al 2017) has been used. In addition, radar reflectivity data from 10 countries covered by the DKA domain are assimilated for 2/3 of control members. For COMEPS-HIRLAM, only conventional data, ATOVS and AMV data are assimilated.

Since Sept 2016, the real time COMEPS setup has been in pre-operational running. Assessment on the daily performances and validation statistics about pre-operational COMEPS so far has demonstrated consistent and satisfactory results in model intercomparisons. Figure 4 shows e.g. comparison of CRPS scores for key forecast parameters in December 2016 for COMEPS in comparison to the scores of the operational DMI-EPS and HIRLAM GLAMEPS (Sattler et al 2015) for Danish stations in which the score advantage of COMEPS is clear and consistent..Technically, pre-operational COMEPS appears to be stable and delivers stably. At present, COMEPS is nearing the final phase of operationalisation.

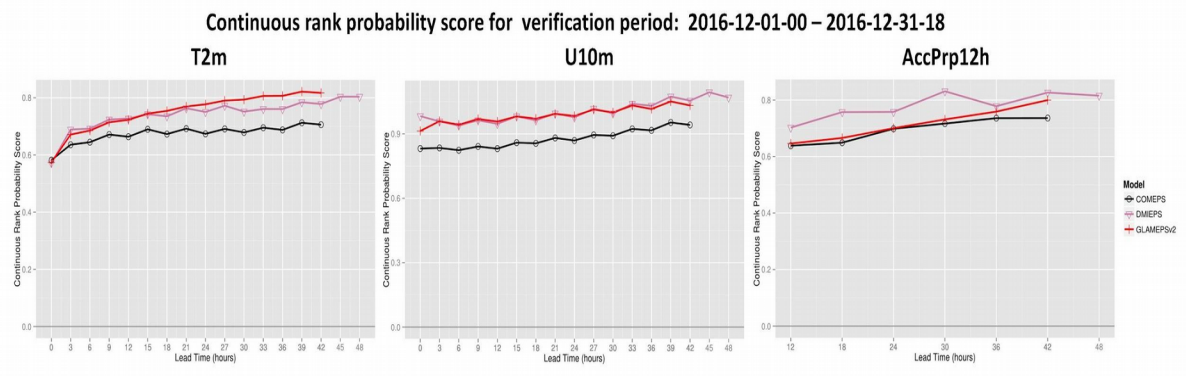

Figure 4: Comparison of probabilistic forecast skill as measured by Continuous Rank Probabilistic Score (CRPS) along forecast lead-time for Danish stations over December 2016 between COMEPS (in black) and the operational DMI-EPS (in pink) and the operational HIRLAM multimodel EPS GLAMEPS (in red)
for a) 2 metre temperature, b) 10 metre wind and c) 12h accumulated precipitation forecast.

Acknowledgement

Thanks to Alexander Mahura for technical assistance with graphics used in this report.

Reference

Bengtsson, L., Andrae, U., Aspelien, T., Batrak, Y., Calvo, J., de Rooy, W., Gleeson, E., Sass, B. H., Homleid, M., Hortal, M., Ivarsson, K.-I., Lenderink, G., Niemelä, S., Nielsen, K. P., Onvlee, J., Rontu, L., Samuelsson, P., Santos Muñoz, D., Subias, A., Tijm, S., Toll, V., Yang, X., Køltzow, M. Ø., 2017: The HARMONIE-AROME model configuration in the ALADIN-HIRLAM NWP system, Monthly Weather Weather Review, accepted for publication, January 2017

Ebisuzaki, W. and E. Kalnay, 1992: A Modified Lagged-average-forecast Ensemble. WMO Research activities in atmospheric and oceanic modelling. Report 17, pp. 6.31-6.32.

Feddersen, H., 2009: A Short-range Limited Area Ensemble Prediction System. DMI Technical Report no. 09-14, 2009.
(http://www.dmi.dk/fileadmin/Rapporter/TR/tr09-14.pdf).

Fisher, M, Y Tremolet, H. Auvinen, D. Tan and P. Poli, 2011, Weak-Constraint and Long-Window 4D-Var, ECMWF Technical Memorandum, 655, 2011.

Iversen, T., A. Deckmyn, C. Santos, K. Sattler, J. B. Bremnes, H. Feddersen, and I.-L. Frogner, 2011: Evaluation of 'GLAMEPS'— A proposed multimodel EPS for short range forecasting. Tellus, 63A , 513–530

Sattler K., A. Deckmyn, X. Yang, 2015, The GLAMEPS real-time production system, Joint ALADIN-HIRLAM Newsletter 5, 15-25, 2015

Yang, X., H. Feddersen, B. H. Sass and K. Sattler, 2016: Construction of a Continuous Mesoscale EPS System, Conference proceedings of the international symposium on extreme precipitation and hazards, Wuhan, China, March 2016.

Yang, X., B S Andersen, M Dahlbom, B H Sass, S Zhuang, B Amstrup, C Petersen, K P Nielsen, N W Nielsen, A Mahura, 2017: NEA, the Operational Implementation of HARMONIE 40h1.1 at DMI, Joint ALADIN-HIRLAM Newsletter 8, 2017

Summary of Ljubljana workshop on "Mesoscale data assimilation and the role of winds in limited-area models for NWP in Europe"

Nedjeljka Žagar[1], Jelena Bojarova[2], Nils Gustafsson[2], Tijana Janjić[3], Gert-Jan Marseille[4], Michael Rennie[5], Ad Stoffelen[4] and Matic Šavli[1] , *[1]UL-FMF, Slovenia; [2]SMHI, Sweden; [3]LMU, Germany; [4]KNMI, The Netherlands; [5]ECMWF, UK*

1 Background

Over the past two decades, limited area models (LAMs) for numerical weather prediction (NWP) have become operational in practically every country across Europe. Clustered around the four major development centres: the UK MetOffice, Meteo-France, Deutsche Wetterdienst and the HIRLAM group, the European LAMs initially focused mainly on the downscaling of global analyses and forecasts produced by their own global NWP systems or by the ECMWF. In the new millennium, developments have become better focused on advanced methods for mesoscale data assimilation (DA), first using the 3D-Var, followed by the 4D-Var, the ensemble Kalman filter and, most recently, hybrid methods. Over the same period, the ECMWF model and other global models have steadily increased their horizontal grids that are now approaching 10 km.

Mesoscale data assimilation (MDA) is expected to provide initial conditions for km-scale forecasts that outperform the global model forecasts on the short range (few hours to 1-day). In this range of spatio-temporal scales, MDA affects processes with timescales of hours in contrast to the processes with timescales of days addressed by global models. A lack of frequent and accurate high-resolution observations, especially wind observations, makes the challenge of MDA only greater.

The workshop on "Wind profiles and mesoscale data assimilation" at the Faculty of mathematics and physics, University of Ljubljana, addressed the potential impact of the forthcoming wind profile measurements by the ESA's ADM-Aeolus satellite in mesoscale models. The participants discussed the modelling of the background-error covariances for MDA in a couple of presentations based on hybrid MDA methods. Sensitivity studies with several new wind observations (e.g. Mode-S) showed mixed results in spite of the observation high quality. The potential of the line-of-sight ADM-Aeolus measurements in mesoscale observing system simulation experiments (OSSE) suggested that improvements in the analysis of the amplitude and location of the baroclinic development in the northern Atlantic will be possible thanks to the ADM-Aeolus wind profiles. The workshop presentations are available at http://meteo.fmf.uni-lj.si/en/workshop.

In the following, we summarize the workshop discussion of challenges and recommendations for further research in the mesoscale NWP and DA communities.

2 Challenges in mesoscale NWP modelling

Representation of mesoscale dynamics

Observations and numerical model simulations provide increasing evidence that at scales around 500 km atmospheric dynamics becomes predominantly unbalanced, i.e., that the divergent component of circulation becomes comparable to the rotational component. In other words, flow variability is produced to a larger extent by the internal inertio-gravity and gravity waves than by the Rossby waves. Consequently, the energy spectrum becomes shallower (changing from a slope of -3 to -5/3). So far,

the mesoscale NWP models have not been applying the criterion of a -5/3 slope of the energy spectrum as a strong constraint in their model validation.

A recent decomposition of the mesoscale energy spectra in the ALADIN model into rotational and divergent components showed that divergent energy, used as a synonym for inertio-gravity waves in the mid-latitudes, comprises about 50% of kinetic energy in the free troposphere [1]. In the stratosphere this percentage increases and the energy spectra become shallower. A similar shallowing of the spectra takes place close to the surface in relation to the strong orography forcing. In the free troposphere, the slope of the kinetic energy spectrum in mesoscale NWP models may significantly deviate from the expected -5/3. Furthermore, some methods for the computation of spectra in limited-area domains produce somewhat biased slopes at the shortest range of scales [2]. Several studies also showed that the slope can be greatly altered by the applied numerical diffusion [3].

Research practice in NWP is to tune mesoscale NWP models to produce optimal forecasts regardless of the slope of the spectrum. An established efficient method to smooth apparently noisy forecasts is the horizontal diffusion [3]. The spatial characteristics of LAMs can be verified by covariance methods on collocated model and observation fields [4].

An inter-comparison exercise with the European operational mesoscale NWP models regarding their ability to produce the -5/3 spectrum would help address this issue in a systematic manner.

Lateral boundary conditions and scale interactions

The need for a large domain for mesoscale models has been well recognized in the NWP community. At the same time, domains applied in practice are a compromise between the applied grid density and available computer resources to frequently provide updated forecasts in real time. The grid issue is usually considered only with regard to the horizontal. Thus, the mesoscale NWP models applied in Europe may have a smaller number of vertical levels in the troposphere than the ECMWF model.

Some domain dimensions, currently used with a horizontal grid distance of around 2 km, are such that the impact of lateral boundaries (LBs) reaches the centre of the domain within 24 hours, especially in the upper troposphere. Traditionally, the forecast-error growth in mesoscale models focused on the growth of errors in small scales and their upscale cascades. However, it is now understood that the errors grow from the start of the forecast on all scales [5]. Furthermore, there is also a downscale cascade of the initial-state error from the synoptic scales to smaller scales [6]. The errors cascading downscale and the errors growing in the small scales interact from the start of the forecast across all scales represented by a mesoscale model.

We consider it crucial to push for a more intense research on the scale-dependent growth of forecast errors in a mesoscale model and the interaction with the errors in LBs, especially on larger meso scales.

3 Mesoscale data assimilation

Identification of the forecast errors

It is recognized that spatio-temporal error structures that are only partially observed may cause rather artificial analysis updates (in the engineering community commonly referred to as aliasing) [7]. Should thus MDA be restricted to analyse only those spatial and temporal scales that are well resolved by the density of the observation network? Does this imply that due to lack of frequent high-resolution observations background error covariances with broad structure functions should be employed, relying on the model itself to constrain the small scales accordingly?

Structure functions produced by the ensembles of high-resolution simulations are characterized by sharp spatial gradients [8]. However, can we rely on the ability of currently applied ensemble generation techniques to realistically simulate processes with a short length of life (order of an hour)? Are the currently applied hybrid ensemble methods and/or methods copied from the global NWP model (perturbed observations) capable to realistically simulate flow-dependent forecast errors on scales around 10 km? What information on error propagation do we get from ensemble simulations?

Are these simulations at short forecast ranges affected by artifacts of ensemble generation approaches and do they to a large extent reflect the adjustment processes or are they provoked by noise and imbalances?

Provided that the mesoscale ensemble reliably simulates the errors of the hour, should the small scales be treated only using the error covariances? What are the small scales? One idea is that this can be defined as the scale where the energy spectrum has a slope -5/3 reflecting divergence-dominated dynamics.

It is well known that surface conditions play an important role in initializing convection. Presuming that processes driven by orography have increased predictability, should the lower troposphere be the focus of MDA? Or, are the errors in the free atmosphere more relevant (e.g. deep convection, large-scale errors in initial and lateral boundaries)?

A lack of wind observations

Basic understanding of the coupling between the mass and the wind field in the NWP models is based on the adjustment process as first discussed by C.G. Rossby almost 80 years ago. It suggests that for the initialization of mesoscale processes we need wind observations more strongly than the observations of mass variables. Although this argument originally applied to dynamical processes involving no changes of the phase of water, it has successfully served the NWP community over several decades. The same argument has also been successfully employed to argue about a significant benefit of the profiles of line-of-sight winds from the ADM-Aeolus mission [9]. It was shown that wind profile observations distributed in space and time are needed especially in the tropics and on the mesoscale.

At the same time, recent results from DA studies with scatterometer data and aircraft data of types Mode-S and GADS agree that adding new wind observations is a challenging task [10,11,12,13]. In spite of relatively small estimated observation errors, the impact of new observations is quickly lost in forecasts. One clear reason is model bias. Observational information is lost within a couple of hours when the model returns to its biased climatology. Other reasons remain poorly understood and they may be related to the impact of the applied background-error covariances in relation to the mesoscale model (im)balance and model dynamics, including the errors in synoptic scales in the initial state as well as in LB fields. In any case, we can question if DA, which corrects the errors of the hour, is expected to produce improved forecasts for longer than a few hours? Is an initial three-hour long improvement in the convection forecast what the MDA can at most achieve with respect to global NWP models due to the predictability of these scales? These questions may be addressed in OSSE-type experiments, taking into account the initial and LB errors on the synoptic scales.

Mesoscale data assimilation and balance issues

The basic question is whether the balance matters at the mesoscale, especially in hybrid ensemble DA methods? If balance in MDA does matter, what are the relevant balance constraints? Are analytically derived balances that describe climatology of short-term forecast errors at mesoscale still useful? How significant is the harm caused by the applied homogeneity and isotropy assumptions? The climatological balances are based on the hydrostatic approximation and produce hydrostatic DA increments. An open question is whether non-hydrostatic increments added during the DA step would improve the initialization of the model?

Following the spectrum of atmospheric energy, energy variance on the mesoscales is of the order of a couple of Joules per kg. In other words, the mesoscale analysis increments added in a DA step are energetically very small. Superposed on synoptic-scale features, they can be quickly lost for many reasons, even if they result from high-quality wind observations, as discussed above.

In spite of all progress in DA, transient features following moist adjustment are not well understood. In the ECMWF model global 4D-Var DA, significant wind increments are coming from the humidity observations and they lead to better short-range forecasts [14]. This however does not mean that the coupling between the moisture and winds in 4D-Var is well understood. Furthermore, when deep convection is not parametrized, natural question arises as to whether the hydrometeors, especially

when assimilating radar data, should be updated in the analysis step or if this should be left to the microphysics scheme.

Mesoscale DA studies have shown that significant mesoscale forecast failures are related to a poorly initialized moisture field. Moreover, imposed structure functions are shown to degrade both moisture analysis and forecast quality if they poorly represent the actual situation, indicating the importance of flow-dependent balance relationships [11]. Analysis of the moisture is especially difficult due to Gaussian error assumptions of all data assimilation methods used operationally today. At present the ensemble techniques are used to carry on the evolution of flow-dependent uncertainty, advocating this approach by dispensing with expensive developments of tangent linear and adjoint simplified physics which is required for 4D-Var. The complication here is that the covariance inflation and the covariance localization, which are commonly applied in the ensemble techniques to allow for an affordable ensemble size, affect the coupling between the mass and wind fields in the model and its forecast errors. Even simple multiplicative inflation can affect enstrophy leading to even greater importance of wind observations in order to control it [15].

The coupling between the moisture and wind fields is considered crucial for the optimal initial state. With both fields poorly observed, idealized and OSSE studies of DA with simulated mesoscale observations may be a way to better understand the mesoscale balance issues and the need and prospects for the initialization of inertio-gravity waves in a saturated moist atmosphere.

4 Concluding remarks

In global models, OSSE experiments have usually been used to estimate the potential impact of new observing systems. In particular, the perfect-model OSSEs provides an understanding of dynamical and physical aspects free of the model error. The significant challenges in MDA listed in this summary suggest that controlled, OSSE type of experiments with mesoscale models can be useful for the quantification of the relative impact of the various issues discussed. Primarily, the implications of the evidently significant role of analysis uncertainties on larger scales and the short-range error growth on small scale NWP are yet to be quantified. Some inertio-gravity waves may be possible to initialize better in DA step by a multivariate approach. This and similar topics call for a stronger collaboration between the weather services and atmospheric science research at European universities.

5 References

[1] Blažica, V. et al., 2013: Rotational and divergent kinetic energy in the mesoscale model ALADIN. Tellus 65A, 18918.

[2] Blažica, V. et al., 2015: The impact of periodization methods on the kinetic energy spectra for limited-area numerical weather prediction models. Geosci. Model Dev. 8, 87-97.

[3] Bengtsson, L. et al., 2012: Impact of Flow-Dependent Horizontal Diffusion on Resolved Convection in AROME. J. Appl. Meteorol. Clim. 51, 54-67.

[4] Vogelzang, J. et al., 2015: Spatial variances of wind fields: their sensitivity to sampling strategy and their relation to second-order structure functions and spectra, J. Geophys. Res. 120, doi:10.1002/2014JC010239

[5] Žagar, N. et al., 2015: A three-dimensional multivariate modal analysis of atmospheric predictability with application to the ECMWF ensemble. J. Atmos. Sci. 72, 4423-4444.

[6] Durran, D. R. and M. Gingrich, 2014: Atmospheric Predictability: Why Butterflies Are Not of Practical Importance. J. Atmos. Sci. 71, 2476-2488.

[7] WMO CGMS IWWg: https://groups.ssec.wisc.edu/groups/iwwg/activities/high-resolution-winds-1/nwp-data-assimilation, visited 18 Nov 2016.

[8] Gustafsson, N. and J. Bojarova, 2014: Four-dimensional ensemble variational (4D-En-Var) data assimilation for the HIgh Resolution Limited Area Model (HIRLAM). Nonlin. Processes Geophys. 21, 745–762.

[9] Stoffelen, A. et al., 2005: The atmospheric dynamic mission for global wind measurements. Bull. Amer. Meteor. Soc. 86, 73-87.

[10] de Haan, S. and A. Stoffelen, 2012: Assimilation of high-resolution Mode-S wind and temperature observations in a regional NWP model for nowcasting applications. Wea. Forecasting 27, 918–937.

[11] Strajnar et al., 2015: Impact of new aircraft observations Mode-S MRAR in a mesoscale NWP model. J. Geophys. Res. Atmos. 120, 3920–3938.

[12] Lange, H. and T. Janjić, 2016: Assimilation of Mode-S EHS Aircraft Observations in COSMO-KENDA, Mon. Wea. Rev. 144, 1697.

[13] Marseile, G.J. and A. Stoffelen, 2016: Toward Scatterometer Winds Assimilation in the Mesoscale HARMONIE Model, IEEE Journal of Selected Topics in Applied Earth Observations and Remote Sensing, doi 10.1109/JSTARS.2016.2640339, in print.

[14] Geer, A. J. et al., 2008: Lessons learnt from the 1D+4D-Var assimilation of rain and cloud affected SSM/I observations at ECMWF. Q. J. R. Meteorol. Soc. 134, 1513-1525.

[15] Zeng Y. and T. Janjić, 2016: Study of Conservation Laws with the Local Ensemble Transform Kalman Filter, Q. J. R. Meteorol. Soc. 142-699, 2359–2372.

Report from ALARO-1 Working days 2016

Luc Gerard, Neva Pristov, Radmila Brožková, Ján Mašek

1 Introduction

ALARO developers and users gathered at ALARO-1 Working Days in Brussels for three days in mid September 2016. Overview of developments during the last two years, users experiences and the outcome of discussions on further developments are summarized in this report.

2 Scope

The development of new physics for high resolution to be part of the ALARO-1 has been the holy Graal for more than 5 years, now. The wide ambition of the initial plans has not been lost. The different modules that have been developed along these years have reached the step of the individual tuning and validation; the tuning and further validation of the whole model where these modules interact together is going on.

The recent developments of ALARO-1 physics have concerned:

- an improved radiation scheme (ACRANEB2) and its interaction with clouds
- the turbulence scheme TOUCANS, including handling of shallow clouds transport using a simplified mass-flux-type scheme;
- computation of screen-level properties (diagnostic at 2m)
- cloud overlap strategies
- non saturated downdraught scheme
- improved scale-aware deep convection scheme (CSD)

Further efforts will have to be put also on SURFEX and microphysics.

3 Local ALARO experience

Comparisons and case studies have been performed in different countries. Experiments have been performed down to 1.3km resolution, showing already benefits of the high resolution with the ALARO-1vA in cy40t1 version.

Climate experiments are done in Belgium and in Sweden.

Belgium participates to the Coordinated Regional Climate Downscaling Experiment (CORDEX) using the ALARO-0 model at 50km and 12.5km resolution with runs over 30-year periods, in the past (1979-2010, using ERA-interim reanalysis) and in the future based on different climate scenarios. The runs for the evaluation period show good performance of ALARO-0 compared to other models. The local CORDEX-BE project makes a further downscaling at 4km resolution around Belgium with ALARO-0, COSMO-CLM and MAR, to provide an ensemble of high-resolution climate runs to feed local impact models.

Sweden continues with ALARO experiments over Europe at 15 and 6km resolutions, and with AROME experiments over Central Europe at 2km resolution, including case studies of heavy rainfall and sensitivity studies of deforestation. This allows to make apparent some biases of the model as well as their improvement with the new cycles and configurations.

4 Points of attention and further developments

- The newly introduced shallow cloud treatment in TOUCANS uses internally a `shallow cloud fraction'; however this value is a separate diagnostic, while the interaction with the model fields takes place through transport. Hence the (so-called 'stratiform') Xu-Randall cloud scheme condensation automatically includes the condensation in shallow clouds. This is different from (complementary) deep convection condensation computed explicitly in a separate parametrisation.
- A big issue is the harmonisation of radiative cloud fraction and condensates with the microphysical cloud fraction and prognostic condensates.

  Presently (LNEB_FP=.F.), the radiative condensates are re-estimated. The 'stratiform' part is obtained from total water using a critical relative humidity profile (HUC) that (contrary to the cloud scheme) does not include phase and mesh size dependencies. The convective condensates are re-estimated from the historic convective cloud fraction. These two re-estimated condensates are added, and the radiative cloud fraction is obtained by direct application of the XR formula (with parameter QXRAL corresponding to QXRAL_ADJ in the cloud scheme). Additional parameters further affect the estimation of radiative condensates and cloud fraction.

  At short term, the radiative cloudiness should be further re-tuned, in the spirit to reduce the difference with the adjustment; a re-unification of adjustment and radiative cloudiness is desirable at longer term (possibly a direct use of prognostic condensates and adjustment cloud fraction into radiation, with LNEB_FP=.T.).

- TOUCANS: some parts and options have further to be tested / improved:
  - different functional dependencies to Ri of the stability functions: model I, model II, emulation and extension of turbulence schemes EFB, QNSE,
  - mixing length combinations (CGMIXELEN='EL0' to 'EL6'), conversion between the TKE-based mixing lengths and Prandtl mixing lengths (RMC01),
  - impact of the Third Order Moments (TOMs),
  - further tuning and improvement of shallow convection part,
  - interfacing TOUCANS with SURFEX (TOMs interact strongly with surface fluxes, while these should stay externalised => conflict to be solved, especially for urban areas (TEB)).
- Radiation: parameters have rather fixed physical values, so that tuning possibilities are very limited. Recent developments include intermittent update of the shortwave gaseous transmissions, revised cloud optical properties and optical saturation, optimal bracketing of the exchange between layers, introduction of generalized cloud overlap and improved sunshine duration estimation. Further improvements may concern the treatment of aerosols, considering the radiative effect of falling hydrometeors, and parameterizing impact of clouds on the broadband surface albedo.

  A big challenge are 3D cloud effects. For lower horizontal resolutions they can be parameterized within 1D radiative framework. In kilometric and finer resolutions, however, 3D cloud effects become resolved. Unfortunately, cost and complexity of truly 3D radiative calculations are beyond the scope of NWP. For the time being it is not clear what the optimal solution will look like. Literature on the subject should be monitored.
- Non-saturated downdraught: the new scheme is able to produce a better correlation between the downdraughts and the precipitation. A fixed version of the code is in CY43T2, and a first tuning with 3MT has been validated.
- Convection: the CSD updraught scheme has shown to produce a smoother transition towards fully explicit convection at very high resolution. The dynamical behaviour (location and evolution of the precipitation fields) is generally improved. The tuning and validation is going on in ALARO-1, with some interactions with the tuning of the cloud scheme (adjustment) and the radiative clouds.

  The behaviour at high resolution when deep clouds are substantially resolved by the model grid is sensitive to the turbulent diffusion tuning; it can also be improved by the use of cellular automaton in the convective scheme. The code in CY43T2 includes this option.
- Microphysics: prognostic graupel has been coded by Michiel V., should be phased. Prognostic hail does not appear important. At longer term, could go to a 1.5 moment scheme (i.e. introducing number concentration for rain only).
- New physics-dynamics interface is working; the DDH (diagnostics on horizontal domains) should now work properly with the flexible interface in CY43T1.

5 Prospects on ALARO-1 versions

The first well tuned version was ALARO-1vA available in February 2015 (export cy40t1, also modset for cy38t1), in May 2016 the improvement of the screen-level properties (modset for cy40t1 and cy38t1) was distributed. Now next well tuned version named ALARO-1vB has been prepared (is already used at CHMI). Its ingredients (in addition to ALARO-1vA, screen-level interpolation) are: mass flux type of shallow convection scheme in TOUCANS, exponential-random cloud overlaps in radiation and cloud diagnostics, improved sunshine duration, direct solar flux at surface and 10m wind interpolation. This code is available in cy43t2 and it was proposed to prepare a modset for cy40t1. Updates of the CSD code also entered cy43t2. It was proposed that the current code in cy43t2 is a base for further developments and tunings, also for the coupling with SURFEX.

Foreseen future version (ALARO-1vC) could have non-saturated downdaught and possible additional novelties (prognostic graupel, revision of mixing length and TOMs inOUCANS). And finally, a baseline version of the full ALARO-1 will contain CSD.

Steps to the full ALARO-1 baseline are as follows, including validations and proposed namelist settings:

- complete TOUCANS with mass flux type of shallow convection
- idem + non-saturated downdraught
- possible additional novelties (prognostic graupel, revision of mixing length and TOMs in TOUCANS)
- idem + CSD will make a baseline version of the full ALARO-1

6 References

Presentations: http://www.rclace.eu/?page=163

Overview of the operational configurations

Patricia Pottier

1 Introduction

Our 26 NMSs run 46 deterministic LAM configurations . The table below gives their main fictures. More details about the configurations and more maps can be found on the operational page on the ALADIN website.

Operational configurations	Horiz resol (km)	Size (grid-point)	Vertic levels	Version	Coupled with	Computer	Configu-ration	DA	DA (details)
1. Algeria: ALADIN-ALGE	8.00	450 x450	70	CY40T1.bf5	ARPEGE	IBM-HPC ALGERIE	ALADIN	NO	
2. Algeria: ALADIN_DUST	14.00	250 x250	70	CY38T1.bf03	ARPEGE	IBM-HPC ALGERIE	ALADIN	NO	
3. Algeria: AROME-NORD-ALGE	3.00	500 x500	41	CY40T1.bf5	ALADIN -ALGE	IBM-HPC ALGERIE	AROME	NO	
4. Austria: ALARO5-AUSTRIA	4.82	540 x600	60	CY36T1	IFS	SGI ICE-X	ALARO	YES	CANARI
5. Austria: AROME-AUSTRIA	2.50	432 x600	90	CY40T1.bf5	IFS	SGI ICE-X	AROME	YES	3DVAR + OI Main
6. Belgium: ALARO-7km	6.97	240 x240	46	CY38T1.bf03	ARPEGE	SGI Altix 4700	ALARO	NO	
7. Belgium: ALARO-4km	4.01	181 x181	46	CY38T1.bf03	ARPEGE	SGI Altix 4700	ALARO	NO	
8. Bulgaria: ALADIN-Bulgaria	7.00	144 x180	70	CY38T1.bf03	ARPEGE	Linux cluster	ALADIN	NO	
9. Croatia: HR-ALARO-88	8.00	216 x240	37	CY38T1.bf03	IFS	SGI Altix	ALARO	YES	3DVAR + CANARI
10. Croatia: HR-ALARO-44	4.00	432 x480	73	CY38T1.bf03	IFS	SGI Altix	ALARO	YES	3DVAR + CANARI
11. Croatia: HR-ALARO-22	2.00	450 x450	37	CY36T1.bf08	HR-alaro-88	SGI Altix	ALARO	NO	
11. Croatia: HR-alaro-HRDA	2.00	450 x450	15	CY38T1.bf03	HR-alaro-88	SGI Altix	ALARO	YES	
12. Czech Rep: CZ-ALARO	4.71	432 x540	87	38T1.bf03 + local dev ALARO1	ARPEGE	NEC SX-9	ALARO	YES	3DVAR + CANARI+ DFI_blending

Operational configurations	Horiz resol (km)	Size (grid-point)	Vertic levels	Version	Coupled with	Computer	Configu-ration	DA	DA (details)
13. Denmark: AROME-NEA	2.50	1080 x1200	65	CY40H1.1	IFS	Cray XC30	AROME	YES	3DVAR+CANARI,OI,SODA for SURFEX
14. Denmark&Iceland: AROME-IGA	2.50	800 x1000	65	CY40H1.1	IFS	Cray XC30	AROME	YES	BLENDING+CANARI, OI,SODA for SURFEX
15. Finland: AROME-FMI	2.50	800 x720	65	CY38H1.2 + local adapt.	IFS	Cray XC30	AROME	YES	3DVAR + CANARI OI, SODA for SURFEX
16. France: AROME-France	1.30	1440 x1536	90	CY41T1	ARPEGE	BULLx B710 DLC	AROME	YES	3DVAR + OI Main
17. France: AROME-Indian	2.50	900 x1600	90	CY41T1	IFS	BULLx B710 DLC	AROME	NO	
18. France: AROME-Polynesia	2.50	600 x600	90	CY41T1	IFS	BULLx B710 DLC	AROME	NO	
19. France: AROME-Caledonia	2.50	600 x600	90	CY41T1	IFS	BULLx B710 DLC	AROME	NO	
20. France: AROME-Guyana	2.50	384 x500	90	CY41T1	IFS	BULLx B710 DLC	AROME	NO	
21. France: AROME-Antilles	2.50	576 x720	90	CY41T1	IFS	BULLx B710 DLC	AROME	NO	
22. Hungary: ALARO-HU determinis	7.96	320 x360	49	CY38T1	IFS	IBM iDataPlex Clust.	ALARO	YES	3DVAR + CANARI
23. Hungary: AROME-HU	2.50	320 x500	60	CY38T1	IFS	IBM iDataPlex Clust.	AROME	YES	3DVAR + OI Main
24. Iceland: AROME-IMO	2.50	500 x480	65	CY38H1.2 + local adapt.	IFS	ECMWF (cca/ccb)	AROME	YES	CANARI OI, SODA for SURFEX
25. Ireland: AROME-IRELAND25	2.50	500 x540	65	CY37H1.1	IFS	SGI ICE X	AROME	YES	CANARI OI + SURFEX OI
26. Lithuania: AROME-LHMS	2.50	432 x432	65	CY37H1.2	IFS	SGI Altix Ice	AROME	YES	Upper air blending +CANARI, OI_Main for SURFEX
27. Morocco: ALADIN-NORAF	18.00	324 x540	70	CY41T1	ARPEGE	IBM HPC	ALADIN	YES	DA (3DVAR + CANARI) in CY36T1 version only
28. Morocco: ALADIN Maroc	7.50	400 x400	70	CY41T1 with SURFEX	ARPEGE	IBM HPC	ALADIN	NO	
28. Morocco: ALADIN Maroc 3DVar	10.00	320 x320	60	CY36T1	ARPEGE	IBM HPC	AROME	YES	3DVAR+Canari is ongoing for CY40t1

Operational configurations	Horiz resol (km)	Size (grid-point)	Vertic levels	Version	Coupled with	Computer	Configu-ration	DA	DA (details)
29. Morocco: AROME Maroc	2.50	800 x800	60	CY41T1	ALADIN Maroc 3DVar	IBM HPC	AROME	NO	
30. Netherlands: AROME-KNMI	2.50	800 x800	90	CY36H1.4	HIRLAM	BULLX B500	AROME	YES	3DVAR + CANARI OI, OI_MAIN for SURFEX
31. Norway: AROME-Arctic	2.50	960 x750	65	CY38H1.2 + local adapt.	IFS	SGI, Intel Sandy Br.	AROME	YES	3DVAR + CANARI OI, SODA for SURFEX
32. No&Se&Fi: AROME-MetCoOp	2.50	960 x750	65	CY40H1.1	IFS	Frost	AROME	YES	3DVAR + CANARI OI, SODA for SURFEX
33. Poland: E040-ALARO	4.00	800 x800	60	CY40T1.bf5	ARPEGE	Linux cluster	ALARO	NO	
34. Poland: P020-AROME	2.04	810 x810	60	CY40T1.bf5	ALARO-E040	Linux cluster	AROME	NO	
35. Portugal: ALADIN-ATP	9.00	288 x450	46	CY38T1	ARPEGE	IBM POWER7+	ALADIN	NO	
36. Portugal: AROME-PT2	2.50	540 x480	46	CY38T1	ARPEGE	IBM POWER7+	AROME	NO	
37. Portugal: AROME-Madeira	2.50	200 x192	46	CY38T1	ARPEGE	IBM POWER7+	AROME	NO	
38. Portugal: AROME-Azores	2.50	270 x360	46	CY38T1	ARPEGE	IBM POWER7+	AROME	NO	
39. Romania: ALARO-RO	6.50	240 x240	60	CY40T1	ARPEGE	cluster IBM BLADE	ALARO	NO	
40. Slovakia: ALARO-SK	4.50	576 x625	63	CY40T1.bf6	ARPEGE	IBM Power7	ALARO	YES	CANARI+ DFI_blending
41. Slovenia: sis4-ALARO	4.40	432 x432	87	38T1	IFS	SGI ALTIX ICE 8200	ALARO	YES	3DVAR + CANARI
42. Spain: IBERIA	2.50	800 x648	65	CY38H1.2 + local adapt.	IFS	ECMWF (cca/ccb)	AROME	YES	3DVAR + CANARI OI, SODA for SURFEX
43. Spain: CANARIAS	2.50	576 x480	65	CY38H1.2 + local adapt.	IFS	ECMWF (cca/ccb)	AROME	YES	Blending + CANARI OI, SODA for SURFEX
44. Tunisia: ALADIN-Tunisia	7.50	216 x270	70	CY38T1.bf03	ARPEGE	IBM PS690	ALADIN	NO	
45. Turkey: ALARO-Tk	4.50	450 x720	60	CY38T1.bf03	ARPEGE	Altix 4700	ALARO	NO	
46. Turkey: AROME-Tk	2.50	512 x1000	60	CY38T1.bf03	ARPEGE	SGI UV2000	AROME	NO	

2 All over the world …

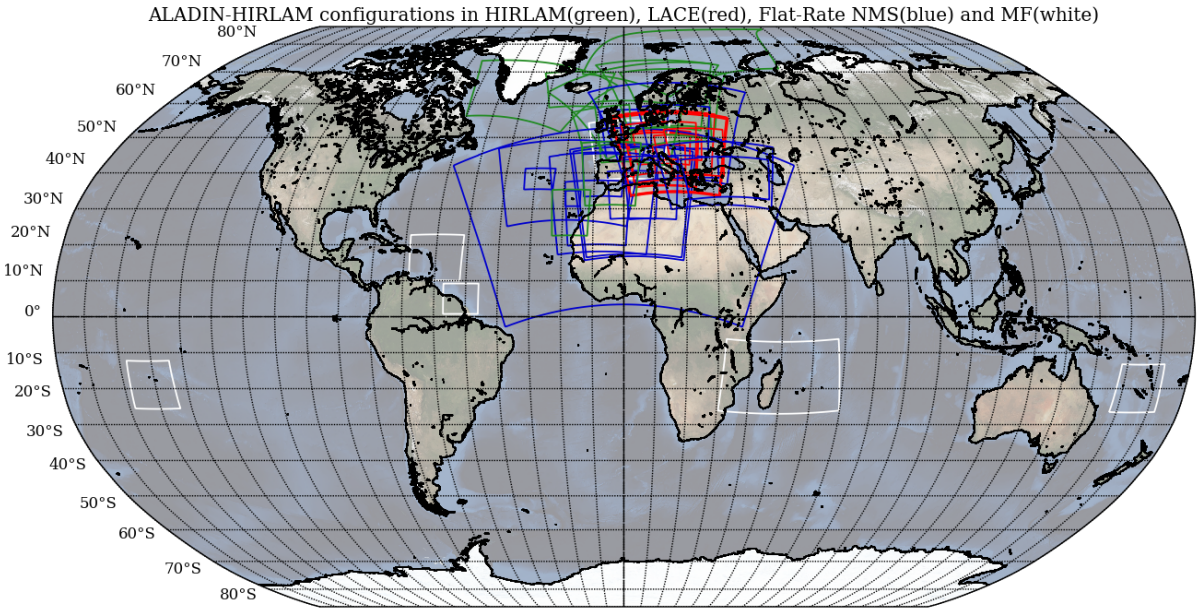

3 Vertical discretization

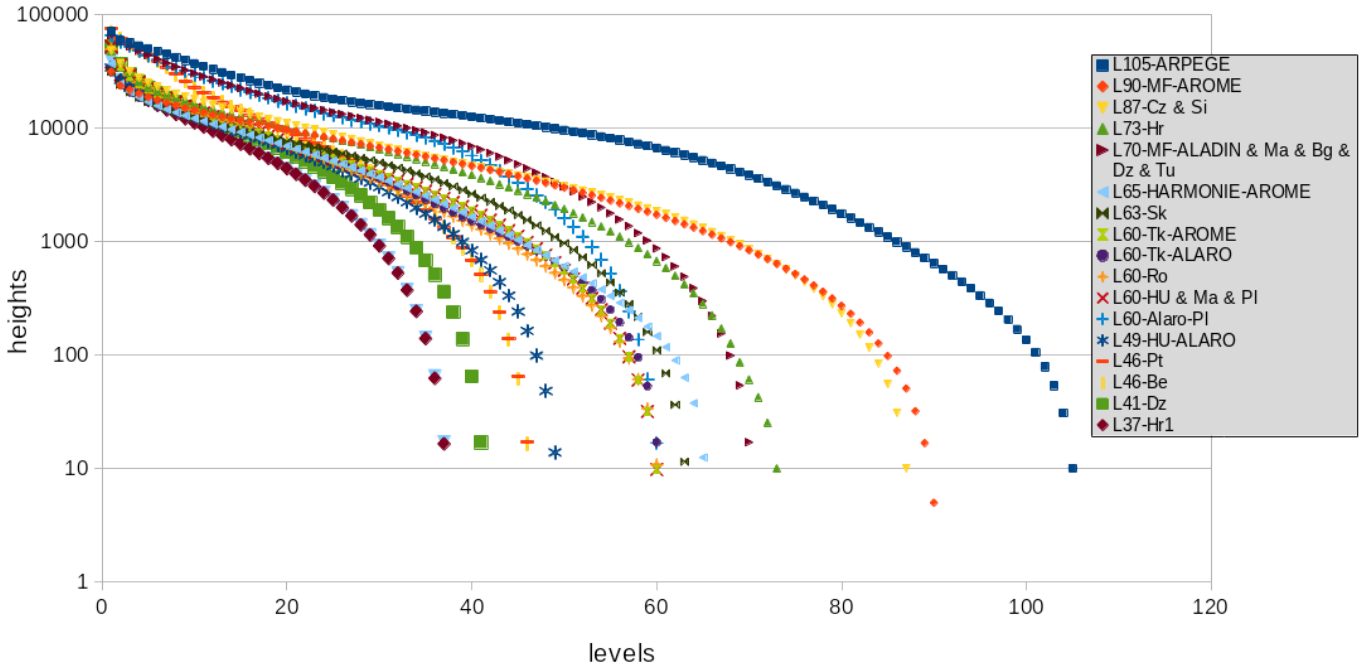

Vertical levels used in operational systems and their standard atmosphere heights

4 The 46 configurations

Operational configurations in ALADIN and HIRLAM consortia

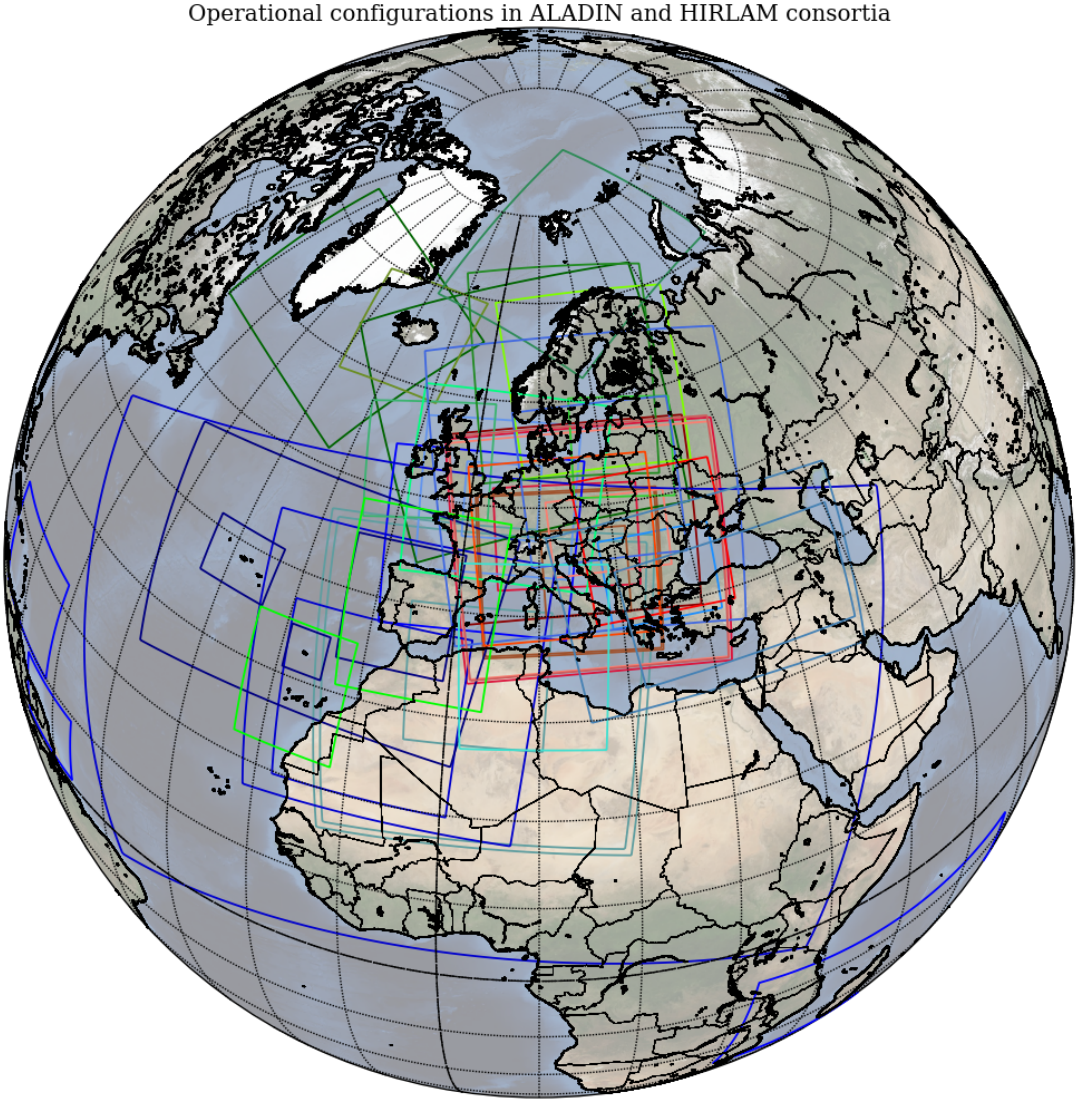

1. Algeria: ALGE (aladin)
2. Algeria: ALADIN_DUST
3. Algeria: AROME-NORD-ALGE
4. Austria: ALARO5-AUSTRIA
5. Austria: AROME-AUSTRIA
6. Belgium: Belgium-Alaro-7km
7. Belgium: Belgium-alaro-4km
8. Bulgaria: aladin-Bulgaria
9. Croatia: HR-alaro-88
10. Croatia: HR-alaro-44
11. Croatia: HR-alaro-22
12. Czech Rep: CZ-alaro
13. Denmark: AROME-NEA (Denmark)
14. Denmark: AROME-IMO (Ic+S.Gre)
15. Finland: AROME-FMI
16. France: Arome-France
17. France: AROME-Indian
18. France: AROME-Polynesia
19. France: AROME-Caledonia
20. France: AROME-Guyana
21. France: AROME-Antilles
22. Hungary: ALARO-HU determinis
23. Hungary: Arome-HU
24. Iceland: AROME-IMO
25. Ireland: AROME-IRELAND25
26. Lithuania: AROME-LHMS
27. Morocco: aladin-Mo1
28. Morocco: aladin-Mo2
29. Morocco: AROME Maroc
30. Netherlands: AROME-KNMI
31. Norway: AROME-Arctic
32. Fi&No&Se: AROME-MetCoOp
33. Poland: E040-alaro
34. Poland: P020-arome
35. Portugal: ALADIN-Portugal(ATP)
36. Portugal: AROME-Portugal(PT2)
37. Portugal: AROME-Madeira(MAD)
38. Portugal: AROME-Azores(AZO)
39. Romania: ALARO-RO
40. Slovakia: Slovakia-alaro
41. Slovenia: sis4-alaro
42. Spain: IBERIA
43. Spain: CANARIAS
44. Tunisia: Tunisia-aladin
45. Turkey: Turkey-alaro
46. Turkey: Turkey-Arome

5 AROME, ALARO, ALADIN configurations

ALADIN-HIRLAM model configurations : AROME (red) ALARO (green) ALADIN (blue)

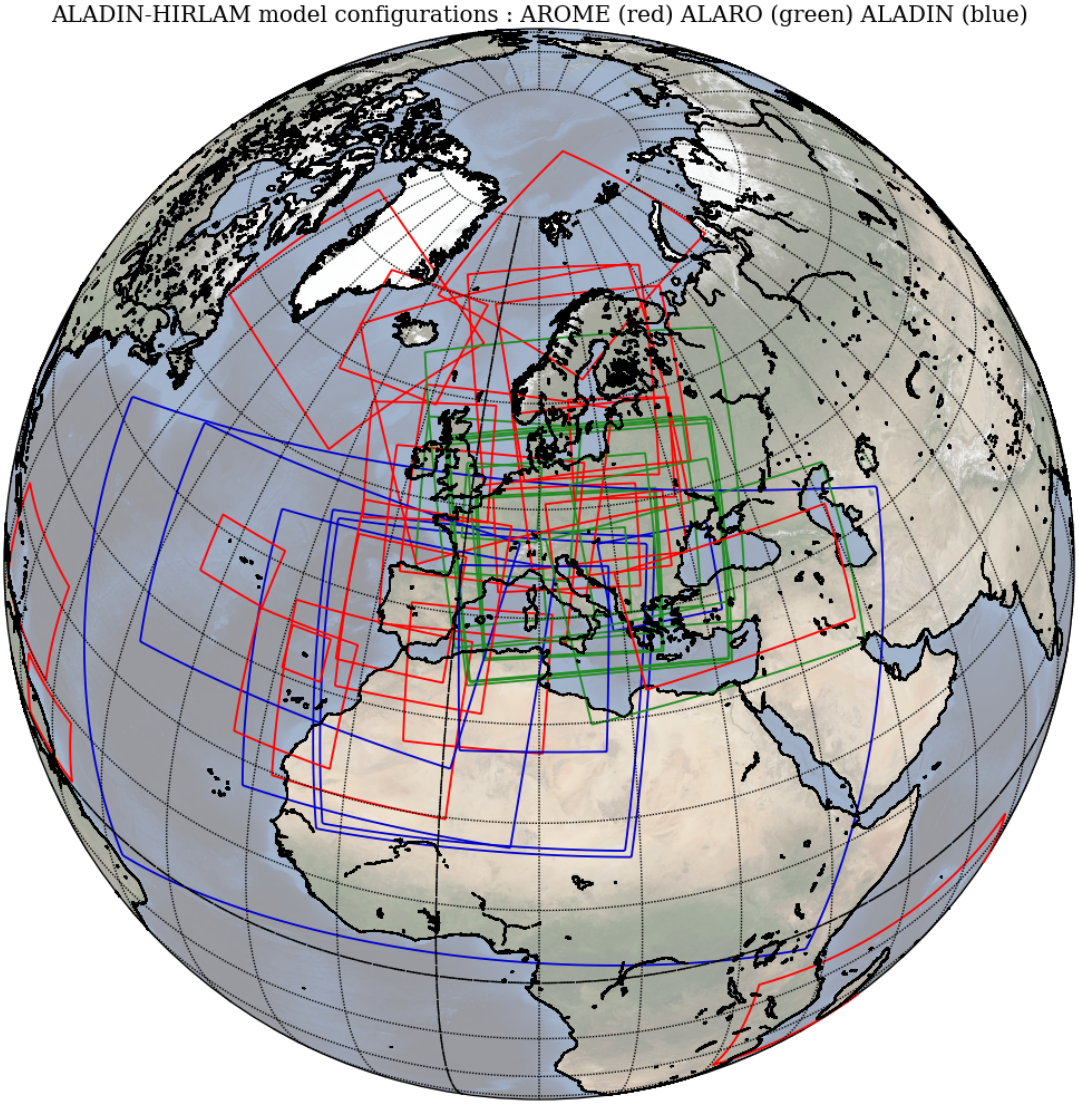

1. Algeria: ALGE (aladin)
2. Algeria: ALADIN_DUST
3. Algeria: AROME-NORD-ALGE
4. Austria: ALARO5-AUSTRIA
5. Austria: AROME-AUSTRIA
6. Belgium: Belgium-Alaro-7km
7. Belgium: Belgium-alaro-4km
8. Bulgaria: aladin-Bulgaria
9. Croatia: HR-alaro-88
10. Croatia: HR-alaro-44
11. Croatia: HR-alaro-22
12. Czech Rep: CZ-alaro
13. Denmark: AROME-NEA (Denmark)
14. Denmark: AROME-IMO (Ic+S.Gre)
15. Finland: AROME-FMI
16. France: Arome-France
17. France: AROME-Indian
18. France: AROME-Polynesia
19. France: AROME-Caledonia
20. France: AROME-Guyana
21. France: AROME-Antilles
22. Hungary: ALARO-HU determinis
23. Hungary: Arome-HU
24. Iceland: AROME-IMO
25. Ireland: AROME-IRELAND25
26. Lithuania: AROME-LHMS
27. Morocco: aladin-Mo1
28. Morocco: aladin-Mo2
29. Morocco: AROME Maroc
30. Netherlands: AROME-KNMI
31. Norway: AROME-Arctic
32. Fi&No&Se: AROME-MetCoOp
33. Poland: E040-alaro
34. Poland: P020-arome
35. Portugal: ALADIN-Portugal(ATP)
36. Portugal: AROME-Portugal(PT2)
37. Portugal: AROME-Madeira(MAD)
38. Portugal: AROME-Azores(AZO)
39. Romania: ALARO-RO
40. Slovakia: Slovakia-alaro
41. Slovenia: sis4-alaro
42. Spain: IBERIA
43. Spain: CANARIAS
44. Tunisia: Tunisia-aladin
45. Turkey: Turkey-alaro
46. Turkey: Turkey-Arome

6 Configurations with / without Data Assimilation

ALADIN-HIRLAM configurations with DA (blue) and without (red)

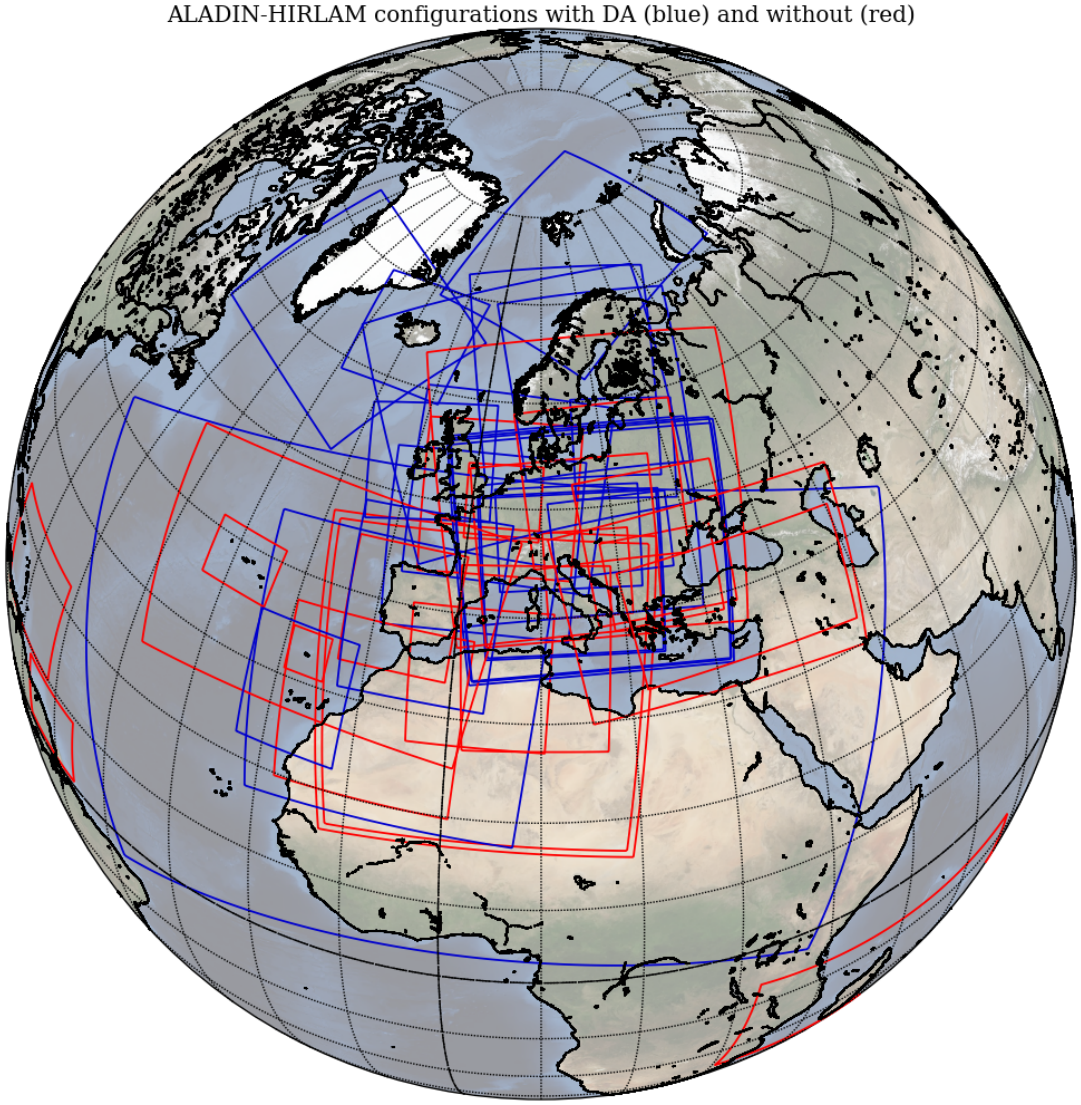

1. Algeria: ALGE (aladin)
2. Algeria: ALADIN_DUST
3. Algeria: AROME-NORD-ALGE
4. Austria: ALARO5-AUSTRIA
5. Austria: AROME-AUSTRIA
6. Belgium: Belgium-Alaro-7km
7. Belgium: Belgium-alaro-4km
8. Bulgaria: aladin-Bulgaria
9. Croatia: HR-alaro-88
10. Croatia: HR-alaro-44
11. Croatia: HR-alaro-22
12. Czech Rep: CZ-alaro
13. Denmark: AROME-NEA (Denmark)
14. Denmark: AROME-IMO (Ic+S.Gre)
15. Finland: AROME-FMI
16. France: Arome-France
17. France: AROME-Indian
18. France: AROME-Polynesia
19. France: AROME-Caledonia
20. France: AROME-Guyana
21. France: AROME-Antilles
22. Hungary: ALARO-HU determinis
23. Hungary: Arome-HU
24. Iceland: AROME-IMO
25. Ireland: AROME-IRELAND25
26. Lithuania: AROME-LHMS
27. Morocco: aladin-Mo1
28. Morocco: aladin-Mo2
29. Morocco: AROME Maroc
30. Netherlands: AROME-KNMI
31. Norway: AROME-Arctic
32. Fi&No&Se: AROME-MetCoOp
33. Poland: E040-alaro
34. Poland: P020-arome
35. Portugal: ALADIN-Portugal(ATP)
36. Portugal: AROME-Portugal(PT2)
37. Portugal: AROME-Madeira(MAD)
38. Portugal: AROME-Azores(AZO)
39. Romania: ALARO-RO
40. Slovakia: Slovakia-alaro
41. Slovenia: sis4-alaro
42. Spain: IBERIA
43. Spain: CANARIAS
44. Tunisia: Tunisia-aladin
45. Turkey: Turkey-alaro
46. Turkey: Turkey-Arome

ALADIN and HIRLAM organisational charts

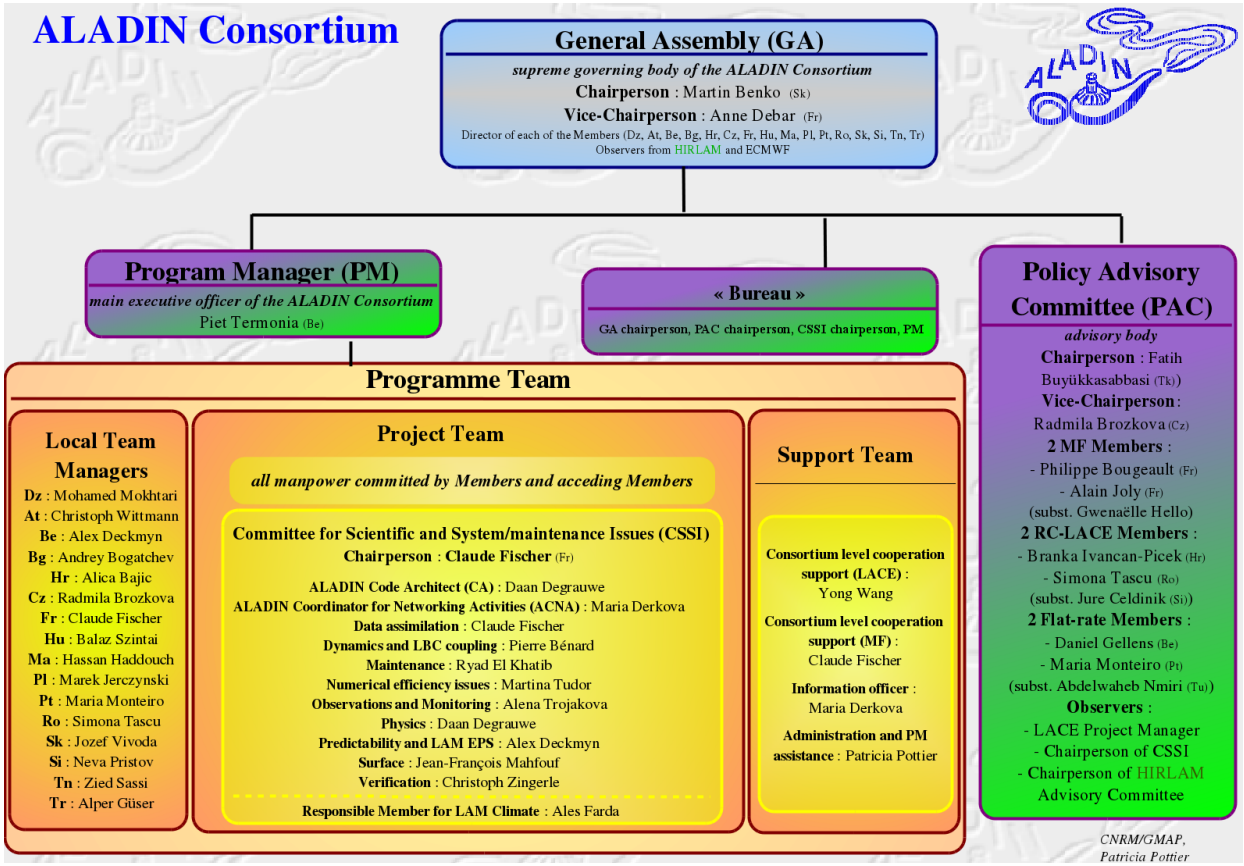

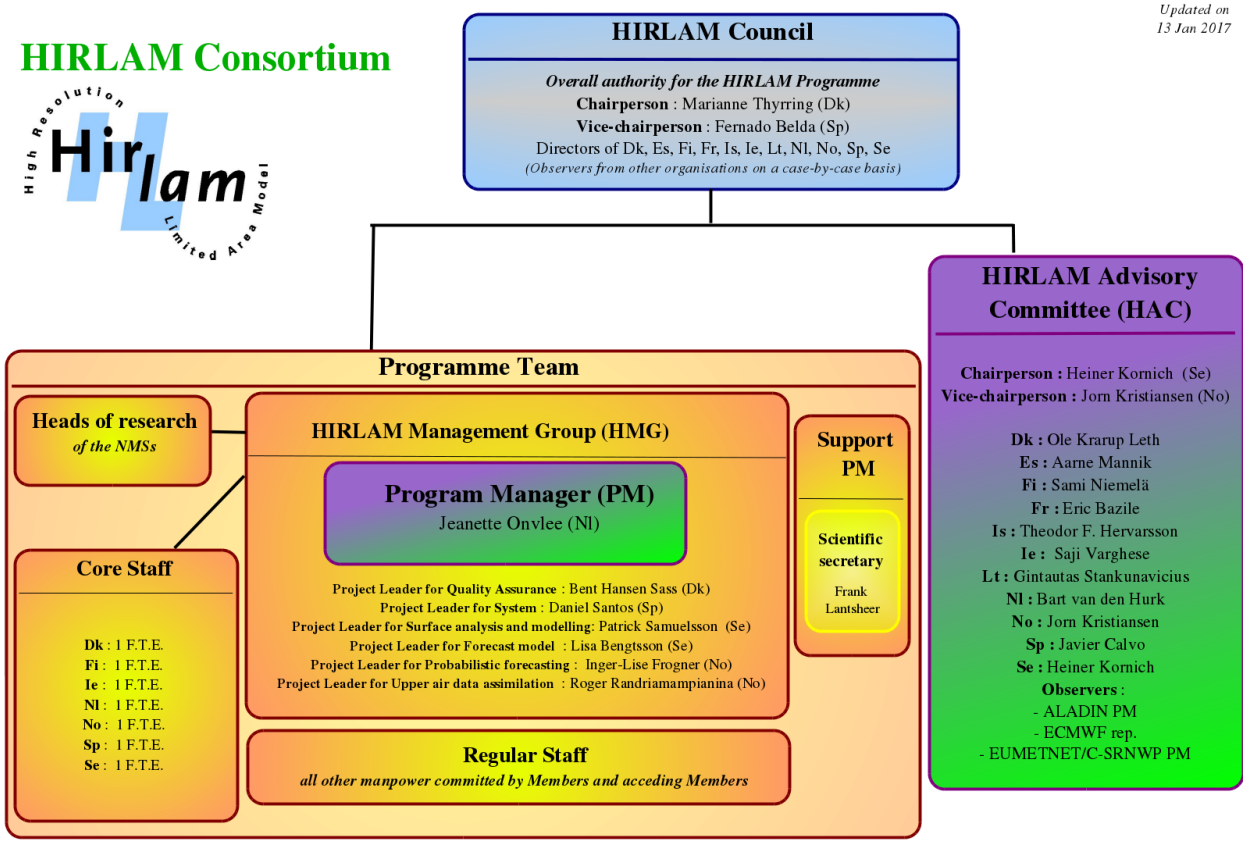

ALADIN-HIRLAM Newsletters : previous issues

No. 1, Sept 2013

No. 2, April 2014

No. 3, Sept 2014

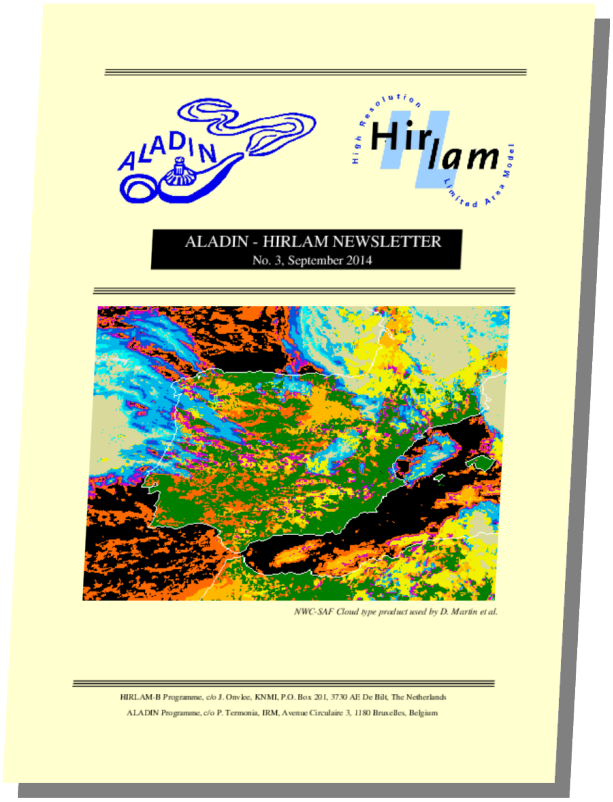

No. 4, Feb 2015

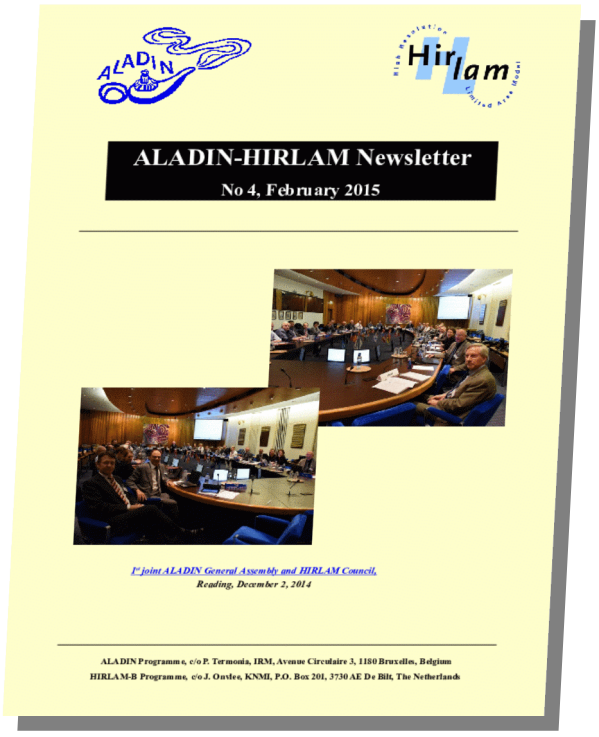

ALADIN-HIRLAM Newsletters : previous issues

No. 5, Aug 2015

No. 6, Fev 2016

No. 7, Sep 2017